AUS DEM INSTITUT FÜR KLINISCHE ZYTOBIOLOGIE UND ZYTOPATHOLOGIE
GESCHÄFTSFÜHRENDER DIREKTOR: PROF. DR. ROLAND LILL
DES FACHBEREICHS MEDIZIN DER PHILIPPS-UNIVERSITÄT MARBURG

BIOGENESIS OF PEROXISOMES IN MAMMALIAN CELLS: CHARACTERIZATION OF THE PEX11 PROTEINS AND THEIR ROLE IN PEROXISOMAL GROWTH AND DIVISION

INAUGURAL-DISSERTATION ZUR ERLANGUNG DES DOKTORGRADES DER HUMANBIOLOGIE
(DR. RER. PHYSIOL.)

DEM FACHBEREICH MEDIZIN DER PHILIPPS-UNIVERSITÄT MARBURG
VORGELEGT VON

HANNAH KATHARINA DELILLE
AUS KÖLN

MARBURG, 2010

Angenommen vom Fachbereich Medizin der Philipps-Universität Marburg am:
11.11.2010
Gedruckt mit Genehmigung des Fachbereichs.

Dekan: Prof. Dr. Matthias Rothmund
Referent: Prof. Dr. Ralf Jacob
Korreferent: Prof. Dr. Uta-Maria Bauer

TABLE OF CONTENTS

1 INTRODUCTION

1.1 Peroxisomes – an overview

1.1.1 General features of the organelle

Peroxisomes are essential organelles found in virtually all eukaryotic cells. They were one of the last organelles to be discovered and have been first described as spherical and oval microbodies in electron microscope images (Rhodin 1954). Later on, the discovery of their metabolic functions in hydrogen peroxide processing as well as the discovery of the enzyme catalase finally coined the name "peroxisome" (De Duve & Baudhuin 1966). The development of the alkaline 3, 3'-diaminobenzidine (DAB) staining exploiting catalase activity allowed the specific staining of peroxisomes for electron and light microscopy and facilitated studies on the organelle in different tissues and organisms (Fahimi 1968, 1969; Novikoff & Goldfischer 1969). Afterwards, their important role in lipid metabolism and the existence of a peroxisomal β-oxidation pathway have been discovered (Lazarow & De Duve 1976). Nowadays, it is known that peroxisomes, which together with glycosomes, glyoxisomes and Woronin bodies belong to the microbody family (Michels et al. 2005), fulfil a wide range of metabolic functions. Peroxisomal malfunctions lead to severe (congenital) disorders, rendering peroxisomes essential for human health and development.

Although peroxisomes are ubiquitous organelles, their morphological appearance and number as well as protein composition and metabolic functions vary widely among species, cell types and developmental stages (Schrader & Fahimi 2006b). Peroxisomes are single membrane-bounded organelles mainly found as spherical bodies, with a diameter between 0.1 and 0.3 µm, or as rod-like forms (0.3 to 0.5 µm). But also tubular structures (up to 5 µm) or even interconnecting compartments forming tubular networks are found (Purdue & Lazarow 2001). Electron microscopy (EM) images reveal diverse ultrastructural peroxisomal appearances (Figure 1.1). Peroxisomes often contain a crystalline matrix, such as e.g. urate oxidase cores in rat liver or crystalline inclusions of L-α-hydroxyacid oxidase B (HAOX-B), which create polyehedral shapes of peroxisomes in beef kidneys (Hruban & Swift 1964; Zaar et al. 1991). Woronin bodies of *Neurospora crassa* contain hexagonal crystals (Jedd & Chua 2000). In mammals, a particular high number of peroxisomes is found in kidney and liver cells, with around 1,000 peroxisomes per hepatocyte. In contrast, fungi such as the yeast *Saccharomyces cerevisiae* pos-

sess usually only a few peroxisomes (Figure 1.1 C). Number, size and shape of peroxisomes depend on various factors, as the compartment is highly dynamic adjusting to cellular needs.

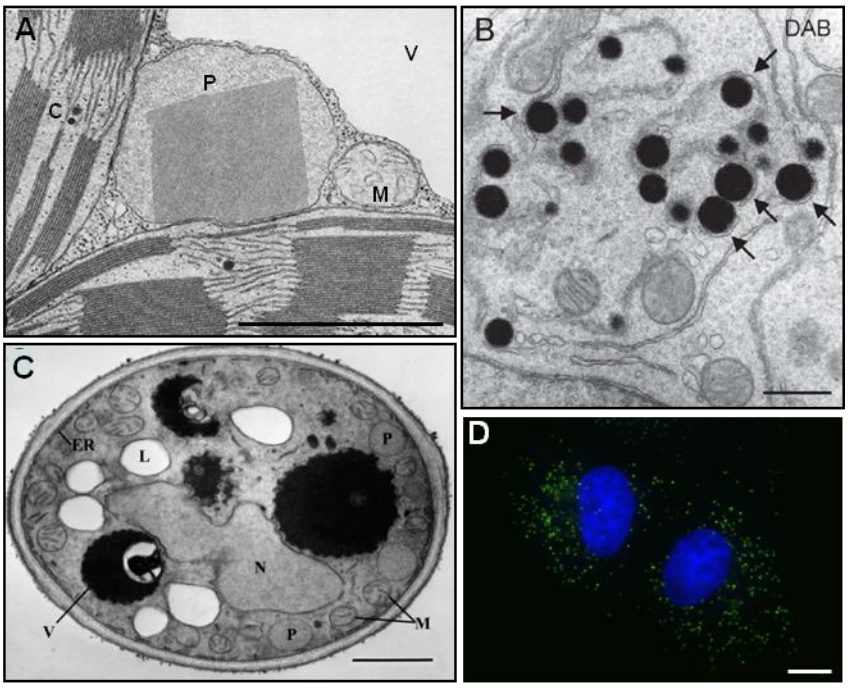

Figure 1.1: Peroxisomes
(A) Peroxisomes with crystalline inclusions in tobacco leaf cells (from Frederick & Newcomb 1969). **(B)** Peroxisomes stained by DAB (black) in rat hepatoma cells. Note the close association with the smooth ER (arrows; from Schrader & Fahimi 2004). **(C)** *S. cerevisiae* (from Purdue & Lazarow 2001). **(D)** Mouse fibroblasts. Peroxisomes are shown in green (GFP-SKL) and nuclei blue (Hoechst 33528). ER, endoplasmic reticulum; L, lipid droplet; M, mitochondrium; N, nucleus; P, peroxisome; V, vacuole. Bars, 1 µm (A and C), 500 nm (B), 10 µm (D).

Peroxisomes do not contain DNA and all peroxisomal proteins are encoded by the nuclear genome. About 61 yeast and 85 human genes encoding peroxisomal proteins have been identified so far. Many of them are enzymes with metabolic functions, while the other group of proteins, termed peroxins, is required for biogenesis and maintenance of functional peroxisomes (see section 1.2).

1.1.2 Metabolic functions of peroxisomes

Peroxisomes are "multipurpose organelles" (Opperdoes 1988) that are involved in a wide range of metabolic processes (see Figure 1.2 and Table 1.1 for an overview), and their specific metabolic functions vary depending upon organism and cell type, as well as developmental and environmental conditions (reviewed in Wanders & Waterham 2006b). In mammals about 50 peroxisomal metabolic proteins have been identified. Furthermore, peroxisomes cooperate with other organelles such as the endoplasmic reticulum (ER) or mitochondria (Camoes et al. 2009; Schrader & Yoon 2007).

Lipid metabolism

Peroxisomes have a very central role in lipid metabolism. They possess their own β-oxidation system and in plant cells and many eukaryotic microorganisms peroxisomes are the only sites of β-oxidation (Cooper & Beevers 1969; Kunau et al. 1988; Poirier et al. 2006; Shen & Burger 2009), which renders them essential for the utilization of fatty acids in these organisms.

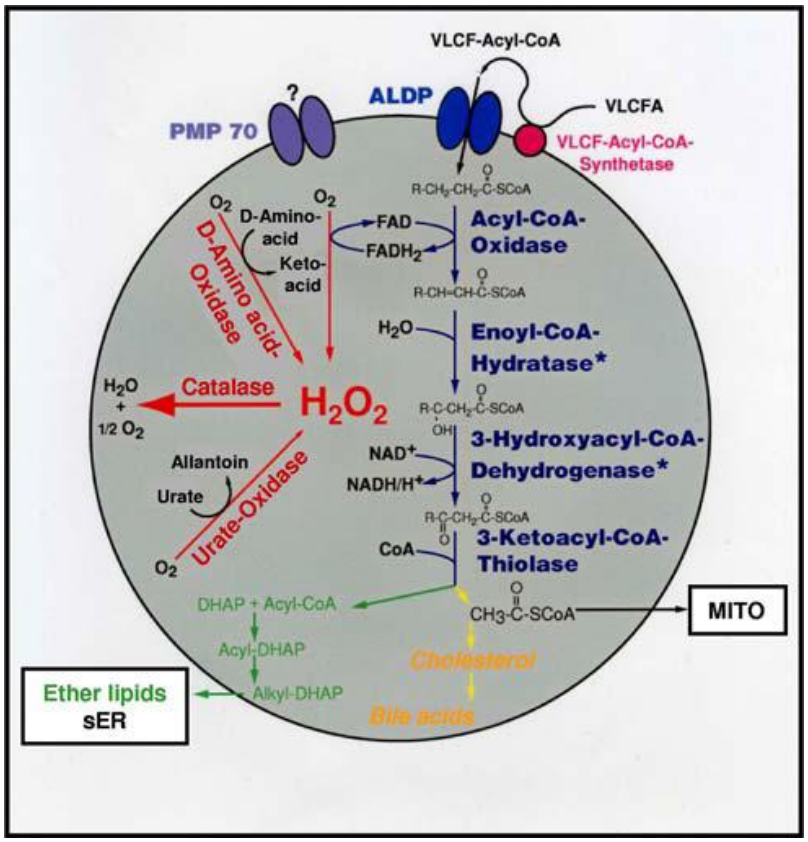

Figure 1.2: The major peroxisomal metabolic pathways
Peroxisomal metabolism in the mammalian liver. Adapted from Baumgart et al. (1997) and Schrader & Fahimi (2008).

In mammalian cells very long-chain fatty acids (VLCFA, ≥C_{24}) are degraded by peroxisomes and not by mitochondria (Reddy & Hashimoto 2001). VLCFA are probably imported into peroxisomes as acyl-CoA esters by ABC transporters (e.g. ABCD1 = adrenoleukodystrophy protein, ALDP). After chain shortening by peroxisomal β-oxidation the resulting (medium-chain) acyl-CoA esters can be transferred to mitochondria for full oxidation to CO_2 and H_2O. This is one example for the close metabolic cooperation between mitochondria and peroxisomes (Camoes et al. 2009; Schrader & Yoon 2007). The final degradation of fatty acids in mitochondria supplies the cell with ATP, as the peroxisomal β-oxidation is not coupled to an electron transfer chain. Instead, electrons are transferred to oxygen via $FADH_2$, generating hydrogen peroxide (H_2O_2; Figure 1.2). Therefore, the obtained energy is not used to power ATP synthesis, but is

instead released as heat (contributing to thermogenesis; Lazarow 1987). Besides VLCFA, other substrates such as prostaglandins and leukotriens, bile acid intermediates, pristanic acid, certain polyunsaturated fatty acids, and the vitamins E and K are degraded by peroxisomal β-oxidation (Ferdinandusse et al. 2002; Wanders & Waterham 2006b). Trans-unsaturated fatty acids, i.e. those containing a methyl group at the C-3 position such as e.g. phytanic acid and xenobiotic compounds, cannot undergo β-oxidation and are thus first decarboxylated in peroxisomes by fatty acid α-oxidation (Casteels et al. 2003; Jansen & Wanders 2006; Wanders & Waterham 2006b).

Function	Enzymes, substrates, products
Peroxide metabolism, ROS/RNS metabolism*	catalase and H_2O_2-generating oxidases
Lipid biosynthesis	ether phospholipids/plasmalogens, bile acids, fatty acid elongation, (cholesterol and dolichol)
Fatty acid β-oxidation*	very long-chain fatty acids, dicarboxylic acids, branched-chain fatty acids, unsaturated fatty acids, arachidonic acid metabolism
Fatty acid α-oxidation	phytanic acid, xenobiotic compounds
Long/very long-chain fatty acid activation	
Regulation of acyl-CoA/CoA ratio	
Glycerol biosynthesis	
Protein/amino acid metabolism*	biosynthesis of cysteine and sulphur assimilation, D-amino acid degradation, L-lysine metabolism, degradation of polyamines, proteases, transaminases
Catabolism of purines	
Glyoxylate and dicarboxylate metabolism	
Hexose monophosphate pathway	
Nicotinate and nicotinamide metabolism	
Retinoid metabolism	

Table 1.1: Metabolic functions of peroxisomes
Adapted from Schrader & Fahimi (2008). *Functional cooperation of peroxisomes with mitochondria.

Additionally, catabolic processes also take place in peroxisomes. The synthesis of ether-phospholipids such as plasmalogens is a cooperative process between peroxisomes and the endoplasmic reticulum (Brites et al. 2004; Gorgas et al. 2006; Heymans et al. 1983). Plasmalogens are essential components of myelin, thus they account for roughly 80% of the white matter of the brain (Wanders & Waterham 2006a), and represent around 18% of the total phospholipid mass. The formation of the characteristic ether linkage is catalyzed by the peroxisomal enzyme alkyl-DHAP synthase while further biosynthesis is conducted in the smooth ER (Wanders & Waterham 2006b). Moreover, bile acid and

glycerol biosynthesis are also performed by peroxisomal enzymes. The synthesis of cholesterol and dolichol in peroxisomes is debated (Hogenboom et al. 2004; van den Bosch et al. 1992; Wanders & Waterham 2006b).

ROS metabolism and other functions

Peroxisomes contain a number of O_2-consuming oxidases that produce H_2O_2 by oxidizing a large collection of substrates. H_2O_2 is ascribed to "reactive oxygen species" (ROS), as it can easily be converted into more aggressive radical species. Although ROS have been shown to have physiological functions (e.g. in signalling), increased oxidative stress can provoke serious cell damage (Bonekamp et al. 2009). Therefore a tight regulation of ROS metabolism is required. In addition to the enzymes involved in fatty acid α- and β-oxidation (see above), oxidases metabolising other substrates such as lactate, glycolate, other α-hydroxy acids, D-amino acids, oxalate, and urate (not in primates) produce H_2O_2. Xanthin oxidase (XOx), an enzyme involved in the catabolism of purines, even produces superoxide radicals ($O_2^{\bullet-}$) (Angermuller et al. 1987).

Type of ROS/RNS produced	**Generating reaction**	**Produced in PO by**	**Scavenged in PO by**
Hydrogen peroxide (H_2O_2)	$O_2^{\bullet-} + H^+ \rightarrow HO_2^{\bullet-}$, $2\ HO_2^{\bullet-} \rightarrow H_2O_2 + O_2$	Acyl-CoA oxidase (several types), Urate oxidase, Xanthine oxidase, D-amino acid oxidase, D-aspartame oxidase, Pipecolic acid oxidase, Sarcosine oxidase, L-α-hydroxy acid oxidase, Polyamine oxidase	Catalase, Glutathione peroxidase, Peroxiredoxin I, PMP20
Superoxide anion ($O_2^{\bullet-}$)	$O_2 + e^- \rightarrow O_2^{\bullet-}$	Xanthine oxidase	MnSOD, CuZnSOD
Nitric oxide ($^{\bullet}NO$)	L-Arg + NADPH + H^+ + O_2 → NOHLA + $NADP^+$ + H_2O, NOHLA + ½ NADPH + ½ H^+ + O_2 → L-citrulline + ½ $NADP^+$ + $^{\bullet}NO$ + H_2O	Nitric oxide synthase	

Table 1.2: Overview of ROS/RNS generated in mammalian peroxisomes.
Adapted from Bonekamp et al. (2009). PO, peroxisomes; NOHLA, N^{ω}-hydroxy-L-arginine.

On the other hand, antioxidant enzymes located in peroxisomes counteract the production of H_2O_2 and $O_2^{\bullet-}$, the most prominent being catalase (reviewed in Bonekamp et al. 2009; Schrader & Fahimi 2006a). While catalase and other enzymes (see Table 1.2) de-

compose H_2O_2, superoxide anions and hydroxyl radicals (•OH, generated from hydrogen peroxide via Fenton-catalyzed reduction) are scavenged by manganese and copper-zinc superoxide dismutases (MnSOD, CuZnSOD) (Dhaunsi et al. 1992; Immenschuh & Baumgart-Vogt 2005; Singh et al. 1994; Singh 1996).

Furthermore, the toxic metabolite glyoxylate is converted into glycine by alanine:glyoxylate aminotransferase (AGT), which localizes exclusively to peroxisomes in humans (Danpure 2006), and enzymes of the hexose monophosphate pathway are found in peroxisomes as well (Antonenkov 1989). More specialized functions are for instance fulfilled in the glyoxysomes of the parasite *Trypanosoma*, which contain enzymes of the glyoxylate cycle for the production of lipid-derived compounds required for gluconeogenesis, or in Woronin bodies, which seal septal pores in the hyphae of filamentous fungi (Jedd & Chua 2000; Kunze et al. 2006). Additionally, peroxisomes are involved in several quite diverse processes such as penicillin biosynthesis, photorespiration in plants, or luciferase-based glowing of a firefly (Gould et al. 1987; Muller et al. 1992; Reumann & Weber 2006).

1.1.3 Peroxisomal disorders

Due to the important metabolic roles of peroxisomes in eukaryotic cells, disturbance of their functions can lead to severe pathologies. Peroxisomal disorders are divided into two main subgroups: peroxisomal biogenesis disorders (PBDs, 1.1.3.1) and peroxisomal enzyme deficiencies (PEDs, 1.1.3.2). Peroxisomal disorders are often associated with neurological and developmental defects. Apart from the inherited peroxisomal disorders, peroxisomes have been linked to other pathological conditions (e.g. associated with oxidative stress), such as inflammation, carcinogenesis, ischemia-reperfusion injury, fatty liver disease and type-2 diabetes, or neurodegenerative diseases such as Parkinson's or Alzheimer's disease (Cimini et al. 2009) (reviewed in Delille et al. 2006; Schrader & Fahimi 2006a, 2008). Interestingly, the induction of peroxisome proliferation might exert a protective effect (Santos et al. 2005). In addition, peroxisomes have been linked to ageing (Terlecky et al. 2006).

1.1.3.1 Peroxisomal Biogenesis Disorders

PBDs (reviewed in Brosius & Gartner 2002; Faust et al. 2005; Steinberg et al. 2006; Wanders & Waterham 2005; Weller et al. 2003) result from defects in the so-called per-

oxins (Pex), i.e. proteins important for the biogenesis of peroxisomes (1.2). Therefore, peroxisomes are often absent from cells, or only present as empty, non-functional membrane "ghosts" if solely the import of peroxisomal matrix proteins is impaired. PBD patients suffer from severe metabolic dysfunctions, as most peroxisomal metabolic pathways are affected (Wanders & Waterham 2006b). Most PBDs belong to the Zellweger syndrome spectrum (ZSS), which include the fatal cerebro-hepato-renal syndrome (Zellweger syndrome, ZS) itself, neonatal adrenoleukodystrophy (NALD), and infantile Refsum's disease (IRD). Mutations in at least 12 different peroxins have been identified to lead to ZSS disorders (Table 1.3). Complementation studies with PBD patient fibroblasts in combination with transfection experiments using peroxin-encoding plasmids have been used to identify the affected PEX genes. The presently known complementation groups (CG) are shown in Table 1.3 (Sacksteder & Gould 2000; Steinberg et al. 2006).

Gene	CG-Dutch	CG-Japan	CG-KKI	Clinical phenotypes	Proportion of ZSS[1]
PEX1	2	E	1	ZS NALD IRD	70%
PEX2	5	F	10	ZS IRD	3%
PEX3		G	12	ZS	<1%
PEX5	4		2	ZS NALD	<2%
PEX6	3	C	4, 6	ZS NALD IRD	10%
PEX7	1	R	11	RCDP1	-
PEX10		B	7	ZS NALD	3%
PEX12			3	ZS NALD IRD	5%
PEX13		H	13	ZS NALD	<1%
PEX14		K		ZS	<1%
PEX16		D	9	ZS	<1%
PEX19		J	14	ZS	<1%
PEX26		A	8	ZS NALD IRD	5%

Table 1.3: Complementation groups of peroxisomal biogenesis disorders
CG, complementation group; Dutch, group at University of Amsterdam; Japan, group at Gifu University School of Medicine; KKI, Kennedy Krieger institute. [1]Estimates of CG frequency is derived from the KKI data. Adapted from Steinberg et al. (2006).

The disturbed peroxisomal metabolism results in an accumulation of peroxisomal substrates like VLCFAs, pristanic acid, phytanic acid, bile acid intermediates and pipecolic acid. This is combined with a lack of peroxisomal products, for instance plasmalogens/ether glycerolipids, cholic and chenodeoxycholic acid, and docosahexaenoic acid. Additionally, the cell-protective function of peroxisomes due to the degradation of ROS, reactive nitrogen species and other toxic metabolites (Wanders & Waterham 2006b) is impaired. Clinical symptoms are diverse but generally comprise liver dysfunction, se-

vere neurodevelopmental impairment, retinopathy, perceptive deafness, dysmorphic features and skeletal abnormalities with ZS being the most and IRD the least severe disorder (Brosius & Gartner 2002; Steinberg et al. 2006). Peroxisomal metabolism is essential for normal brain development. Studies on Pex5 knockout mice have revealed that peroxisomes provide oligodendrocytes with an essential neuroprotective function against axon degeneration, dysmyelination and neuroinflammation, which is relevant for human demyelinating diseases (Baes & Aubourg 2009; Hulshagen et al. 2008; Kassmann et al. 2007). Onset of ZSS disorders is usually in the first months of life and they lead to death of the patients within the first year(s), although IRD patients may even reach adulthood. Another PBD is Rhizomelic chondrodysplasia punctata type 1 (RCDP1), which results from mutation in the peroxin Pex7p, the PTS2 import factor (see section 1.2.1). Main symptoms are growth and neuronal defects, while the lifespan can range from early childhood up to young adulthood (Braverman et al. 2002; Steinberg et al. 2006; White et al. 2003).

1.1.3.2 Single Peroxisomal Enzyme Deficiencies

Most peroxisomal disorders belong to the class of single enzyme deficiencies (reviewed in Wanders & Waterham 2006a). The phenotypes can vary broadly, even if the affected enzymes act in the same metabolic pathway. The PEDs can be divided into subgroups depending on the peroxisomal metabolic pathway affected (Wanders & Waterham 2006a), which are (a) ether lipid synthesis, (b) peroxisomal β-oxidation, (c) peroxisomal α-oxidation, (d) glyoxylate detoxification, and (e) H_2O_2-metabolism. The X-linked adrenoleukodystrophy (X-ALD) is the most frequent PED with an incidence of 1:21,000 to 1:15,000 males and affects peroxisomal β-oxidation. Onset of the childhood cerebral ALD (CCALD) is between 3-10 years of age, but there are also adolescent and adult forms (ACALD) with later onset, as also seen in the non-cerebral phenotype (adrenomyeloneuropathy, AMN). Mutations in the ALD gene result in dysfunction of an ABC transporter important for import of VLCFAs (Figure 1.2), and therefore in the inability to metabolize VLCFAs and their subsequent accumulation in the blood (Wanders et al. 2010). Main symptoms are a progressive demyelination/neurodegeneration as well as adrenal insufficiency (Berger & Gartner 2006; Moser et al. 2007). Interestingly, studies on *ABCD1* knockout mice indicate that early oxidative damage might underlie neurodegeneration in X-ALD (Fourcade et al. 2008). D-bifunctional protein (DBP) deficiency is now known

to be relatively frequent among PEDs, as patients with previously unidentified or doubtful diagnosed peroxisomal β-oxidation deficiencies have been shown to suffer from this disorder (Ferdinandusse et al. 2006). Which of both enzyme activities is deficient does not seem to influence the pathology, which resembles ZS (Wanders & Waterham 2006a). Generally, the diagnosis of peroxisomal disorders involves laboratory analysis of blood and urine samples in regard to e.g. VLCFAs, bile acids, and erythrocyte plasmalogen levels followed by biochemical, morphological, and molecular studies in patient fibroblasts cell lines (Depreter et al. 2003; Steinberg et al. 2008; Steinberg et al. 2006). Treatment of peroxisomal disorders is still rare and mostly supportive, being difficult due to the prenatal development of abnormalities especially in PBDs. Nevertheless, there are some therapeutic strategies such as allogenic stem cell transplantation (Krivit 2004). One of the few treatable disorders is Refsum disease, where a mutation in phytanol-CoA hydroxylase interferes with α-oxidation of branched-chain fatty acids, characterized by elevated phytanic acid levels. A restriction of phytanic acid intake may stop the progression of the phenotypes and improve some symptoms (Wanders & Waterham 2006a). Hyperoxaluria type 1 is caused by mutations in AGT leading to reduced activity or mistargeting of the enzyme to mitochondria (Danpure 2006). This results in deposition of oxalate in all types of tissues, especially kidneys, and finally in kidney failure. Therapeutic strategies are aimed at an increase of the solubility of oxalate and a decrease in synthesis by treatment with the AGT cofactor pyridoxal phosphate, which can interestingly even diminish the mistargeting of AGT to mitochondria (Wanders & Waterham 2006a).

1.2 Peroxisome biogenesis

Peroxisomal biogenesis requires a special set of proteins, the peroxins (Pex proteins), which are encoded by PEX genes (Distel et al. 1996). Peroxisomes do not contain DNA – in contrast to mitochondria and chloroplasts – and peroxisomal proteins are translated on free polyribosomes in the cytoplasm and imported post-translationally (Lazarow & Fujiki 1985). Exceptions are discussed in section 1.2.3. The peroxins can be divided into three groups according to their role in peroxisomal biogenesis: (a) peroxins involved in the import of peroxisomal matrix proteins (1.2.1), (b) peroxins required for peroxisomal membrane assembly/import of peroxisomal membrane proteins (PMPs, 1.2.2), and (c) peroxins regulating peroxisomal proliferation (1.3.3). At present around 31 peroxins have been discovered in lower eukaryotes (*S. cerevisiae*, *Pichia pastoris*, *Yarrowia lipolytica*, or *N. crassa*) and around 18 mammalian and 23 plant peroxin homologues have been identified (Table 1.4) (Kiel et al. 2006; Platta & Erdmann 2007). Most of the additional peroxins present in lower eukaryotes appear to be specific for one species and/or functional redundant (Kiel et al. 2006; Schluter et al. 2006).

Peroxin	Organism	Localization	Domains	Proposed function
Pex1p	m p f y	membrane (cytosol)[1]	AAA ATPase	Matrix protein import, export of Pex5p
Pex2p	m p f y	integral PMP	Zinc RING finger	Matrix protein import, translocation
Pex3p	m p f y	integral PMP		Membrane biogenesis, PMP import
Pex4p	p f y	peripheral PMP	E2 enzyme[2]	Matrix protein import, Pex5p ubiquit-ination
Pex5p[3]	m p f y	cytosol/membrane	TPRs	Matrix protein import, PTS1 (and PTS2) receptor
Pex6p	m p f y	membrane (cytosol)[1]	AAA ATPase	Matrix protein import, export of Pex5p
Pex7p	m p f y	cytosol/membrane	WD40 repeats	Matrix protein import, PTS2 receptor
Pex8p	f y	peripheral PMP (matrix)		Matrix protein import
Pex9p	*Yl*	(ORF wrongly identified, antisense sequence of Pex26p)		
Pex10p	m p f y	integral PMP	Zinc RING finger	Matrix protein import, translocation
Pex11p[4]	m p f y	integral PMP[5]		Proliferation and division
Pex12p	m p f y	integral PMP	Zinc RING finger	Matrix protein import translocation
Pex13p	m p f y	integral PMP	SH3	Matrix protein import, docking
Pex14p	m p f y	(integral) PMP	Coiled-coil	Matrix protein import, docking
Pex15p	*Sc*	integral PMP		Matrix protein import, Pex1p/Pex6p anchor
Pex16p	m p f *Yl*	integral PMP[6]		Membrane biogenesis
Pex17p	y	peripheral PMP	Coiled-coil	Matrix protein import, docking

Peroxin	Organism	Localization	Domains	Proposed function
Pex18p	*Sc*	cytosol/membrane		Matrix protein import, PTS2 import
Pex19p	m p f y	cytosol/membrane	Farnesylation motif	Membrane biogenesis, PMP import
Pex20p	f y	cytosol/membrane		Matrix protein import, PTS2 import
Pex21p	*Sc*	cytosol/membrane		Matrix protein import, PTS2 import
Pex22p	p f y	integral PMP		Matrix protein import, Pex4p anchor
Pex23p	f y	integral PMP	Dysferlin	Proliferation
Pex24p	f y	integral PMP		Proliferation
Pex25p	y	peripheral PMP		Proliferation
Pex26p	m f y[7]	integral PMP		Matrix protein import, Pex1p/Pex6p anchor
Pex27p	*Sc*	peripheral PMP		Proliferation
Pex28p	*Sc*	integral PMP		Proliferation (Pex24p ortholog)
Pex29p	y	integral PMP		Proliferation
Pex30p	*Sc*	integral PMP	Dysferlin	Proliferation (Pex23p ortholog)
Pex31p	*Sc*	integral PMP	Dysferlin	Proliferation
Pex32p	y	integral PMP	Dysferlin	Proliferation

Table 1.4: Peroxisomal biogenesis proteins (Peroxins)
Organisms: m, mammals; p, plants; f, filamentous fungi; y, yeasts; *Sc*, *S. cerevisiae* only; *Yl*, *Y. lipolytica* only. RING, really interesting new gene; SH3, Src-Homology 3.[1]Dual localization of Pex1p and Pex6p due to species difference. [2]The mammalian E2 is UbcH5/a/b/c (Grou et al. 2008). [3]Mammals contain two isoforms, Pex5pS and Pex5pL, the latter harbouring a Pex7p binding site. [4]Mammalian cells contain three PEX11 genes encoding Pex11pα, Pex11pβ, and Pex11pγ and plants have five Pex11p isoforms (a-e). [5]Pex11p from *Sc* might be a peripheral PMP (Marshall et al. 1995). [6]Pex16p in *Yl* appears to be intraperoxisomal (Eitzen et al. 1997). [7]Pex26 is absent from *Sc* and related yeasts. (Kiel et al. 2006; Nito et al. 2007; Purdue & Lazarow 2001; Weller et al. 2003).

1.2.1 Import of matrix proteins

The import of matrix proteins from the cytosol into peroxisomes (Lazarow & Fujiki 1985) differs from most other protein translocation systems (e.g. into ER or mitochondria) (Schnell & Hebert 2003). Interestingly, fully folded, co-factor bound or oligomeric proteins can be transported across the peroxisomal membrane (Glover et al. 1994; McNew & Goodman 1994), and even gold particles with a diameter up to 9 nm have been shown to be imported into peroxisomes (Walton et al. 1995). The specific import of peroxisomal matrix proteins is mediated by targeting signals which are recognized by cytosolic receptors. According to the "extended shuttle model" (Figure 1.3), based on the concept of cycling receptors (Dammai & Subramani 2001), the import process can be divided into four steps: (a) cargo recognition in the cytosol, (b) docking of the cargo-loaded receptor to distinct proteins at the peroxisomal membrane, (c) translocation across the peroxisomal membrane, and (d) export of the receptor back to the cytosol (Girzalsky et al. 2010).

Most peroxisomal matrix proteins contain a type 1 peroxisomal targeting signal (PTS1) consisting of three C-terminal amino acids, serine-lysine-leucine (SKL), or conserved variants (S/A/C-K/R/H-L) (Gould et al. 1989). Nowadays, PTS1 has been redefined as dodecamer, as additional amino acids might be crucial for receptor-cargo interaction (Brocard & Hartig 2006). PTS2 is N-terminally localized and comprised by the degenerated nonapeptide R-L/V/I/Q-x-x-L/V/I/H-L/S/G/A-x-H/Q-L/A (Lazarow 2006; Swinkels et al. 1991). Pex5p is the cytosolic receptor for PTS1 proteins and contains a tetratricopeptide repeat (TPR) domain which mediates PTS1 binding (Gatto et al. 2000). PTS2 proteins are bound by the soluble receptor Pex7p, which contains six WD40 repeats (Marzioch et al. 1994). Interestingly, Pex7p requires the assistance of species-specific auxiliary proteins. In mammals and plants this function is fulfilled by a longer splice variant of Pex5p (Pex5pL; Dodt et al. 2001; Otera et al. 2000; Woodward & Bartel 2005). Proteins neither containing PTS1 nor PTS2 (non-PTS proteins) can be imported into peroxisomes by binding to a different region of Pex5p (van der Klei & Veenhuis 2006a) or "piggyback" by formation of a complex with PTS-containing proteins (Islinger et al. 2009; McNew & Goodman 1994; Titorenko et al. 2002; Yang et al. 2001).

Two intrinsic peroxisomal membrane proteins, Pex13p and Pex14p, are both crucial for docking of the cargo-receptor complex at the peroxisomal membrane and for translocation of the cargo proteins across the membrane, although their exact roles are still matter of discussion (Azevedo & Schliebs 2006; Urquhart et al. 2000; Williams & Distel 2006). Importantly, neither Pex13p nor Pex14p have the capacity to bind peroxisomal matrix proteins, suggesting that Pex5p does not just deliver its cargoes to these membrane proteins. Indeed, Pex5p acquires transient transmembrane topology and is thought to translocate cargo proteins across the organelle membrane by itself (Grou et al. 2009a). The translocation might be performed via a "transient pore", which could be dynamically formed by the import receptors/docking proteins themselves (Erdmann & Schliebs 2005). The mechanism of how cargo is released from the receptors inside peroxisomes remains unknown, and the only peroxin which has been connected to this process is Pex8p, which is not present in higher eukaryotes (Table 1.4) (Girzalsky et al. 2010; Rayapuram & Subramani 2006; Rehling et al. 2000).

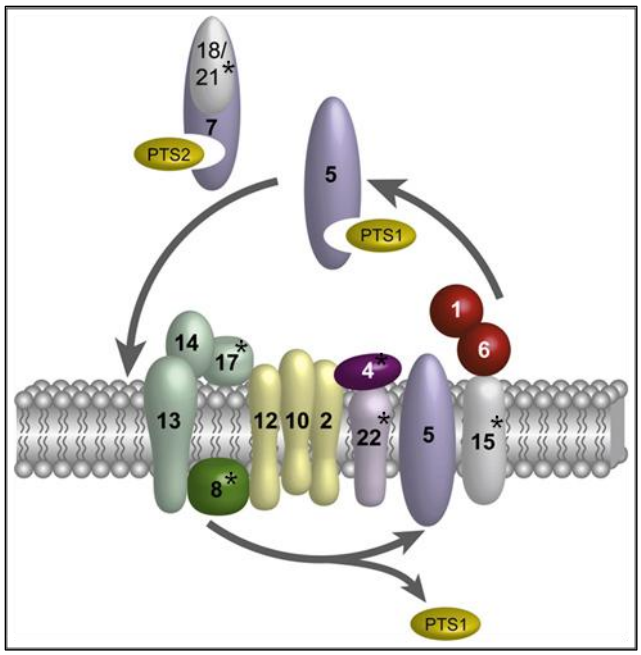

Figure 1.3: Peroxisomal matrix import
The cycling receptor model in yeast. Differences in mammalian cells are marked by asterisks: The proteins Pex17p and Pex8p do not exist. Furthermore, the function of Pex18p/Pex21p is fulfilled by Pex5pL and the function of Pex22p/Pex4p by UbcH5a/b/c. Pex15p is replaced by Pex26p. For detailed explanations see text. From Girzalsky et al. (2010).

After cargo translocation Pex5p returns to the cytosol in an ATP-dependent process. Recently, it has been discovered that Pex5p has to be monoubiquitinated at a conserved cysteine residue to be exported (Carvalho et al. 2007; Platta et al. 2007). In yeast the E2 ubiquitin-conjugating enzyme is Pex4p, which is anchored at the peroxisomal membrane through Pex22p. Mammals lack both proteins and ubiquitination is assisted by UbcH5a/b/c (Grou et al. 2008). The RING-finger proteins Pex2p, Pex10p, and Pex12p are protein-ubiquitin ligases (E3), with Pex12p being responsible for monoubiquitination and receptor recycling (Girzalsky et al. 2010; Platta et al. 2009; Williams et al. 2008). Afterwards, extraction of ubiquitinated Pex5p is catalyzed by Pex1p and Pex6p, two members of the AAA-protein family (Miyata & Fujiki 2005; Platta et al. 2005), which are anchored to the peroxisomal membrane by Pex15p/Pex26p (Matsumoto et al. 2003). Subsequent removal of the ubiquitin moiety could be performed by a yet undefined deubiquitinating enzyme, but recent *in vitro* data showed that the thiolester bond can also be broken by a non-enzymatic nucleophilic attack of glutathione (Grou et al. 2009b). Finally, Pex5p is once again available for promoting further cycles of protein transportation (Figure 1.3).

1.2.2 Import of membrane proteins

The import of peroxisomal membrane proteins (PMPs) occurs independently of matrix import via a different set of import factors. Many mechanistic details are still unclear, but three proteins were identified to be required for peroxisomal membrane assembly:

Pex3p, Pex16p, and Pex19p. The loss of any one of these proteins/genes leads to complete loss of peroxisomes, for instance seen in patients suffering from a ZSS disorder (1.1.3.1), while defects in matrix protein import result in formation of empty peroxisomal "ghosts" (Brosius & Gartner 2002; Honsho et al. 1998; Santos et al. 1988).

Pex19p is a farnesylated, predominantly cytosolic protein, but is also found at the peroxisomal membrane (Gotte et al. 1998; Matsuzono et al. 1999; Rucktaschel et al. 2009). It is thought to act as a cytosolic receptor by binding PMPs and delivering them to the peroxisomal membrane. Additionally, a chaperone-like function preventing PMP aggregation in the hydrophilic environment of the cytosol has been ascribed to Pex19p (Jones et al. 2004; Shibata et al. 2004). Therefore, a model with a dual role for Pex19p as both chaperone and cycling receptor is favoured (Figure 1.4) (Fujiki et al. 2006; Jones et al. 2004; Matsuzono & Fujiki 2006). Pex19p binds to (type I) intrinsic and peripheral PMPs (Fransen et al. 2001; Sacksteder et al. 2000; Snyder et al. 2000), and the peroxisomal membrane targeting signal (mPTS) can be defined as a Pex19p binding motif together with a membrane anchor sequence (transmembrane domain, TMD, or protein-binding module) (Girzalsky et al. 2010; Purdue & Lazarow 2001; Van Ael & Fransen 2006). In many cases the Pex19p binding motif consists of positively charged amino acid residues or a mixture of basic and hydrophobic amino acids, but no general consensus sequence could be deduced (Halbach et al. 2005; Rottensteiner et al. 2004).

The membrane docking factor for the receptor-cargo complex is Pex3p, an integral PMP (Fang et al. 2004; Fujiki et al. 2006; Muntau et al. 2003; Pinto et al. 2006). Thus, Pex3p binds to Pex19p at a region different from other PMPs (Fang et al. 2004; Matsuzono et al. 2006; Shibata et al. 2004). How PMP insertion into the peroxisomal membrane is achieved is not known. Another puzzling protein involved in PMP import is Pex16p, as its exact role in the import process has not yet been defined (Girzalsky et al. 2010). It is an integral membrane protein essential for peroxisome membrane biogenesis in mammalian cells, but absent in most yeast and intraperoxisomal in *Y. lipolytica* (Table 1.4) (Eitzen et al. 1997; Honsho et al. 2002). It might act as tethering/recruitment factor for Pex3p, or contribute to a putative membrane-insertion machinery (Kim et al. 2006; Matsuzaki & Fujiki 2008; Toro et al. 2009).

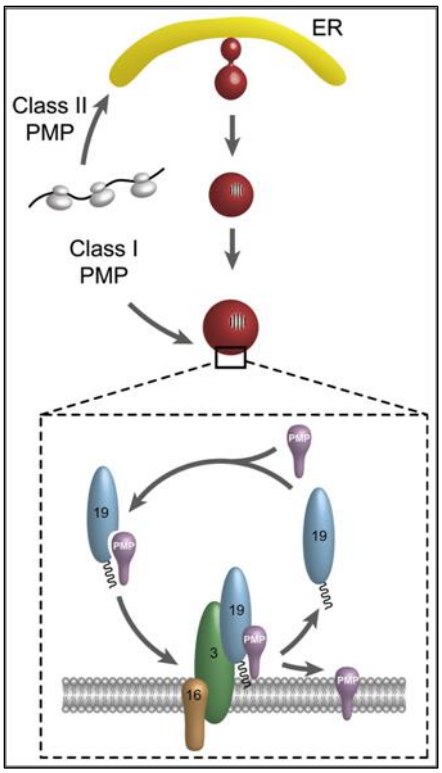

Figure 1.4: Import of peroxisomal membrane proteins
For explanations see text. From Girzalsky et al. (2010).

Pex3p itself is not inserted into the peroxisomal membrane via Pex19p, but rather targeted to the membrane of the ER and delivered to peroxisomes via a undefined vesicular (?) pathway (Hoepfner et al. 2005; Kragt et al. 2005; Tam et al. 2005; Toro et al. 2009). Thus, a second membrane targeting mechanism for so-called type II PMPs was proposed, in which proteins are routed to peroxisomes via the ER (Figure 1.4) (Jones et al. 2004). Controversially, direct – Pex16p and Pex19p-dependent – import of Pex3p into peroxisomes was described in mammalian cells (Matsuzaki & Fujiki 2008). Recently, the peroxisomal protein targeting was further complicated by discovery of a novel vesicular transport pathway from mitochondria to peroxisomes (Neuspiel et al. 2008). This pathway is supposed to involve unique mitochondria-derived vesicles (MDVs) which emanate from the sides of mitochondria, and a subpopulation of these MDVs was observed to fuse with a subpopulation of peroxisomes. A putative physiological function of this transport pathway is presently unknown (Andrade-Navarro et al. 2009; Schrader & Fahimi 2008; Schumann & Subramani 2008).

1.2.3 "Growth and division" vs. "*de novo* synthesis"

The early steps of peroxisome biogenesis are still controversially discussed (Lazarow 2003; Tabak et al. 2006). The observation that peroxisomal matrix and membrane pro-

teins are directly imported into peroxisomes from the cytosol led to the classical view that peroxisomes are autonomous organelles and the proposal of the "growth and division" model for multiplication (Lazarow & Fujiki 1985). Accordingly, peroxisomes grow by import of newly synthesized proteins and are subsequently divided into daughter organelles. The source of phospholipids for the peroxisomal membrane was suggested to be the ER, as lipid transfer could be achieved for example via sites of close association previously observed in morphological studies (Novikoff & Shin 1964; Raychaudhuri & Prinz 2008). Growth and division of peroxisomes is a well characterized multistep process including peroxisome elongation, constriction, and final fission (Koch et al. 2004; Koch et al. 2003; Koch et al. 2005; Schrader & Fahimi 2006b). For a detailed discussion see section 1.3.

However, cell lines missing Pex3p, Pex6p, or Pex19p lack any detectable peroxisomal remnants but are still able to restore *de novo* peroxisome formation upon reintroduction of the missing gene (Matsuzono et al. 1999; Muntau et al. 2000; South & Gould 1999). The restoration of peroxisomes appears to involve the ER and therefore an ER-dependent "*de novo* synthesis" model for peroxisomal biogenesis and maintenance was suggested (Kunau 2005; Tabak et al. 2006). Several independent observations point to a general role of the ER in peroxisome formation (reviewed in Nagotu et al. 2010). In mouse dendritic cells, peroxisomal proteins were partially located in specialized regions of the ER in close proximity to peroxisomes (Geuze et al. 2003; Tabak et al. 2003). Pex3p and Pex16p were shown to travel to peroxisomes via the ER in yeast and plants (1.2.2) (Karnik & Trelease 2007; Titorenko & Rachubinski 1998) and during *de novo* formation of peroxisomes Pex3p targets first to the ER, then concentrates in foci, finally buds off in a Pex19p-dependent manner and matures to functional peroxisomes in *S. cerevisiae* (Hoepfner et al. 2005; Kragt et al. 2005; Tam et al. 2005). Toro et al. (2009) have recently demonstrated that also in human fibroblasts Pex3p-dependent *de novo* formation can be initiated in the ER. Furthermore, it was shown that Pex16p can travel from the ER to peroxisomes in wild type mammalian cells (Kim et al. 2006).

In contrast, a recent study showed that newly synthesized Pex3p is targeted directly to peroxisomes (Matsuzaki & Fujiki 2008). Mammalian Pex3p mistargets to mitochondria when overexpressed in both normal and Pex19-deficient cells and has not been found in the ER compartment in a number of studies (Fang et al. 2004; Ghaedi et al. 2000; Muntau et al. 2000; Muntau et al. 2003; Sacksteder et al. 2000; Soukupova et al. 1999; South et al. 2000; Voorn-Brouwer et al. 2001). Peroxisome regeneration is independent

of COPI- and COPII-mediated vesicle budding and the ER translocation factors Sec61 and Ssh1p (South et al. 2001; South et al. 2000; Voorn-Brouwer et al.). Furthermore, most studies supporting the *de novo* synthesis model use engineered overexpressed membrane proteins, truncated or tagged versions, all of which are frequently associated with mistargeting events, generally to the ER (in yeast). Finally, growth and division has been demonstrated to be the major source for peroxisome biogenesis in yeast cells (Motley & Hettema 2007).

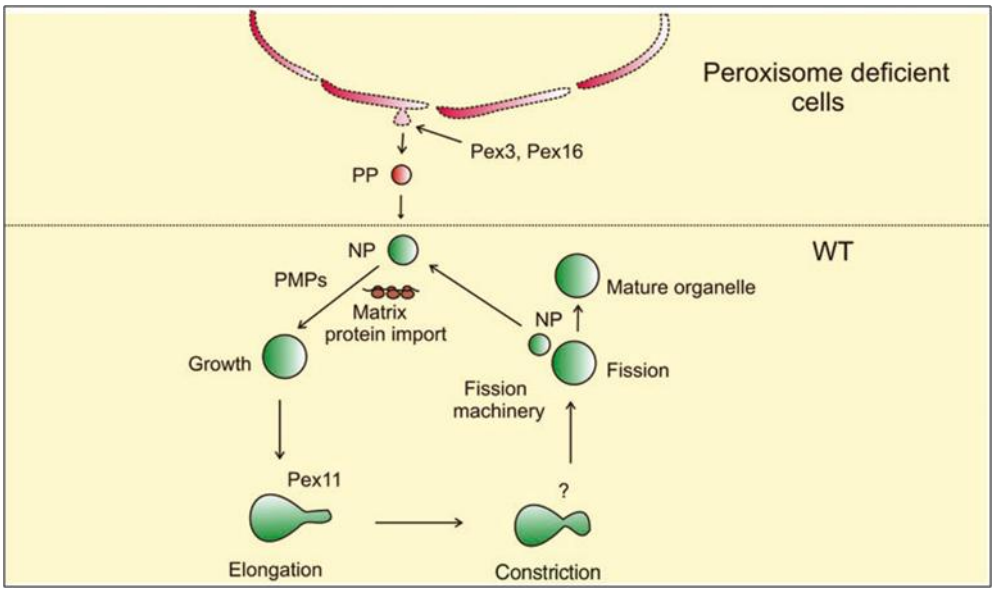

Figure 1.5: Model for peroxisome proliferation
In wild type (WT, lower panel) cells PMPs are targeted to existing (nascent, NP) peroxisomes which grow by importing newly synthesized proteins. Elongation, constriction, and fission are events of the division process (section 1.3). Pex3p, Pex16p (and Pex19p) are essential proteins for membrane formation required for *de novo* formation from the ER in cells lacking peroxisomes (due to loss of one of these proteins, upper panel). PP, pre-peroxisome. From Nagotu et al. (2010).

Altogether, it seems more likely that *de novo* formation of peroxisomes represents a backup system of the cell to cope with a situation where the organelle is lost and may reflect its evolutionary origin (Figure 1.5) (Nagotu et al. 2010). Peroxisome multiplication occurs by growth and division. *De novo* formation from the ER would begin with Pex16p, which serves as docking site for Pex3p (in a Pex3p-Pex19p-complex) and its insertion, generating a pre-peroxisome that may mature towards complete and functional entities (Matsuzaki & Fujiki 2008; South & Gould 1999; Toro et al. 2009).

1.2.4 Peroxisomal dynamics

1.2.4.1 Proliferation

Peroxisomes are dynamic organelles displaying a large plasticity. Their number and size can vary broadly and peroxisome proliferation – as well as degradation – is stimulated and regulated by a number of factors. Pharmacological studies with so-called peroxisome proliferators (e.g. hypolipidemic drugs such as clofibrate and plasticizers) led to the first observation that peroxisomes can remarkably increase in number and size, especially in the liver of rodents (Bentley et al. 1993; Fahimi et al. 1982; Hess et al. 1965; Svoboda & Azarnoff 1966). Such a peroxisome proliferation is often accompanied by an increase in the synthesis of peroxisomal enzymes, and can result in formation of hepatic tumors, mainly in rodents (Moody et al. 1991; Reddy et al. 1980; Reddy et al. 1982). Primates are so-called "low-responders" and for humans there is apparently no risk in taking hypolipidemic drugs (Peters et al. 2005; Rao & Reddy 1987). The selective induction of peroxisomal genes is mediated by peroxisome proliferator activated receptor-α (PPARα), which belongs to the family of nuclear transcription factors (Issemann & Green 1990; Pyper et al. 2010) and acts as heterodimeric partner with retinoid X receptor (RxR) by binding to the peroxisome proliferator response elements (PPREs) (Issemann et al. 1993; Tugwood et al. 1992). PPARα functions mainly as a lipid sensor in the liver responding to the influx of fatty acids and activating genes involved in β-oxidation in peroxisomes and mitochondria, as well as in the microsomal ω-oxidation system (Feige et al. 2006; Lefebvre et al. 2006). Another model system for peroxisome proliferation is the regenerating rat liver after partial hepatectomy (Yamamoto & Fahimi 1987). Proliferating peroxisomes display a marked polymorphism with various morphologies such as tail-like tubular protrusions emerging from spherical peroxisomes, elongated (tubular) peroxisomes, tubules with a constricted morphology, and interconnections between peroxisomal structures (Bernhard & Rouiller 1956; Luers et al. 1993; Schrader & Fahimi 2006b; Yamamoto & Fahimi 1987). Furthermore, peroxisomal β-oxidation and/or proliferation are stimulated by thyroid hormones, cold adaptation, unsaturated fatty acids, and acetylsalicylic acid.

In fungi and yeasts, peroxisome number and size depends mainly on the carbon source. Peroxisome proliferation can be induced when the cells are shifted to nutrients whose metabolism requires peroxisomal functions and enzymes for cellular growth, for example alkanes, oleic acid, methanol, D-amino acids, purines, and primary amines (van der

Klei & Veenhuis 2006b). In *S. cerevisiae* and *Y. lipolytica* an increase in number and size of peroxisomes is induced when fatty acids such as oleic acid are the sole carbon source (Veenhuis et al. 1987). In methylotrophic yeast species (*Candida bodinii*, *Hansenula polymorpha*, and *P. pastoris*} some of the enzymes required to utilize methanol are located in peroxisomes and those species show a prominent peroxisome proliferation. In *H. polymorpha* up to 80% of the total cytoplasmic volume may be occupied by peroxisomes when grown in methanol-containing cultures (Veenhuis et al. 2003). Similar to the mammalian system, it has been shown in *S. cerevisiae* that promoters of fatty acid inducible genes contain an oleate response element (ORE) that represents the binding target for Pip2p-Oaf1p (peroxisome induction pathway; oleate activation factor), a heterodimeric transcription factor complex (Rottensteiner et al. 2003a).

Proteins of the Pex11 family are known to be involved in regulation of peroxisome number and size (1.3.3). In mammals, there are three Pex11 isoforms (Pex11pα, β and γ), in plants five (Pex11a-e), and two Pex11-related peroxins (Pex25p and Pex27p) have been identified in *S. cerevisiae* in addition to Pex11p (Table 1.4). In general, overexpression of Pex11 proteins induces peroxisome proliferation, while a loss of function leads to fewer, enlarged peroxisomes. Furthermore, in yeasts a number of additional proteins has been identified which affect peroxisome size and number and are supposed to function in peroxisome proliferation (*Yl*Pex24p, *Yl*Pex26p, *Sc*Pex28p-*Sc*Pex32p). Pex11 proteins are discussed in detail in section 1.3.3.

1.2.4.2 Degradation

Upon withdrawal of a peroxisome proliferating stimulus, the process is reversed and excess particles are removed by autophagic processes. In yeast, the selective degradation of peroxisomes is called pexophagy (Sakai et al. 2006), and most studies originate from the methylotrophic yeasts *H. polymorpha* and *P. pastoris* (reviewed in Dunn et al. 2005; Platta & Erdmann 2007; Sakai et al. 2006). In general, autophagic processes are regulated by conserved ATG genes, supported by additional organism-specific factors which specifically regulate pexophagy (Meijer et al. 2007; Schroder et al. 2007). Around 30 proteins have been shown to be involved in these pathways (Platta & Erdmann 2007; Sakai et al. 2006). Two distinct mechanisms have been described: macropexophagy and micropexophagy. During macropexophagy organelles are sequestered into autophagosomes, which in turn fuse with lysosomes/vacuoles. This process is restricted to

mature organelles. Two peroxins, Pex3p and Pex14p, have been shown to be involved in macropexophagy in yeast (Bellu et al. 2001; Bellu et al. 2002; Zutphen et al. 2008). During micropexophagy membrane events occur on the surface of the vacuole/lysosome which then engulfs the cell components to be digested resulting in the formation of microautophagic bodies (Farre & Subramani 2004; Sakai et al. 1998; Schrader & Fahimi 2008).

Although autophagic processes in mammalian cells have been noted quite early (Leighton et al. 1975; Moody & Reddy 1976; Staubli et al. 1977) and the morphological aspects are well characterized (Yokota 2003), the molecular aspects are only poorly understood. An implication of Atg7 in peroxisome degradation has been demonstrated in studies using *ATG7*-deficient mice (Iwata et al. 2006). Pex14p might play a role in autophagic protein degradation dependent on LC3, a microtubule-bound protein (Hara-Kuge & Fujiki 2008). While 70-80% of excess peroxisomes are degraded by autophagic processes (Iwata et al. 2006), two additional pathways have been implicated in degradation of the remaining excess peroxisomes (Yokota & Fahimi 2009). 15-lipoxygenase – known to be involved in cell organelle degradation in differentiating lens fibres and maturation of reticulocytes (Bassnett & Mataic 1997; Matsui et al. 2006; Schewe et al.) – has been suggested to play a role in peroxisome degradation (Yokota et al. 2001). 15-lipoxygenase binds selectively to membranes of organelles and induces the diffusion of their content (van Leyen et al. 1998). Additionally, a peroxisome-specific isoform of Lon protease (POLP), an ATP-dependent protease with chaperone-like activity, has recently been identified in peroxisome proteomics studies (Islinger et al. 2007; Kikuchi et al. 2004). Interestingly, POLP can be induced by peroxisome proliferators, reaching its maximum level 3 days after discontinuation of the proliferator while β-oxidation enzyme levels decrease immediately (Yokota et al. 2008).

1.2.4.3 Inheritance and motility

Peroxisomes have been shown to frequently change size and shape *in vivo* and to move in a motor protein-dependent manner along cytoskeletal tracks throughout the cell (Muench & Mullen 2003; Schrader et al. 2003). Rapid and directional movement of peroxisomes in yeast and plants requires the actin cytoskeleton and type-V myosins (Hoepfner et al. 2001; Jedd & Chua 2002; Mano et al. 2002; Mathur et al. 2002). Instead, mitochondria-based movement of peroxisomes was proposed in fission yeast

(*Schizosaccharomyces pombe*) (Jourdain et al. 2008). Segregation of mother and daughter organelle after peroxisome division is likely to require directional movements. During cell division in yeast, peroxisomes have to be transported into the daughter cell (bud), initiated by binding of the myosin Myo2p to its peroxisomal receptor Inp2 (Fagarasanu et al. 2006; Saraya et al. 2010). The peroxisomal peripheral membrane protein Inp1p on the other hand is a negative regulator of peroxisome inheritance (Fagarasanu et al. 2005). Mother cells lacking Inp1p display an inability to retain a subset of peroxisomes, whereas its overexpression results in immobilized peroxisomes that fail to be partitioned to the bud. Inp1p is thought to link peroxisomes to a cortical anchor (Fagarasanu et al. 2007). A role for Pex3p as Inp1p receptor has been suggested from studies in *S. cerevisiae* (Munck et al. 2009). In *Y. lipolytica* a Pex3p paralog (Pex3Bp) may fulfil the function of Inp2p (Chang et al. 2009). Additionally, the small GTPase Rho1p is recruited to peroxisomes via interaction with Pex25p and is suggested to be involved in the reorganization of actin on peroxisomes (Marelli et al. 2004).

In mammalian cells peroxisomes have been shown to bind to and move along microtubules *in vivo* and *in vitro* (Huber et al. 1999; Kural et al. 2005; Rapp et al. 1996; Schrader et al. 1996; Schrader et al. 2000; Schrader et al. 2003; Thiemann et al. 2000; Wiemer et al. 1997). Microtubule-based peroxisome movement involves dynein, kinesin and the dynein activator complex dynactin (Kural et al. 2005; Schrader et al. 2000). *In vivo* studies revealed that 85-90% of peroxisomes exhibit a slow, energy- and microtubule-independent oscillatory movement, while the remaining 10-15% display a fast, directional movement that requires energy and is microtubule-dependent (Schrader et al. 2003). These peroxisomes move with average velocities of 0.6 µm/s (0.1-1 µm/s) and are able to translocate over long distances (up to 10 µm; Rapp et al. ; Schrader et al. 2000; Wiemer et al. 1997). Recently, it was shown in *Drosophila melanogaster* cells that peroxisome motility can also be achieved by motion of the underlying microtubule track itself (Kulic et al. 2008). The distribution (and multiplication) of peroxisomes to the daughter cells during mitosis appears to be random in mammalian cells (Wiemer et al. 1997). However, a cell-cycle dependent replication of peroxisomes has been described in plant cells (Lingard et al. 2008). Cytoskeletal tracks and motor proteins may be required to exert different tensions on the organelle membrane thus assisting in organelle fission. However, microtubules appear not to be essential for the formation and maintenance of peroxisomes (Schrader et al. 1996; Schrader et al. 2000; Schrader et al. 1998a). Tubular peroxisomes can be generated in the complete absence of microtubules and

surprisingly, peroxisome elongation is even promoted by microtubule-depolymerising agents (Schrader et al. 1996; Schrader et al. 1998a). Although segmentation and division of elongated peroxisomes (see section 1.3) can proceed in the absence of microtubules, the proper intracellular distribution after division is disturbed. Furthermore, microtubules are required for rapid and directed peroxisome motility, for positioning of peroxisomes and for maintenance of their uniform distribution within the cell (Schrader et al. 2003). Although microtubules are not required for the import of peroxisomal proteins (Brocard et al. 2005), they have been suggested to facilitate the regulated import of matrix proteins (Chuong et al. 2005). Furthermore, a requirement for microtubules and dynein motors in the early stages of peroxisome biogenesis has been demonstrated (Brocard et al. 2005). Peroxisome *de novo* formation upon Pex16p-reintruduction into *PEX16*-mutant cells failed in the absence of microtubules or after inhibition of the dynein/dynactin motor complex. In addition, binding to microtubules and trafficking along them has been linked to peroxisome proliferation and division (Nguyen et al. 2006). In (most) PBD- and PED-patient cells peroxisomes are enlarged and significantly less abundant and exhibit clustering and loss of alignment along microtubules. Expression of Pex11pβ to induce peroxisome proliferation re-established the alignment of peroxisomes along microtubules (Nguyen et al. 2006). Thus, peroxisome proliferation might trigger the binding and transport of newly formed peroxisomes along microtubules. A loss of trafficking and disturbed cytoplasmic distribution of peroxisomes might lead to a regional loss of essential peroxisomal activities and thus, to cell damage and degeneration (Schrader & Fahimi 2006b). Interestingly, overexpression of the microtubule-associated tau protein, which inhibits kinesin-dependent transport of peroxisomes (and other organelles) into neurites, rendered neurons vulnerable to oxidative insults and led to their degeneration (Stamer et al. 2002).

1.3 The division machinery

In recent years, the peroxisomal growth and division process (1.2.3) was characterized as a multistep pathway. First, elongated (tubular) peroxisomes are formed, which become constricted leading to a "beads-on-a-string"-like morphology (Schrader et al. 1996). At this step certain peroxisomal proteins (e.g. Pex11pβ and matrix proteins) are segregated from each other. Finally, fission of the constricted tubules occurs to form new spherical peroxisomes (Figure 1.6).

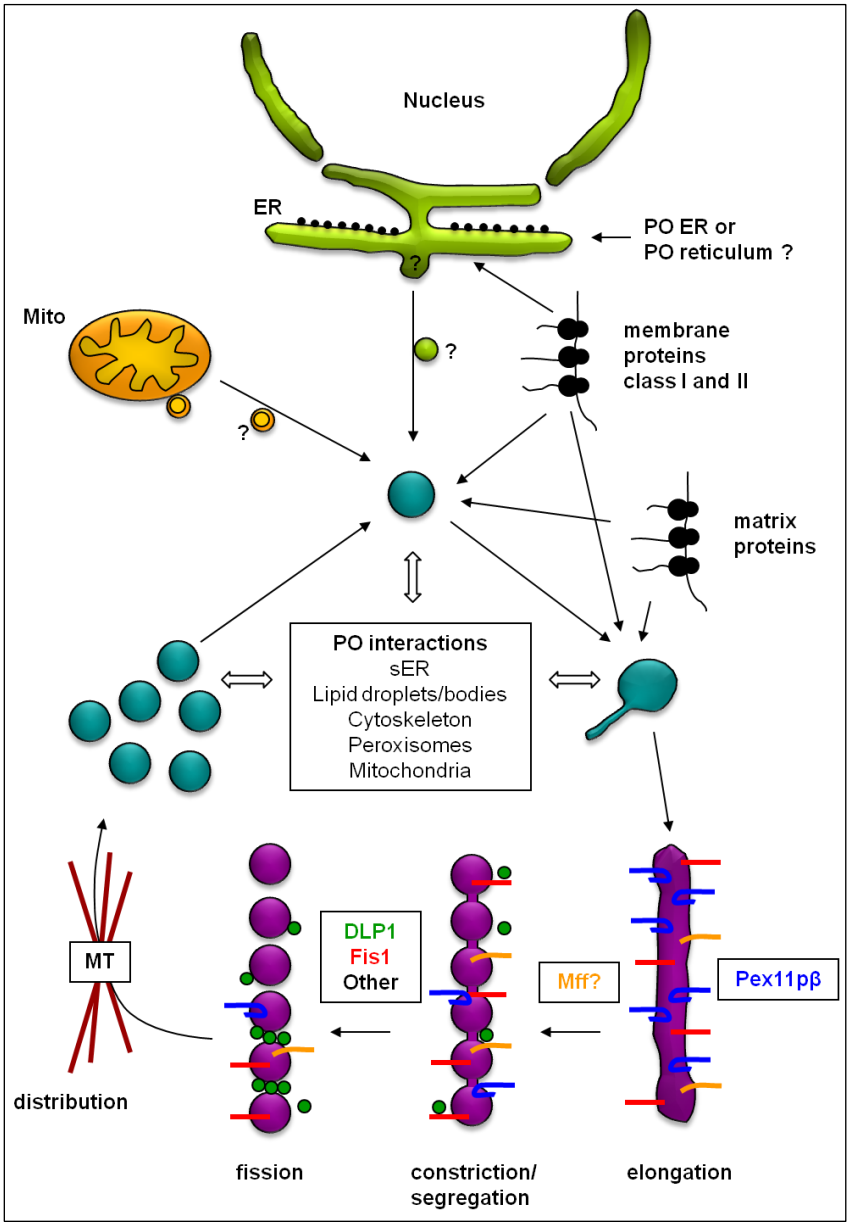

Figure 1.6: Peroxisome biogenesis model
Peroxisomal membrane proteins (PMPs) are directly imported into pre-existing organelles or routed via the ER, presumably by vesicular transport. Also mitochondria-derived vesicles (MDVs) might be targeted to peroxisomes. A well defined sequence of morphological changes of peroxisomes contributes to peroxisome proliferation: elongation (growth), constriction, and final fission (division). Pex11pβ induces peroxisome elongation, whereas DLP1 and Fis1 mediate peroxisome fission. The exact function of Mff is unknown. Microtubules (MT) and motor proteins are required for proper intracellular distribution. Adapted from Camoes et al. (2009).

Each step is thought to require its own set of molecular components. Several proteins involved in this process have been identified in mammals, plants and yeast/fungi. Pex11 proteins, in mammals Pex11pβ, are required for peroxisome elongation and prolifera-

tion (section 1.3.3). The mechanisms leading to protein segregation in elongated peroxisomes and to tubule constriction are unknown. Interestingly, molecular components of the division machinery are shared by peroxisomes and mitochondria (Table 1.5). Dynamin-like proteins are required for organelle fission (section 1.3.1), and are recruited to the membranes by Fis1 (section 1.3.2).

Plants		Yeast		Mammals			
PO	Mito	PO	Mito	PO	Mito	Family	Function
Fis1a, b	Fis1a, b	Fis1	Fis1	hFis1	hFis1	TA protein TPR motif	Membrane adapter
		-	-	Mff	Mff	TA protein	Membrane adapter?
?	ELM[1]	Mdv1 Caf4[2]	Mdv1 Caf4[2]	?	?	WD protein other	Cytosolic linker
DRP3A, B DRP5B[3]	DRP3A, B DRP1C, E	Dnm1 Vps1[4]	Dnm1	DLP1	DLP1	Large GTPase	Final scission
Pex11 (a-e)		Pex11 (Pex25, Pex27)	Mmm1, 2 Mdm (10, 12, 31-33)	Pex11 (α, β, γ)			Membrane tubulation

Table 1.5: Shared components of the peroxisomal and mitochondrial division machineries
[1]Identified in *A. thaliana* (Arimura et al. 2008). [2]Only present in *S. cerevisiae* and *C. glabrata*. [3]Involved also in the division of chloroplasts (Zhang & Hu 2010). [4]Required in *S. cerevisiae* but not in *H. polymorpha*. Mito, mitochondria; PO, peroxisomes. Adapted from Delille et al. (2009).

1.3.1 Peroxisomal fission by dynamin-like proteins

Dynamin-like proteins (DLP or Drp, dynamin-related proteins) were the first components to be identified as key players in peroxisome fission (Koch et al. 2003; Li & Gould 2003). DLPs belong to the dynamin family of large GTPases known to function in tubulation and fission events of cellular membranes. These cytosolic proteins are recruited to organelle membranes and assemble, probably as rings or spirals, in multimeric complexes around constricted parts of the organelle, where they induce GTP-dependent final membrane scission. Thus, dynamin proteins are supposed to act as pinchase-like mechanoenzymes. Classical dynamins have a size of approximately 100 kDa and possess five domains: GTPase domain, middle domain, Pleckstrin homology domain (PH), GTPase effector domain (GED), and proline-rich domain (PRD). DLPs lack the SH3-binding PRD domain and the PH domain required for membrane association (Hinshaw 2000; Praefcke & McMahon 2004; Roux et al. 2010; Roux et al. 2006; Sweitzer & Hinshaw 1998; Yoon & McNiven 2001).

DLP1 was discovered to be involved in peroxisomal and mitochondrial fission. It is not equally distributed along the organelle membranes but concentrated in focal spots at

constriction sites and tips (Bleazard et al. 1999; Koch et al. 2003; Smirnova et al. 2001). A loss of DLP1 function results in formation of highly elongated peroxisomes (and mitochondria) (Koch et al. 2003). These elongated peroxisomes still have a constricted morphology, indicating that DLP1 is required for final scission, but not for organelle constriction (Koch et al. 2004). Similar morphologies were observed in fibroblasts from a patient, leading to discovery of a new lethal disorder based on a mutation in *DLP1* (Waterham et al. 2007). Overexpression of DLP1 does not induce organelle fragmentation, demonstrating that the division is regulated by other factors.

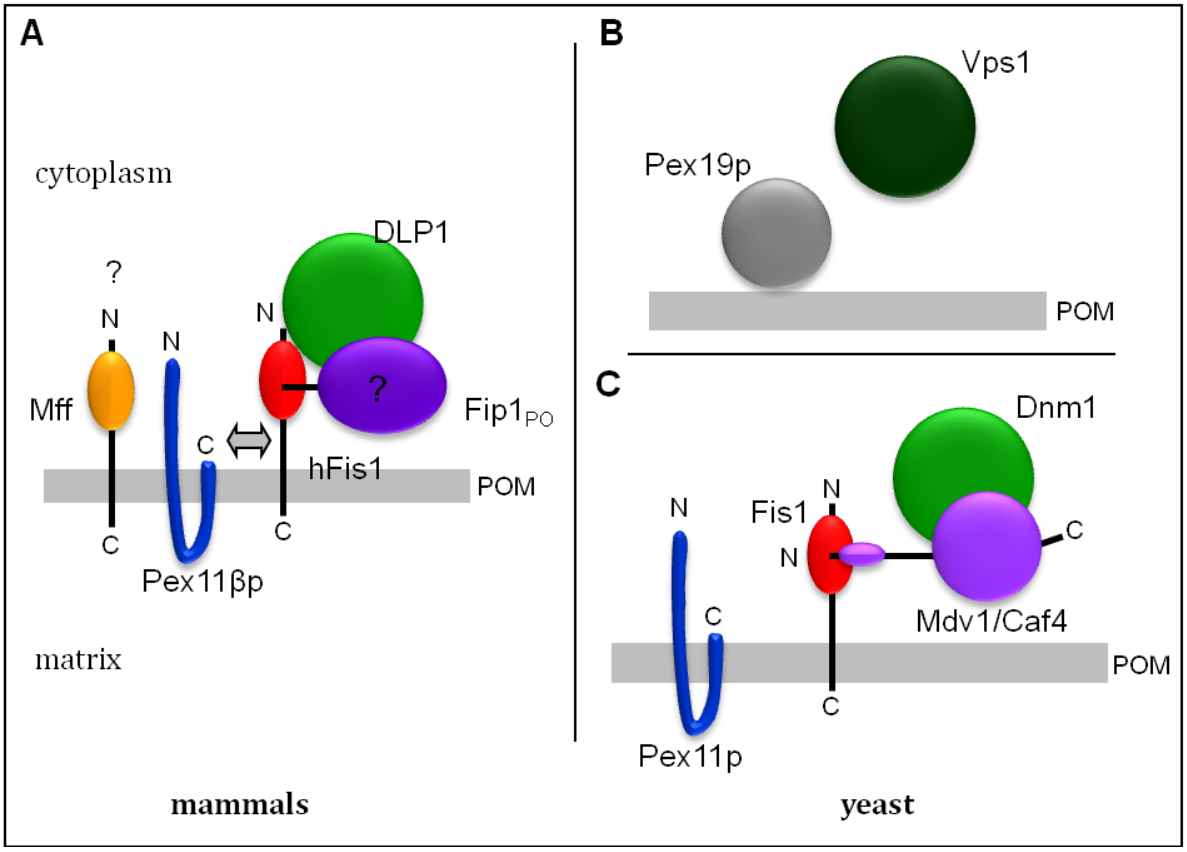

Figure 1.7: The peroxisomal division machineries in mammals and yeast
(A) Peroxisomal fission in mammals is dependent upon DLP1 and hFis1. Mff was likewise shown to be involved. hFis1 is supposed to interact with the elongation factor Pex11pβ. The involvement of peroxisome-specific hFis1-interacting proteins (Fip1$_{PO}$) is likely, but has so far not been verified. **(B-C)** Peroxisomes in yeast can be divided by two independent machineries: By Vps1, which might be recruited by Pex19p (B), or by Dnm1, which is recruited by Fis1 and requires the soluble adapter proteins Mdv1 and Caf4 (C). POM, peroxisomal membrane. Adapted from Camoes et al. (2009).

Similar, homologues of mammalian DLP1 are required for peroxisome fission in other species, such as Dnm1 in yeasts (Table 1.5). Interestingly, if *S. cerevisiae* is grown on glucose, peroxisome division depends on the dynamin-related GTPase Vps1 (vacuolar protein sorting-associated protein 1), which might be recruited to the organelles by Pex19p (Figure 1.7 B). Under growth conditions that induce peroxisome proliferation (1.2.4.1),

peroxisomes appear to be divided by the same machinery as mitochondria including Dnm1 (Figure 1.7 C) (Hoepfner et al. 2001; Jourdain et al. 2008; Kuravi et al. 2006; Motley & Hettema 2007; Nagotu et al. 2008b). *De novo* formation of peroxisomes appears to be Dnm1-independent (Nagotu et al. 2008b). In plants (*A. thaliana*), DRP3A and B have been implicated in peroxisomal and mitochondrial division (Table 1.5) (Fujimoto et al. 2009; Lingard et al. 2008; Mano et al. 2004), while DRP5B appears to be shared by peroxisomes and chloroplasts (Zhang & Hu 2010).

As DLP1 lacks a PH domain it requires a membrane adapter for membrane association. DLP1 was shown to be recruited to peroxisomes and mitochondria by hFis1, a tail-anchored membrane protein (section 1.3.2). In yeast, additional cytosolic adapter proteins have been identified: Mdv1 and Caf4 (Motley et al. 2008; Nagotu et al. 2008a). These WD proteins are supposed to mediate the interaction of Dnm1 and Fis1 (Figure 1.7 C). There are no obvious homologues of Mdv1/Caf4 in higher eukaryotes (Table 1.5), although mitochondria- or peroxisome-specific Fis1-interacting proteins could be part of the scission complexes (Figure 1.7 A) (Camoes et al. 2009).

1.3.2 Fis1 – an adapter protein

The mammalian hFis1 (fission) protein was the second component discovered to be involved in both, peroxisomal and mitochondrial fission, as well as its yeast (Fis1p) and plant homologues (Fis1a, b) (Koch et al. 2005; Kuravi et al. 2006; Lingard et al. 2008; Motley et al. 2008; Zhang & Hu 2008). Fis1 belongs to the class of tail-anchored (TA) proteins, which possess a N-terminal cytosolic domain and a hydrophobic segment close to the C-terminus which serves as membrane anchor. The short C-terminus (in the case of hFis1 consisting of five amino acids) protrudes into the organelle lumen (Mozdy et al. 2000; Yoon et al. 2003). Fis1 has a molecular size of 17 kDa and the cytosolic domain consists of a TPR-like fold formed by six α-helices (Figure 1.8) (Dohm et al. 2004; Suzuki et al. 2003; Suzuki et al. 2005). TPR motifs typically mediate protein-protein interactions. The helix bundle of hFis1 creates a concave face containing hydrophobic amino acids, which is likely to serve as binding region. It was shown that DLP1 interacts with the TPR motif, whereas the most N-terminal α1-helix is supposed to have a regulatory function (Suzuki et al. 2005; Yu et al. 2005). Deletion of this helix leads to increased hFis1-oligomerization, indicating that the α1-helix functions as a negative regulator of the hFis1 self-interaction (Serasinghe & Yoon 2008) and Dnm1 binding (Wells et al.

2007). The N-terminus of *S. cerevisiae* Fis1p is longer and might function as interaction or recruitment site for Mdv1/Caf4 (Suzuki et al. 2005). Also blocking the N-terminus by addition of a GFP-Tag or by microinjection of an antibody directed to the N-terminus interferes with proper hFis1 function, probably due to sterical hindrance of protein-protein interactions (Koch et al. 2003; Yoon et al. 2003).

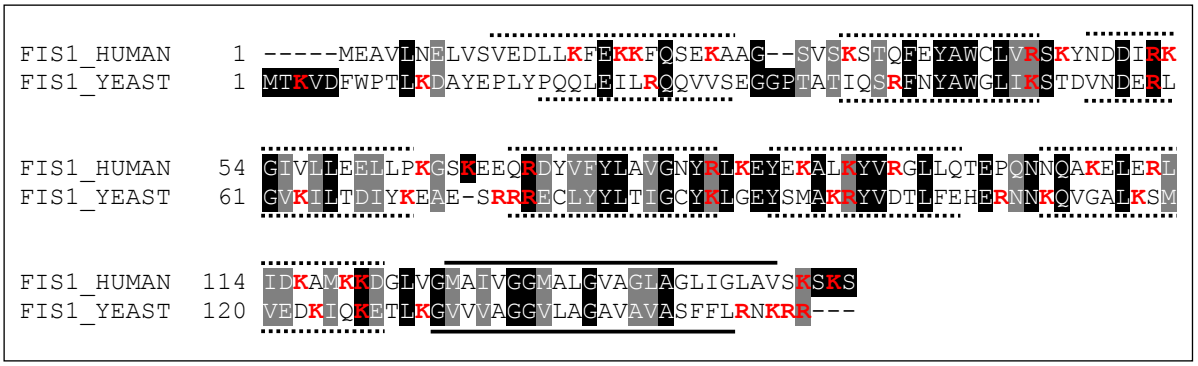

Figure 1.8: Amino acid sequence of Fis1 from *H. sapiens* (human) and *S. cerevisiae* (yeast)
Basic amino acids are printed red, identical residues are shaded black and similar residues are shaded grey. Alignment was performed using ClustalW (www.ch.embnet.org/software/ClustalW.html) and Boxshade 3.21 (www.ch.embnet.org/software/BOX_form.html) software. Putative transmembrane domains are under-/overlined and location of six α-helices is indicated by dotted bars (Suzuki et al. 2005).

hFis1 is equally distributed along the membranes of peroxisomes and mitochondria. The association of hFis1 (and DLP1) with peroxisomes from rat liver is increased after induction of peroxisome proliferation by bezafibrate (Koch et al. 2005). Increasing the amount of hFis1 by overexpression promotes peroxisome and mitochondria division, whereas inhibition of hFis1 function results in elongation of both organelles (Koch et al. 2005; Yoon et al. 2003). The division depends on functional DLP1, demonstrating that hFis1 itself does not perform organelle fission. Furthermore, hFis1 is not required for organelle constriction, as tubular peroxisomes induced by hFis1 inhibition have a constricted morphology. Therefore, hFis1 is supposed to serve as adapter (and regulatory?) protein recruiting DLP1 to the membrane. Additional proteins, such as Mdv1/Caf4 in yeast, might be involved and could also provide an organelle-specific regulation. Furthermore, an interaction of hFis1 with Pex11pβ has been shown (Kobayashi et al. 2007). The targeting of hFis1 to peroxisomes and mitochondria requires an intact C-terminus. Addition of a C-terminal GFP- or Myc-tag interferes with its targeting, as well as removal of the five amino acids located at its extreme C-terminus. It was shown that the 26 C-terminal amino acids, comprising those five residues together with the transmembrane domain (TMD), are necessary and sufficient for peroxisomal and mitochondrial targeting

(Koch et al. 2005; Yoon et al. 2003). Two lysine residues are found at position 149 and 151 in the luminal domain (Figure 1.8 and Figure 3.2) and it was demonstrated that mutation of these two amino acids disturbs the mitochondrial targeting of hFis1 (Stojanovski et al. 2004). These findings are in agreement with the general model for TA protein targeting, which differs from regular protein import. All TA proteins have to be inserted into their target membranes post-translational – even into the ER membrane – as protein translation is completed before the hydrophobic, putative SRP-interacting (signal-recognition particle) region is accessible outside of the ribosome (Borgese et al. 2003). Mitochondrial import of TA proteins has been shown to be independent of the regular import machinery and cytosolic factors (Kemper et al. 2008; Setoguchi et al. 2006). Therefore, an unassisted insertion of TA proteins into their target membranes is discussed (Borgese et al. 2007; Rabu et al. 2009). TA proteins were thought to be targeted to peroxisomes via the ER or ER-subdomains (Elgersma et al. 1997), but Pex26p/Pex15p were shown to be targeted to peroxisomes in a Pex19p-dependet manner (Halbach et al. 2006). The targeting signals of TA proteins are generally located in the C-terminus including the TMD. Length and hydrophobicity of the TMD together with the charge of the surrounding amino acids seem to be important (Borgese et al. 2003; High & Abell 2004; Wattenberg & Lithgow 2001). The assumed targeting from the ER towards peroxisomes is supposed to be regulated by positively charged amino acids in the luminal domain. The mitochondrial targeting signal consists of a rather short TMD (< 20 amino acids) and a neighbouring basic region (Beilharz et al. 2003; Borgese et al. 2003; Hwang et al. 2004; Rapaport 2003). It is not known, how hFis1 is targeted to peroxisomes and if the same signals and/or sequences as utilized for mitochondrial targeting (K149 and K151) are required. Furthermore, it is not known how the dual targeting of hFis1 to both organelles is achieved. hFis1 is involved in organelle division, and therefore also in induction of apoptosis (Yu et al. 2005), and a stringent regulation of its targeting and/or function is necessary.

Recently, another tail-anchored protein targeted to peroxisomes and mitochondria was discovered. Mff (mitochondrial fission factor) has been proposed to function as a novel adapter protein in a complex different from hFis1 (Gandre-Babbe & van der Bliek 2008). The loss of Mff function results in the elongation of both organelles and it is possible that Mff is involved in the assembly of the constriction machinery. Interestingly, Mff seems to be restricted to metazoans (Table 1.5).

1.3.3 Pex11 proteins in peroxisome proliferation

Proteins of the Pex11 family regulate peroxisome proliferation, i.e. they are able to increase peroxisome number and size. It is the only component of the growth and division machinery identified so far being unique for peroxisomes. *Sc*Pex11p was the first protein discovered being involved in peroxisome proliferation or division (Erdmann & Blobel 1995; Marshall et al. 1995). Meanwhile, a large number of Pex11 proteins, or proteins affecting peroxisome number, have been identified (PPPs, Pex11-type peroxisome proliferators; reviewed in Thoms & Erdmann 2005). Every organism studied so far contains several Pex11 orthologs. The three mammalian Pex11 proteins are encoded by different genes and termed Pex11pα, Pex11pβ, and Pex11pγ. Plants (*A. thaliana*) possess five different Pex11 isoforms, *At*Pex11a to *At*Pex11e (Lingard & Trelease 2006; Orth et al. 2007), while yeast and trypanosomes contain both three Pex11 proteins (Pex11p, Pex25p, and Pex27p, or *Tb*Pex11, GIM5A, and GIM5B, respectively). Pex11 proteins have a molecular weight of 27-32 kDa and a length of roughly 230 to 260 amino acids. Pex25p and Pex27p from *S. cerevisiae* show only weak homology to *Sc*Pex11p (Figure 1.9) (Rottensteiner et al. 2003b). They contain an extended N-terminus and are much larger (~45 kDa). Additionally, *Yl*Pex24p and the related *Sc*Pex28p and *Sc*Pex29p, as well as *Yl*Pex23 and the related *Sc*Pex30p, *Sc*Pex31p, and *Sc*Pex32p are supposed to affect peroxisome numbers (Table 1.4) (Brown et al. 2000; Tam & Rachubinski 2002; Vizeacoumar et al. 2004; Vizeacoumar et al. 2003). *Sc*Pex11p was shown to have a significant amino acid sequence similarity with the ligand-binding domain of nuclear receptors, in particular PPARs (Barnett et al. 2000), and a function for Pex11p in lipid binding is discussed. Different functions have been attributed to Pex11 proteins, such as playing a role in β-oxidation in *S. cerevisiae* (van Roermund et al. 2000), organelle inheritance (Krikken et al. 2009), determination of the membrane structure (Voncken et al. 2003), or direct regulation of peroxisome size and number. Overexpression of Pex11p in *Penicicilium chrysogenum* increases penicillin production (Kiel et al. 2005). Common among all Pex11 proteins is the observation that modulations of their protein levels affect the number of peroxisomes (Erdmann & Blobel 1995; Lingard & Trelease 2006; Lorenz et al. 1998; Marshall et al. 1995; Schrader et al. 1998b). In general, an increase of Pex11 levels induces peroxisome proliferation, while inhibition of its function reduces the peroxisome number or impairs peroxisome proliferation.

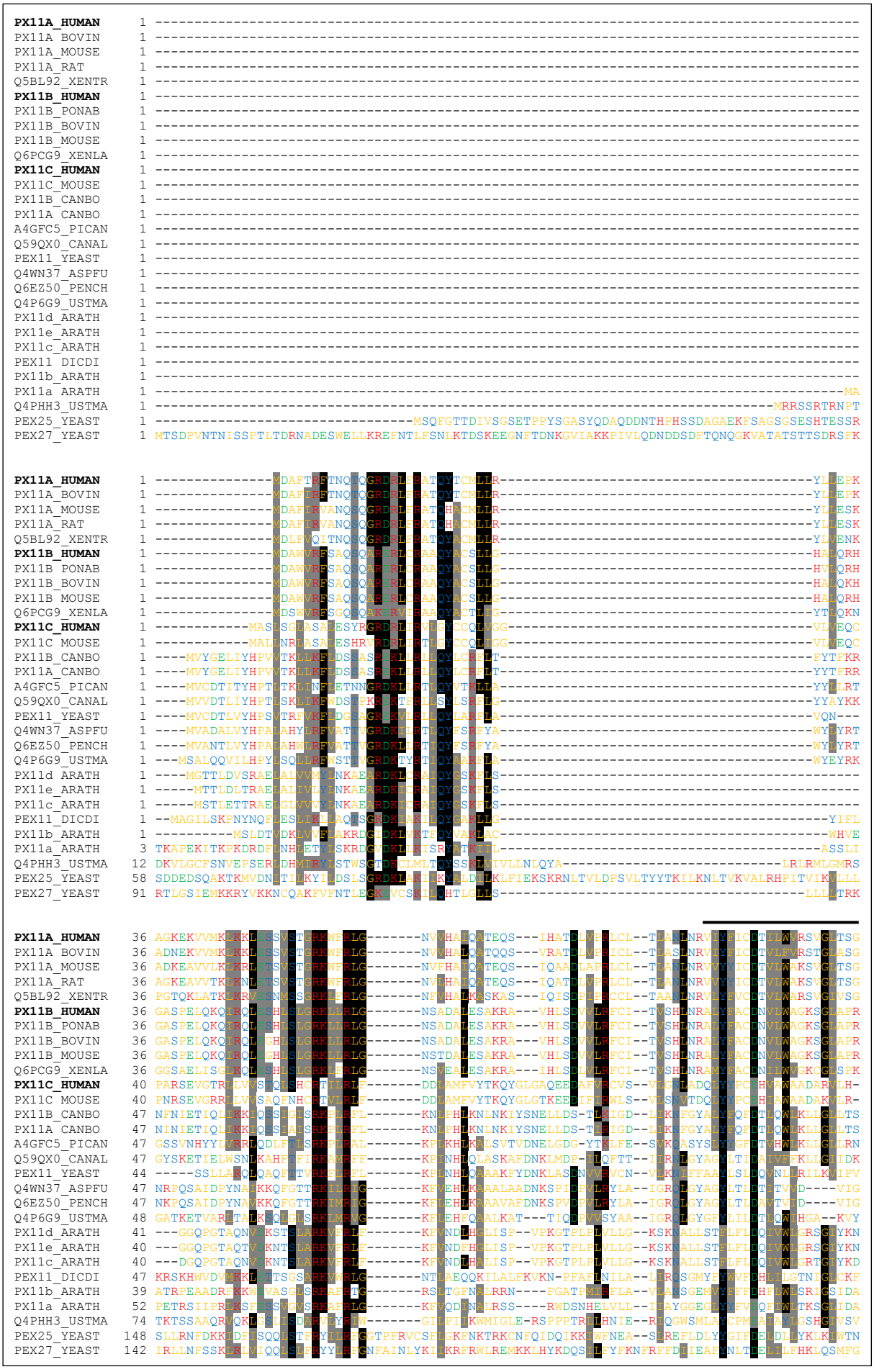
PX11A_HUMAN
PX11A_BOVIN
PX11A_MOUSE
PX11A_RAT
Q5BL92_XENTR
PX11B_HUMAN
PX11B_PONAB
PX11B_BOVIN
PX11B_MOUSE
Q6PCG9_XENLA
PX11C_HUMAN
PX11C_MOUSE
PX11B_CANBO
PX11A_CANBO
A4GFC5_PICAN
Q59QX0_CANAL
PEX11_YEAST
Q4WN37_ASPFU
Q6EZ50_PENCH
Q4P6G9_USTMA
PX11d_ARATH
PX11e_ARATH
PX11c_ARATH
PEX11_DICDI
PX11b_ARATH
PX11a_ARATH
Q4PHH3_USTMA
PEX25_YEAST
PEX27_YEAST

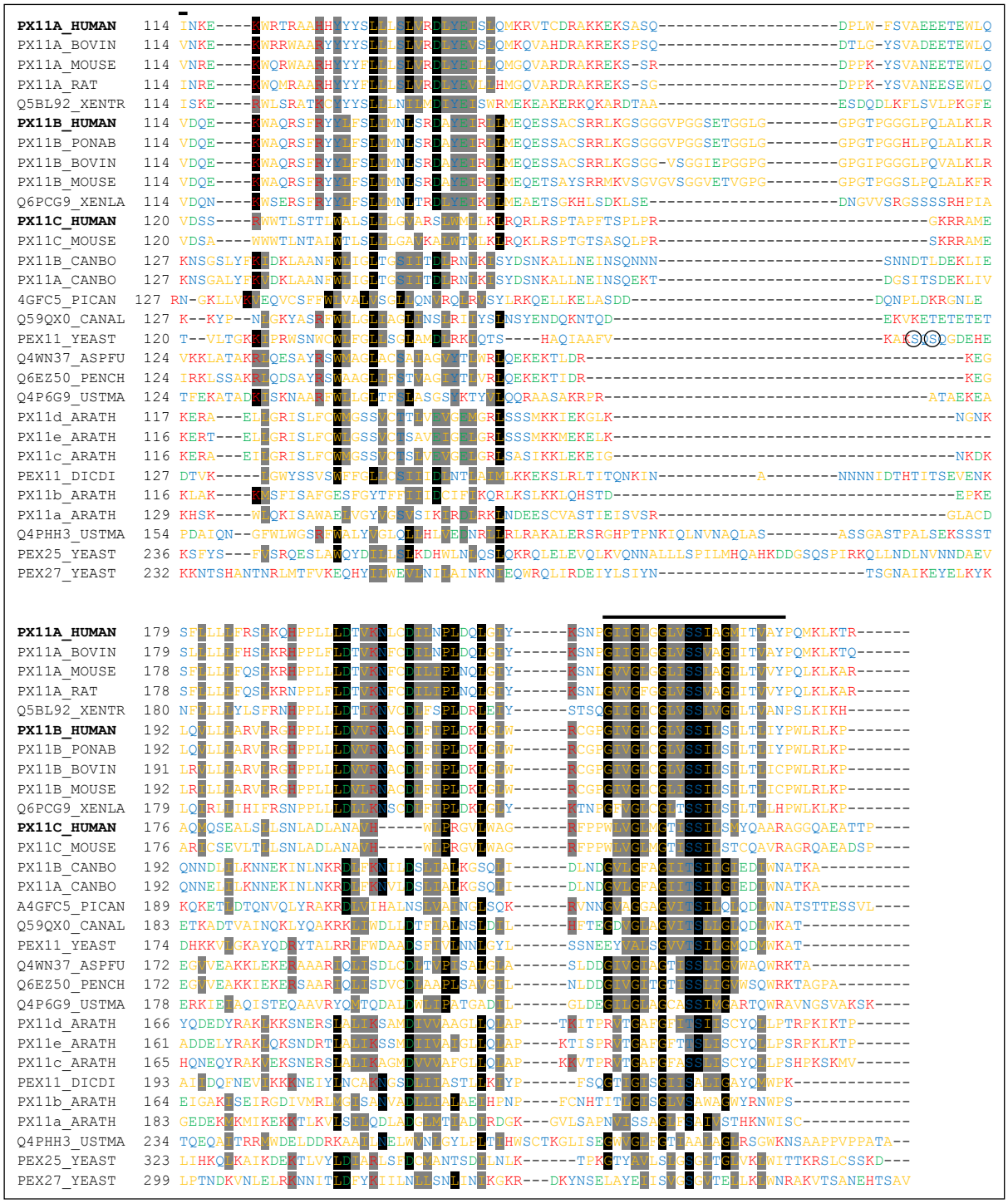

Figure 1.9: Comparison of Pex11 sequences
Alignment was performed using ClustalW (www.ch.embnet.org/software/ClustalW.html) and Boxshade 3.21 (www.ch.embnet.org/software/BOX_form.html) software. Sequences are ordered according to the alignment. Species: arath, *Arabidopsis thaliana*; aspfu, *Aspergillus fumigates*; bovin, *Bos taurus*; canal, *Candida albicans*; canbo, *Candida boidinii*; dicdi, *Dictyostelium discoideum*; human, *Homo sapiens*; mouse, *Mus musculus*; pench, *Penicillium chrysogenum*; pican, *Pichia angusta*; ponab, *Pongo abelii*; rat, *Rattus norvegicus*; ustma, *Ustilago maydis*; xenla, *Xenopus laevis*; xentr, *Xenopus tropicalis*; yeast, *S. cerevisiae*. Amino acids are colored according to their charge: blue, neutral polar; green, negative; red, positive; yellow, neutral nonpolar. Putative transmembrane domains (human Pex11pα) are overlined. Putative phosphorylated residues (yeast) are encircled. Identical residues are shaded black and similar residues are shaded grey.

The extent of these effects differs between the isoforms. For example, *Sc*Pex11p has the most dominant effect compared to *Sc*Pex25p and *Sc*Pex27p (Rottensteiner et al. 2003b).

In mammals, Pex11pβ induces the most prominent peroxisome proliferation. First, peroxisomes become elongated and after 24 to 48 hours the tubules are divided into numerous small peroxisomes (Schrader et al. 1998b). Before, Pex11pβ appears to be concentrated in focal spots along the tubule, segregating at least from peroxisomal matrix proteins. It was shown that Pex11pβ-induced peroxisome proliferation occurs independently of peroxisome metabolism (Li & Gould 2002). Pex11pα has been reported to induce peroxisome division, while Pex11pγ has been hardly studied (Li et al. 2002a; Passreiter et al. 1998; Tanaka et al. 2003).

Mammalian Pex11 proteins are predicted to possess two transmembrane domains (Figure 1.9), one located roughly in the middle of the protein and the other close to the C-terminus (Schrader et al. 1998b). The middle TMD of Pex11pβ has the lowest hydrophobicity score. While three to four transmembrane domains are predicted for the *At*-Pex11 proteins (Lingard & Trelease 2006), *Sc*Pex11p, Pex25p and Pex27p appear to be peripheral membrane proteins (Marshall et al. 1995; Rottensteiner et al. 2003b; Smith et al. 2002; Tam et al. 2003). The N- and C-termini of all Pex11 isoforms are exposed to the cytosol, except for the C-terminus of *At*Pex11a (Abe et al. 1998; Li et al. 2002a; Lingard & Trelease 2006; Lorenz et al. 1998; Passreiter et al. 1998; Schrader et al. 1998b; Tanaka et al. 2003). All Pex11 proteins interact with themselves and are likely to form homo-oligomers or homo-dimers (Li & Gould 2003; Lingard et al. 2008; Lorenz et al. 1998; Marshall et al. 1996; Marshall et al. 1995; Rottensteiner et al. 2003b; Tam et al. 2003). The N-terminal domain of Pex11pβ was shown to be required for the homo-oligomerization and to be indispensable for its peroxisome-proliferating activity (Kobayashi et al. 2007). Furthermore, *At*Pex11 proteins were shown to hetero-oligomerize with each other (Lingard et al. 2008), as were Pex25p and Pex27p (Rottensteiner et al. 2003b; Tam et al. 2003).

Pex11pα as well as *At*Pex11c-e and trypanosome *Tb*Pex11 contain a C-terminal dilysine motif (KxKxx) and Pex11pα from rat has been shown to bind coatamer *in vitro*. Consequently, a role for Pex11pα in ARF- and coatamer-dependent vesiculation or budding of peroxisomes has been proposed (Lay et al. 2005; Passreiter et al. 1998). However, mutation of the C-terminus did not affect Pex11 function (Maier et al. 2000) and the dilysine motif is not conserved in other Pex11 homologues such as *Hs*Pex11pβ, *Hs*Pex11pγ or *Sc*Pex11p (Figure 1.9).

From the mammalian isoforms only Pex11pα is induced by peroxisome-proliferating agents (1.2.4.1) (Abe & Fujiki 1998; Abe et al. 1998; Li et al. 2002a; Schrader et al.

1998b; Tanaka et al. 2003). Its expression varies between different tissues, with liver, testis and kidney displaying the highest levels (Li et al. 2002a; Schrader et al. 1998b). Pex11pβ levels are equal in all tissues, but generally higher than those of Pex11pα (Schrader et al. 1998b), while Pex11pγ expression is again tissue-specific with high levels in liver and levels below the detection limit in some other tissues or cells (Li et al. 2002a). It is tempting to speculate that Pex11pα is responsible for peroxisome proliferation in response to external stimuli, whereas Pex11pβ is required for constitutive peroxisome biogenesis. However, Pex11pα is dispensable for PPARα-mediated peroxisome proliferation and only required for PPAR-independent peroxisome proliferators, which was shown in *PEX11α*$^{-/-}$ mice (Li et al. 2002a). The *PEX11α*$^{-/-}$ mouse is viable with no obvious effect on peroxisome number or metabolism, and morphologically indistinguishable from wild type mice. In contrast, knockout of *PEX11β* causes neonatal lethality with a number of defects reminiscent of Zellweger syndrome, such as neurological pathologic features (Li et al. 2002b). However, these mice are only mildly affected in peroxisome protein import and metabolism. These observations demonstrate that the pathological features of ZS are rather caused by a disturbed peroxisomal biogenesis and subtle effects on signalling pathways during development, e.g. involving peroxisomal products, than by gross metabolic disturbances. Double knockout mice of *PEX11α* and *PEX11β* do not have greater defects than mice only lacking *PEX11β*, and Pex11pγ levels are not increased (Li et al. 2002a).

Up to now it remained unclear if and how Pex11 activities could be modulated by rapid signalling or if post-translational modifications of Pex11 proteins occur. Very recently, Knoblach et al. (2010) demonstrated that *Sc*Pex11p is reversible phosphorylated at residues S165 and/or S167 in response to nutritional changes. Studies based on phosphomimicking mutants revealed that expression of the phosphorylated form of *Sc*Pex11p induced peroxisomal phenotypes resembling those of *Sc*Pex11p overexpression (peroxisome hyperproliferation). On the other hand, phenotypes induced by the dephosphorylated form of *Sc*Pex11p resembled somehow *PEX11* gene knockouts (clustered peroxisomes). Furthermore, overexpression of cyclin-dependent kinase Phos85p resulted in hyperphosphorylation of *Sc*Pex11p and peroxisome proliferation, indicating that phosphorylation can activate *Sc*Pex11p to regulate peroxisome dynamics.

Nevertheless, it is unclear how the effects on peroxisome size and number mediated by PPPs are exerted. The rapid tubulation of the peroxisomal membrane induced by Pex11pβ overexpression may be indicative for a change in membrane lipid composition

or a modification of peroxisome lipids, which could affect membrane curvature. Studies in *H. polymorpha* point to a significant role in peroxisome elongation before fission, as *Hp*Pex11p localizes at the site of peroxisome elongation in *dnm1* cells incapable of organelle division (Nagotu et al. 2008b). Thus, PPPs could be structural components of the peroxisomal membrane and/or recruit other proteins to the membrane. In line with this, *At*Pex11 proteins were shown to bind Fis1b (Lingard et al. 2008). The data regarding a direct binding of Pex11pβ to hFis1 are inconsistent. While our laboratory did not detect a direct hFis1-Pex11pβ interaction (Koch et al. 2005), Kobayashi et al. (2007) showed that hFis1 interacts with Pex11pβ, which involved the C-terminal region of Pex11pβ. Furthermore, Pex11pβ, hFis1, and DLP1 appeared to be form a ternary complex. Moreover, *Sc*Pex25p turned out to be a receptor for the GTPase Rho1p involved in actin reorganization (Marelli et al. 2004). Fact is that overexpression of other peroxisomal membrane proteins does not induce peroxisome proliferation and Pex11pβ-induced membrane elongation is followed by assembly of the hFis1-DLP1 fission complex at the site of fission. Furthermore, the exact functions of the different Pex11 isoforms in each species are hardly known. Are the proteins redundant in function? Or are they required under specialized proliferation conditions? A comprehensive study comparing the different mammalian Pex11 isoforms is missing so far.

1.4 Objectives

Peroxisomes are multifunctional organelles involved in various metabolic processes. Peroxisomal malfunctions lead to numerous mostly severe disorders, rendering peroxisomes essential for human health and development. Peroxisomes have the remarkable capacity to proliferate in response to nutritional or environmental stimuli, and peroxisomal abundance can be adjusted to the cellular needs. However, the molecular components/machineries involved in the formation, growth, division and dynamics of peroxisomes are far from being understood. In previous studies from our laboratory and other groups Pex11pβ, DPL1 and hFis1 were identified as the first molecular components involved in proliferation and division of peroxisomes in mammals. Surprisingly, DLP1 and hFis1 were shown to be involved in both mitochondrial and peroxisomal division. Furthermore, evidence was presented that peroxisomal growth and division is a multistep process involving peroxisome elongation, constriction and final fission.

Aim of this study is to further reveal the molecular mechanisms of peroxisomal proliferation and division. One focus is set on the regulation/recruitment of the peroxisomal division machinery, in particular on the dual targeting of hFis1 to peroxisomes and mitochondria. Furthermore, three Pex11 isoforms have been identified in mammals but their exact functions are so far unknown. It is assumed that the proteins are key components of the regulation of peroxisome abundance in mammals. Thus, this study intends to characterize this class of proteins and their functions in more detail. These experiments will also provide insights into the early events of peroxisomal growth and division. Finally, this work intends to enlighten some regulatory aspects of peroxisome proliferation. The results are thought to help in clarification of the following basic cell biological questions:

1) How does the targeting of (peroxisomal) hFis1 occur? What are the targeting signals and import factors of this tail-anchored protein? How is the dual targeting to peroxisomes and mitochondria regulated?
2) What are the respective functions of the three mammalian Pex11p isoforms? How redundant or specialized function these proteins? What are special characteristics of the different Pex11 proteins?
3) Is it possible to unravel the early steps of peroxisomal growth and division, e.g. by manipulation of Pex11pβ? How does Pex11pβ-mediated peroxisome proliferation occur?

4) Which signals mediate morphological changes and proliferation of peroxisomes? Is the cytoskeleton involved in peroxisomal growth and division? Is Pex11pβ the only effector inducing elongation (and proliferation) of peroxisomes?

2 MATERIAL AND METHODS

2.1 Equipment

Centrifuges

- Avanti Centrifuge J-251, Rotors JA-25.50 and JA-14 (Beckman Coulter, Fullerton, USA)
- Centrifuge 5810R (Eppendorf, Hamburg, Germany)
- Heraeus Fresco 17 Centrifuge (Thermo Scientific, Hanau, Germany)
- Heraeus Pico 17 Centrifuge (Thermo Scientific, Hanau, Germany)
- Minispin plus (Eppendorf, Hamburg, Germany)
- Optima LE-80K Ultracentrifuge, Rotor Ki80 (Beckman Coulter, Fullerton, USA)

Incubators and shakers

- Incubator for bacterial cultures (Binder, Tuttlingen, Germany)
- Incubator shaker for bacterial cultures Innova 4400 (New Brunswick Scientific, Edison, USA)
- Magnetic stirrer Agimatic-N (JP Selecta, Barcelona, Spain)
- Mini Rocker MR-1 (Biosan, Riga, Latvia)
- Shaker REAX 2 (Heidolph Instruments, Heidelberg, Germany)
- Shaker, horizontal Unimac 1010 (Heidolph Instruments, Heidelberg, Germany)
- Thermomixer comfort (Eppendorf, Hamburg, Germany)
- Ultra Low -80°C freezer (Sanyo, Sakata, Japan)
- Vortex Genius 3 (IKA, Staufen, Germany)
- Water bath (Memmert, Schwabach, Germany)

Cell culture

- CO_2 incubator (Sanyo, Sakata, Japan)
- CO_2 incubator HeraCell (Heraeus/Kendro Laboratory Products, Hanau, Germany)
- Electro Cell Manipulator ECM 630 (BTX Harvard Apparatus, Holliston, USA)
- Microinjector Femto Jet (Eppendorf, Hamburg, Germany)
- Micromanipulator InjectMAN N1 2 (Eppendorf, Hamburg, Germany)
- Peristaltic pump Masterflex 701572 (Cole-Parmer, Vernon Hills, USA)
- Pump Laboport (KNF Neuberger, Freiburg, Germany)

- Safety cabinet HeraSafe (Heraeus/Kendro Laboratory Products, Hanau, Germany)

Optical equipment and microscopes

- AlphaImager HP (Alpha Innotech, San Leandro, USA)
- Calibrated Imaging Densitometer GS-710 (Bio-Rad, Munich, Germany)
- Camera F-View II CCD and Soft Imaging software (Soft Imaging Systems, Münster, Germany)
- Leica DMIL microscope (Leica, Heidelberg, Germany; cell culture)
- Olympus BX 61 microscope; Plan-Neofluar 100x/1.35 oil objective (Olympus Optical, Hamburg, Germany)
- Olympus IX81 microscope; PlanApo 100x/1.40 oil objective (Olympus Optical, Hamburg, Germany)
- Photometer Ultrospec 100 pro (Amersham Biosciences, Uppsala, Sweden)
- Qubit fluorometer (Molecular Probes/Invitrogen, Eugene, USA)
- Spectrophotometer Cary 50 Bio (Varian, Walnut Creek, USA)
- Zeiss Axiovert 10 (Zeiss, Oberkochen, Germany; microinjection)
- Zeiss EM 109S Electron Microscope (Zeiss, Oberkochen, Germany)
- Zeiss LSM 510 confocal microscope; Plan-Apochromat 63x and 100x/1.4 oil objectives (Carl Zeiss, Oberkochen, Germany)
- Zeiss LSM 510 live cell equipment: Heating insert P, CTI controller 3700 digital, Tempcontrol 37-2 (PeCon, Erbach, Germany)

Electrophoretic and blotting equipment

- Horizontal PerfectBlue Gel System Mini (Peqlab Biotechnology, Erlangen, Germany)
- Electrophoresis power supply EPS 2A200 (Amersham Biosciences, Uppsala, Sweden)
- Electrophoresis power supply EPS 601 (Amersham Biosciences, Uppsala, Sweden)
- Hoefer SE 600 Ruby gel chamber (Amersham Biosciences, Uppsala, Sweden)
- Slap mini gel chamber (Keutz, Reiskirchen, Germany)
- Trans-Blot SD SemiDry transfer cell (Bio-Rad, Munich, Germany)

Other equipment

- AES 1010 SpeedVac System (Thermo Savant, Waltham, USA)
- Autoclave Uniclave 88 (AJC, Lisbon, Portugal)
- Bag Sealer Folio (Severin, Sundern, Germany)
- Balance Vicon (Acculab/Sartorius, Göttingen, Germany)
- Balance, analytical BP 221S (Sartorius, Göttingen, Germany)
- Centrifuge beakers, 250 ml (Beckman, Munich, Germany)
- Centrifuge tubes, 50 ml (Nalgene, Rochester, USA)
- Cryomed N_2 storage (Forma Scientific, Waltham, USA)
- Drying Oven (Sanyo, Sakata, Japan)
- Easypet (Eppendorf, Hamburg, Germany)
- Microwave KOR-63A5 (Daewoo, Butzbach, Germany)
- pH meter PB-11 (Sartorius, Göttingen, Germany)
- Research pipettes, 2.5 µl, 10µl, 100 µl, 1000 µl (Eppendorf, Hamburg, Germany)
- Thermal Cycler MyCycler (Bio-Rad, Munich, Germany)
- X-Ray cassette (Roth, Karlsruhe, Germany)

2.2 Consumables

Product	**Source**
Coverslips, round, Ø 12 and 18 mm	Menzel, Braunschweig, Germany
Cryovials, 2 ml	Greiner Bio-One, Frickenhausen, Germany
Cuvettes, semimicro	Plastibrand/Brand, Wertheim, Germany
Dishes for agar plates	Greiner Bio-One, Frickenhausen, Germany
Dishes for tissue culture, 6 and 12 well	Greiner Bio-One, Frickenhausen, Germany
Dishes for tissue culture, 35, 60, 100 mm	Greiner Bio-One, Frickenhausen, Germany
Electroporation cuvettes, 4 mm gap	Molecular BioProducts, San Diego, USA
Femtotips, glass capillaries	Eppendorf, Hamburg, Germany
Filter for medium, Sartolab P20, 0.2 µm	Sartorius, Goettingen, Germany
Folded filters	Macherey-Nagel, Düren, Germany
Glass bottom dishes, 35 mm	MatTek, Ashland, USA
Hyperfilm ECL	Amersham Biosciences, Uppsala, Sweden
Microcentrifuge tubes, 0.5, 1.5, 2 ml	Greiner Bio-One, Frickenhausen, Germany
Microloader	Eppendorf, Hamburg, Germany
Microscope slides, frosted end	Menzel, Braunschweig, Germany
Needle, Sterican 26 G x 1”, 0.45 x 25 mm	B. Braun, Melsungen, Germany
Pipette tips, 20, 200, 1000 µl	Sarstedt, Nümbrecht, Germany
Protran Nitrocellulose Transfer Membrane	Whatman, Dassel, Germany

Product	Source
Reaction tubes for PCR, 0.2 ml	Axygen, Union City, USA
Reaction tubes, 15, 50 ml	Greiner Bio-One, Frickenhausen, Germany
Serological pipettes, 5, 10 ml	Greiner Bio-One, Frickenhausen, Germany
Silica Gel Orange	Roth, Karlsruhe, Germany
Syringe Inject, 10 ml	B. Braun, Melsungen, Germany
Syringe Omnifix-F, 1 ml	B. Braun, Melsungen, Germany
Tubes for bacterial cultures, 14 ml	Greiner Bio-One, Frickenhausen, Germany
Whatman filter paper, 3 mm	Whatman, Dassel, Germany

Table 2.1: Disposable material

2.3 Chemicals and reagents

2.3.1 Chemicals

Chemical	Source
2, 4, 6-Tris(dimethylaminomethyl)phenol	Serva, Heidelberg, Germany
2-Dodecenylsuccinic acid anhydride	Serva, Heidelberg, Germany
3, 3'-Diaminobenzidine	Fluka, Buchs, Switzerland
Acetic acid	Merck, Darmstadt, Germany
Acrylamide – RotiphoreseGel 30	Roth, Karlsruhe, Germany
Agar	Formedium, Hunstanton, England
Agarose NEEO	Roth, Karlsruhe, Germany
Albumin Fraction V (BSA)	Roth, Karlsruhe, Germany
Ammonium persulphate (APS)	Sigma, Steinheim, Germany
Ampicillin	Sigma, Steinheim, Germany
β-Mercaptoethanol	Sigma, Steinheim, Germany
Bromophenol blue	Sigma, Steinheim, Germany
Cacodylic acid sodium salt	Merck, Darmstadt, Germany
Calcium chloride	Sigma, Steinheim, Germany
CHAPS	Roth, Karlsruhe, Germany
Chloroform	Merck, Darmstadt, Germany
D(+)glucose monohydrate	Fluka/Sigma, Steinheim, Germany
Digitonin	Sigma, Steinheim, Germany
Dimethyl sulphoxide (DMSO)	Sigma, Steinheim, Germany
Dithiobis(succinimidyl propionate) (DSP)	Pierce, Rockford, USA
Dithiothreitol (DTT)	Sigma, Steinheim, Germany
ECL advanced western blot detection kit	Amersham Biosciences, Uppsala, Sweden
Ethanol	Merck, Darmstadt, Germany
Ethidium bromide solution	Fluka/Sigma, Steinheim, Germany
Ethylenediaminetetraacetic acid salt dehydrate (EDTA)	Sigma, Steinheim, Germany
FOY-305 protease inhibitor	Sanol-Schwarz, Monheim, Germany

Chemical	Source
G418	Sigma, Bornem, Belgium
Glutaraldehyde	Serva, Heidelberg, Germany
Glycerol	Roth, Karlsruhe, Germany
Glycid ether 100 (EPON 812)	Serva, Heidelberg, Germany
Glycine	Sigma, Steinheim, Germany
HaloTag R110Direct ligand	Promega, Madison, USA
HaloTag TMR ligand	Promega, Madison, USA
HEPES sodium salt	Sigma, Steinheim, Germany
Hoechst 33528	Polysciences, Warrington, USA
Hydrochloric acid	Merck, Darmstadt, Germany
Hydrogen peroxide	Merck, Darmstadt, Germany
Isopropyl alcohol	Merck, Darmstadt, Germany
Kanamycin disulphate salt	Sigma, Steinheim, Germany
LB-Broth Miller	Formedium, Hunstanton, England
Lead nitrate	Merck, Darmstadt, Germany
Maleic acid	Merck, Darmstadt, Germany
Methanol	Merck, Darmstadt, Germany
Methylnadic anhydride	Serva, Heidelberg, Germany
Milk, powder, low fat (Molico)	Nestlé, Linda-a-Velha, Portugal
MOPS sodium salt	Sigma, Steinheim, Germany
Mowiol 4-88 reagent	Calbiochem/Merck, Darmstadt, Germany
Nocodazole	Sigma, Steinheim, Germany
Osmium tetroxide	Roth, Karlsruhe, Germany
Paraformaldehyde (powder)	Sigma, Steinheim, Germany
Phenylmethylsulphonyl fluoride (PMSF)	Sigma, Steinheim, Germany
Pikric acid	Merck, Darmstadt, Germany
Ponceau S	Roth, Karlsruhe, Germany
Potassium chloride	Sigma, Steinheim, Germany
Potassium ferrocyanide	Merck, Darmstadt, Germany
Potassium phosphate dibasic	Sigma, Steinheim, Germany
Propyl gallate	Fluka/Sigma, Steinheim, Germany
Protein A-gold (10 nm)	J. Slot, University of Utrecht, The Nether-lands
Protein A-sepharose, 1 mg/ml	Sigma, Steinheim, Germany
Protein assay (Bradford)	Bio-Rad, Munich, Germany
Sodium azide	Sigma, Steinheim, Germany
Sodium bicarbonate	Sigma, Steinheim, Germany
Sodium chloride	Sigma, Steinheim, Germany
Sodium deoxycholate monohydrate	Sigma, Steinheim, Germany
Sodium dodecyl sulphate (SDS)	Sigma, Steinheim, Germany
Sodium hydroxide	Merck, Darmstadt, Germany
Sodium phosphate dibasic	Sigma, Steinheim, Germany

Chemical	Source
Sucrose	Sigma, Steinheim, Germany
Tannic acid	Serva, Heidelberg, Germany
Tetramethylethelenediamine (TEMED)	Fluka/Sigma, Steinheim, Germany
Trasylol (protease inhibitor)	Bayer, Leverkusen, Germany
Tris	Roth, Karlsruhe, Germany
Tri-Sodium citrate	Merck, Darmstadt, Germany
Triton X-100	Sigma, Steinheim, Germany
Uranyl acetate	Merck, Darmstadt, Germany

Table 2.2: Frequently used chemicals

Further chemicals not listed in Table 2.2 were purchased from Sigma (Steinheim, Germany), Merck (Darmstadt, Germany), or Roth (Karlsruhe, Germany).

2.3.2 Loading dyes and markers

Product	Source
6x Orange Loading Dye	Fermentas, Burlington, Canada
Gene Ruler DNA Ladder Mix	Fermentas, Burlington, Canada
Kaleidoscope Precision Plus Protein Standard	Bio-Rad, Munich, Germany

Table 2.3: Loading dyes and markers

2.3.3 Kits

Product	Source
Illustra Plasmid Prep Mini Spin Kit	GE Healthcare, Buckinghamshire, UK
Jetstar 2.0 Plasmid Maxiprep Kit	Genomed, Löhne, Germany
Nucleobond Xtra Midi Kit	Macherey-Nagel, Düren, Germany
Qiaprep Spin Miniprep Kit	Qiagen, Hilden, Germany
Qiaquick Gel Extraction Kit	Qiagen, Hilden, Germany
Quant-iT dsDNA BR Assay Kit	Molecular Probes/Invitrogen, Eugene, USA
Quant-iT RNA Assay Kit	Molecular Probes/Invitrogen, Eugene, USA
RNeasy Protect Mini Kit	Qiagen, Hilden, Germany

Table 2.4: Kits

2.3.4 Cell culture reagents

Product	Source
Chloroquine diphosphate	Fluka/Sigma, Steinheim, Germany
DEAE-Dextran hydrochloride	Sigma, Steinheim, Germany

Product	Source
DMEM high glucose with L-glutamine	PAA Laboratories, Pasching, Austria
DMEM with L-glutamine, without sodium bicarbonate and phenol red, powder (supplemented with 3.7 g/l sodium bicarbonate and filtered upon use)	Sigma, Steinheim, Germany
Fetal Bovine Serum "Gold" (FBS)	PAA Laboratories, Pasching, Austria
Lipofectamine reagent	Invitrogen, Karlsruhe, Germany
Lipofectamine RNAiMax reagent	Invitrogen, Karlsruhe, Germany
PEI (polyethylenimine) 25 kD	Sigma, Steinheim, Germany
Penicillin/Streptomycin, 100x concentrate	PAA Laboratories, Pasching, Austria
Trypsin EDTA	PAA Laboratories, Pasching, Austria

Table 2.5: Cell culture reagents

2.4 Immunological reagents

2.4.1 Primary antibodies

Antibody/Name	Source	Dilution
Mouse mc anti-GFP	Clontech, Saint-Germain-en-Laye, France	IP 1:1000
Mouse mc anti-HA.11 epitope	Covance, Berkeley, USA	IMF 1:200; WB 1:1000
Mouse mc anti-Myc epitope 9E10	Santa Cruz Biotechnology, Santa Cruz, USA	IMF 1:200; WB 1:1000
Mouse mc anti-Myc epitope 9E10 agarose conjugate	Santa Cruz Biotechnology, Santa Cruz, USA	IP 1:25
Mouse mc anti-p115	BD Transduction Laboratories, San Diego, USA	IMF 1:100
Mouse mc anti-Pex19	BD Biosciences, San Jose, USA	WB 1:250
Mouse mc anti-Tom20	BD Transduction Laboratories, San Diego, USA	IMF 1:200
Mouse mc anti-α-Tubulin	Synaptic Systems, Göttingen, Germany	IMF 1:100; WB 1:1000
Mouse anti-VDAC1	Abcam, Cambridge, UK	WB 1:1000
Rabbit pc anti-carboxypeptidase A	Rockland Immunochemicals, Gilbertsville, USA	IMF 1:800
Rabbit pc anti-DLP1-MiD	M. McNiven, University of Rochester, USA (Koch et al. 2003; Yoon et al. 1998)	WB 1:3000
Rabbit pc anti-DLP1-N	M. McNiven, University of Rochester, USA (Yoon et al. 1998)	WB 1:6000

Antibody/Name	Source	Dilution
Rabbit pc anti-Fis1	Alexis/Axxora, Grünberg, Germany	WB 1:1000
Rabbit pc anti-GFP	Invitrogen, Karlsruhe, Germany	IMF 1:100; WB 1:1000
Rabbit pc anti-Marburg Virus Glycoprotein (MBGV-GP)	S. Becker, University of Marburg (Becker et al. 1996)	IMF 1:100
Rabbit pc anti-Pex14	D. Crane, Griffith University, Brisbane, Australia	IMF 1:1000
Rabbit pc anti-PMP70	A. Völkl, University of Heidelberg, Germany (Luers et al. 1993)	IMF 1:200, WB 1:1000
Rabbit pc anti-Tom22C	M. Ryan, La Trobe University, Melbourne, Australia	IMF 1:100

Table 2.6: Primary antibodies
Abbreviations: IMF, immunofluorescence; IP, immunoprecipitation; mc, monoclonal; pc, polyclonal; WB, Western blot.

2.4.2 Secondary antibodies

Antibody/Name	Source	Dilution
Donkey pc anti-mouse IgG conjugated to tetramethylrhodamine 5 isothiocyanate (TRITC)	Jackson ImmunoResearch, West Grove, USA	IMF 1:100
Donkey pc anti-rabbit IgG conjugated to TRITC	Jackson ImmunoResearch, West Grove, USA	IMF 1:100
Donkey pc anti-mouse IgG conjugated to Alexa Fluor 488	Invitrogen, Karlsruhe, Germany	IMF 1:400
Donkey pc anti-rabbit IgG conjugated to Alexa Fluor 488	Invitrogen, Karlsruhe, Germany	IMF 1:500
Goat anti-mouse IgG conjugated to horseradish peroxidase (HRP)	Bio-Rad, Munich, Germany	WB 1:2000
Goat anti-rabbit IgG conjugated to HRP	Bio-Rad, Munich, Germany	WB 1:2000

Table 2.7: Secondary antibodies
Abbreviations: IMF, immunofluorescence; pc, polyclonal; WB, Western blot.

2.5 Molecular biology reagents

2.5.1 Enzymes and other reagents

Reagent	Source
Antarctic phosphatase	New England Biolabs, Ipswich, USA

Reagent	Source
dNTP's	Invitrogen, Karlsruhe, Germany
KOD Hot Start DNA polymerase	Novagen/Merck, Darmstadt, Germany
Oligo-dT(15) primer	Roche, Basel, Switzerland
Restriction enzymes: *Bam*HI, *Bgl*II, *Eco*RI, *Not*I, *Xho*I	New England Biolabs, Ipswich, USA; Fermentas, Burlington, Canada; Invitrogen, Karlsruhe, Germany
M-MuLV reverse transcriptase	Stratagene, LaJolla, USA; New England Biolabs, Ipswich, USA
RNase block	Stratagene, LaJolla, USA; New England Biolabs, Ipswich, USA
T4 DNA ligase	New England Biolabs, Ipswich, USA
Taq DNA polymerase	New England Biolabs, Ipswich, USA
TriFast peqGOLD	Peqlab Biotechnology, Erlangen, Germany
Water, treated with DEPC	Roth, Karlsruhe, Germany

Table 2.8: Enzymes and other molecular biology reagents

2.5.2 Plasmids

Name	Source/Reference
Carboxypeptidase A-UT	H. Borta, University of Marburg, Germany
HaloTag-HsCatalase	Marc Fransen, Katholieke Universiteit Leuven, Belgium
DLP1-K38A-GFP	M. McNiven, University of Rochester, USA (Koch et al. 2003; Pitts et al. 1999)
DLP1-K38A-UT	M. McNiven, University of Rochester, USA (Pitts et al. 1999)
GFP-hFis1	Y. Yoon, University of Rochester, USA (Koch et al. 2005; Yoon et al. 2003)
Myc-hFis1	Y. Yoon, University of Rochester, USA (Koch et al. 2005; Yoon et al. 2003)
Myc-hFis1-ΔC	Y. Yoon, University of Rochester, USA (Koch et al. 2005; Yoon et al. 2003)
Myc-hFis1-ΔTM/C	Y. Yoon, University of Rochester, USA (Koch et al. 2005; Yoon et al. 2003)
hFis1-YFP-TM/C	Y. Yoon, University of Rochester, USA (Koch et al. 2005; Yoon et al. 2003)
GFP-hFis1$^{K149/151A}$	M. T. Ryan, La Trobe University, Melbourne, Australia (Stojanovski et al. 2004)
MBGV-GP	S. Becker, University of Marburg (Becker et al. 1996)
Pex3-Myc	G. Dodt, University of Tübingen, Germany
Pex3-GFP	G. Dodt, University of Tübingen, Germany
Pex11α-YFP	(Delille & Schrader 2008)
Pex11β-Myc	(Schrader et al. 1998b)
HA_2-Pex11γ	Y. Fujiki, Kyushu University, Fukuoka, Japan

Name	Source/Reference
Pex12-Myc	S. Gould, Johns Hopkins University School of Medicine, Baltimore, USA
Myc-Pex16	G. Dodt, University of Tübingen, Germany
HA-Pex19	P. U. Mayerhofer, University of Munich, Germany
YFP-Pex19	P. U. Mayerhofer, University of Munich, Germany
Pxmp2/PMP22-HA	G. Lüers, University of Marburg, Germany
PMP70-Myc	S. Gould, Johns Hopkins University School of Medicine, Baltimore, USA
GFP-SKL	S. Gould, Johns Hopkins University School of Medicine, Baltimore, USA
mRuby-PTS1	J. Wiedenmann, University of Southampton, UK (Kredel et al. 2009)
pDsRed-Peroxi	Clontech, Saint-Germain-en-Laye, France
ER-mRuby-KDEL	J. Wiedenmann, University of Southampton, UK (Kredel et al. 2009)
Mito-RFP	Invitrogen, Karlsruhe, Germany
pmEYFP-N1	Clontech, Saint-Germain-en-Laye, France; (Glebov & Nichols 2004)
pmEYFP-C1	Clontech, Saint-Germain-en-Laye, France; (Glebov & Nichols 2004)
pcDNA3	Invitrogen, Karlsruhe, Germany
pCMV-Tag3A	Stratagene, La Jolla, USA
pCMV-HA	Clontech, Saint-Germain-en-Laye, France

Table 2.9: Plasmids for protein expression in mammalian cells
UT, untagged.

2.5.3 Constructs

Name	Template	Primer	Enzymes	Vector
Myc-Pex11α§	Pex11pα-YFP	Pex11α-up & Pex11α-down-f.l.	*Bgl*II & *Eco*RI	pCMV-Tag3A
Myc-Pex11αΔ8§	Pex11pα-YFP	Pex11α-up & Pex11α-downΔ8	*Bgl*II & *Eco*RI	pCMV-Tag3A
Myc-Pex11αΔ30	Pex11pα-YFP	Pex11α-up & Pex11α-downΔ30	*Bgl*II & *Eco*RI	pCMV-Tag3A
Pex11β-UT	Pex11β-Myc	Pex11β-up & Pex11β-wt-down	*Bam*HI & *Eco*RI	pcDNA3
HA-Pex11β	Myc-Pex11β	Pex11β-up-HA & Pex11β-down-NotI	*Eco*RI & *Not*I	pCMV-HA
Myc-Pex11β*	Pex11β-Myc	Pex11β-up & Pex11β-wt-down	*Bam*HI & *Eco*RI	pCMV-Tag3A

Name	Template	Primer	Enzymes	Vector
Myc-Pex11βΔ5*	Pex11β-Myc	Pex11β-up & Pex11βΔ5down	*Bam*HI & *Eco*RI	pCMV-Tag3A
Myc-Pex11βΔ30*	Pex11β-Myc	Pex11β-up & Pex11βΔ30down	*Bam*HI & *Eco*RI	pCMV-Tag3A
Myc-Pex11βΔ60*	Pex11β-Myc	Pex11β-up & Pex11βΔ60down	*Bam*HI & *Eco*RI	pCMV-Tag3A
Pex11β-YFP#	Pex11β-Myc	Pex11β-up-N & Pex11β-down-N	*Eco*RI & *Bam*HI	pmEYFP-N1
YFP-Pex11β#	Pex11β-Myc	Pex11β-up-C & Pex11β-down-C	*Eco*RI & *Bam*HI	pmEYFP-C1
Pex11γ-YFP	HA-Pex11γ	Pex11γ-up-N & Pex11γ-down-N	*Eco*RI & *Bam*HI	pmEYFP-N1
Myc-Pex11γ	Pex11γ-YFP	Pex11γ-up & Pex11γ-down-f.l.	*Bam*HI & *Eco*RI	pCMV-Tag3A
Myc-Pex11γΔ11	Pex11γ-YFP	Pex11γ-up & Pex11γ-downΔ11	*Bam*HI & *Eco*RI	pCMV-Tag3A
Myc-Pex11γΔ30	Pex11γ-YFP	Pex11γ-up & Pex11γ-downΔ30	*Bam*HI & *Eco*RI	pCMV-Tag3A

Table 2.10: Plasmids cloned during this study
Marked constructs were cloned by *H. Borta, #W. Ackermann (Department of Cell Biology and Cell Pathology, University of Marburg, Germany), or §Rui Batista and Fátima Camões (Centre for Cell Biology, University of Aveiro, Portugal).

In frame insertion of all constructs was verified by sequencing (Eurofins MWG Operon, Ebersberg, Germany).

2.5.4 Primer

Name	Sequence (5' to 3')
GPO1	ACT CCT ACG GGA GGC AGC AGT A
MGSO	TGA ACC ATC TGT CAC TCT GTT AAC CTC
Pex11β-up	TTG GAT CCT *ATG* GAC GCC TGG GTC CGC TTC
Pex11β-wt-down	TG AAT TC**T CA**G GGC TTG AGT CGT AGC CAG GG
Pex11βΔ5down	TTG AAT TC**T CA**C CAG GGA TAG ATT AGG GTG AC
Pex11βΔ30down	TTG AAT TC**T CA**G CGC CAG AGG CCT AGT TTG TC
Pex11βΔ60down	TTG AAT TC**T CA**T CGA GCC AGG AGC AGG ACT TG
Pex11β-up-N	TT GAA TTC *ATG* GAC GCC TGG GTC CGC TTC
Pex11β-down-N	T TGG ATC CAT GGG CTT GAG TCG TAG CCA GGG
Pex11β-up-C	TTG AAT TCT *ATG* GAC GCC TGG GTC CGC TTC
Pex11β-down-C	TT GGA TCC **TCA** GGG CTT GAG TCG TAG CCA GGG
Pex11β-up-HA	TT GA ATT CTC *ATG* GAC GCC TGG GTC CGC TTC
Pex11β-down-NotI	T TGC GGC CGC **TCA** GGG CTT GAG TCG TAG CCA G
Pex11α-up	TA GAT CTT *ATG* GAC GCC TTC ACC CGC TTC ACC

Name	Sequence (5' to 3')
Pex11α-down-f.l.	TT GAA TTC **TCA** ACG GGT CTT CAG CTT CAT CTG
Pex11α-downΔ8	TT GAA TTC **TCA** ATA TGC CAC AGT GAT CAT GC
Pex11α-downΔ30	TT GAA TTC **TCA** GGA TTT ATA GAT CCC CAG CTG
Pex11γ-up-N	TT GAA TTC *ATG* GCG TCG CTG AGC GGC CTG
Pex11γ-down-N	T TGG ATC CGG GGT AGT GGC CTC GGC CTG
Pex11γ-up	AAG GAT CCT *ATG* GCG TCG CTG AGC GGC CTG G
Pex11γ-down-f.l.	TT GAA TTC **TCA** GGG GGT AGT GGC CTC GGC CTG
Pex11γ-downΔ11	TT GAA TTC **TCA** GGC CGC CTG GTA CAT GCT GAG
Pex11γ-downΔ30	TT GAA TTC **TCA** CGG CGG GAA GCG GCC GGC

Table 2.11: Primer sequences used for PCR/cloning in this study
Restriction sites are underlined, start codons are printed italic, and stop codons are printed bold. All primers were purchased from Eurofins MWG Operon (Ebersberg, Germany).

2.6 Frequently used buffers and solutions

All solutions were prepared with distilled water (ROpure infinity reverse osmosis water system; Barnstead, Dubuque, USA) if not indicated otherwise.

Blocking solution for immunofluorescence

- 1% (w/v) BSA in PBS

Blocking solution for western blots

- 5% (w/v) milk powder in PBS

Fixative for immunofluorescence

- 4% (w/v) Paraformaldehyde in PBS, pH 7.4

Cell culture medium for COS-7 and HepG2 cells

- DMEM, high glucose (4.5 g/l) with L-glutamine
- 10% (v/v) FBS
- 100 U/ml Penicillin
- 100 µg/ml Streptomycin

HBS – HEPES buffered saline, pH 7.15, for electroporation

- 5 g/l HEPES
- 8 g/l Sodium chloride
- 0.37 g/l Potassium chloride
- 0.1 g/l Sodium phosphate dibasic
- 1.08 g/l D(+)Glucose

LB medium

- 2.5% (w/v) LB-Broth Miller

LB plates

- 2.5% (w/v) LB-Broth Miller
- 1% (w/v) Agar

Lysis buffer, hypotonic

- 10 mM Tris, pH 7.5
- 1 mM EDTA

Lysis buffer, pH 8.0

- 25 mM Tris
- 50 mM Sodium chloride
- 0.5% (w/v) Sodium deoxycholate
- 0.5% (w/v) Triton X-100

Mounting medium for immunofluorescence

- 3 volumes Mowiol stock
- 1 volume Propylgallat stock

Mowiol stock

- 12 g Mowiol 4-88
- 40 ml PBS, stir over night
- 20 ml Glycerol, stir over night
- Centrifuge 1 hour, 15,000 rpm, 4°C
- Sodium azide added to the supernatant

PBS – phosphate buffered saline, pH 7.35

- 140 mM Sodium chloride
- 2.5 mM Potassium chloride
- 6.5 mM Sodium phosphate dibasic
- 1.5 mM Potassium phosphate dibasic

Permeabilization for immunofluorescence

- 0.2% (v/v) Triton X-100 in PBS

Permeabilization for immunofluorescence

- 1 mg/ml Digitonin stock solution
- 1:400 diluted in PBS

Peroxisome homogenization buffer, pH 7.4

- 5 mM MOPS
- 250 mM Sucrose
- 1 mM EDTA
- (0.1% (v/v) Ethanol)

Propyl gallate stock (bleach protection)

- PBS
- 2.5% (w/v) Propyl gallate
- 50% (v/v) Glycerol

Protease inhibitor mix (final concentrations)

- 0.1 mM PMSF
- 0.01 mM FOY 305
- 0.25% (v/v) Trasylol

SDS loading buffer (Laemmli 1970)

- 60 mM Tris, pH 6.8
- 2% (w/v) SDS
- 10% (v/v) Glycerol
- 0.005% (w/v) Bromophenol blue
- 20 mM DTT
- 5% (v/v) β-Mercaptoethanol (fresh)

SDS running buffer

- 25 mM Tris
- 190 mM Glycine
- 0.1% (w/v) SDS

Semidry blotting buffer

- 48 mm Tris
- 39 mM Glycine
- 0.4% (w/v) SDS
- 20% (v/v) Methanol

50x TAE – Tris-Acetate-EDTA, pH 8.0

- 40 mM Tris
- 20 mM Acetic acid
- 1 mM EDTA

TBS – Tris buffered saline

- 50 mM Tris, pH 7.5
- 150 mM Sodium chloride
- 1 mM EDTA

Tris buffer separation gel (pH 8.8)

- 2 M Tris (60.56 g in 250 ml water)

Tris buffer stacking gel (pH 6.8)

- 1 M Tris (30.28 g in 250 ml water)

Wash buffer I for immunoprecipitation

- PBS, pH 7.35
- 0.5% (w/v) Sodium deoxycholate
- 0.5% (w/v) Triton X-100

Wash buffer II for immunoprecipitation, pH 8.0

- 500 mM Sodium chloride
- 125 mM Tris
- 10 mM EDTA
- 0.5% (w/v) Triton X-100

2.7 Cell lines

COS-7

- Source: ATCC (American Type Culture Collection, Rockville, USA); CRL-1651
- *Cercopithecus aethiops* (African green monkey), kidney
- SV40 transformed, produce large T antigen,
- adherent, fibroblast morphology

COS-GFP-SKL

- Source: G. Lüers, University of Marburg, Germany (Koch et al. 2004)
- COS-7 cells stably transfected with GFP-SKL

HepG2

- Source: ATCC (American Type Culture Collection, Rockville, USA); HB-8065
- *Homo sapiens* (human), liver
- hepatocellular carcinoma
- adherent, epithelial morphology

2.8 Cell culture

COS-7, COS-GFP-SKL, and HepG2 cells were cultured in Dulbecco's modified Eagle medium (DMEM) high glucose (4.5 g/l) supplemented with 10% FBS, 100 U/ml Penicillin, and 100 µg/ml Streptomycin. Cells were cultured at 37°C, 5% CO_2 aeration, and 95%

humidity. Cell culture work was performed in a sterile laminar flow safety cabinet and all materials and solutions were sterilized by filtration, autoclaving or heat sterilization. Routinely, cells were grown in 100 mm dishes and seeded on coverslips in 60 mm dishes for immunofluorescence experiments. Cell number was determined using a Fuchs-Rosenthal hemocytometer.

2.8.1 Cell passage

Routinely, passaging or splitting of cell was performed twice per week, after the cells reached confluency (~$1.7x10^4$ cells/cm^2). Cells were washed with PBS to remove debris and residues of FBS which might inhibit trypsin activity and incubated with 1.5 ml trypsin EDTA solution (0.5 mg/ml trypsin and 0.22 mg/ml EDTA) for five minutes at 37°C. The protease trypsin cleaves extracellular adhesion proteins. Additionally, EDTA, a chelating agent, binds Ca^{2+} ions required for cell-cell-adhesions formed by cadherins and thus supports cell detachment. Cells were resuspended in 10 ml medium containing FBS and pelleted by centrifugation for 5 minutes at 500x g. The pellet was resuspended in medium and cells were seeded as single cell suspension in a dilution of 1:10 (10^4 cells/ml). In between cell passaging the culture medium was changed every two days to provide fresh nutrients, to remove toxic products, and to prevent pH changes, which are also indicated by the pH indicator dye (phenol red) included in the medium.

2.8.2 Cell freezing

For long term storage, cells were frozen and stored in the vapour phase of liquid nitrogen. Cell pellets prepared as described above (2.8.1) were resuspended in freezing medium containing 20% FBS and 10% DMSO to avoid crystal formation. Cell suspension aliquots of 1 ml were filled into cryovials, slowly frozen overnight at -80°C and subsequently transferred into the liquid nitrogen storage tank. For unfreezing cells were thawed quickly in a water bath (37°C) or by mixing with pre-warmed culture medium, and the cells were seeded with pre-warmed medium in a regular dish. After adhesion of the cells to the bottom of the dish, the medium was changed to remove DMSO and debris.

2.8.3 Mycoplasma detection

Mammalian cell cultures get easily contaminated by mycoplasmas, a genus of bacteria insensitive to most antibiotics. Mycoplasmal contaminations can lead to cell damage, interfere with proper cell growth and metabolism, and might impede applications like cell transfection. Due to the small size of these bacteria, mycoplasma contaminations are not detectable by normal microscopy and two different techniques were used on a regular basis to test for contaminations.

2.8.3.1 Hoechst staining test

Hoechst 33528, a reagent intercalating into DNA, allows the visualization of DNA using a fluorescence microscope. After excitation with ultraviolet (UV) light at 359 nm the dye integrated into DNA appears blue (emission wave length: 461 nm). By staining of the DNA with Hoechst, mycoplasmas can be detected in between the nuclei of the cells as rod-like forms or chains of rods.

Protocol: Cells were seeded on coverslips and after 24 hours cells were fixed using 4% paraformaldehyde (see 2.9.1). The Hoechst staining (0.2 µg/ml in PBS) was performed by incubation of the cells for two to three minutes. After thorough washing, the coverslips were mounted using Mowiol (2.6) and examined for mycoplasma contamination using a fluorescence microscope.

This low cost technique is easy to perform, but small degrees of contamination might not be detected.

2.8.3.2 Mycoplasma PCR test

PCR is a highly sensitive method which allows the amplification and detection of low amounts of a certain DNA (see also 2.11.3). Using a genus-specific primer set (Table 2.11) with oligonucleotide sequences complementary to 16S rRNA conserved regions of mycoplasma (van Kuppeveld et al. 1992) a sensitive screening for mycoplasma contaminations was possible.

Protocol: After two days of culture samples (100 µl) of the cell culture medium were taken and heated for five minutes at 95°C to lyse the cells. After centrifugation at 13,000 rpm for one minute to pellet cell debris, 1.5 µl of the supernatant were used as sam-

ple/template (Table 2.12) for the PCR (Table 2.13). Positive (mycoplasma containing) and negative (fresh medium) controls were treated in the same way.

Subsequently, the samples were analyzed by gel electrophoreses using a 1% agarose gel (see 2.11.5). In positive samples (positive control and contaminated cell lines) a DNA fragment with a size of 715 bp appears, but a band in the negative control indicates cross-contamination of the samples.

Template	1.5 µl
Primer GPO1 (100 pmol/µl)	0.5 µl
Primer MGSO (100 pmol/µl)	0.5 µl
10x Thermo-Pol buffer	3.0 µl
50x dNTP's (10 mM each)	0.6 µl
Taq DNA polymerase (5 U/µl)	0.6 µl
Water	23.3 µl
Final volume	30.0 µl

Table 2.12: Mycoplasma PCR mix

Initial denaturation	95°C	5 minutes	
Denaturation	95°C	30 seconds	35 cycles
Annealing	55°C	30 seconds	
Elongation	72°C	1 minute	
Cooling	4°C	∞	

Table 2.13: PCR program

2.8.4 Transfection of mammalian cells

Several methods were used for the transfection of COS-7 and COS-GFP-SKL cells, the introduction of a DNA or RNA sequence into the cells, depending on the application. Cells were transfected with plasmid DNA containing a cDNA sequence to induce expression of the respective protein or with siRNA (2.8.5) to reduce the amount of a target protein in the cell. In this study only transient transfections were performed. The transfection methods are based on different mechanisms of DNA/RNA uptake, e.g. endocytosis, membrane fusion, or diffusion. The transfection efficiency, cell mortality, and morphological influence on the cells varies in between the different methods, cell types, and conditions used, thus requiring optimization of the transfection method for each cell line and application.

2.8.4.1 PEI transfection

For morphological experiments like immunofluorescence studies cells were usually transfected using PEI (polyethylenimine). The cationic and branched polymer PEI binds to the negatively charged DNA backbone which allows endocytotic uptake of the complex by the cells. The correct DNA/PEI ratio is crucial for optimal complex formation. The so called "proton-sponge-effect" of PEI prevents lysosomal degradation of the DNA. The high number of amino groups of PEI provides a high buffer capacity at physiological conditions. In acidic compartments like lysosomes this effect results in an increased uptake of protons and the balancing anions like chloride ions, leading to an osmotic influx of water and finally to rupture of the endosomal structures and DNA release.

Protocol: 24 hours before transfection cells were seeded on coverslips in 60 mm dishes. 10 µg DNA were diluted in 750 µl 150 mM sodium chloride, and 100 µl PEI (0.9-1 mg/ml in water) were diluted with 650 µl sodium chloride solution. After 15 minutes of incubation at room temperature the PEI solution was added drop-wise to the DNA solution and the mixture was incubated for additional 15 minutes. 500 µl of the mixture were added drop-wise to 2.5 ml medium into the cell dish and the cells were incubated for 3 to 6 hours at 37°C. Afterwards cells were washed with PBS and incubated for 24 to 48 hours in fresh medium before fixation and processing for immunofluorescence (2.9.1). For time-course experiments cells were fixed 5, 10, 24, 48, and 72 hours after the start of transfection.

2.8.4.2 DEAE-Dextran transfection

For immunoprecipitations COS-7 cells were usually transfected using Diethylaminoethyl(DEAE)-Dextran. The DNA binds to the polycationic DEAE-Dextran forming complexes, which are adsorbed at the cell surface and endocytosed. To avoid lysosomal degradation cells are incubated with chloroquine preventing the pH decrease and therefore the activation of acidic hydrolases.

Protocol: 10 µg DNA and 9 µl DEAE-Dextran (50 mg/ml) were diluted in 1.5 ml DMEM without FBS and incubated at room temperature for 15 minutes. A dish with cells at 50-70% confluence was washed with PBS, incubated with the DEAE-Dextran mixture for 90 minutes at 37°C, and was carefully shaken every 15 minutes. Subsequently, the medium was renewed and the cells were incubated with 60 µg/ml chloroquine for 2.5

hours. Maximal expression of the transfected genes was achieved 48 hours after transfection.

2.8.4.3 Electroporation

Electroporation is the only method used which requires cells in suspension. For some cell types electroporation results in a high mortality rate, but the great advantage of this technique is the high transfection efficiency and the possibility to transfect cells which are usually difficult to transfect. In particular for the transfection with siRNA (2.8.5) electroporation turned out to be the method of choice due to the very high transfection rate. Adherent cells have to be trypsinized before transfection. It is not entirely clear how the nucleic acids enter the cell, probably the electric pulse leads to disruption of the cellular membrane potential which results in transient permeability of the cell membrane and diffusion of the DNA/RNA into the cell. The electroporation parameters (voltage/Volt, capacitance/Farad, resistance/Ohm) have to be optimized for every cell type.
Protocol: A confluent dish of cells was trypsinized as described in 2.8.1. The cell pellet was washed by resuspension in 5 ml HBS buffer (2.6) and re-centrifugation. HBS buffer has low ion strength which is required for safe and efficient application of the electric pulse. The cell pellet was resuspended in 0.5 to 1 ml HBS buffer and 0.5 ml of this cells suspension were mixed with DNA (10 µg) or siRNA (2.8.5) in a 4 mm gap electroporation cuvette. Electroporation of COS-7 or COS-GFP-SKL cell was performed at 230 V, 1500 µF, and 125 Ω. Subsequently, the cells were mixed quickly with 1 ml of complete medium and seeded in dishes prepared with pre-warmed medium.

2.8.4.4 Microinjection

Microinjection is a transfection method in which DNA is mechanically injected directly into the cell nucleus using a fine glass capillary. Precise pressure application induces the injection of the low amounts of DNA solution (femtoliters) from the capillary into the cell. An advantage of this method is the possibility to transfect non-dividing cells or cells which have been manipulated in ways interfering with other transfection methods, e.g. the depolymerisation of the cytoskeleton (see 3.4). Disadvantages are the low number of transfected cells, as every single cell has to be injected, and the difficulty to find the correct parameters, otherwise the injection results in rupture of the cells.

Protocol: A semiautomatic microinjection system (Eppendorf) was used, which allows a sequence of microinjections once the injection parameters and the injection level are established. The DNA solution was diluted to a concentration of 50 ng/µl in water and centrifuged for 15 minutes at 13,000 rpm to remove particles which might block the capillary. Using microloader pipette tips 3 µl of the DNA solution were filled into the glass capillary (Femtotips, 0.5 µm inner and 1.0 µm outer diameter) which was then connected to the microinjector. Cell dishes with cells growing on coverslips were placed onto an inverse microscope (40-fold magnification). The micromanipulator (InjectMan NI 2) controls the position of the capillary and triggers the injection performed by the microinjector (FemtoJet; 0.8 to 1 bar for 0.5 to 1 second). Usually 300 to 600 cells were transfected per session and cells were fixed after 24 hours.

2.8.4.5 Lipofection

The lipofection technique is based on the formation of liposomal structures which fuse with the cell membrane and enter the cell by endocytosis. The lipofectamine reagent (Invitrogen), a mixture of cationic and neutral lipids binds to the negatively charged DNA and forms a liposomal complex around it which allows the DNA delivery. For transfection of plasmid DNA the lipofectamine reagent and for transfection of siRNA the lipofectamine RNAiMax reagent were used.

Protocol: The DNA/siRNA was diluted in medium without antibiotics and FBS (Solution A) and incubated at room temperature for 15 minutes. A dilution of the transfection reagent with medium (Solution B) was incubated at the same time. After careful mixture of the two solutions, the transfection mix is again incubated for 15 minutes at room temperature and subsequently added drop-wise to the cell medium (without FBS and antibiotics). After five hours or the next day the medium was changed to complete medium. For the exact amounts used please refer to Table 2.14.

Dish	Seeding medium	Solution A		Solution B	
		Medium	DNA (siRNA)	Medium	Lipofectamine (RNAiMax)
100 mm	5 ml	500 µl	8 µg (120 pmol)	500 µl	30 µl (10 µl)
60 mm	2 ml (2.5 ml)	200 µl (250 µl)	3.2 µg (60 pmol)	200 µl (250 µl)	12 µl (5 µl)
12 well	400 µl	50 µl	0.8 µg (12 pmol)	50 µl	2 µl (1 µl)

Table 2.14: Lipofectamine transfection
Values for siRNA transfection with Lipofectamine RNAiMax are in brackets. 12 well plate amounts are given per well.

2.8.5 RNA interference

RNA interference (RNAi) is a method for specific inhibition of the synthesis of a certain protein. By degradation of the respective mRNA the protein expression can be reduced up to 90% of the normal level, which is called "knock down" or "silencing" of the protein. For this purpose an intracellular mechanism comparable with the "immune system of the genome" is utilized, which is normally targeted against viral genomes or transposons to maintain genomic stability, or to regulate gene expression with genomically encoded microRNAs. A short double-stranded RNA molecule with a length of 21 to 23 base pairs, called small interfering RNA (siRNA) is introduced into the cell (see 2.8.4). It is also possible to use longer double-stranded RNA molecules, which are intracellular cleaved into siRNAs by an enzyme called Dicer. The siRNA is incorporated into a RNA protein complex, the RNA-induced silencing complex (RISC), where one of the RNA strands is removed. The remaining (guide) strand mediates the binding of RISC to the complementary (target) mRNA which is cleaved and degraded. The amounts of the target mRNA are drastically reduced, which inhibits further synthesis of the encoded protein (Elbashir et al. 2001). The maximal protein "knock down" is reached 2 to 3 days after transfection.

Protocol: siRNA was purchased as lyophilized duplexes from Ambion (Austin, USA) which were resuspended in nuclease free water according to the manual (50 µmol/l), aliquoted and stored frozen at -20°C. Transfection with siRNA was performed by electroporation (2.8.4.3) using 20 µl siRNA (1 nmol) per approach. The siRNA sequences used are listed in Table 2.15. If several sequences are indicated a mix of those was applied. siRNA targeted to luciferase, a non-mammalian protein, was used as control sequence.

Target gene	Sequence
Pex19 #1	5'-GGAGAUCACAGAAAAGUAUtt-3'
Pex19 #2	5'-GGAGACACUGCCAAAGAUGtt-3'
Pex19 #3	5'-GGAACUAUUCGACAGUGAAtt-3'
Pex19 #4 (Jones et al. 2004)	5'-GAGAUCGCCAGGAGACACUtt-3'
DLP1 (Koch et al. 2004)	5'-UCCGUGAUGAGUAUGCUUUtt-3'
Luciferase	5'-CGUACGCGGAAUACUUCGAtt-3'

Table 2.15: siRNA sequences

For experiments combining DLP1 knock down and protein expression (3.4), cells were re-transfected after 48 hours with plasmid DNA by electroporation, seeded on cover-

slips, and fixed after 24 hours. For import studies after Pex19p silencing (3.1), cells were also re-transfected after 48 hours but fixed after 3, 6, and 24 hours.

2.9 Microscopic techniques

2.9.1 Immunofluorescence

Immunofluorescence (IMF) is a method which allows the specific staining of proteins in fixed cells and their subsequent examination using a fluorescence or confocal microscope. It utilizes the specific binding of antibodies, which are conjugated to fluorescent dyes, to their epitopes. Indirect immunofluorescence takes advantage of the application of two types of antibodies. The primary antibodies are not labelled and bind to their respective target proteins. Secondary antibodies, which are coupled to fluorescent dyes, recognize the Fc domain of the primary immunoglobulin. This results in signal amplification, as the complete Fc domain can be bound by the secondary antibody, and it allows the utilization of a small number of fluorochrome-coupled antibodies in a broad range of applications. Proteins introduced by transfection are often fused to a tag like Myc or HA, a short amino acid sequence which can be recognized by specific antibodies. This is in particular useful if antibodies directed to the protein itself are not available.

Several preparative steps are necessary before cells can be processed for immunofluorescence. (1) To avoid degradation and for stabilization of e.g. certain structures, the cells have to be fixed, which is achieved with formaldehyde. Formaldehyde cross-links proteins by formation of methylene bridges in between the amino groups of lysine side chains and the nitrogen atom of a peptide linkage (Kiernan 2000). (2) For the antibodies to have access to intracellular structures, cells have to be permeabilized. Routinely, Triton X-100 was used, a non-ionic detergent which removes lipids from the membranes creating pores. To achieve a differential permeabilization only affecting the plasma membrane and not the peroxisomal membrane, digitonin was used. This glycoside acts as a detergent mainly on cholesterol, which is only present in low amounts in the peroxisomal membrane. The permeabilization with digitonin was also applied in all studies including Myc-tagged Pex11 proteins (see 3.2.2) to avoid the observed loss-of-signal with Triton X-100 (Schrader et al. 1998b). (3) The high number of protein epitopes within the cell and the presence of free aldehyde groups might lead to unspecific interac-

tions with the antibodies (e.g. due to charge), requiring the block of these binding sites with a protein solution, e.g. bovine serum albumin (BSA).

Protocol: Cells grown on coverslips were washed twice with PBS to remove residual medium and fixed with 4% formaldehyde (2.6) for 20 minutes at room temperature. The cells were washed tree times with PBS and washing was performed in between all further incubation steps. Cellular membranes were permeabilized using 0.2% Triton X-100 for 10 minutes or 2.5 µg/ml digitonin for 5 minutes. Afterwards unspecific binding sites were blocked by incubation with 1% BSA for 10 minutes. Incubation with the primary antibodies was performed for 1 hour in a humid and dark environment to avoid drying of the cells, followed by incubation with the secondary antibodies in the same way. If a set of several (primary or secondary) antibodies was used, the incubation occurred simultaneously. For the dilution of the antibodies see section 2.4. For visualization of the cell nuclei the DNA was stained using Hoechst dye as described (2.8.3.1). The coverslips were washed with distilled water to avoid crystal formation of the salts present in PBS, mounted on glass slides using Mowiol and dried over night before microscopic examination.

2.9.2 Fluorescence microscopy

The fluorescence microscopy is based on the characteristics of a specific group of substances, the fluorophores. Each fluorophore can be excited by light of a specific wave length, which leads to emission of light with a longer wavelength, appearing in a different colour. In this study fluorophores were mainly used coupled to antibodies in immunofluorescence preparations (2.9.1). The utilization of fluorophores with different excitation and emission spectra (see Table 2.16) in combination with a specific filter set allows the visualization of several proteins or structures in the same sample.

In fluorescence microscopes illumination of the sample occurs via the objective onto the specimen and the emitted fluorescent light passes through the same objective towards the detector, which might be the eye or a CCD camera. Light source is a mercury-vapor lamp and an excitation filter selects the excitation wave length directed to the specimen by a dichroic mirror. The dichroic mirror works like a selective filter and only the light emitted by the fluorochrome passes. It is directed to an emission filter and focused in the ocular. For morphological studies the Olympus BX-61 and IX81 (inverted) microscopes were used. Digital images were taken with the CCD camera F-View II and selected

and optimized for contrast and brightness using Olympus Soft Imaging Viewer, Adobe Photoshop and Microsoft Power Point software.

Name	**Excitation** [nm] max.	**Emission** [nm] max.	**Colour** (approx.)
AlexaFluor 350	346	442	
DAPI Hoechst 33258	359	450	blue
CFP	383	445	
GFP	395	475	green
YFP	434	477	
AlexaFluor 488	495	519	green-yellow
FITC	492	520	
R110Direct ligand	502	527	
TRITC	550	570	orange-red
TMR ligand	555	585	
DsRed/RFP	558	583	
mRuby	558	605	red
Texas Red	596	620	

Table 2.16: Characteristics of selected fluorophores and fluorescent proteins

2.9.2.1 Image deconvolution

In a conventional fluorescence microscope (2.9.2) the entire specimen (also outside the focal plane) is illuminated and emits fluorescent light, resulting in high background signals and low contrast. One method to deal with the "out-of-focus" signals is the computational approach of image deconvolution. A series of images in different focal planes (stack) is obtained creating a blurred three-dimensional image. Afterwards, a computer program calculates the theoretical blurring of each point and removes the equivalent blur (deconvolution) from the image. This results in a series of clear optical sections (Alberts et al. 2002). Images for deconvolution were taken at 200 nm intervals with a Plan-Neofluar 100x/1.35 oil objective on an Olympus BX-61 microscope and deconvolution was performed using Soft Imaging software.

2.9.3 Confocal microscopy

As described above (2.9.2.1), an ordinary fluorescence microscope has optical limitations in achieving clear and focussed images. In particular in co-localization studies, the signal from above or below the focal plane can lead to false-positive results. In a confocal

laser scanning microscope (CLSM), a laser beam is focused on one point of the specimen by the objective. The emitted fluorescent light has to pass a pinhole, which prevents the passage of light outside of the focal point, before it is detected by a photomultiplier. The focal point and the pinhole are arranged in an optically conjugated – confocal – plane. The laser beam scans the specimen point-by-point creating a complete digital image. Three dimensional images can be created by successive scans in different focal planes. A disadvantage compared to conventional fluorescence microscopy is the low fluorescence intensity which can require long exposure times/slow scanning speeds. For confocal microscopy a Zeiss LSM 510 confocal microscope and the associated software was used. Images were selected and optimized for contrast and brightness using Zeiss LSM Image Browser and Adobe Photoshop software.

2.9.4 Quantitative examination

For quantification of the peroxisomal morphology 100 to 200 cells per coverslip were characterized, two coverslips per experiment were analyzed and each experiment was performed two to four times. Usually, peroxisomes were categorized as spherical and rod-like (0.1 to 1 µm) or as tubular (> 1 µm) (Schrader et al. 1996). Data analysis and preparation of diagrams was done using Microsoft Excel software. Data are presented as means ± standard deviation (SD). An unpaired t-test was used to determine statistical differences between experimental groups. P values < 0.05 are considered as significant and P values < 0.01 are considered as highly significant.

For import assays (3.1.2), fluorescence intensities were determined on digital images acquired with identical settings by encircling single peroxisomes (or mitochondria), and the GFP/TRITC ratio was calculated. Images were processed and quantified using LSM 510 software (Carl Zeiss). 60-140 peroxisomes per cell were analyzed in about 60 control as well as treated cells.

2.9.5 Live cell imaging

The expression of proteins fused to fluorescent proteins allows the direct observation with a fluorescence or CLS microscope. The most common fluorescent protein are the green fluorescent protein (GFP) and its yellow (YFP) and cyan (CFP) variants isolated from the jellyfish *Aequorea victoria*. The fluorophore properties originate from three

internal amino acids (Ser 65 – Tyr 66 – Gly 67, Prasher et al. 1992; Tsien 1998; Yang et al. 1996). Also red fluorescent proteins like DsRed/RFP (from the reef coral Discosoma sp. Baird et al. 2000; Matz et al. 1999), and mRuby (from Entacmaea quadricolor, an anemone, Kredel et al. 2009) are available. For the emission and excitation wavelengths see Table 2.16. Fluorescent tagged proteins can be observed in fixed or living cells.

Protocol: The Zeiss LSM-510 confocal microscope was equipped with a closed chamber which was aerated with 5% warm (37°C) CO_2 to create normal culture conditions. Cells growing in glass bottom dishes in medium without phenol red (2.3.4) were placed in the warm chamber and live cell time-lapse imaging was performed. Usually images were taken in time intervals of 1 second.

2.9.6 FRAP

FRAP (fluorescence recovery after photobleaching) is a technique which allows measuring or comparison of the mobility of fluorescent-tagged proteins in a membrane. In a live cell setup a certain area of the cell (region of interest, ROI; e.g. a part of a peroxisomal tubule or of the ER) expressing the fluorescent protein is bleached and the fluorescence recovery in this region is measured. Recovery occurs by lateral diffusion of non-bleached proteins from the surrounding membrane into the ROI. The time required for recovery and the degree of recovery depends on the mobility of the protein in the membrane (Lippincott-Schwartz et al. 2001).

Protocol: In a 12 bit acquisition unidirectional scan setting (zoom 2.6) a 200x200 pixel region of the cell was selected. In this region a 20x20 pixel square was chosen as bleach ROI. Bleaching was performed by a single iteration at 100% power of all four argon laser lines (458, 477, 488, 514 nm) with 6.39 µs pixel time. Usually, 230 scans with 1 second time interval were recorded and the bleaching was performed after 30 scans (t = 0 s). Fluorescence intensity was recorded for the acquisition ROI and the bleach ROI, as well as a background and a non-bleached ROI of the same size. For analysis the intensity in the bleached region was normalized for the general acquisition bleaching by scanning using the non-bleached ROI. The mean pre-bleach value was set 100%, the first post-bleach value (minimum) was set 0% and the intensities were plotted against time. Following equation was used:

$$I_t = \frac{\left(\frac{Ib_t}{Ic_t} - \left(\frac{Ib}{Ic}\right)_{min}\right)}{\left(\frac{Ib_t}{Ic_t} - \left(\frac{Ib}{Ic}\right)_{min}\right)_{max}} \times 100$$

I_t, intensity at a time point t; Ib, intensity bleach ROI; Ic, intensity control ROI; min, intensity at t=0 (bleach); max, mean of the pre-bleach intensities.

2.9.7 HaloTag technology

HaloTag is a protein tag generated from a modified haloalkane dehalogenase (Los et al. 2008). It covalently binds to synthetic ligands which comprise a chloralkane linker attached to a molecule of choice, such as e.g. fluorescent dyes. Thus, the tag can be adapted to differing experimental requirements without altering the underlying genetic construct. In this study, a HaloTag-catalase fusion protein was used in combination with two differently coloured fluorophores to selectively label the peroxisomal matrix at different times within the cell (Huybrechts et al. 2009). The experiments were performed in cooperation with Prof. Dr. Marc Fransen (Katholieke Universiteit Leuven, Belgium).

Protocol: First, COS-7 cells expressing HaloTag-catalase were enriched by cultivation of transfected cells in the presence of 600 µg/ml G418 for at least 4 weeks. To investigate the matrix protein import competence of pre-existing and newly-formed peroxisomal structures upon overexpression of Pex11pβ, the cells were incubated for 48 hours with the cell-permeable HaloTag TMR ligand at a final concentration of 250 nM. Cells were extensively washed with PBS and incubated in standard growth medium for 24 hours. Afterwards, cells were transfected with a plasmid encoding Pex11pβ-Myc by electroporation, and immediately cultivated in the presence of the cell-permeable HaloTag R110Direct ligand at a final concentration of 10 nM. Cells were fixed after 24 hours at the onset of peroxisome division and processed for immunofluorescence microscopy.

2.9.8 Electron microscopy

Electron microscopy (EM) is used for ultra structural studies with a resolution of up to 2 nm, possible because of the short wavelengths of electrons (< 1 nm). It requires irradiation under vacuum conditions to avoid scattering of the electrons by air molecules. The overall design of a transmission electron microscope is similar to a light microscope, with magnetic coils – like optical lenses – focussing the electron beam. Electrons are scattered by electron-dense (stained) material of the specimen leaving dark areas in the

image detected by a photographic plate or phosphorescent screen (Alberts et al. 2002). The specimens have to be specifically processed by fixation, dehydration, embedding and contrasting and they have to be very thin to allow passage of the electrons. The embedding in special resins (e.g. EPON) allows the preparation of these ultrathin sections. Copper grids are used as specimen holder. Ultrathin sections were analyzed using a Zeiss EM 109 transmission electron microscope. Photographs were digitalized by scanning.

2.9.8.1 Buffer and solutions

Cacodylate buffer

- 0.1 M Cacodylic acid sodium salt, pH 7.35

DAB medium, alkaline (pH 10.5)

- 0.2% 3, 3'-Diaminobenzidine
- 0.15% Hydrogen peroxide
- in Cacodylate buffer

EPON

Mixture A

- 62 ml Glycid ether (Epon 812)
- 100 ml 2-Dodecenylsuccinic acid anhydride

Mixture B

- 100 ml Glycid ether (Epon 812)
- 89 ml Methylnadic anhydride

Mixture C

- 1:1 Mixture A and mixture B
- 0.18-0.2% (v/v) 2,4,6-Tris(dimethylaminomethyl)phenol

Ito-fixative

- 2.5% (w/v) Paraformaldehyde
- 2.5% (w/v) Glutaraldehyde
- 0.05% (v/v) Pikric acid
- 0.1 M Cacodylic acid, pH 7.35

Lead citrate

- 26.6 g/l Lead nitrate ($Pb(NO_3)_2$)
- 35.2 g/l Trisodium citrate ($Na_3(C_6H_5O_7)$ x $2H_2O$)
- 16% (v/v) 1N Sodium hydroxide

Reduced osmium tetroxide

- 1% (w/v) Osmium tetroxide (OsO_4)
- 1.5% (w/v) Potassium ferrocyanide ($K_4Fe(CN)_6$)

Uranyl acetate

- 0.3% Uranyl acetate
- 50 mM Maleate, pH 5.0

2.9.8.2 Embedding in EPON

For routine electron microscopy, cultured cells (35 mm dishes) were fixed with Ito-fixative (Ito & Karnovsky 1968) for 30 minutes at room temperature and washed three times with cacodylate buffer. Postfixation with reduced osmium tetroxide was performed for 1 hour at 4°C, which binds to and stabilizes lipid bilayers as well as proteins (Alberts et al. 2002). Samples were stained with 0.3% uranyl acetate overnight at 4°C. The samples were dehydrated in a graded series of alcohol (first addition of 50% ethanol ratio 1:1, then only ethanol 50%, 70%, 90%, and 100%, 10 minutes each) followed by embedding in EPON. The cells were incubated for 30 minutes each with ethanol:EPON ratios 3:1, 1:1, 1:3, and then over night with EPON. EPON-filled gelatine capsules were put on top and EPON was polymerized at 60°C for 48 hours. Ultrathin sections (70 nm) were prepared using a diamond knife, put on copper or nickel grids and stained with lead citrate.

2.9.8.3 Immunoelectron microscopy

For immunostaining, samples were embedded in Lowicryl K4M to preserve the antigenic properties of the cells. Analogous to immunofluorescence (2.9.1), proteins can specifically be localized using antibodies. The visualization occurs with electron-dense gold particles. Cells were fixed in cacodylate buffer containing 2% paraformaldehyde

and 0.1% glutaraldehyde for 2 hours at 4°C. The cells were washed three times with cacodylate buffer, collected by scraping, incubated for one hour with 1% (v/v) tannic acid/0.05 M cacodylate buffer and washed again for 10 minutes with cacodylate buffer and water. The samples were dehydrated in a graded series of alcohol (50%, 70%, 90%, 100%, 2 minutes each), incubated with ethanol/K4M (1:1) for 10 minutes, and embedded in K4M overnight at 4°C. Cells were filled in BEEM capsules and polymerized at -20°C and UV light (360 nm) for 72 hours. Thin sections (80 nm) were prepared and, after blocking with 1% BSA in PBS for 30 minutes, sections were incubated with polyclonal antibodies directed against GFP/YFP in a dilution of 1:200 to 1:500, and visualized using 10 nm protein A-gold-containing solution at a dilution of 1:60 or 1:70 (both in 1% BSA in PBS for 1 hour), washed with PBS and water, and stained with uranyl acetate/lead citrate.

2.9.8.4 Alkaline DAB staining

Alkaline DAB (diaminobenzidine) staining is a method for cytochemical localization of catalase (Angermuller & Fahimi 1981; Fahimi 1969, 2009), one of the most abundant enzymes in the peroxisomal matrix (see 1.1.2). The method exploits the peroxidative activity of catalase, as DAB oxidized by catalase forms a brown, insoluble, and electron dense precipitate. HepG2 cells (35 mm dishes) were incubated in alkaline DAB medium for 1 hour at 37°C followed by postfixation in reduced osmium tetroxide and 2% uranyl acetate (Schrader et al. 1994). The samples were dehydrated in a graded series of alcohol and embedded in EPON as described in section 2.9.8.2.

2.10 Biochemical techniques

2.10.1 Preparation of cell lysates

To analyze the protein content of cells, e. g. after RNA interference experiments (2.8.5) or similar approaches, a lysate of mammalian cells was prepared.

Protocol: A confluent dish (60 mm or 100 mm) of cells was rinsed with PBS and the cells were harvested by scraping with a rubber policeman in 1 to 1.5 ml PBS. The cells were pelleted by centrifugation (800 g for 5 minutes) and resuspended in 0.5 to 1 ml lysis buffer containing protease inhibitor mix (2.6) on ice. The cells were passed ten times

through a 26 G needle followed by over-head rotation for 30 minutes at 4°C to guarantee complete lysis. To remove DNA and left cell debris the lysate was cleared by centrifugation at 13,000 rpm and 4°C for 15 minutes.

2.10.2 Preparation of peroxisome-enriched fractions

To isolate subcellular components from cultured cells or tissue, they have to be released from the cells by homogenization. It is crucial not to damage the organelles and to protect proteins from degradation, achieved by choosing the right buffer conditions and by addition of protease inhibitors. The homogenate containing organelles, membrane fragments and cytosol with its soluble components can be subfractionated by centrifugation. The differences in density and size (sedimentation coefficients) allow a separation of the organelle fractions by differential centrifugation. Increasing speed and time, organelles pellet in the following order: nuclei, mitochondria, peroxisomes, and microsomes, the vesicular endosomal compartment. The obtained fractions are only enriched in the respective organelle populations and for further purification of the organelle fractions density gradient centrifugation has to be applied. In this study only fractions enriched in peroxisomes and mitochondria were prepared.

Protocol: Two confluent 100 mm dishes of COS-7 cells were rinsed with PBS and the cells were harvested in a total volume of 4 ml PBS. The cells were pelleted by centrifugation (5 minutes, 800 g), resuspended in 1 ml peroxisome homogenization buffer containing protease inhibitors (2.6) and transferred to a microcentrifuge tube on ice. The cells were homogenized by passing ten times through a 26 G needle. Remaining intact cells were pelleted by centrifugation (5 minutes, 500x g, 4°C), the supernatant was collected and the cell pellet was re-homogenized as described. This procedure was performed twice, and the nuclei were removed from the collected supernatant by centrifugation at 800x g for 5 minutes. The mitochondria-enriched fraction was prepared by centrifugation at 2,000x g for 10 minutes at 4°C. The supernatant was transferred to a Beckman centrifuge tube and centrifuged for 20 minutes at 25,000x g and 4°C to prepare a peroxisome-enriched fraction. To generate a microsome-enriched fraction, the supernatant was transferred to an ultracentrifuge tube and the sedimentation occurred by centrifugation at 125,000x g for 1 hour. The remaining supernatant represents the cytosolic fraction. The organelle pellets were carefully resuspended in small volumes of homogenization or lysis buffer, depending on the downstream application.

2.10.3 Protein precipitation

Proteins were precipitated to remove lipids, detergents or other interfering components and to concentrate protein samples. Routinely, precipitation was performed using chloroform and methanol (Wessel & Flugge 1984).

Protocol: One volume of protein-containing sample (100 µl) was mixed with three volumes of methanol (300 µl), followed by mixing with one volume of chloroform (100 µl) and three volumes of water (300 µl). Centrifugation for 3 minutes at 13,000 rpm separated the solution in two phases divided by a white interphase containing the proteins. The top aqueous phase was removed and discarded, and three volumes of methanol (300 µl) were added. After another centrifugation step (3 minutes, 13,000 rpm) the precipitated proteins were found in the bottom pellet and the supernatant was discarded. The pellet was air-dried and dissolved, e. g. in SDS loading buffer (25 to 50 µl).

2.10.4 Measurement of protein concentration

Measurement of the protein concentration, e.g. for equal gel loading, was performed using the Qubit quantification kit (2.3.3), a fluorophore-based method, or the Bradford assay. The Bradford assay is a colour-based method using Coomassie brilliant blue. This dye binds (unspecific) to cationic and non-polar amino acid side chains. The binding to proteins (or an acidic environment) leads to a shift of the absorption maximum from 465 nm to 595 nm. Therefore, the colour intensity at 595 nm correlates to the amount of protein present in the sample and can be measured. As reference a number of standards containing specific amounts of BSA is used. The Bradford assay can be disturbed by the following substances: Triton X-100 (> 0.5%), SDS (> 0.1%), and sodium deoxycholate (Lottspeich & Engels 2006).

Protocol: Standards containing 1 to 20 µg BSA, blank, and samples (1 to 10 µl) were filled up to 100 µl with 0.1 M NaOH. Proteinassay (Bradford) solution was diluted 1:5 with distilled water and 1 ml of the solution was added to each sample. All standards and samples were prepared as triplicates. After 15 minutes of incubation at room temperature the absorption at 595 nm compared to the blank was measured. Using the standard curve prepared from the mean values, the protein concentration of the samples was calculated.

2.10.5 SDS-PAGE

Electrophoresis describes the movement of charged particles in an electric field, where differences in charge or size of the particles result in differences in the electrophoretic mobility. The one-dimensional polyacrylamide gel electrophoresis (PAGE) separates proteins according to their molecular weight. The separating matrix is formed by a net of acrylamide polymers, which are cross-linked by N'N'-methylenebisacrylamide. The size of the pores in the net is determined by the concentration of the acrylamide monomers and the degree of cross-linking. The polymerization is initiated by decay of peroxide sulphate ions (APS) leading to a radical chain reaction. The radicals activate tetramethylethelenediamine (TEMED) which initiates the cross-linking.

In order to separate proteins in a polyacrylamide gel via electrophoresis they have to be equally charged, meaning the charge/size ratio has to be equal for all proteins to achieve a fractionation depending only on the protein molecular weight. Sodium dodecyl sulphate (SDS) is an anionic detergent which binds to hydrophobic regions of proteins and provides them with a negative charge corresponding to the protein size. Approximately one SDS molecule binds per two amino acids, masking the intrinsic charge of the protein. The negatively charged proteins move towards the anode during the gel electrophoresis. Before loading of the proteins on the gel, they are denatured at 95°C for 5 minutes in SDS-containing loading buffer (2.6). Additionally, reducing agents in the loading buffer (DTT and β-mercaptoethanol) help in the denaturation process by cleavage of disulphide bonds.

In this study discontinuous Tris-chloride/Tris-glycine buffer systems according to Laemmli (1970) were used. The separation of the proteins occurs in the "separating gel" at pH 8.8. To achieve clear and focussed protein bands, the first part of the gel is a "stacking gel" at pH 6.8 for protein concentration and pre-separation. In the stacking gel glycine is barely charged and has therefore low mobility during the electrophoresis (terminating ion), while chloride anions are highly mobile (leading ion). Proteins move in between these ions in an electrical field gradient and form a protein stack according to their mobility. At the border of the two gels the proteins accumulate and the protein bands are focused, while the small glycine moves into the gel. Thus, the proteins are in a homogenous buffer and the proteins are separated according to their size.

Protocol: Standard SDS-PAGE was performed with 12.5% separating and 5% stacking gels. To exclude oxygen, which inhibits the polymerization process, the gel solution was

covered with a layer of isopropyl alcohol or 0.1% SDS. Gel recipes are presented in Table 2.17. Gel electrophoresis in mini slap gel chambers was conducted for approximately 30 minutes at 80 V until the proteins entered the resolving gel and continued at 130 V for approximately 90 minutes. Electrophoresis of large gels (e.g. gradient gels) was performed for around 4 hours. The gel chambers were filled with 1x SDS running buffer (2.6). To mark protein size a pre-stained molecular weight marker (Rainbow, 2.3.2) was used and the sample running front was visualized by bromophenol blue added to the loading buffer.

	Stacking gel	**Separation gel**		
	5%	7.5%	12.5%	15%
30% Polyacrylamide	1.66 ml	4.0 ml	6.67 ml	8.0 ml
2 M Tris pH 8.8 (360 mM)	-	2.89 ml	2.89 ml	2.89 ml
1 M Tris pH 6.8 (125 mM)	1.25 ml	-	-	-
20% SDS (0.1%)	50.0 µl	80.0 µl	80.0 µl	80.0 µl
dH_2O	6.95 ml	8.89 ml	6.22 ml	4.89 ml
TEMED (0.1%/0.05%)	10.0 µl	8.0 µl	8.0 µl	8.0 µl
10% APS (0.8%/0.3%)	80.0 µl	48.0 µl	48.0 µl	48.0 µl
Total volume	10.0 ml	16.0 ml	16.0 ml	16.0 ml

Table 2.17: Gel solutions for SDS-PAGE
Final concentrations are in brackets.

2.10.6 Immunoblotting

Immunoblotting is a method for specific detection of proteins in a sample that was prior separated by SDS-PAGE. The proteins are electrophoretically transferred – blotted – from the polyacrylamide gel onto a (nitrocellulose) membrane, a process called Western blot (Burnette 1981; Towbin et al. 1979). The proteins on the membrane are immobilized and can be detected, e.g. by an indirect immune reaction. A specific primary antibody recognizes specifically the protein band on the membrane and a secondary antibody directed to its Fc domain is used for detection. The secondary antibody is coupled to a fluorophore or an enzyme which catalyzes a detectable (e. g. colour) reaction. In this study secondary antibodies coupled to horseradish peroxidase (HRP) were used (2.4) for detection by enhanced chemiluminescence (ECL). HRP oxidizes luminol and transfers it into an excited state. Upon return to the ground state, a photon (light) is liberated and can be detected by a photosensitive film. After development and fixation, illuminated areas appear as dark bands on the film.

Protocol: Protein transfer to the membrane was performed by semi-dry Western blotting (Kyhse-Andersen 1984). The nitrocellulose membrane and two Whatman filter papers (3 mm) were soaked with semidry blotting buffer (2.6) and a stack of Whatman filter, membrane, gel, and Whatman filter was formed. Air bubbles in between the layers had to be removed to guarantee complete transfer. The stack was put into a semidry transfer chamber and the proteins were blotted for 40 minutes at 12 V. As the proteins are still covered with SDS, they move towards the anode.

After the transfer unspecific binding sites on the membrane were blocked by incubation with 5% low fat powdered milk in PBS for 1 hour. For incubation with the primary antibody the membrane was sealed into a plastic bag with the respective antibody dilution (2.4) in PBS and incubated with shaking over night at 4°C or for 2 to 3 hours at room temperature. Afterwards the membrane was washed three times for 10 to 15 minutes to remove excess (unbound) antibody. The incubation with the secondary antibody was performed for 1 to 2 hours at room temperature. For the ECL reaction, ECL 1 (containing luminol) and ECL 2 (phenol-containing enhancer) solutions were mixed (ratio 1:1) and the membrane was incubated for 2 minutes. Film exposition (3 to 30 minutes), development and fixation were performed in a light protected environment. For presentation and quantification the films were scanned with a Bio-Rad GS-710 Calibrated Imaging Densitometer and densitometric analysis for quantification was done using Bio-Rad Laboratories Quantity One software.

2.10.7 Immunoprecipitation

2.10.7.1 Co-immunoprecipitation

Immunoprecipitations (IPs) are used to prove the interaction of two proteins or to show that two (or more) proteins are part of the same complex. A target protein is isolated out of a protein mixture, such as a cell lysate, by antibody binding and precipitation of the antigen-antibody-complex e. g. by conjugation to large particles and centrifugation. The (co-immunoprecipitated) proteins attached to the initial target protein can be identified by SDS-PAGE and immunoblot analysis or by mass spectrometry. For analysis of weak or transient interactions, the proteins can be cross-linked with bi-reactive agents (see 2.10.7.2).

In this study, co-immunoprecipitations were performed with antibodies bound to agarose or sepharose particles, so-called beads. Antibodies directly conjugated to agarose beads (anti-Myc, see 2.4) or Protein A-coupled sepharose (PAS) beads in combination with regular antibodies were used. Protein A isolated from *Staphylococcus aureus* binds reversible to the Fc domain of many immunoglobulins, generating a tool for binding a large spectrum of antibodies to beads.

Protocol: Protein A-sepharose was incubated twice over night in PBS (5 ml PAS in 50 ml PBS) at 4°C and for storage 0.1% sodium azide was added. For co-immunoprecipitations (see Table 2.18) two confluent 100 mm dishes of COS-7 cells co-transfected with the plasmids encoding the respective proteins by DEAE-Dextran (2.8.4.2) or electroporation (2.8.4.3) were used. The cells were washed with PBS and carefully harvested in a total volume of 5 ml PBS by scraping. All further steps were performed on ice. A cell pellet was prepared by centrifugation (5 minutes, 500x g) and resuspended in 500 µl lysis buffer containing protease inhibitors (2.6). The cells were lysed by passing ten times through a 26 G needle followed by over-head rotation for 30 minutes at 4°C. In order to remove DNA and cell debris the lysate was cleared by centrifugation at 13,000 rpm and 4°C for 15 minutes. A pre-clearing was performed to avoid unspecific binding to PAS. The cell lysate was incubated with 30 µl PAS and rotated for 1 hour at 4°C. The beads were removed by centrifugation at 5,000 rpm for 1 minute. The supernatant was pre-incubated with the antibody (2.4) for 1 hour before PAS (50 µl) was added. The pre-incubation was not performed when anti-Myc agarose beads were used. To allow complex formation the samples were incubated over night with over-head rotation. Afterwards, the beads were precipitated by centrifugation (1 minute, 5,000 rpm) and the supernatant was removed. Samples of the cell lysate and the supernatant (100 µl) were precipitated with chloroform and methanol (see 2.10.3) and used as expression controls (input). The beads were washed twice with wash buffer I, wash buffer II and PBS and resuspended in SDS loading buffer (2.6). Proteins were detached from the beads and from each other by heating at 95°C for 5 minutes before further analysis by SDS-PAGE and immunoblotting. Controls were performed in parallel without addition of antibodies.

Plasmid A	Plasmid B	Cross-link	Antibody
Pex11pβ-Myc	YFP-Pex19p	-	anti-Myc agarose
YFP-Pex19p	Myc-hFis1	+	anti-GFP/YFP, PAS

Plasmid A	Plasmid B	Cross-link	Antibody
pEYFP-N1	Myc-hFis1	+	anti-GFP/YFP, PAS
-	-	-	anti-hFis1, PAS
Myc-hFis1	-	-	anti-hFis1, PAS
Myc-hFis1	pEYFP-N1	-	anti-Myc agarose
Myc-hFis1	YFP-Pex19p	-	anti-Myc agarose
Myc-hFis1-ΔC	YFP-Pex19p	-	anti-Myc agarose
Myc-hFis1-ΔTM/C	YFP-Pex19p	-	anti-Myc agarose
GFP-hFis1	HA-Pex19p	-	anti-GFP/YFP, PAS
hFis1-YFP-TM/C	HA-Pex19p	-	anti-GFP/YFP, PAS
GFP-hFis1$^{K149/151A}$	HA-Pex19p	-	anti-GFP/YFP, PAS
pEGFP-N1	HA-Pex19p	-	anti-GFP/YFP, PAS

Table 2.18: Co-immunoprecipitations performed in this study

2.10.7.2 Cross-linking

To improve the analysis of protein interactions cross-linking agents can be used. This might be necessary if protein interactions are rather transient or weak. Dithio-bis(succinimidyl propionate) (DSP) is an example of a cross-linking agent. This molecule is membrane permeable and can enter the cells and organelles by diffusion. It is homobi-functional and has two identical reactive groups, activated esters, which react with pri-mary amines of proteins and are separated by a spacer. The spacer is cleavable and the cross-link can be removed by reducing agents as they are contained in SDS loading buffer.

Protocol: 20 mg DSP were freshly dissolved in DMSO and added drop-wise to 50 ml PBS resulting in a final concentration of 400 µg/ml. Before harvesting the cells (see 2.10.7.1) they were incubated with DSP for 45 minutes at room temperature. DSP reactivity was quenched by Tris present in the lysis buffer.

2.10.7.3 Endogenous co-immunoprecipitation

For co-immunoprecipitation of endogenous, not exogenously expressed proteins (hFis1 and Pex19p) the utilization of a different buffer system turned out to work better. All other steps were conducted as described for regular co-immunoprecipitation (2.10.7.1). After preparation of the cell lysate the protein amount in each sample was measured and identical protein concentrations were used for immunoprecipitation.

Lysis buffer

- 50 mM Tris
- 120 mM Sodium chloride
- 4% (w/v) CHAPS
- Protease inhibitors

Washing buffer

- 50 mM Tris
- 120 mM Sodium chloride

2.10.7.4 Peroxisome immunoprecipitation

An organelle immunoprecipitation aims at precipitating whole membrane pieces and the containing proteins. The protein content for example of the peroxisomal membrane can be analyzed and compared under different conditions. The membranes were precipitated using an antibody targeted to the tag of an expressed peroxisomal membrane protein (Pex11pα-YFP). The peroxisomes from a peroxisome-enriched fraction were opened using a hypotonic buffer before precipitation of the peroxisomal membranes.
Protocol: A peroxisome-enriched fraction from four confluent 100 mm dishes of COS-7 cells was prepared as described in section 2.10.2. The organelle pellet was resuspended in 400 µl hypotonic lysis buffer (2.6) leading to osmotic rupture of the organelles. Immunoprecipitation was performed using an anti-GFP antibody and PAS according to section 2.10.7.1. The beads were washed with TBS buffer containing protease inhibitors. By precipitation with chloroform and methanol (2.10.3) and resuspension in SDS loading buffer, proteins were removed from the membranes and could be analyzed by SDS-PAGE and immunoblotting.

2.11 Molecular biology techniques

2.11.1 RNA isolation

RNA isolation and subsequent transcription into cDNA can be used for two different purposes. To amplify the cDNA of a specific protein by PCR for cloning into an expres-

sion vector or for measuring the mRNA level of a protein or set of proteins by quantitative PCR approaches.

Protocol: Two different methods for RNA isolation were used. For isolation using the RNeasy Kit (Qiagen, 2.3.3) cellular pellets were frozen at –80°C or used freshly and homogenized in the provided buffer by means of a 20 G needle. The RNA is isolated by binding to a silica membrane. Elution was performed using two times 30 µl RNase-free water.

RNA isolation using TriFast (2.5.1), also known as Trizol, was performed according to the manufacture's protocol. A confluent 60 mm dish of COS-7 cells was lysed by addition of 1 ml TriFast and passing the lysate several times though the pipette. The amount of TriFast used depends on the area of the culture dish. The lysate was incubated at room temperature for 5 minutes before 200 µl chloroform were added. The tube was shaken vigorously by hand for 15 seconds and incubated at room temperature for 5 minutes. Centrifugation at 12,000x g and 4°C for 5 to 15 minutes leads to phase separation into a lower red, phenol-chloroform phase containing proteins, an interphase containing DNA and an upper, colourless aqueous phase containing RNA. The aqueous phase was transferred to a new reaction tube and RNA was precipitated by addition of 500 µl isopropyl ethanol and incubation at 4°C for 10 minutes. A gel-like RNA pellet was formed by centrifugation (12,000x g, 4°C) for 10 minutes and washed twice with 1 ml 75% ethanol followed by centrifugation. The RNA was dissolved in 30 µl RNase-free water. RNA concentration was measured as described in 2.11.13.

2.11.2 cDNA synthesis

Reverse transcriptases are RNA-dependent DNA polymerases isolated from viruses. They are used for RT-PCR (reverse transcription-PCR) to transcribe mRNA into so called complementary DNA (cDNA). cDNA contains all transcribed genes of a cell present at a certain moment and the number of cDNAs coding for a particular protein correlates to its number of mRNAs. cDNA is more stable than mRNA and can be used as template for regular PCRs. cDNA does not contain introns, in contrast to genomic DNA, and facilitates the cloning of genes into expression vectors. Determination of cDNA levels is a common method to quantify the mRNA levels of a cell, e.g. by semi-quantitative (SQ-) PCR (2.11.4). Reverse transcriptases require a starting point for cDNA synthesis, usually provided by an oligo(dT) primer annealing to the poly(A) tail of the mRNA.

Protocol: Reverse transcriptase isolated from *Moloney Murine Leukemia Virus* (M-MuLV-RT) was used and 3 µg RNA were transcribed per reaction (see 2.5.1 and Table 2.19). Annealing of the primer occurred during 10 minutes incubation at room temperature, followed by transcription at 42°C for 90 minutes (shaking). The enzyme was inactivated at 99°C for 5 minutes and cDNA was stored at –20°C.

3.0 µg	mRNA
0.5 µl	M-MuLV reverse transcriptase (200 U/µl)
2.8 µl	Oligo(dT) primer (100 µM)
0.6 µl	50x dNTP mix (10 mM each)
3.0 µl	10x RT buffer
0.5 µl	RNase inhibitor (40 U/µl)
x µl	DEPC-treated water
30 µl	Finale volume

Table 2.19: Reverse transcription

2.11.3 PCR

The polymerase chain reaction (PCR) is a technique for amplification of (known) DNA sequences. A thermostable DNA-dependent DNA polymerase, most common is Taq polymerase isolated from *Thermus aquaticus*, synthesizes a DNA strand complementary to the template, starting at free 3'-OH ends. Forward (up) and reverse (down) primers, each providing a free 3'OH end, are used to amplify the DNA strand enclosed by the two primers (see 2.5.4). Primers are oligonucleotides with a length of 20 to 30 nucleotides. They are complementary to a short sequence in the selected gene and specifically bind to or hybridize with this sequence. The forward primer binds to the coding and the reverse primer to the non-coding DNA strand. The chosen primers define which piece of DNA is amplified. It is possible to add additional (non-complementary) nucleotides to the ends of the primers, in order to add for example cutting sites for certain restriction enzymes to each end of a coding sequence. The template of a PCR can be genomic DNA, cDNA or a plasmid containing the gene of interest. During the PCR each newly synthesized DNA strand can be used as a template itself and hybridizes with the primers, leading to exponential amplification of the DNA molecules. The basic steps of a PCR are as follows: The complementary DNA strands are separated during a denaturation phase at 95°C. During the following annealing phase the primers bind to their complementary DNA strands (anneal) and form the starting point for the DNA synthesis in the subse-

quent elongation phase at 72°C. This three-step cycle is repeated 25 to 35 times during a PCR reaction. The temperature of the annealing phase depends on the melting temperatures (T_m) of the primer pair and has to be optimized for each reaction. Usually an annealing temperature 5 to 10 degrees below the lowest T_m of the primer pair is chosen. A high annealing temperature can inhibit primer binding to the DNA strand, while a low annealing temperature might result in unspecific binding of the primer to other DNA sequences and their amplification.

For sequence sensitive applications such as cloning, usage of proofreading polymerases, for example Pfu DNA polymerase isolated from *Pyrococcus furiosus* or KOD DNA polymerase from *Thermococcus kodakaraensi*, is recommended. This type of polymerases has 3'-5' exonuclease activity and the ability to remove wrongly incorporated nucleotides from the newly synthesized DNA strand resulting in a much lower mutation frequency. KOD Hot Start DNA polymerase used in this study needs to be activated in the beginning of the PCR as the enzyme is blocked by monoclonal antibodies to avoid degradation of the primers/templates during PCR assembly.

The PCRs performed for cloning in this study are listed with template, primer pair, restriction endonuclease cutting sites, and target vector in Table 2.10. For standard PCR conditions see Table 2.20 and Table 2.21. Due to the G/C-rich sequence of Pex11γ higher denaturation temperatures (98°C) were used in those PCRs.

x µl	Template
0.5 µl	Primer forward (100 pmol/µl)
0.5 µl	Primer reverse (100 pmol/µl)
5.0 µl	dNTP's (2 mM each)
2.0 µl	$MgSO_4$ (25 mM)
5.0 µl	10x Buffer
1.0 µl	KOD hot start DNA polymerase (1 U/µl)
x µl	ddH2O
50 µl	Final volume

Table 2.20: Standard PCR assembly

Denaturation & activation	95°C	2 min	
Denaturation	95°C	45 sec	35 cycles
Annealing*	53°C	30 sec	
Elongation* (20 s/kbp)	72°C	45 sec	
Elongation	72°C	3 min	
Cooling	4°C	∞	

Table 2.21: Standard PCR protocol
*Annealing temperature was adjusted to the respective primer pair and elongation time to template length.

2.11.4 Semi-quantitative RT-PCR

Conduction of a semi-quantitative RT-PCR (SQ-PCR) aims on determination of the expression level of a certain mRNA in the cells/tissues analyzed. It can e.g. be used to analyze if the expression of an mRNA species is induced or repressed by a certain stimulus. The SQ-PCR is based on the correlation of the amount of PCR product with the amount of template during the exponential phase of a PCR. The abundance of the template (cDNA) represents the target mRNA level. First, the exponential phase has to be determined. The relative expression levels of the mRNA (protein) of interest are then determined in relation to appropriate controls.

Protocol: RNA was isolated and transcribed into cDNA as described in sections 2.11.1 and 2.11.2. Transcription of identical amounts of mRNA was performed for all samples and same amounts of cDNA were used as templates for the SQ-PCR (section 2.11.3 and Table 2.22 and Table 2.23). To determine the exponential phase for each template, samples were taken during the PCR after certain cycle numbers (21, 24, 27, and 30 cycles for Pex11 samples and 12, 15, 18, and 21 cycles for the housekeeping gene GAPDH) and separated on an agarose gel (2.11.5). During the exponential PCR phase the intensity of the bands increased with longer PCR duration. SQ-PCR was performed for all templates (Pex11α, Pex11β, Pex11γ, and GAPDH as control) in parallel for samples isolated from treated (nocodazole) and control cells. Samples (10 µl) were taken after the optimal cycle number for each template or samples were taken after 3 different time points to overcome fluctuations in the cDNA. Analysis of the samples, i.e. quantification of the PCR products, was done by agarose gel electrophoresis (2.11.5).

2 µl	cDNA (template)
1 µl	Primer forward (0.2 µM final concentration)
1 µl	Primer reverse (0.2 µM final concentration)
1 µl	dNTP's mix (10 mM each)
5 µl	ThermoPol Taq Reaction buffer (10x)
0.5 µl	Taq polymerase (5 U/µl)
x µl	ddH2O
50 µl	Final volume

Table 2.22: Standard SQ-PCR assembly

94°C	5 min	
94°C	45 sec	40 cycles
T_m-5°C	30 sec	
72°C	90 sec	
72°C	5 min	
4°C	∞	

Table 2.23: Standard SQ-PCR protocol

2.11.5 Agarose gel electrophoresis

To separate and analyze DNA strands of different sizes agarose gel electrophoresis is used. The separation occurs according to DNA size (length) and shape. The negatively charged phosphate backbone provides equal charge per size and the DNA migrates towards the anode in an electric field. Agarose is a galactose polymer which can be dissolved by boiling in water or buffer and forms a gel matrix during cooling. The density of the gel depends on the amount of agarose (usually in between 0.5 and 2% w/v). DNA is visualized in the gel by staining with ethidium bromide, which intercalates into the DNA and becomes visible upon UV irradiation.

Protocol: Agarose was dissolved in TAE buffer (2.6) by boiling in a microwave. The solution was cooled down until being hand-hot, ethidium bromide was added (0.5 µg/ml) and the gel was poured into a horizontal gel chamber containing a comb to form loading wells. Routinely 0.8 to 1% (w/v) gels were used. DNA samples were mixed with 6x loading buffer and a co-migrating DNA ladder was used to mark DNA sizes (2.3.2). Separation was performed at maximal 5 V per cm electrode distance (60 to 130 V) for 30 to 60 minutes. Digital images were taken using AlphaImager HP and quantification was done with the provided software.

2.11.6 Gel extraction

PCR products or other DNA samples were isolated from agarose gels using a gel extraction kit (Qiagen, 2.3.3). The DNA bands visible with UV light were cut with a scalpel and transferred to a reaction tube. Agarose was melted at 50°C and the DNA was extracted with spin columns. Elution was performed using 30 µl distilled water.

2.11.7 Digestion with restriction enzymes

Restriction endonucleases (REs) are enzymes isolated from bacteria which cut DNA double strands at a specific, sequence-dependent position. They are part of a bacterial restriction-modification system intended to protect from phage DNA. In contrast to the bacterial DNA, phage DNA is not methylated at the respective sequences and is therefore degraded by the REs. There are a large number of different REs from different bacterial strains (see Table 2.24). REs usually recognize palindrome sequences with a length of 4 to 8 base pairs and cut inside this sequences (Type II RE). This can result in overhanging, sticky DNA ends, meaning that 5'- and 3'-strands differ in length, or in blunt ends with the same strand length. Free DNA strands, in particular sticky ends, are easily (re-) ligated.

Name	Organism	Recognition site	Concentration	Buffer
*Bam*HI	*Bacillus amyloliquefaciens* H	5'...G|GATTCC...3'	20 U/µl	3 + BSA
*Bgl*II	*Bacillus globigii*	5'...A|GATCT...3'	10 U/µl	3
*Eco*RI	*E. coli* RY13	5'...G|AATTC...3'	20 U/µl	EcoRI
*Not*I	*Nocardia otitidis-caviarum*	5'...GC|GGCCGC...3'	10 U/µl	3 + BSA
*Xho*I	*Xanthomonas holcicola*	5'...C|TCGAG...3'	20 U/µl	4 + BSA

Table 2.24: Properties of selected restriction enzymes
The vertical lines in the DNA sequences of the recognition sites mark the cleavage sites. Concentrations and buffer conditions listed refer to enzymes purchased from New England Biolabs. For unit (U) definitions see appendix (8.1.2).

2.11.7.1 Preparative RE digestion

In the field of molecular biology the properties of restriction endonucleases are utilized for cloning of DNA constructs. Two different DNA molecules, e.g. a protein-encoding cDNA and mammalian expression vector, can be ligated with each other if they were digested with (the same) REs resulting in complementary sticky ends. Expression vectors usually contain a multiple cloning site (MCS) with a set of unique RE cutting sites to be used for cloning. RE cutting sites are usually added to the DNA sequence of choice (e.g. a

cDNA sequence) via the primers by PCR (see 2.11.3). Using different RE cutting sites at the 5'- and 3'-end leads to directed ligation of the DNA fragments. It is crucial to choose RE sequences not present at other positions inside the DNA sequences.

Protocol: PCR products extracted from the agarose gel and the target vector were digested with the same two enzymes. Full activity of the REs is only achieved at optimal buffer conditions. Depending on the respective enzymes, a double digest with both enzymes at the same time was possible, or sequential digestions and precipitation of the DNA (2.11.8) in between was required. Routinely, preparative digestions were performed according to Table 2.25 at 37°C over night. Afterwards, successful digestion was checked on an agarose gel, the DNA was isolated and used for ligation.

x µg	DNA (PCR product or vector)
1.0 µl (10 U)	Restriction endonuclease I
1.0 µl (10 U)	Restriction endonuclease II (or separate)
0.5 µl	100x BSA (100 ng/µl; optional)
5.0 µl	10x Buffer
x µl	dH2O
50 µl	Final volume

Table 2.25: Standard RE reaction

2.11.7.2 Analytical RE digestion

Analytical RE digestions were performed to confirm the correct insertion of a DNA sequence into the vector, and to screen DNA isolated from a set of bacterial clones for the correct plasmid. The optimal RE for this control cuts inside the vector and inside the plasmid and creates DNA fragments of characteristic sizes differently from the vector alone. But also a double digest with two (or more) enzymes is possible.

Protocol: DNA (2 µl) obtained by a mini preparation (2.11.12) was digested with 0.2 µl RE at 37°C for 2 to 4 hours. Negative and positive controls were co-digested and parallel analysis on an agarose gel was performed.

2.11.8 DNA precipitation

DNA can easily be isolated from an aqueous solution, e.g. in between two sequential digestions, by precipitation.

Protocol: 2 to 2.5 volumes cold (-20°C) 96% ethanol were added to the DNA sample. The solution can be neutralized by addition of 1/10 volume of sodium acetate. Precipitation occurred at -80°C for 30 minutes and the DNA was pelleted by centrifugation at 4°C for 30 minutes with 13,000 rpm. The pellet was washed with cold (-20°C) 70% ethanol and centrifuged for 5 minutes at 13,000 rpm and 4°C. After air-drying the DNA pellet was resuspended in distilled water.

2.11.9 Dephosphorylation

To avoid false-positive clones after DNA ligation and transformation into bacteria, incubation of the vector with a phosphatase prior to ligation with the DNA insert can be performed. The phosphatase removes the free 5' phosphate residues from the DNA strands, which inhibits the self-ligation of the vector in case of incomplete digestion with the RE. The 5' phosphates present at the DNA insert are sufficient for subsequent ligation.
Protocol: After digestion and isolation the vector was incubated with 1 µl Antarctic phosphatase in the provided buffer for 30 minutes at 37°C. Subsequently, phosphatase was inactivated at 65°C for 10 minutes.

2.11.10 Ligation

To join insert and vector DNA both are enzymatically ligated using the T4 DNA ligase. The insert to vector molecule ratio should be around 5:1 if the insert size is around 1 kb. Following equation allows a rough determination of the DNA amounts needed:

$$mass_{\text{insert}}\ [\text{ng}] = \frac{5 \text{ x } mass_{\text{vector}}[\text{ng}] \text{ x } length_{\text{insert}}[\text{kb}]}{length_{\text{vector}}[\text{kb}]}$$

The complementary sticky DNA ends created by RE digestion of vector and insert hybridize with each other and the DNA backbone is ligated by the DNA ligase.
Protocol: The reaction was assembled according to Table 2.26 and incubated at 16°C over night. The plasmid formed was transformed and amplified in *E. coli* (2.11.11) and screened for correct ligations by analytical RE digestion (2.11.7.2). A control reaction without insert was performed side-by-side.

x ng	Insert
50 ng	Vector
1.0 µl	T4 ligase (400 U/µl)
2.0 µl	10x Ligation buffer
x µl	dH2O
20 µl	Total volume

Table 2.26: Standard ligation reaction

2.11.11 Bacterial culture

For cloning and amplification of DNA plasmids *Escherichia coli* cultures were used. The DH5α derivate of the K12 *E. coli* safety strain was used, which misses certain pathogenic genes like toxins, adhesion and invasion factors (Lottspeich & Engels 2006). The bacteria were cultured in LB medium containing a selective antibiotic (100 mg/ml Ampicillin or 30 µg/ml Kanamycin) at 37°C and 200 rpm in an incubator shaker. Long time storage of *E. coli* cultures was performed as 50% glycerol mixtures at –80°C. For single-cell colonies bacteria were spread on LB agar plates and incubated over night in a 37°C incubator. Plates were short-term stored at 4°C and the bacterial colonies were used for inoculation of liquid cultures (3 to 5 ml).

2.11.11.1 Preparation of competent bacterial cells

For plasmid amplification bacterial cells have to be transformation competent, i.e. to be able to take up plasmid DNA. This requires a modification of the membrane to achieve plasmid permeability. Chemically competent bacteria were used.

Protocol: 5 ml of an *E. coli* DH5α culture grown over night were diluted in 500 ml LB medium and shaken at 37°C for 2 to 3 hours until an optical density of OD_{600nm} = 0.4 was reached. The culture was chilled on ice for 15 minutes and centrifuged at 3,000 rpm, 4°C for 15 minutes. The pellet was resupended in 40 ml ice-cold 0.1 M calcium chloride ($CaCl_2$) solution and incubated on ice for 30 minutes. The bacteria were re-centrifuged, the pellet was resuspended in 20 ml ice-cold 0.1 M calcium chloride solution and 20% (v/v) glycerol was added. After incubation on ice for 2 hours aliquots of 100 µl were frozen in liquid nitrogen and stored at –80°C.

2.11.11.2 Chemical transformation

During the process of chemical transformation the DNA plasmid binds to the membrane of the competent bacteria and the uptake is induced by a heat shock.

Protocol: 100 µl competent *E. coli* cells were mixed with the plasmid DNA (e.g. from a ligation reaction) and incubated on ice for 30 minutes. After a 90 seconds heat shock at 42°C the bacteria were chilled on ice and 700 ml LB medium without antibiotics was added, followed by 1 hour shaking incubation at 37°C. A cell pellet was formed by centrifugation (3 minutes at 5,000 rpm) and resuspended in ca. 50 ml LB medium. The suspension was spread on a LB agar plate containing a selective antibiotic using a Drigalski spatula and grown overnight at 37°C.

2.11.12 Plasmid isolation

Plasmid DNA was isolated from *E. coli* cultures in two different amounts; as small scale (mini) preparation from 3 to 5 ml cultures or as large scale preparation from 200 ml cultures. Mini preparations for colony screening after cloning were done with mini spin columns (Qiagen or GE Healthcare, 2.3.3) or according to the protocol described below. Large scale preparations were performed using a maxi or midi kit (Genomed or Macherey-Nagel, 2.3.3). All methods are based on alkaline lysis: Bacteria are resuspended in EDTA-containing buffer chelating magnesium and chloride ions required for membrane stability. The addition of alkaline SDS solution leads to lysis of the cells and denaturation of proteins and DNA. The mixture is neutralized with potassium acetate buffer, which re-natures the small plasmid DNA but precipitates proteins and genomic DNA with potassium dodecyl sulphate, which can be removed by centrifugation. The plasmid DNA is isolated by columns with silica membrane or by precipitation and resuspended in water.

Protocol: 3 ml E. coli cultures inoculated from single colonies were grown over night and sedimented once or twice by centrifugation at 5,000 rpm for 5 minutes. The supernatant was carefully removed and the pellet was completely resuspended in 100 µl cold solution I. 200 ml solution II were added and mixed by inverting the tube five times (maximal 5 minutes). After addition of 150 µl cold solution III and mixing by inverting the lysate was incubated on ice for 3 to 5 minutes. The precipitate formed was removed by centrifugation at 13,000 rpm, 4°C for 10 minutes and the supernatant was transferred to a new tube. The DNA was precipitated by addition of 2 volumes 96% ethanol, incubation

at room temperature for 2 minutes and centrifugation at 13,000 rpm, 4°C for 5 minutes. The pellet was washed with 1 ml 70% ethanol and centrifuged for 5 minutes at 13,000 rpm, 4°C. After air-drying the pellet was resuspended in 50 ml water supplemented with 20 µg/ml RNase, if the RNase has not been added to solution I.

The DNA precipitation of midi preparations was performed with 0.7 volumes isopropyl alcohol and centrifugation at 15,000x g, 4°C for 30 minutes. The pellet was washed with 5 ml 70% ethanol and re-centrifuged for 10 minutes. The DNA was resuspended in approximately 400 µl of water to achieve a final DNA concentration of 1 to 2 µg/µl, aliquoted, and frozen at –20°C until usage, for example for transfection of mammalian cells (2.8.4). DNA concentrations were measured as described in 2.11.13.

Solution I, pH 8.0, autoclave

- 50 mM glucose
- 25 mM Tris
- 10 mM ETDA
- (100 µg/ml RNase)

Solution II

- 0.2 M Sodium hydroxide
- 1% (w/v) SDS

Solution III

- 3 M Potassium acetate
- pH 4.8 with glacial acetic acid (~11.5% v/v)

2.11.13 Measurement of DNA and RNA concentrations

DNA and RNA concentrations were measured in two different ways, either using the Qubit fluorometer and the respective fluorometric assay (2.3.3) or by measuring the optical density at a wavelength of 260 nm (maximal absorption of the aromatic rings of the bases). An optical density of OD_{260} = 1.0 refers to 50 µg/µl DNA or 30 µg/µl RNA. As proteins absorb light with a wavelength of 280 nm, the ratio of the OD_{260} to OD_{280} provides a tool to determine the purity of a DNA or RNA preparation. A clean DNA preparation should have an OD_{260}/OD_{280} ratio of 1.8 and a RNA preparation of 2.0.

Protocol: 1 µl of a DNA midi preparation (2.11.12) was diluted 1:500 in water and measured in a quartz cuvette with water as blank. RNA preparations (2.11.1) were usually diluted 1:50.

3 RESULTS

Peroxisomes are capable to proliferate and multiply, or be degraded in response to nutritional and environmental stimuli (Yan et al. 2005). In this context, elongation and fission processes of peroxisomes have been observed either under conditions of rapid cellular growth or stimulation of cultured cells by e.g. substrates or growth factors, and have been proposed to contribute to peroxisome proliferation (Schrader 2006; Schrader et al. 1996; Schrader & Fahimi 2004; Schrader et al. 2003). At present, however, little information is available on the exact function of the resulting complex tubular or reticular peroxisomal structures, their dynamic behaviour and the molecular machinery required for their formation and division. This work aims at understanding the underlying molecular components of the peroxisomal machinery to provide insight into the mechanisms regulating peroxisomal dynamics, growth and division by investigation of the proteins Pex11p, hFis1 and DLP1.

The first section addresses the question of how hFis1 – the membrane anchor of DLP1 – is targeted to peroxisomes (3.1). Furthermore, the members of the Pex11 protein family were morphologically and functionally characterized (3.2). The main focus of this work was placed on the detailed characterization of a dominant-negative Pex11pβ mutant that gives insight into the peroxisome formation by growth and division (3.3). Finally, another study was focused on the different signals resulting in peroxisomal elongation (3.4).

3.1 Pex19-dependent targeting of hFis1 to peroxisomes

Three molecular components of the peroxisomal division machinery have been identified: Pex11pβ, DLP1 and hFis1 (Kobayashi et al. 2007; Koch et al. 2003; Koch et al. 2005; Li & Gould 2003; Schrader et al. 1998b). Pex11pβ promotes peroxisome proliferation and elongation (1.3.3) and has been suggested to interact with hFis1 (Kobayashi et al. 2007). hFis1, a tail-anchored (TA) protein, regulates membrane fission of peroxisomes and mitochondria by DLP1 recruitment, which then in turn mediates final membrane scission (1.3). Increasing the amount of hFis1 on peroxisomes and mitochondria has been shown to promote peroxisomal and mitochondrial division (Koch et al. 2005; Yoon et al. 2003). Apparently, both organelles have to compete for DLP1. However, it is cur-

rently not understood how the dual targeting of hFis1 to peroxisomes and mitochondria is achieved.

The membrane targeting of TA proteins is controversially discussed and an unassisted membrane insertion for mitochondrial and ER-localized TA proteins has been proposed (Brambillasca et al. 2006; Brambillasca et al. 2005; Colombo et al. 2009; Kemper et al. 2008; Setoguchi et al. 2006). Peroxisomal TA proteins are suggested to be delivered to the organelles via a passage through the ER (Elgersma et al. 1997). Delivery of membrane (and TA) proteins to peroxisomes *per se* can be mediated by direct insertion from the cytosol, by transit through the ER (or a subdomain) (Van Ael & Fransen 2006), and via mitochondria by a population of MDVs (1.2.2) (Nagotu et al. 2010; Neuspiel et al. 2008). However, most peroxisomal membrane proteins (PMPs) are likely to be inserted into peroxisomes directly from the cytosol. This process requires Pex19p, a mainly cytosolic protein which acts as a chaperone and/or import factor for most PMPs (Fransen et al. 2001; Halbach et al. 2005; Jones et al. 2004; Rottensteiner et al. 2004; Sacksteder et al. 2000; Snyder et al. 2000) and directs them to the peroxisomal membrane by interaction with Pex3p (1.2.2) (Fang et al. 2004; Fujiki et al. 2006; Matsuzono et al. 2006; Muntau et al. 2003). In a recent study it has been reported that the peroxisomal TA protein Pex26p and its yeast homologue Pex15p utilize the regular machinery for the import of PMPs and are targeted by binding of Pex19p (Halbach et al. 2006). This section of the thesis presents as a whole the investigation performed on the membrane targeting of mammalian hFis1. This work is a continuation of the diploma thesis (Delille 2006).

3.1.1 Interaction of Pex19p and hFis1

To investigate if the PMP import factor Pex19p is involved in the peroxisomal targeting of hFis1, co-immunoprecipitation experiments were performed. COS-7 cells were co-transfected with the respective plasmids encoding the tagged proteins. After 48 hours cells were lysed and immunoprecipitations with anti-Myc or anti-GFP/YFP antibodies were performed. First, the assay was tested using Pex11pβ-Myc, which was previously shown to bind Pex19p (Jones et al. 2004; Rottensteiner et al. 2004). Pex11pβ-Myc was able to precipitate YFP-Pex19p in this system (Figure 3.1 A). Next, we co-transfected the cells with several hFis1 and Pex19p constructs (see Table 2.18). Myc-hFis1 was observed to co-precipitate with YFP-Pex19p (Figure 3.1 B), and YFP-Pex19p also co-precipitated with Myc-hFis1 (Figure 3.3 A, lane a). Please note that only for the co-

precipitation of Myc-hFis1 with YFP-Pex19p the usage of a cross-linking agent (DSP) was necessary.

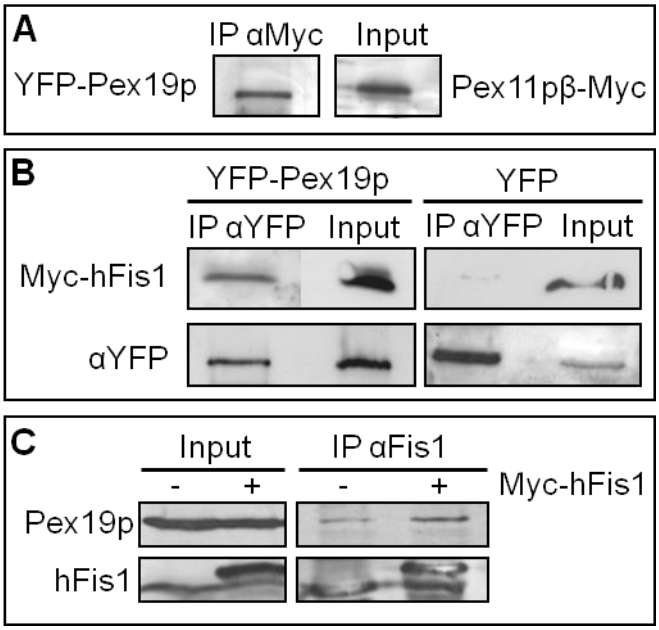

Figure 3.1: Pex19p and hFis1 interact with each other
(A) As a positive control COS-7 cells were co-transfected with Pex11pβ-Myc and YFP-Pex19p and immunoprecipitation (IP) was performed using anti-Myc antibodies (without cross-linking). Pex11pβ-Myc, which is known to interact with Pex19p, forms a complex with YFP-Pex19p. **(B)** COS-7 cells were co-transfected with Myc-hFis1 and YFP-Pex19p (on the left) or cytosolic YFP as negative control (pEYFP-N1; on the right), and incubated for 48 hours. Whole cells were subjected to chemical cross-linking by adding DSP for 45 minutes. Immunoprecipitations were performed with anti-GFP/YFP antibodies and Protein A-sepharose followed by analysis of the samples by SDS-PAGE and immunoblotting using anti-Myc and anti-GFP/YFP antibodies. Note that Myc-hFis1 co-precipitated with YFP-Pex19p, but not with cytosolic YFP. **(C)** COS-7 cells were transfected with Myc-hFis1 or not transfected. Immuno-preciptiation of endogenous (and overexpressed) hFis1 was performed using anti-Fis1 antibodies and Protein A-sepharose, and the co-precipitation of endogenous Pex19p was detected by immuno-blotting using anti-Pex19 antibodies. Note that Myc-tagged hFis1 creates an additional (higher) band.

The results suggested that Pex19p and hFis1 are part of the same complex, and to further consolidate our hypothesis immunoprecipitations of the endogenous proteins were conducted. Non-transfected cells or cells transfected with Myc-hFis1 alone were subjected to immunoprecipitations with anti-Fis1 antibodies. Endogenous Pex19p was found to co-precipitate with endogenous hFis1, and the amount of co-precipitated Pex19p increased when Myc-hFis1 was expressed additionally (Figure 3.1 C). These data further support an interaction between hFis1 and Pex19p.

In order to define the binding region of Pex19p, another set of co-immunoprecipitations was performed. It was previously shown that an intact C-terminus of hFis1 is necessary and sufficient for peroxisomal and mitochondrial targeting (Koch et al. 2005; Yoon et al. 2003), as removal of the short C-terminal tail consisting of five amino acids impaired proper targeting of hFis1 to peroxisomes and mitochondria. Different deletion mutants of hFis1 were used for co-immunoprecipitations (Table 2.18 and Figure 3.2) and it was shown that the C-terminal tail of hFis1 together with the transmembrane domain is indispensable for the binding of Pex19p. Noteworthy, the removal of only five amino acids from the C-terminus of hFis1 impedes the binding of Pex19p (Figure 3.3 A and Figure 3.4 A).

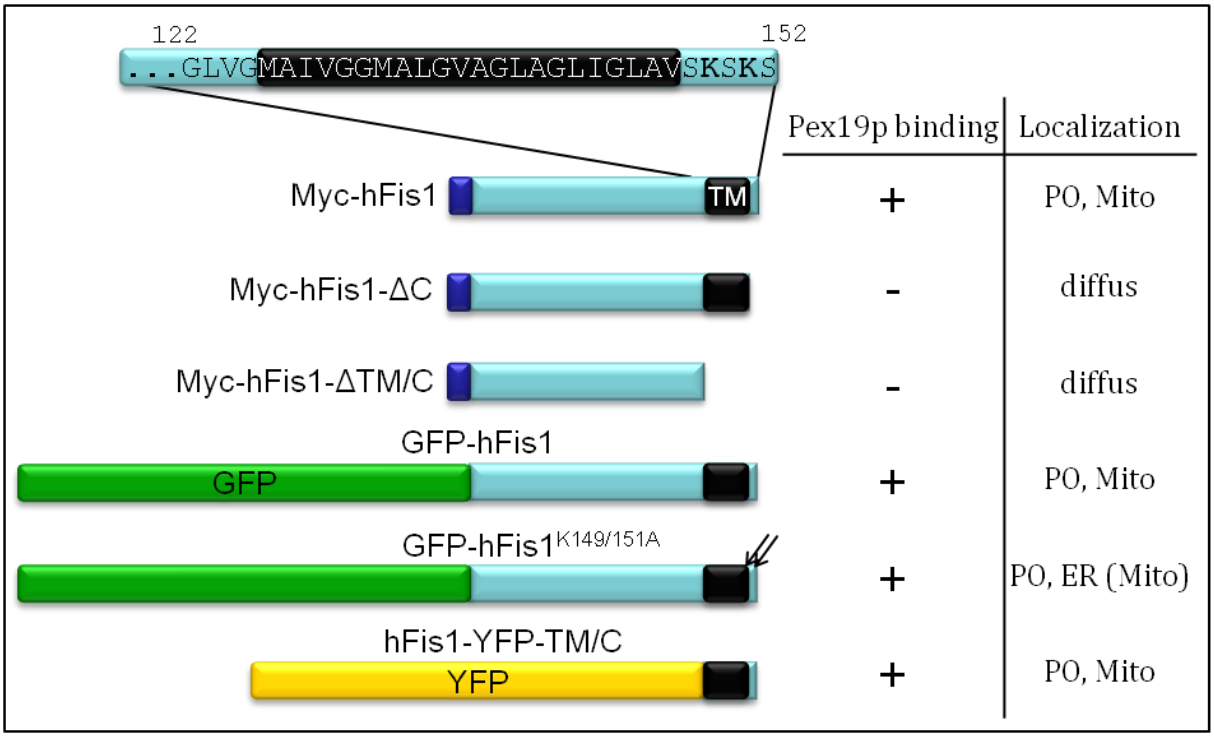

Figure 3.2: Overview of the hFis1 constructs used to study the interaction with Pex19p
The bars on the left represent the proportion of the protein domains of the different tagged and/or truncated hFis1 constructs. Myc-hFis1 and GFP-hFis1 are full length hFis1 constructs N-terminally fused with a Myc epitope tag or green fluorescent protein (GFP), respectively. Myc-hFis1-ΔC has a C-terminal truncation of 5 amino acids while the Myc-hFis1-ΔTM/C construct lacks 26 amino acids (the transmembrane domain (TM) and the C-terminus). In hFis1-YFP-TM/C these 26 amino acids are fused to the C-terminus of yellow fluorescent protein (YFP). GFP-hFis1$^{K149/151A}$ is a full length construct carrying lysine to alanine mutations in the residues 149 and 151 (arrows). The top bar represents the amino acid sequence of the C-terminus (amino acids 122 to 152) of hFis1. The transmembrane domain is depicted in black and basic amino acids (K149 and K151) are printed bold.
An overview of the particular binding to Pex19p (+) and the subcellular localization is given in the table on the right. ER, endoplasmic reticulum; Mito, mitochondria; PO, peroxisomes.

Additionally, a construct only bearing the transmembrane domain and the short tail fused to YFP (hFis1-YFP-TM/C) was sufficient to co-precipitate HA-Pex19 (Figure 3.3 B and Figure 3.4 B) clearly defining these 26 amino acids as a Pex19p binding region.
Basic amino acids close to the transmembrane domain have been shown to be important for the targeting of C-tail anchored proteins (Borgese et al. 2007) as well as for general targeting of peroxisomal membrane proteins (Van Ael & Fransen 2006). hFis1 contains two basic lysine residues at positions 149 and 151, and this overall positive charge was shown to be important for proper mitochondrial targeting of hFis1 (see Figure 3.2) (Stojanovski et al. 2004). To examine whether the targeting to peroxisomes also depends on these lysine residues, the Pex19p-binding of hFis1 carrying the point mutations K149A and K151A was studied. While the targeting to mitochondria was disturbed and some misdirection to the ER was observed (Stojanovski et al. 2004), the targeting to peroxisomes was not affected (Delille & Schrader 2008). Consistent with this, co-immunoprecipitation of HA-Pex19p with GFP-hFis1$^{K149/151A}$ revealed to be just as effec-

tive as with wild type GFP-hFis1 (Figure 3.3 B and Figure 3.4 B). These findings indicate that the overall basic charge within the C-terminal tail of hFis1 is neither crucial for peroxisomal targeting nor essential for binding of Pex19p.

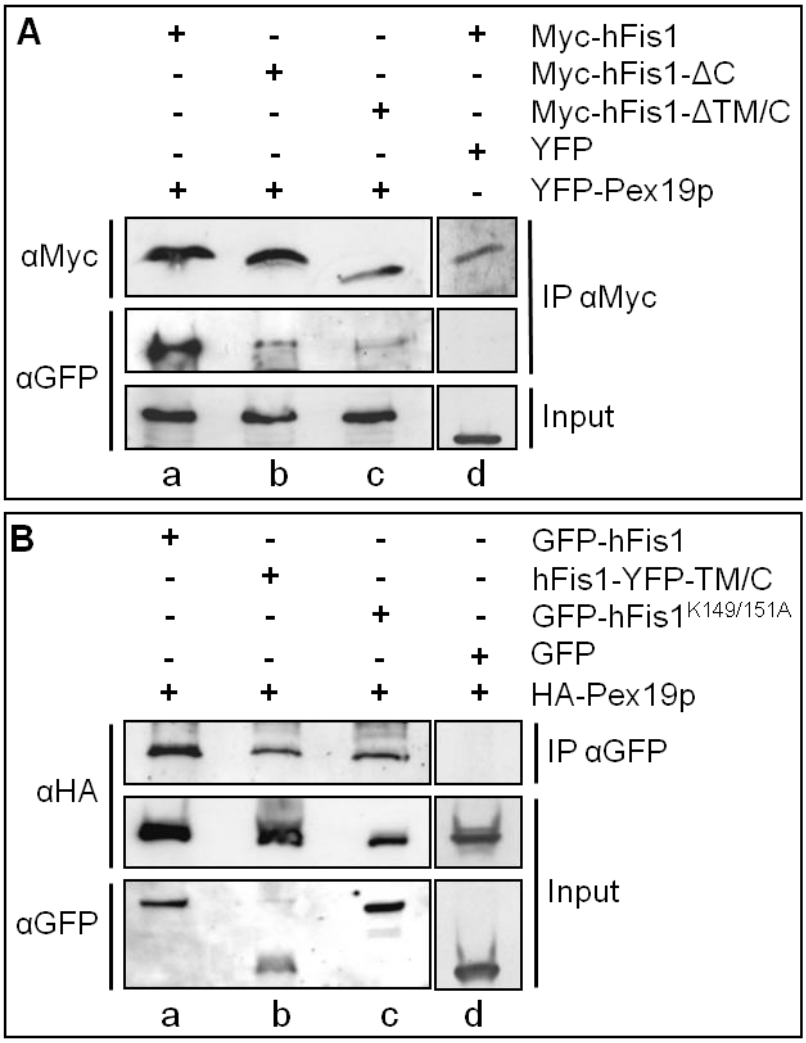

Figure 3.3: The Pex19p binding region is located at the C-terminus of hFis1 and does not require basic amino acids
(A) Co-transfection of COS-7 cells with YFP-Pex19p and Myc-hFis1 (lane a), Myc-hFis1-ΔC (lane b), or Myc-hFis1-ΔTM/C (lane c) followed by immunoprecipitation (IP) with anti-Myc antibodies conjugated to agarose beads. The analysis of the samples was performed by immunoblotting using anti-GFP/YFP antibodies. Note that Pex19p binding to hFis1 is impaired after removal of the C-terminal tail or the transmembrane domain of hFis1 (lanes b and c). To exclude unspecific co-precipitations control experiments were performed with cytosolic YFP (pEYFP-N1) and Myc-hFis1 (lane d). **(B)** COS-7 cells were co-transfected with HA-Pex19p and GFP-hFis1 (lane a), hFis1-YFP-TM/C (lane b), GFP-hFis1$^{K149/151A}$ (lane c), or cytosolic GFP as negative control (pEGFP-N1; lane d). IPs were performed by adding anti-GFP/YFP antibodies and Protein A-sepharose. The samples were analyzed by immunoblotting with anti-HA antibodies. Note that the C-terminal domain of hFis1 (TM/C, 26 amino acids) fused to YFP is sufficient to co-precipitate HA-Pex19p (lane b) and that mutations of the basic amino acids in the very C-terminus of hFis1 do not abolish binding to HA-Pex19p (lane c).

In summary, it was shown that Pex19p, the PMP import receptor, binds to the TA protein hFis1 suggesting a Pex19p-dependent targeting mechanism. Furthermore, the binding region was defined as the TM domain plus the extreme C-terminus (five amino acids), whereas a basic charge in the C-terminus was not required for Pex19p binding. The hFis1 constructs used, their Pex19p binding properties and their subcellular localizations are summarized in Figure 3.2.

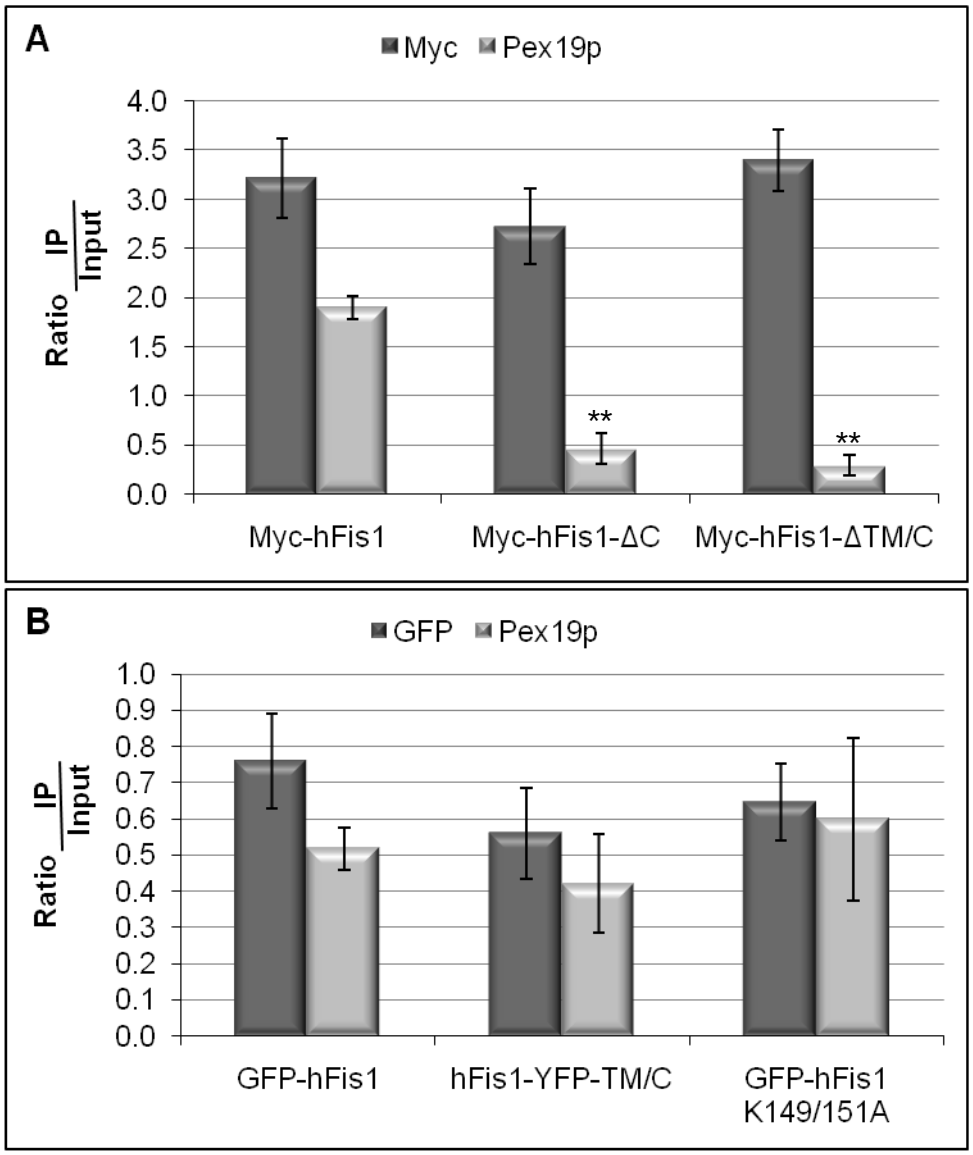

Figure 3.4: Quantitative analyses of immunoprecipitations shown in Figure 3.2
The protein amount ratio of immunoprecipitation (IP) to respective input is shown, to rule out differences in the expression level and to allow comparison between the hFis1-mutants. Note that the removal of the C-terminus (ΔC) of hFis1, and of the transmembrane domain (ΔTM/C), clearly reduces the amount of co-precipitated Pex19p (A), while the mutation of the lysine residues in the C-terminus of hFis1 (K149/151A) does not influence the Pex19p co-precipitation (B). The data are obtained from 3 to 5 independent experiments and are expressed as means ± SD (** $p<0.01$).

3.1.2 Targeting of hFis1 to peroxisomes but not to mitochondria depends on Pex19p

To further prove the role of Pex19p in the peroxisomal targeting of hFis1, the effect of Pex19p silencing by siRNA on targeting of hFis1 to peroxisomes was examined. First, the functionality of the Pex19 knock down was tested in a morphological assay using Pex11pβ-Myc. It was shown before that Pex11pβ also binds to Pex19p (see 3.1.1) (Jones

et al. 2004; Rottensteiner et al. 2004), and therefore the effect of the Pex19p knock down on peroxisomal morphology after expression of Pex11pβ was assessed. The peroxisomal elongation induced by Pex11pβ (1.3.3 and Figure 3.13 A-C) is easy to detect and quantify by microscopic analysis. It was investigated whether the knock down of Pex19p has an effect on the insertion of Pex11pβ into peroxisomal membranes and therefore on peroxisome elongation. Two days after silencing of Pex19p, COS-7 cells were transfected with Pex11pβ-Myc by electroporation and processed for immunofluorescence after 6 to 12 hours. After silencing of Pex19p, the elongation of peroxisomes in Pex11pβ-Myc expressing cells was significantly reduced (55 ± 5.58%, Figure 3.5 B and C) compared to control cells (74 ± 1.71%, Figure 3.5 A and C). Furthermore, many cells with a diffuse or granular, cytoplasmic distribution of Pex11pβ-Myc were observed (data not shown). The knock down does not completely abolish, but strongly reduces the targeting of overexpressed Pex11pβ to peroxisomes, demonstrating the good functionality of the Pex19 knock down by siRNA.

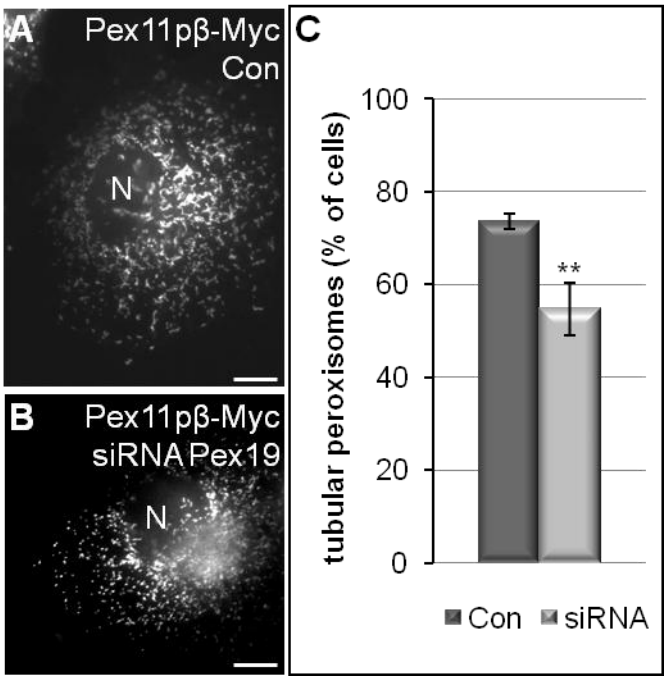

Figure 3.5: Silencing of Pex19p reduces peroxisomal proliferation induced by Pex11pβ
COS-7 cells were transfected with Pex19p siRNA duplexes. After 48 hours the cells were transfected with Pex11pβ-Myc and after additional 6 hours processed for immunofluorescence using anti-Myc (and anti-PMP70) antibodies. **(A)** Control cell (Con) with typical tubular, elongated peroxisomes induced by Pex11pβ expression. **(B)** Silencing of Pex19p (siRNA). In many cases, the peroxisomes exhibit a spherical morphology and are not elongated. **(C)** Quantitative evaluation of peroxisome morphology. Note the reduced frequency of tubular peroxisomes in cells silenced for Pex19p. The data are from 4 independent experiments and are expressed as means ± SD (** $p<0.01$). N, nucleus. Bars, 10 µm.

Next, the targeting of hFis1 was assessed in an import assay. Two days after knock down of Pex19p (Figure 3.6 K) COS-7 cells were transfected with GFP-hFis1 by electroporation. The cells were prepared for immunofluorescence 3 to 5 hours after transfection of GFP-hFis1 and examined for import of GFP-hFis1 into peroxisomes by co-localization with PMP70. In contrast to controls, the number of GFP-hFis1 positive structures which co-localized with peroxisomes labelled by PMP70 was decreased. Many PMP70-positive

peroxisomes exhibited only a very weak staining for GFP-hFis1, or were not labelled at all (Figure 3.6 D-I). In controls, the majority of the PMP70-positive peroxisomes showed co-labelling for GFP-hFis1 (Figure 3.6 A-C) (Koch et al. 2005). These differences were less obvious at later time points, probably due to the fact that silencing of Pex19p does not completely abolish import of PMPs (Halbach et al. 2006; Jones et al. 2004).

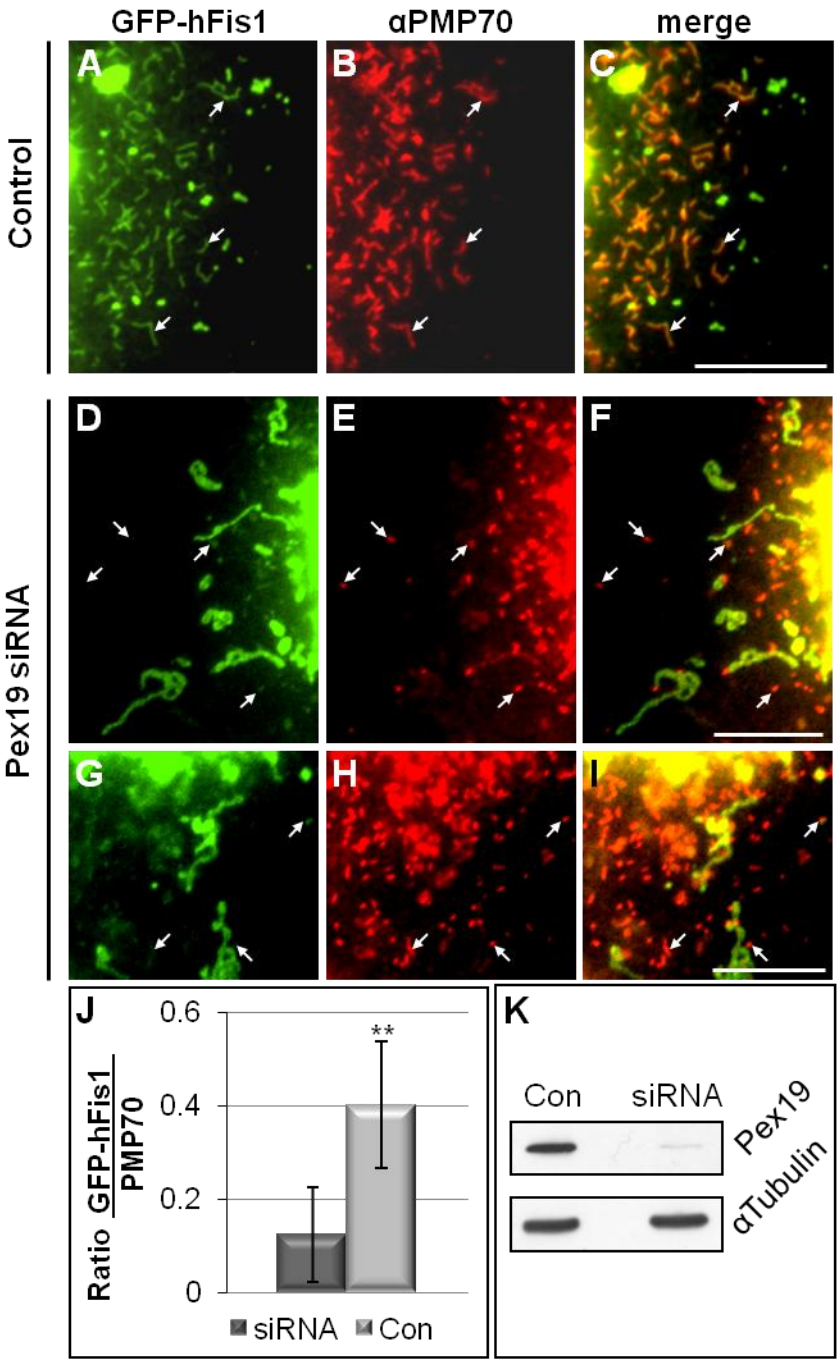

Figure 3.6: Silencing of Pex19p inhibits the peroxisomal targeting of hFis1
Pex19p in COS-7 cells was silenced by transfection with siRNA duplexes (D-I). After 48 hours the cells were transfected with GFP-hFis1, and the targeting of GFP-hFis1 to peroxisomes was assayed after 3 hours. Peroxisomes were immunostained with antibodies to PMP70 (B, E, H). Co-localization of GFP-hFis1 and peroxisomes in control cells (A-C), and in cells silenced for Pex19p (D-I). Arrows in (A-C) highlight regions of co-localization. Note the absence or reduction of co-localization (arrows) of GFP-hFis1 with PMP70 after silencing of Pex19p (D-I). **(J)** Fluorescence intensities of GFP-hFis and PMP-TRITC were determined on digital images by highlighting (encircling) single peroxisomes, and the GFP/TRITC ratios were calculated. 60-140 peroxisomes per cell were analyzed in about 60 control as well as treated cells. Data are expressed as means ± SD (** $p<0.01$). **(K)** Immunoblots of cell lysates prepared after 48 hours from control (Con) and silenced cells (siRNA) using anti-Pex19p and anti-tubulin antibodies (loading control). Equal amounts of protein (35 µg/lane) were loaded onto the gels. Bars, 10 µm.

In a quantitative approach, the fluorescence intensity of peroxisomal GFP-hFis1 and PMP70-TRITC was determined and their ratio was calculated. In agreement with the morphological observations, the GFP-Fis1/PMP70-TRITC ratio was significantly reduced after silencing of Pex19p when compared to controls (Figure 3.6 J). These data further demonstrate that targeting of hFis1 to peroxisomes requires Pex19p. A mistargeting of hFis1 to other organelles (for instance the ER) as seen before for Pex26p and PMP34 (Halbach et al. 2006; Jones et al. 2004) did not occur. On the other hand, the knock down of Pex19p did not influence the mitochondrial targeting of hFis1. A significant reduction or increase of hFis1 targeting to mitochondria after Pex19p knock down was not detected by immunofluorescence or by ratio measurement of fluorescence intensities (Delille & Schrader 2008). The reduction of the peroxisomal import of hFis1 after silencing of Pex19p further supports the assumption that Pex19p functions as a cytosolic receptor for hFis1 targeting to peroxisomes.

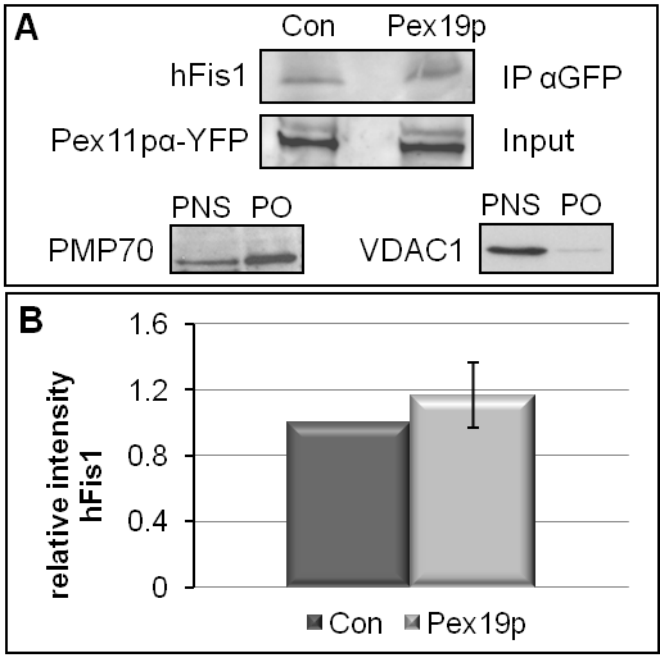

Figure 3.7: Overexpression of Pex19p does not increase peroxisomal targeting of hFis1
(A) Peroxisome immunoprecipitation. COS-7 cells were transfected with Pex11pα-YFP alone (Con) or co-transfected with HA-Pex19p. Peroxisomal membranes were immunoprecipitated from peroxisome-enriched fractions using anti-GFP/YFP antibodies and Protein A-sepharose. Endogenous hFis1 was detected by immunoblotting with anti-hFis1 antibodies. Contamination of mitochondria in the peroxisomal membrane fractions (PO) was low, as shown by immunoblotting with VDAC1 antibodies in the lower panel, in contrast to the enrichment of peroxisomal markers (PMP70). Equal amounts of protein (30µg/lane) were loaded onto the gels. **(B)** Quantitative analysis of the anti-hFis1 immunoblots. Data were normalized using Pex11pα as input references (Con). The data are from 4 independent experiments and are expressed as means ± SD. PNS, post-nuclear supernatant.

Subsequently, we also examined if overexpression of Pex19p leads to a shift in the targeting of hFis1 towards peroxisomes. Peroxisomal membranes of control cells or cells overexpressing Pex19p were immunoprecipitated (see 2.10.7.4) (Li & Gould 2003) and the relative amounts of membrane-associated, endogenous hFis1 were quantified after immunoblotting. Only a very slight increase in the amount of hFis1 associated with peroxisomal membranes after overexpression of Pex19p was observed (Figure 3.7). As a prominent shift of the targeting of hFis1 towards peroxisomes was not induced by sole

overexpression of Pex19p, other rate-limiting factors of the peroxisomal import machinery (for example, Pex3p) are likely to be involved.

3.1.3 Summary

It was shown that the C-terminal domain of hFis1 contains a Pex19p binding site, and that Pex19p is required for peroxisomal but not mitochondrial targeting of hFis1. Pex19p binding is independent of basic amino acid residues in the C-terminus of hFis1, which are instead required for mitochondrial targeting. In contrast, overexpression of Pex19p alone is not sufficient to shift the targeting of hFis1 to peroxisomes. These findings indicate that targeting of hFis1 to peroxisomes and mitochondria are independent events and support a direct, Pex19p-dependent targeting of peroxisomal TA proteins. Thus, TA proteins appear to utilize the existing import machinery of peroxisomes for membrane protein import.

3.2 Comparative characterization of Pex11pα, Pex11pβ, and Pex11pγ

Pex11 proteins are key components of peroxisomal proliferation in all species (Erdmann & Blobel 1995; Kiel et al. 2006; Lingard & Trelease 2006; Schrader et al. 1998b). Pex11 is the only protein of the growth and division machinery identified so far specific for peroxisomes and not shared with mitochondria (Delille et al. 2009). The mammalian Pex11p family consists of three members, Pex11pα, β, and γ, but little is known about differences, redundancies, interactions and specific characteristics or functions of these proteins. Most of the studies published so far are focused on Pex11pβ, the strongest "proliferator" and membrane elongating factor of peroxisomes (Abe & Fujiki 1998; Koch et al. 2004; Koch et al. 2003; Schrader et al. 1998b). In particular Pex11pγ was investigated only scarcely (Li et al. 2002a; Tanaka et al. 2003). Therefore, this part of the work is intended to characterize all mammalian Pex11p isoforms in more detail. The generation and expression of differentially tagged and deleted versions of the three isoforms was followed by monitoring the alterations of peroxisome morphology and formation. This approach was supposed to give insight into the mechanisms and components inducing peroxisomal elongation and proliferation and the role of the different isoforms in the peroxisomal biogenesis process.

3.2.1 The mammalian Pex11 isoforms differ in their membrane elongation-inducing properties

Pex11pβ is known to mediate peroxisomal proliferation by induction of tubulation or elongation of the organelles, a process then followed by constriction and division into small peroxisomes (Schrader et al. 1998b) (section 1.3). Although the effect of Pex11pα on peroxisomal number is controversially discussed – maybe due to the usage of different model systems and external factors (Abe et al. 1998; Li et al. 2002a; Passreiter et al. 1998; Schrader et al. 1998b) – a tubulation of peroxisomes has not been described. In order to compare the effects of the three isoforms on peroxisomal morphology, expression studies in one cellular model system (COS-7) under equal growth conditions were performed. Different tagged and truncated forms were generated (see 2.5.3). The cloning of all three Pex11p isoforms into the same vectors allowed comparable studies under equal expression levels. The proteins were first expressed in COS-GFP-SKL cells as

N-terminally Myc-tagged proteins. This cell line is stably transfected with GFP fused to a SKL tripeptide (PTS1, see 1.2.1 and 2.7), generating GFP-labelled peroxisomes.

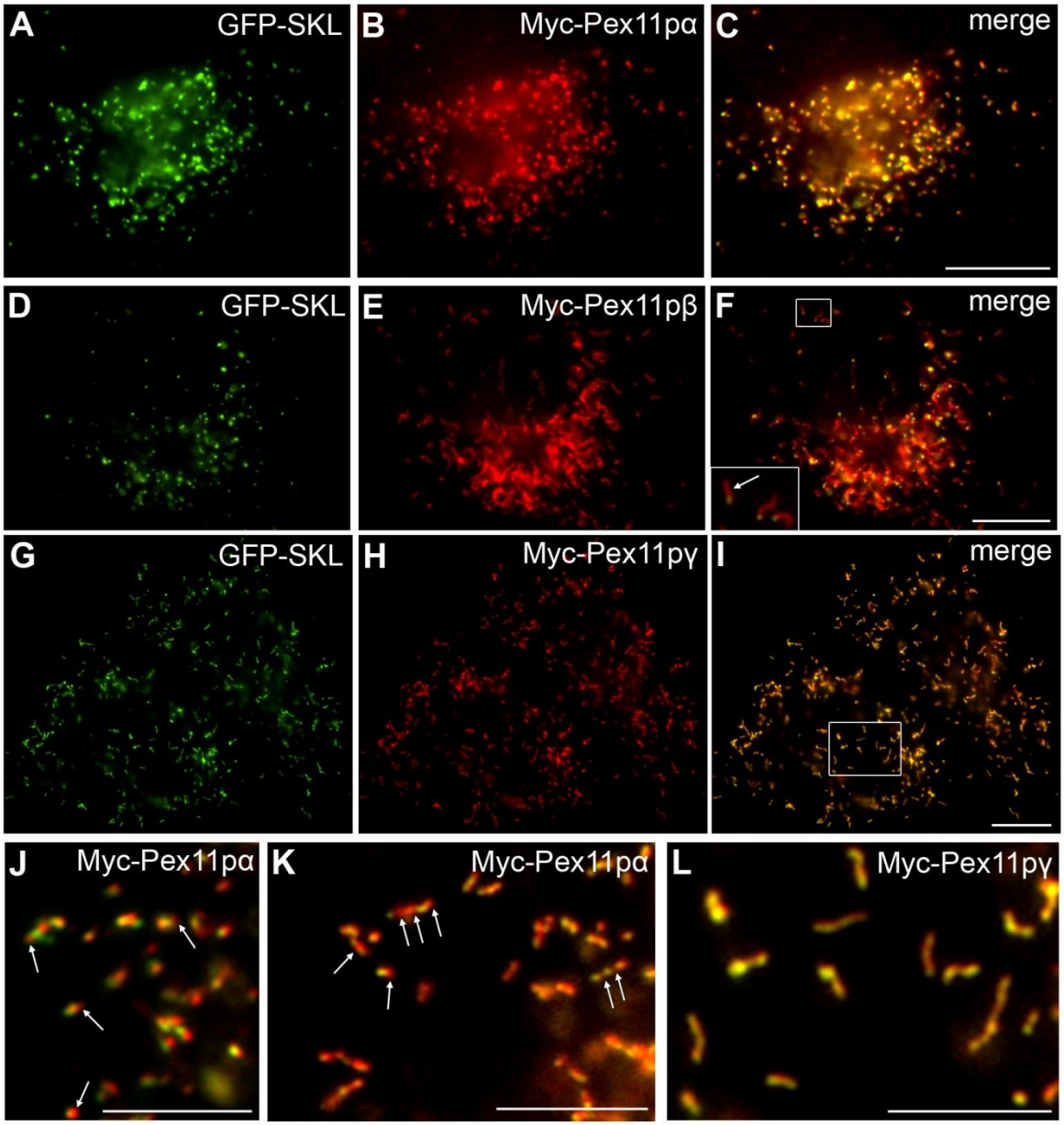

Figure 3.8: The Pex11p isoforms induce different peroxisomal morphologies
COS-GFP-SKL cells were transfected with Myc-Pex11pα (A-C, J-K), Myc-Pex11pβ (D-F), or Myc-Pex11pγ (G-I, L), fixed after 24 hours, and processed for immunofluorescence using an antibody directed against the Myc epitope tag. **(A-C)** Peroxisomes in cells expressing Myc-Pex11pα have a spherical morphology. **(D-F)** Expression of Myc-Pex11pβ induces the formation of elongated peroxisomes. At a certain stage the peroxisomal tubules are mainly positive for Myc-Pex11pβ (arrow) while GFP-SKL is localized to spherical regions at one end of the tubule (inset). **(G-I)** Peroxisomes in cells expressing Myc-Pex11pγ are elongated. The boxed region is shown at higher magnification in **(L)**. Note that GFP-SKL and Myc-Pex11pγ completely co-localize in the peroxisomal tubules. **(J-K)** Higher magnification view of cells expressing Myc-Pex11pα. GFP-SKL is separated from Myc-Pex11pα and is localized to one side of spherical peroxisomes (J) or appears segmented along the peroxisomal tubules while Myc-Pex11pα is more equally distributed (K). Some Myc-Pex11pα-enriched regions are marked by arrows. Bars, 10 µm (A-I), 5 µm (J-L).

Expression of Myc-Pex11pα resulted in a punctate staining pattern usually co-localizing with GFP-SKL (Figure 3.8 A-C) (Abe et al. 1998; Li et al. 2002a; Schrader et al. 1998b). Sometimes Myc-Pex11pα separated from GFP-SKL and localized only to one side of the peroxisome. The expression of Myc-Pex11pα did not result in an increase in tubular peroxisomes, compared to control cells (Figure 3.8 A-C and Figure 3.9). In the minor subset of cells exhibiting tubular peroxisomes (18.0 ± 9.97% after 24 hours), GFP-SKL and Myc-Pex11pα did not completely co-localize but showed an alternating staining of the peroxisomal tubule, with Myc-Pex11pα being more equally distributed than GFP-SKL (Figure 3.8 J and K).

A similar protein segregation or segmentation is also induced by Pex11pβ, although it occurs on much more elongated peroxisomal structures. Before division of the tubule into small peroxisomes, the constriction sites become enriched in Pex11pβ while peroxisomal matrix (and membrane) proteins are preferentially found in between those Pex11pβ spots (Koch et al. 2003; Schrader et al. 1998b) (see Figure 3.20 K-M).

In contrast to Pex11pα, the expression of Myc-Pex11pγ resulted in a pronounced increase of cells with tubular peroxisomes (Figure 3.8 G-I and Figure 3.9). After 24 hours only a subset of the cells (27.75 ± 8.8%) displayed peroxisomes with a spherical morphology. Myc-Pex11pγ always co-localized with GFP-SKL, in spherical and tubular peroxisomes. The peroxisomal tubules were entirely positive for GFP-SKL and Myc-Pex11pγ and did not show any separation of these two proteins or a segmentation of the tubules (Figure 3.8 L). Furthermore, globular endings only positive for GFP-SKL, as seen after expression of Pex11pβ (Figure 3.8 D-F) (Koch et al. 2003; Lay et al. 2006; Schrader et al. 1998b), were not observed.

To evaluate the peroxisome elongating effects of Pex11pα and Pex11pγ in more detail, a time course experiment was performed and the cells were fixed 5 to 72 hours after transfection (Figure 3.9). Interestingly, already 5 hours after transfection of the cells with Myc-Pex11pγ peroxisomes were elongated (in 80.5 ± 6% of the cells). The peroxisomes continued to be tubular over two days but 72 hours after transfection the number of cells with elongated peroxisomes declined (39.0 ± 6.2%). Similar observations were made after expression of Pex11pβ, although the division into spherical peroxisomes occurred at earlier time points, already 24 to 48 hours after transfection (Figure 3.9 and Figure 3.13 A-C) (Koch et al. 2003; Schrader et al. 1998b). Expression of Myc-Pex11pα never increased the number of cells with tubular peroxisomes (Figure 3.9). In control cells and cells transfected with Myc-Pex11pα a slightly elevated number of cells

with tubular peroxisomes was observed (5 and 10 hours after transfection). This was rather induced by the cell culture conditions as such, since the occurrence of tubular peroxisomes also depends on cell density and the time in culture, and a peak of tubular peroxisomes is usually seen 24 hours after seeding (Schrader et al. 1996).

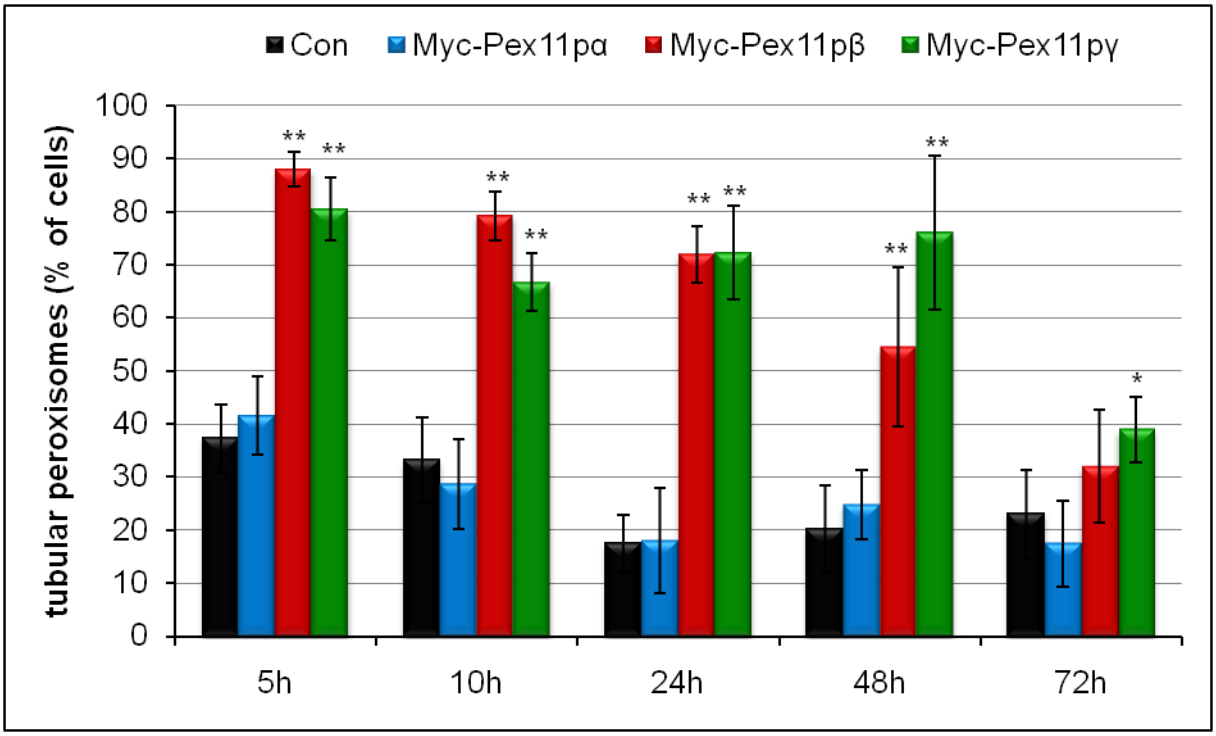

Figure 3.9: Quantitative analysis of peroxisomal morphologies in cells expressing different Pex11p isoforms
COS-7 cells were transfected with Myc-Pex11pα, Myc-Pex11pβ, Myc-Pex11pγ or not transfected (Con) using PEI. Cells were fixed at different time points after the begin of transfection and categorized as cell with tubular or spherical/rod-like peroxisomes. Note the strong increase of tubular peroxisomes in cells expressing Myc-Pex11pβ or Myc-Pex11pγ while cells expressing Myc-Pex11pα are similar to control cells. Data are expressed as means ± SD (** $p<0.01$, * $p<0.05$; compared to control).

The results show that the three isoforms of Pex11p affect the peroxisomal morphology differently. While Pex11pα does not induce peroxisomal elongation, Pex11pγ induces peroxisomal elongation at least as strong as Pex11pβ. But a strong increase in peroxisome number 48 hours after expression, as it is induced by Pex11pβ (Figure 3.13 C) (Schrader et al. 1998b), was not observed. Interestingly, Pex11pα – although not inducing peroxisomal elongation – appears to provoke a separation from peroxisomal proteins similar to Pex11pβ. Therefore, Pex11pα and Pex11pγ functions appear to differ from each other, but each one induces effects (protein segregation or peroxisome elongation, respectively) partly similar to Pex11pβ.

3.2.2 Pex11pα, Pex11pβ, and Pex11pγ differ in their Triton X-100 sensitivity

In previous studies it was shown that Pex11pβ is sensitive to the detergent Triton X-100 (Li & Gould 2003; Schrader et al. 1998b). Interestingly, it was observed that Pex11pβ-Myc is not detectable after permeabilization of formaldehyde-fixed cells with Triton X-100, but after treatment with digitonin (Schrader et al. 1998b) which permeabilizes only the plasma membrane and not the peroxisomal one (Motley et al. 1994). The N- and C-termini of all Pex11p isoforms are exposed to the cytosol and are accessible to antibodies after digitonin permeabilization (Abe et al. 1998; Li et al. 2002a; Schrader et al. 1998b; Tanaka et al. 2003). In biochemical approaches Triton X-100 could also not be used together with Pex11pβ and Pex11pα (Li & Gould 2003). We compared the three Pex11p isoforms in regard to their sensitivity to Triton X-100 in immunofluorescence studies. As shown before, Myc-Pex11pβ was only detectable after permeabilization of the cells with digitonin and never with Triton X-100 (Figure 3.10 D-F) (Schrader et al. 1998b). On the contrary, Myc-Pex11pγ did not show any difference after permeabilization with one or the other detergent (Figure 3.10 G-I). The results for Myc-Pex11pα were ambiguous. In most of the cells permeabilized with Triton X-100 Myc-Pex11pα was not detectable (Figure 3.2 A-C). But in previous studies (Schrader et al. 1998b) and in a minor subset of cells it was possible to detect a signal for Myc-Pex11pα. Additionally, permeabilization experiments with different Triton X-100 concentrations were performed (data not shown). Under standard permeabilization conditions with 0.2% Triton X-100 Myc-Pex11pα was not detectable, but its signal increased with the usage of lower Triton X-100 concentrations (up to 0.02%). This effect was not observed for Pex11pβ. These observations led to the assumption that the Triton X-100 sensitivity depends a) on the Triton X-100 concentration and b) on the expression level of Pex11pα. Triton X-100 might in a way decrease the signal so that it is only visible above a certain protein amount. Interestingly, Pex11p proteins are never sensitive to Triton X-100 permeabilization if they are fused to larger tags like YFP (Figure 3.11; see section 3.3), probably as a result of the better cross-linking by the fixative. As formaldehyde fixation cross-links lysine residues (see 2.9.1), the number of lysines in each of the Pex11p isoforms was determined. There was no correlation in between the total number of lysine residues (Pex11pα 18, Pex11pβ 9, Pex11pγ 3 lysine residues) and the Triton X-100 sensitivity.

In summary, Pex11pβ appears to be the most and Pex11pγ the least Triton X-100 sensitive protein, and Pex11pα is placed somewhere in between those two. The potential lipid-binding properties of Pex11 proteins (1.3.3) may be removed by Triton X-100 resulting in extraction of the protein from the membrane. According to that, the different Triton X-100 sensitivities would reflect different lipid or membrane binding properties of the Pex11p isoforms.

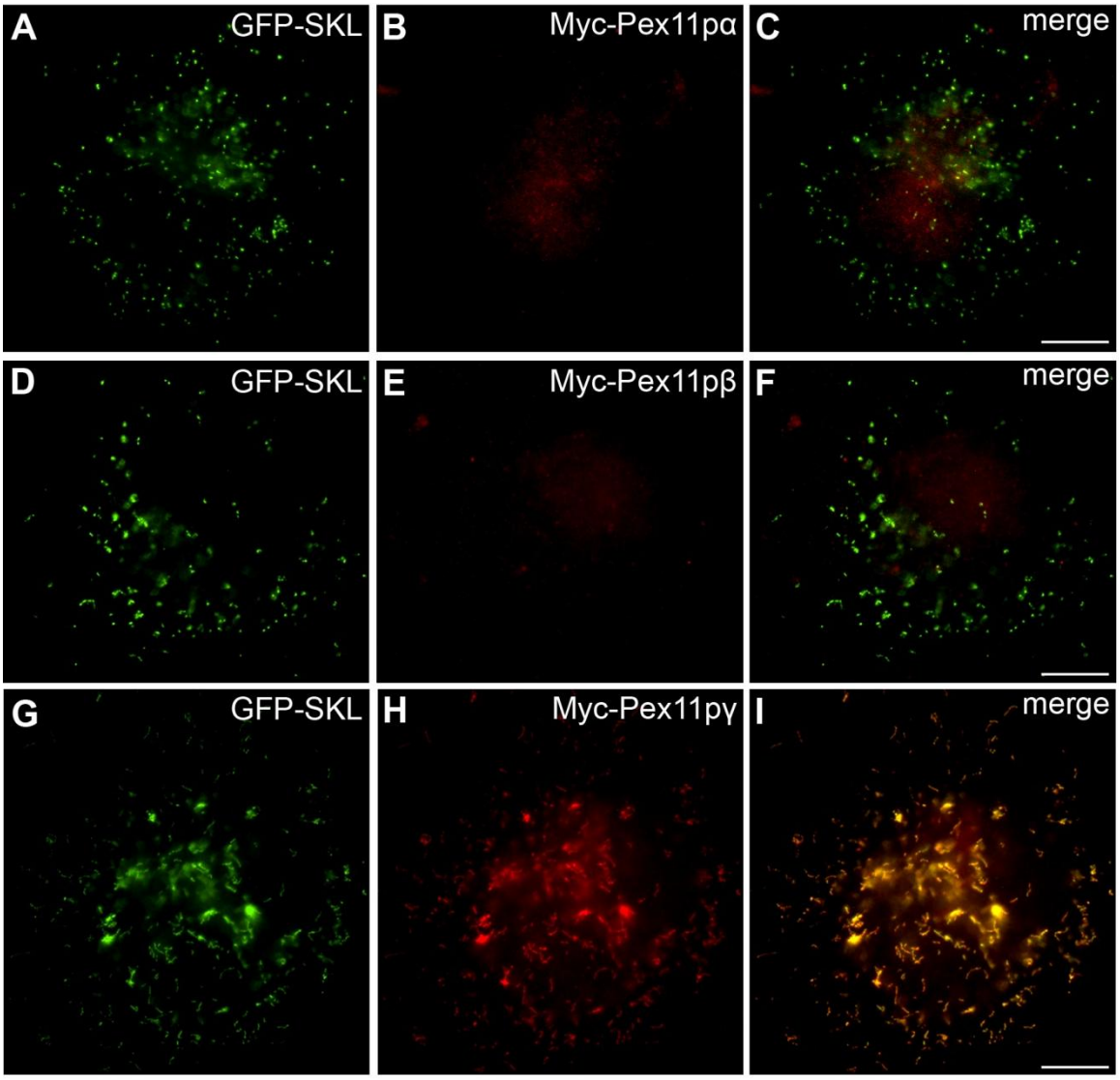

Figure 3.10: Pex11pα and Pex11pβ are sensitive to Triton X-100
COS-GFP-SKL cells were transfected with Myc-Pex11pα (A-C), Myc-Pex11pβ (D-F), or Myc-Pex11pγ (G-I) and subjected to immunofluorescence using 0.2% Triton X-100 (standard protocol). Note that Myc-Pex11pα and Myc-Pex11pβ are not visible upon Triton X-100 permeabilization, while Myc-Pex11pγ appears to be unaffected. Bars, 10 µm.

3.2.3 Pex11pγ-induced peroxisomal tubules are highly motile

Peroxisomes are dynamic organelles exhibiting wriggling and microtubule-dependent long range movements (Rapp et al. 1996; Schrader et al. 2000; Schrader et al. 2003; Wiemer et al. 1997). As immunofluorescence experiments only allow studies in fixed cells, *in vivo* experiments were performed. The Pex11p isoforms were C-terminally fused to monomeric YFP, which enables live cell imaging and *in vivo* visualization of the proteins (see 2.9.5).

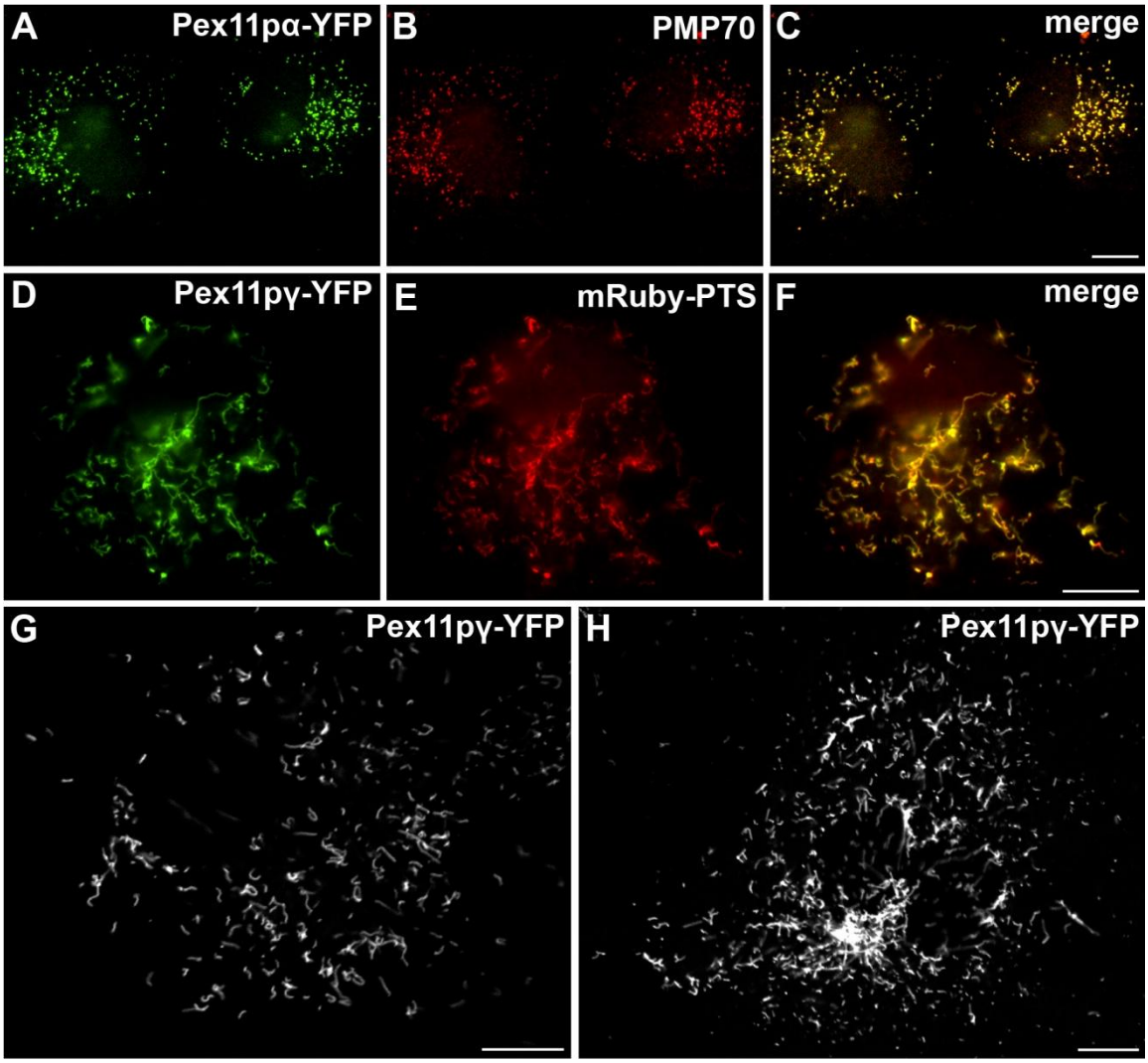

Figure 3.11: Pex11pγ-YFP induces highly elongated peroxisomal tubules
(A-C) Pex11pα-YFP co-localizes with PMP70 and peroxisomes have a spherical morphology. Transfection of COS-7 cells with Pex11α-YFP (A) and staining of peroxisomes with anti-PMP70 antibodies (B). **(D-H)** COS-7 cells were transfected with Pex11pγ-YFP alone (G-H) or co-transfected with mRuby-PTS as peroxisomal marker (D-F). Note the formation of elongated peroxisomes induced by Pex11pγ-YFP. **(G-H)** Confocal images. Bars, 10 µm.

Cells transfected with Pex11pα-YFP showed a similar (spherical) peroxisomal morphology to cells transfected with Myc-tagged Pex11pα (Figure 3.11 A-C) (Delille & Schrader 2008). Interestingly, expression of Pex11pβ-YFP led to an altered peroxisomal pheno-

type, which was studied in detail in part 3.3. The majority of cells expressing Pex11pγ-YFP (66.0 ± 6.6%) displayed tubular peroxisomes (Figure 3.11 D-H), similar to Myc-Pex11pγ, but sometimes also very thin and long tubules or even net-like structures (data not shown). The tubular peroxisomes appeared to be longer (up to 10 μm) compared to Myc-tagged Pex11pγ.

To study the motility and behaviour of the peroxisomal tubules, live-cell imaging was conducted. Pex11pβ-YFP could not be used for this approach (see 3.3) and therefore COS-7 cells were transfected with Pex11pγ-YFP by electroporation, seeded in glass-bottom dishes and motility studies were performed at 37°C under 5% CO_2 atmosphere. The peroxisomal tubules showed high motility and the tubules were crawling throughout the cell, probably along the microtubule network (Figure 3.12 and Movie 2). In the process, the tubules were often seen to bend (and branch?) and to move forwards and backwards.

The induction of tubular peroxisomes by Pex11pγ-YFP did not inhibit or interfere with the peroxisomal motility; in contrast, the tubular peroxisomes were highly motile and interactive. The peroxisomal tubules appeared to be aligned with microtubules and to move along them. Additionally, the membrane mobility of YFP-tagged Pex11pβ and Pex11pγ was determined by FRAP, and it was shown that Pex11pγ has higher membrane mobility in peroxisomal tubules than Pex11pβ (see section 3.3.10).

3.2.4 Summary

By comparison of the morphological alterations induced by the expression of the Pex11p isoforms it was shown for the first time that Pex11pγ induces the formation of peroxisomal tubules in a way similar to Pex11pβ. Furthermore, these tubules appear to be very long and highly motile. On the other hand, expression of Pex11pα does not change the peroxisomal morphology but it separates (at least) from matrix proteins, similar to Pex11pβ. The Pex11 proteins differ in their sensitivity to Triton-X 100, with Pex11pγ being the least and Pex11pβ the most sensitive isoform. In conclusion, Pex11pγ appears to have tubule elongating properties, while Pex11pα function may have protein segregating or tubule constriction activities.

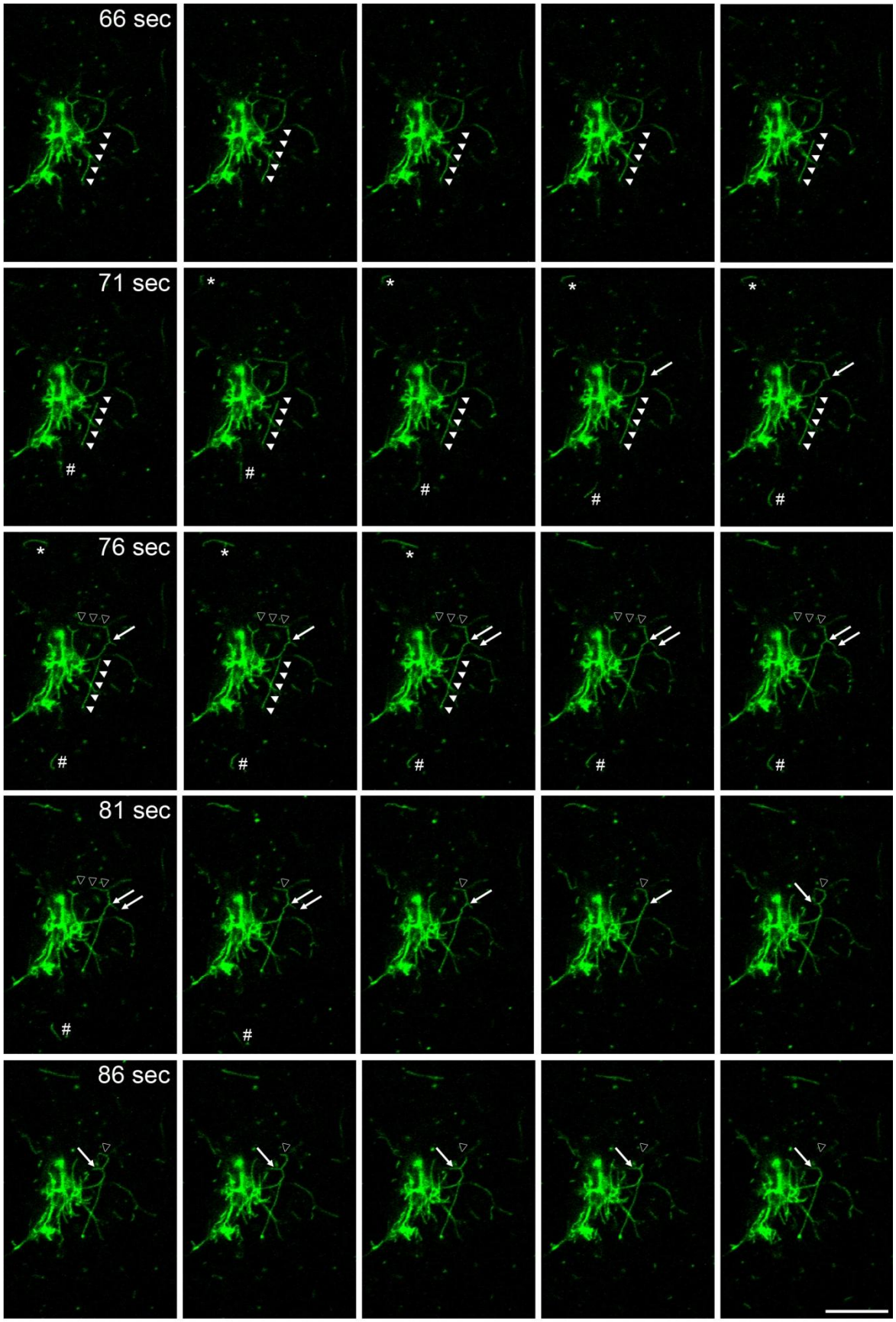

Figure 3.12: Peroxisomal tubules induced by Pex11pγ-YFP are highly motile
Time series of a cell expressing Pex11pγ-YFP. Selection of images (see time indicated) from Movie 1. Time interval between single images was one second. Peroxisomal tubules are highly motile, showing extending and retracting movements as well as bending (and branching), highlighted by arrowheads, arrows, and open arrowheads. * and # mark single peroxisomes moving through the cell which appear in or disappear from the focal plane, respectively. See also Movie 1. Bar, 10 µm.

3.3 Pex11pβ-mediated growth and division of mammalian peroxisomes follows a maturation pathway

In order to manipulate and dissect peroxisomal growth and division, we generated truncated and tagged versions of the Pex11 proteins (3.2). These constructs were expressed in COS-7 cells, which were then screened for alterations of peroxisomal growth and division. When COS-7 cells were transfected with Pex11pβ fused to monomeric YFP_m at the C-terminus (Pex11pβ-YFP), striking morphological changes of the peroxisomal compartment were detected and investigated more precisely.

3.3.1 Pex11pβ-YFP induces tubular peroxisomal accumulations (TPAs) and inhibits the formation of spherical peroxisomes

Expression of Myc-tagged (N- or C-terminally) or untagged Pex11pβ has been shown to induce a pronounced elongation of peroxisomes (Figure 3.13 B), which is followed by peroxisome division and the formation of small spherical peroxisomes (Figure 3.13 C) (Koch et al. 2003; Lingard & Trelease 2006; Schrader et al. 1998b). In contrast, transfection of COS-7 cells with Pex11pβ-YFP led to a strongly altered phenotype. A minority of cells (1-5%) contained spherical peroxisomes (Figure 3.13 D and G), whereas the majority displayed elongated peroxisomal structures, which appeared to form tubular accumulations. These structures were found to be distributed uniformly within the cytoplasm (Figure 3.13 E), or to concentrate at one side of the nucleus (Figure 3.13 F and Figure 3.24 G-I). Usually, several small tubular accumulations were observed, which appeared to be thicker than the tubular peroxisomes found in controls (Figure 3.13 B). This suggests that the tubular morphology is stabilized by expression of Pex11pβ-YFP. Cells with only a few tubular structures were also detected and increased with time in culture (Figure 3.13 G and H). Many of the structures, which were termed TPAs (tubular peroxisomal accumulations), had a twisted, curly or cork-screw-like appearance. Interestingly, the formation of spherical peroxisomes by constriction and fission of tubular peroxisomes, which is promoted by the expression of Myc-tagged (N- or C-terminally) or untagged Pex11pβ (Koch et al. 2003; Lingard et al. 2008; Schrader et al. 1998b), was completely inhibited. TPAs were not observed to constrict or to divide and to give rise to spherical organelles (Figure 3.13 G). Thus, other peroxisomal structures than TPAs appeared to be absent from Pex11pβ-YFP expressing cells (see also Figure 3.17 D-F). Simi-

lar morphological changes of peroxisomes after expression of Pex11pβ-YFP were obtained with a variety of other cell lines of human (HepG2, HeLa) or rodent origin (Fao, AR42J) (data not shown), among which COS-7 cells exhibited very prominent TPAs. As pre-peroxisomal membrane compartments have been associated with the formation of peroxisomes (section 1.2.3), the TPAs were investigated in more detail.

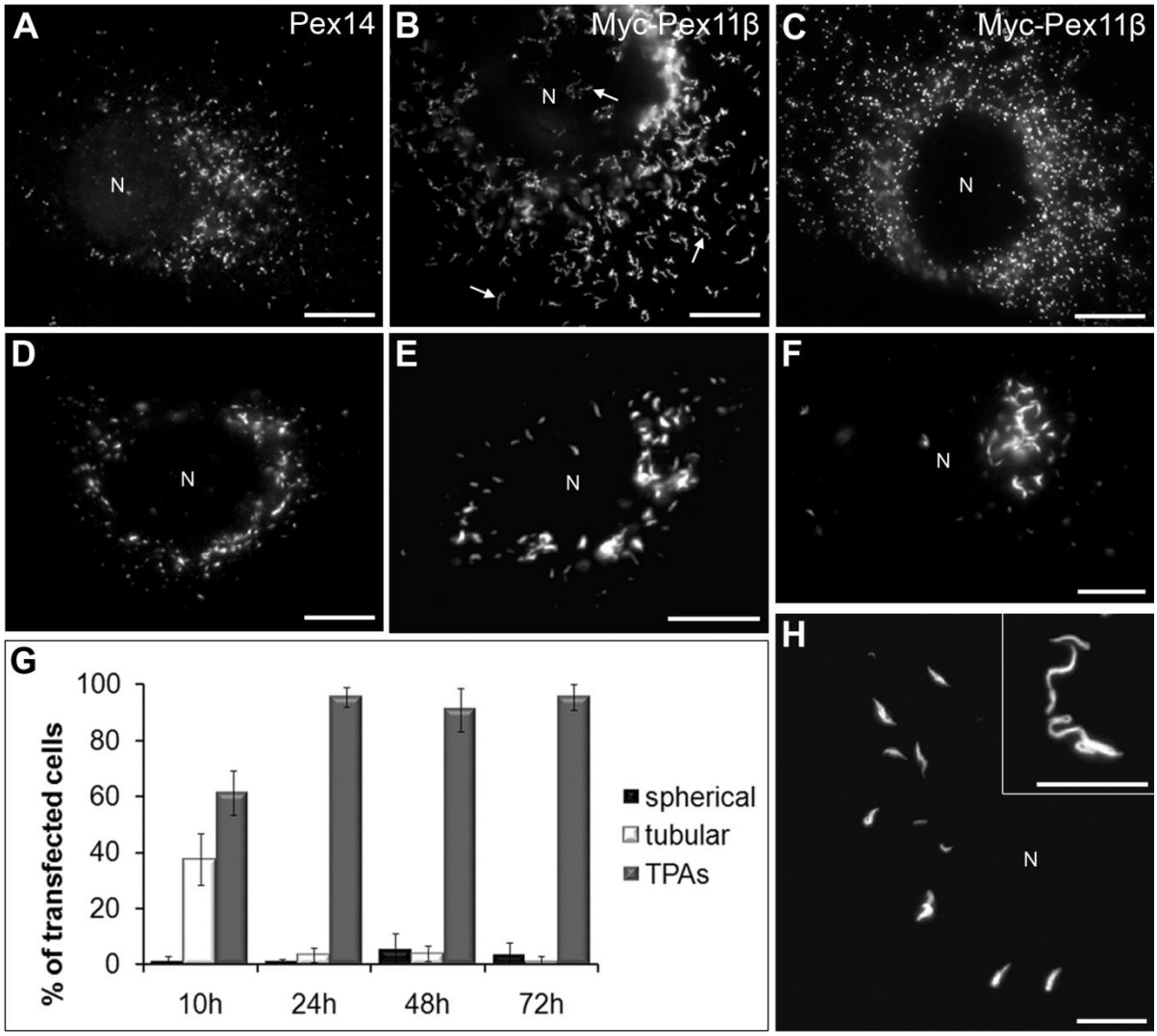

Figure 3.13: Pex11pβ-YFP induces the formation of TPAs (tubular peroxisomal accumulations)
COS-7 cells were transfected with Myc-Pex11pβ (B-C), or Pex11pβ-YFP (D-F, H). Fixed cells were labeled with anti-Pex14p (A, control) or anti-Myc (B-C) antibodies. Pex11pβ-YFP fluorescence is shown in (D-F, H). **(A)** Peroxisomes in control cells have a spherical or rod-shaped morphology. **(B-C)** Myc-Pex11pβ induces peroxisome proliferation by elongation (B), constriction (B, arrows) and division into small spherical peroxisomes (C). **(D-H)** Pex11pβ-YFP induces the formation of TPAs ranging from multiple small peroxisomal accumulations (D, E) to one or few long, curled structures (F, H). Note that in cells forming TPAs no further peroxisomes are detected. **(G)** Quantitative evaluation of peroxisome morphology in cells expressing Pex11pβ-YFP at several time points after transfection. N, nucleus. Bars, 10 µm (A-F, H), 5 µm (insert H).

3.3.2 TPA formation appears to be specific for Pex11pβ-YFP

In order to demonstrate that TPA formation was not just due to the overexpression of Pex11pβ or a YFP/GFP-tagged peroxisomal membrane protein, COS-7 cells were transfected with a Pex11pβ construct bearing the YFP-tag at the N-terminus (YFP-Pex11pβ). The fusion protein was properly targeted to peroxisomes as demonstrated by co-localization with the peroxisomal membrane protein PMP70 (Figure 3.14 A-B). However, formation of TPAs was not observed and YFP-Pex11pβ was able to induce peroxisome elongation and division as demonstrated for Myc-tagged Pex11pβ (Figure 3.14 K). It is important to point out that in order to avoid dimer formation of YFP-tagged fusion proteins a mutated monomeric version of YFP was used for the generation of all constructs. As described above, Pex11pα-YFP had only a slight effect on peroxisome elongation and did not induce TPA formation (see Figure 3.11 A-C) (Delille & Schrader 2008). Similar observations were made when Pex3p-GFP was expressed in COS-7 cells, either alone or in combination with Pex11pβ-Myc (Figure 3.14 C-D). The fusion proteins were successfully targeted to peroxisomes, but TPA formation was not promoted.

These date demonstrate that TPA formation is neither related to the expression of a peroxisomal membrane protein carrying a fluorescent tag, nor to the expression of Pex11pβ. Even the expression of N-terminally tagged YFP-Pex11pβ, or of Pex11pα-YFP, a homologue of Pex11pβ with similar membrane topology, was unable to induce TPAs. TPA formation appeared to be specific for the expression of Pex11pβ-YFP carrying the YFP-tag at the C-terminus.

3.3.3 C-terminal truncations of Pex11pβ inhibit peroxisome elongation

The above observations suggested the possibility that the YFP-tag might block the C-terminal cytoplasmic tail of Pex11pβ, rendering it inaccessible and thus, inhibiting putative protein interactions, for example with components of the peroxisomal division machinery. Removal of different portions of the C-terminus could therefore also lead to TPA formation. C-terminally truncated versions of Pex11pβ with a Myc-tag at the N-terminus were generated and their influence on peroxisomal targeting and TPA formation was examined. As demonstrated, after expression of Myc-Pex11pβ in COS-7 cells, a prominent elongation of peroxisomes but no TPA formation was observed (Figure 3.13 B). Next, Pex11pβ lacking the putative 5-amino-acid cytoplasmic tail (Myc-Pex11pβΔ5)

was expressed. The truncated protein was efficiently targeted to peroxisomes as demonstrated by co-localization with PMP70, but failed to induce the formation of TPAs (Figure 3.14 E-F). In contrast, the capability to promote the elongation of peroxisomes as demonstrated for Myc-Pex11pβ was reduced, although expression levels were equal (data not shown). Interestingly, time course experiments revealed that the elongation of peroxisomes in the presence of Myc-Pex11pβΔ5 was delayed compared to the full length protein (Figure 3.14 K). The C-terminal tail appeared to be dispensable for peroxisome elongation and division.

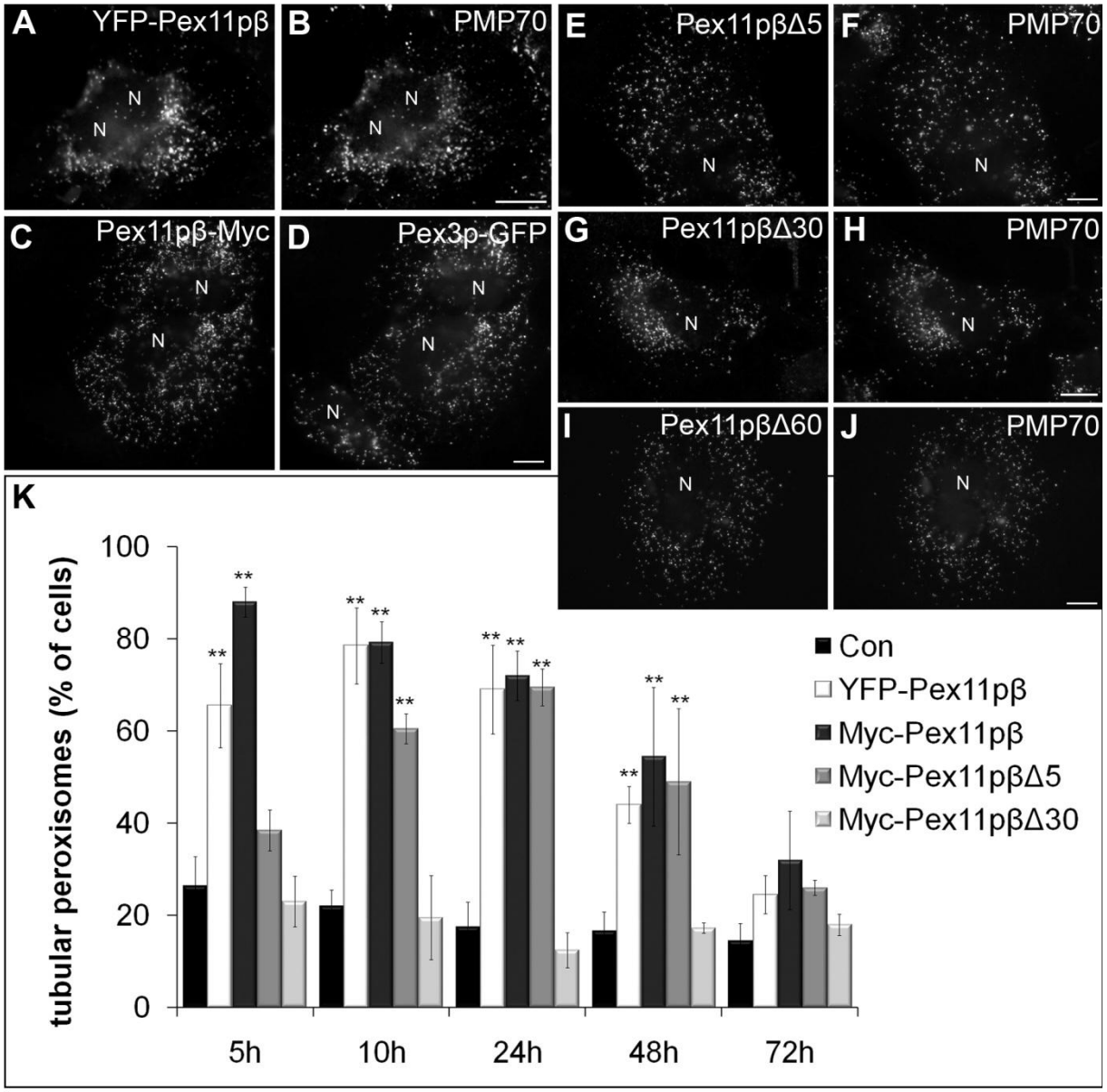

Figure 3.14: TPA formation is specific for Pex11pβ-YFP
COS-7 cells were transfected with YFP-Pex11pβ (A-B), Pex11pβ-Myc plus Pex3p-GFP (C-D), Myc-Pex11pβΔ5 (E-F), Myc-Pex11pβΔ30 (G-H), or Myc-Pex11pβΔ60 (I-J) and labeled with anti-PMP70 antibody (B, F, H, and J). Note that TPA formation is not observed under these conditions. **(K)** Alterations of peroxisome morphology over time. Con, vector only. YFP-Pex11pβ and Myc-Pex11pβ promote peroxisome elongation and division, whereas C-terminal truncations delay/reduce peroxisome elongation. Data are expressed as means ± SD (** $p<0.01$, compared to control). N, nucleus. Bars, 10 µm.

Pex11pβ constructs lacking the putative transmembrane domain (Myc-Pex11pβΔ30) or the last C-terminal 60 amino acids (Myc-Pex11pβΔ60) were expressed next (Figure 3.14 G-J). Both truncated proteins were still targeted to peroxisomes indicating that the targeting information within the N-terminal part is sufficient for peroxisomal localization. However, labelling of peroxisomes with Myc-Pex11pβΔ60 was rather weak suggesting either less efficient targeting and/or degradation of the truncated protein. More interestingly, cells expressing either Myc-Pex11pβΔ30 or Myc-Pex11pβΔ60 exhibited only spherical peroxisomes, and peroxisome elongation was drastically reduced (Figure 3.14 K).

These results show that the last C-terminal 30 amino acids of Pex11pβ are required for the elongation of peroxisomes. The very last 5 amino acids are dispensable for peroxisome elongation and division, but their loss results in a delay in peroxisome elongation. As the addition of a C-terminal YFP does not interfere with the ability of Pex11pβ to elongate peroxisomes, we assume that Pex11pβ-YFP acts as a "dominant-negative" mutant which inhibits other downstream events in the formation of spherical peroxisomes, such as the proper assembly of the constriction and division machineries (see 1.3).

Analogous, C-terminally truncated versions of Pex11pα and Pex11pγ were studied. For both proteins mutants missing the last 30 amino acids including a putative transmembrane domain (Δ30) and mutants lacking the extreme C-terminal amino acids following the TMD (Δ8 for Pex11pα and Δ11 for Pex11pγ) were created and expressed in COS-7 cells. While none of the truncated Pex11pα versions was detectable, no difference to the full length protein was seen after expression of Myc-Pex11pγΔ11 (Figure 3.15). Peroxisomal tubulation was induced in up to 72.0 ± 6.7% of the cells, similar to cells expressing wild type Myc-Pex11pγ. However, tubules were divided into spherical peroxisomes already 48 hours after transfection, compared to 72 hours for the full length protein. On the other hand, Myc-Pex11pγΔ30 was not detected upon expression in COS-7 cells.

These results indicate that the very C-terminus of the three Pex11p isoforms contributes to the stability and properties of the respective proteins in different degrees. Removal of the transmembrane domain always results in complete loss-of-function, and in the case of Pex11pα and Pex11pγ even in total absence of the protein. Removal of the very C-terminus renders Pex11pα (Δ8) unstable or not targeted, while Pex11pγΔ11 is not only targeted properly but also induces peroxisomal elongation normally. Pex11pβΔ5 on

the other hand is targeted to peroxisomes but the induced peroxisomal tubulation/proliferation is delayed compared to the full length protein.

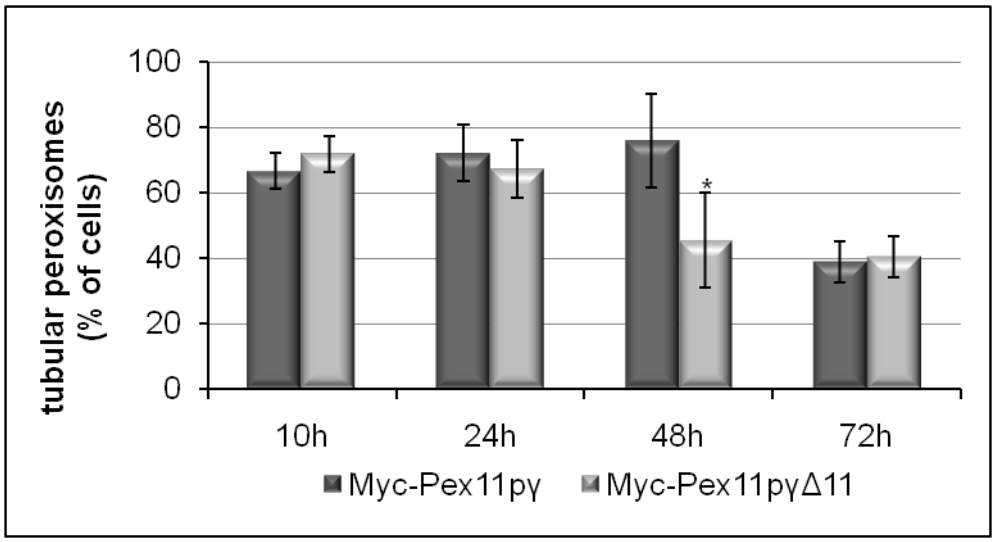

Figure 3.15: Quantitative analysis of tubular peroxisomes induced by Pex11pγ and Pex11pγΔ11
COS-7 cells transfected with Myc-Pex11pγ or Myc-Pex11pγΔ11 were fixed at different time points after transfection and peroxisomal morphology was categorized as tubular or spherical/rod-shaped. Note that C-terminal truncation of Pex11pγ does not hinder peroxisomal tubulation but tubules are less persistent than in cells expressing the full length protein. Data are expressed as means ± SD (* $p<0.05$, compared to control).

3.3.4 TPAs represent a pre-peroxisomal membrane compartment composed out of tubular membrane extensions and mature globular peroxisomes

To examine TPA morphology at the ultrastructural level, electron microscopy of Pex11pβ-YFP transfected cells was performed. As shown in Figure 3.16, consistent with light microscopy, COS-7 cells expressing Pex11pβ-YFP contained accumulations of elongated membranes. In larger accumulations, the tubular membranes were observed to form ordered stack-like structures which are nicely visible in cross-sections of accumulated tubules (Figure 3.16 B, open arrow). Interestingly, the membrane tubules appeared thinner than regular elongated peroxisomes (approx. 35-60 nm vs. 70-150 nm). Immunoelectron microscopy revealed that the membrane tubules could be decorated with an antibody directed to GFP/YFP, indicating that they were containing Pex11pβ-YFP (Figure 3.16 D). More interestingly, bulbous or spherical membrane structures were observed at one end of the membrane tubules (Figure 3.16 A and C, arrows).

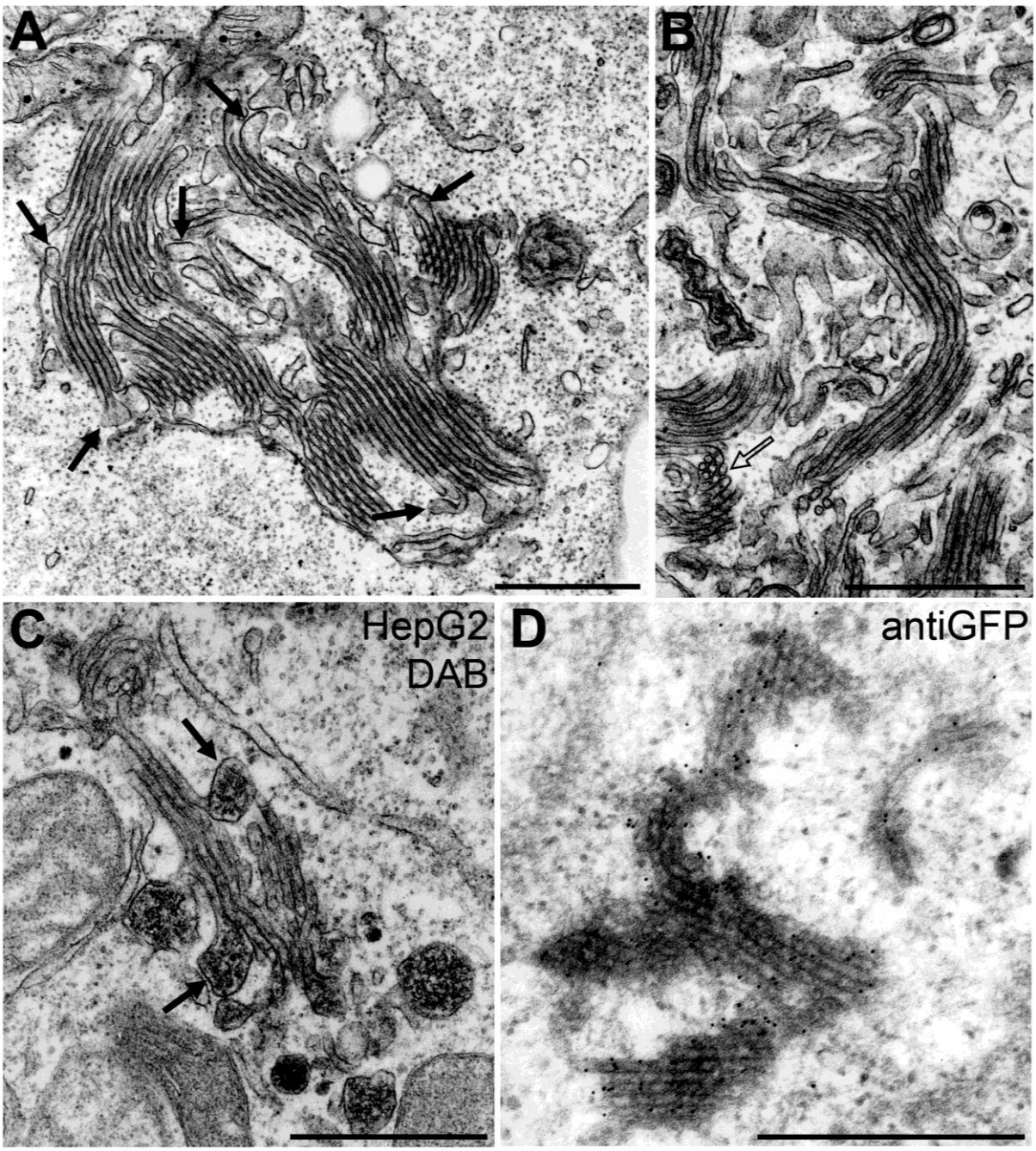

Figure 3.16: TPAs represent a pre-peroxisomal membrane compartment with tubular and globular domains
COS-7 (A-B, D) and HepG2 (C) cells were transfected with Pex11pβ-YFP and processed for electron microscopy. **(A-B)** Ultrastructure of TPAs in COS-7 cells. TPAs represent accumulations of tubular membrane extensions connected to globular domains (arrows in A; open arrow in B points to cross-section). **(C)** DAB cytochemistry for catalase. Catalase concentrates in bulbous structures at tubule endings (arrows). **(D)** Immunoelectron microscopy of TPAs using anti-GFP antibody and Protein-A gold. Bars, 500 nm.

To achieve a specific labelling of peroxisomes, the alkaline DAB-reaction for catalase was used (Angermuller & Fahimi 1981). As this method works less efficient in COS-7 cells (Koch et al. 2004), HepG2 cells were used, which also showed TPA formation after expression of Pex11pβ-YFP, and have already been used successfully for DAB-

cytochemistry (Schrader et al. 1994). Interestingly, DAB staining was predominantly seen in the globular structures at the endings of the tubules (Figure 3.16 C).

These findings confirm that the TPAs formed after expression of Pex11pβ-YFP are composed of ordered, stack-like tubular membranes. Noteworthy, these membrane tubules are in direct luminal and membrane continuity with globular or bulbous structures, which appear to be mature, catalase-containing peroxisomes. At this point it can be hypothesized that these are peroxisomes caught actively during the growth and division process and it can be proposed that the TPAs represent a pre-peroxisomal membrane compartment, which is composed out of tubular membrane extensions and mature (spherical) peroxisomes attached to them (see Figure 3.19).

3.3.5 TPAs show a distinct distribution of matrix proteins

To investigate the distribution of matrix proteins within of TPAs, COS-7 cells were co-transfected with Pex11pβ-YFP and a construct coding for a DsRed fusion protein carrying a peroxisomal targeting signal 1 at the C-terminus (DsRed-PTS1). Like other fluorescent fusion proteins carrying a PTS1 for peroxisomal matrix protein import (for example, EGFP-PTS1, mRuby-PTS1), DsRed-PTS1 was properly and exclusively targeted to peroxisomes in control cells (data not shown). When co-expressed with Pex11pβ-YFP, DsRed-PTS1 was almost exclusively found in the globular structures of the TPAs, and not in the tubular membrane extensions (Figure 3.17 A-C). In contrast, Pex11pβ-YFP mainly localized to the tubular membrane extensions and not to the spherical peroxisomes attached to them, nicely visualized by deconvolution microscopy (Figure 3.17). Similar observations were made when COS-7 cells expressing Pex11pβ-YFP were stained with antibodies directed to peroxisomal catalase or acyl-CoA oxidase, a key matrix enzyme of peroxisomal β-oxidation (data not shown). These findings further confirm that the globular parts of the TPAs represent mature, import competent peroxisomes.

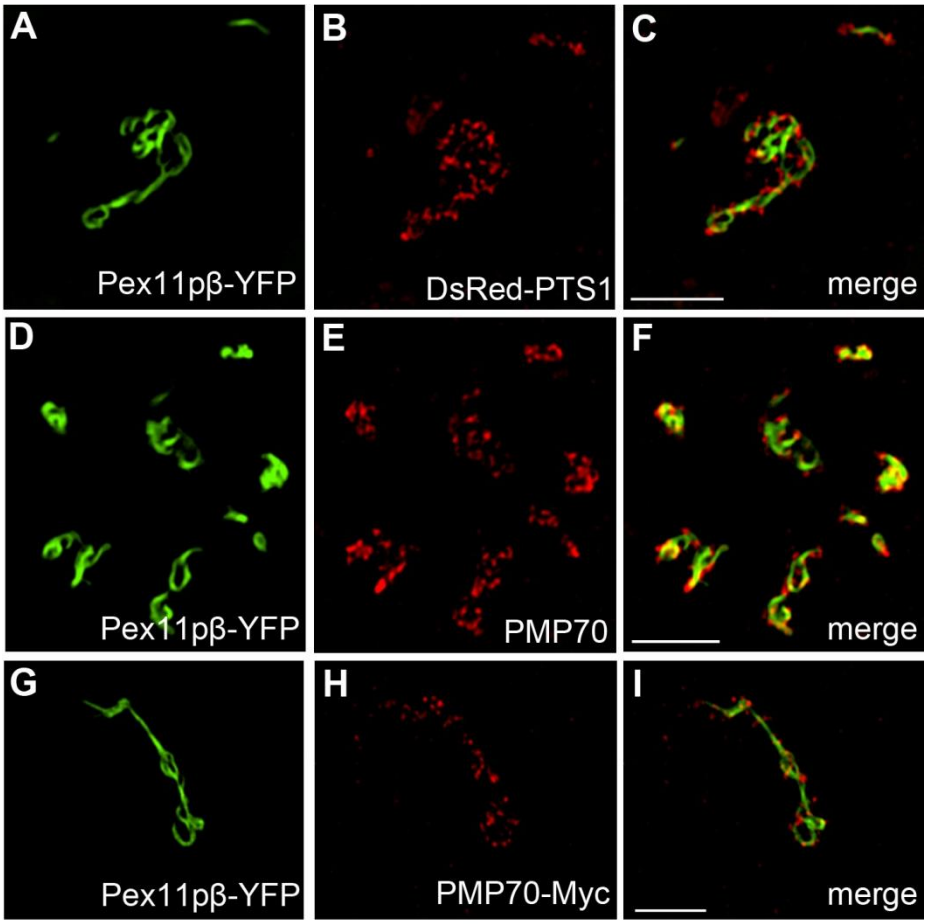

Figure 3.17: Matrix proteins and PMP70 are targeted to the globular domains of TPAs
Deconvolved images of TPAs. COS-7 cells were co-transfected with Pex11pβ-YFP and DsRed-Peroxi (PTS1) (A-C) or PMP70-Myc (G-I), or transfected with Pex11pβ-YFP alone and labeled with anti-PMP70 (D-F). Bars, 5 µm.

3.3.6 TPAs show different distribution of PMPs

Next, the distribution of different peroxisomal membrane proteins (PMPs) in the TPAs was addressed. First, COS-7 cells expressing Pex11pβ-YFP were stained with antibodies directed to PMP70, a peroxisomal ABC transporter (Figure 3.17 D-F). Interestingly, PMP70 was found to localize predominantly to the spherical parts of the TPAs, and not to the tubular membrane extensions labelled by Pex11pβ-YFP. To investigate the localization of newly synthesized PMPs to the TPAs, COS-7 cells were co-transfected with Pex11pβ-YFP and constructs coding for PMP70-Myc, PMP22/Pxmp2-HA, Pex11pβ-Myc, Pex12-Myc, ACBD5.1-Myc, and the "early peroxins" HA-Pex19p, Pex3p-Myc, and Myc-Pex16p (1.2.2; Figure 3.17 to Figure 3.19). As demonstrated for endogenous PMP70, exogenously expressed PMP70-Myc was predominantly targeted to the globular structures of the TPAs (Figure 3.17 G-I). Similar observations were made for PMP22/Pxmp2-HA (data not shown), which has recently been proposed to be a channel-forming perox-

isomal membrane protein involved in metabolite transfer (Rokka et al. 2009). In addition, ACBD5.1-Myc, an acyl-CoA binding protein with a potential transmembrane domain (Islinger et al. 2007) was predominantly targeted to the globular structures (data not shown).

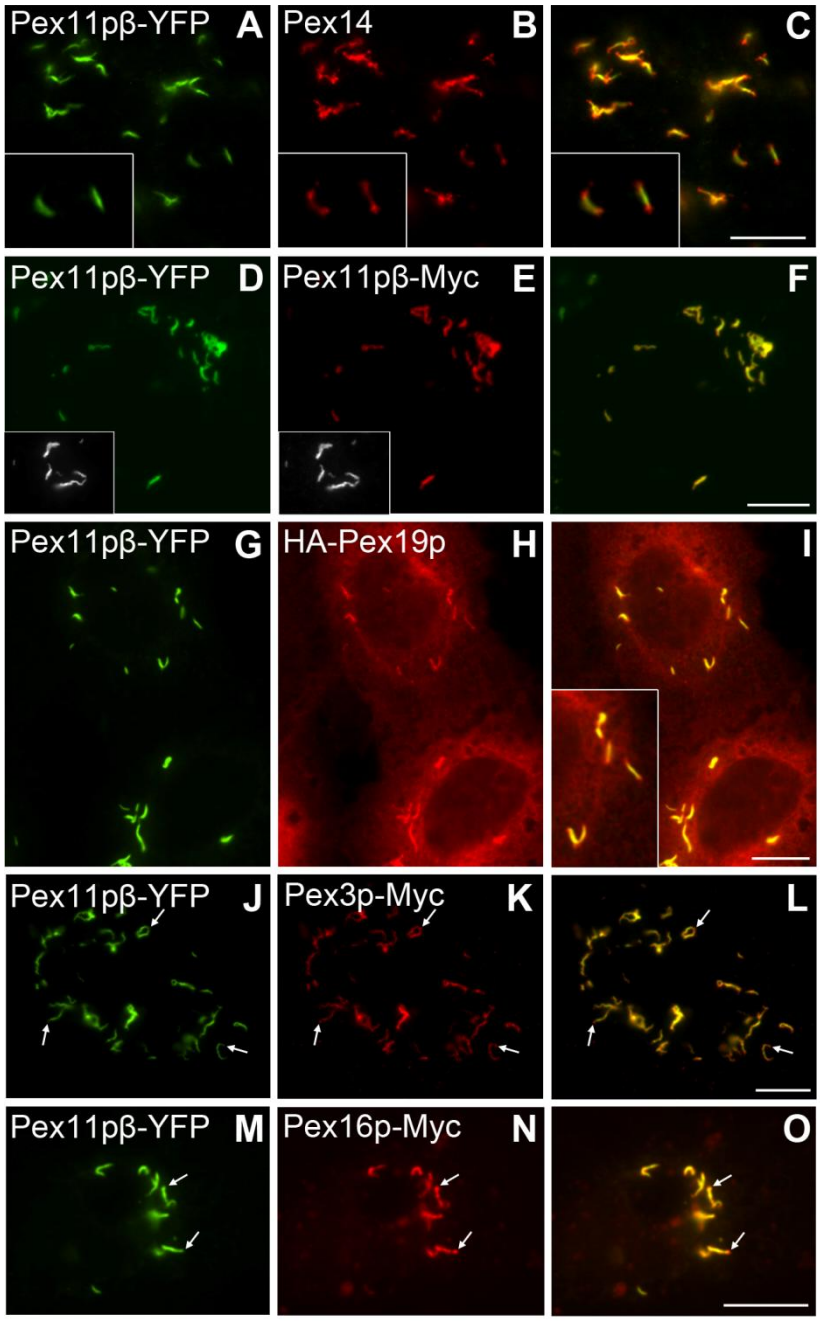

Figure 3.18: Pex11pβ and PMPs show distinct localizations in TPA membranes
COS-7 cells were co-transfected with Pex11pβ-YFP (left panel) and Pex11pβ-Myc (A-C), HA-Pex19p (D-F), Pex3p-Myc (G-I), or Myc-Pex16p (J-L). Arrows highlight localization in globular domains. Boxed regions in (D-E) highlight co-localization. Bars, 10 µm.

As Pex11pβ has been described to promote peroxisomal division and multiplication (Kobayashi et al. 2007; Koch et al. 2003; Koch et al. 2005; Li & Gould 2002; Schrader et al. 1998b), it was investigated whether expression of Pex11pβ-Myc would be sufficient to overcome the Pex11pβ-YFP-mediated block in peroxisomal division. Interestingly,

Pex11pβ-Myc was targeted to the tubular membrane structures of the TPAs, which also contained Pex11pβ-YFP, and not to the globular domains (Figure 3.18 D-F). Furthermore, its expression was not sufficient to release the block in peroxisomal division and did neither result in a division of the TPAs nor in the formation of spherical peroxisomes.

Next, the targeting of the peroxins Pex3p, Pex19p and Pex16p, which have been implicated in membrane biogenesis of peroxisomes and are supposed to act early on in peroxisome biogenesis (section 1.2), was examined. Co-expression of Pex11pβ-YFP and HA-Pex19p revealed targeting of HA-Pex19p to the whole membrane of the TPAs including the spherical compartments as well as the tubular membrane extensions, where it was co-localizing with Pex11pβ-YFP (Figure 3.18 G-I). In addition, a cytoplasmic localization was observed which relates to the role of Pex19p as a cycling receptor/chaperone. When the experiment was performed with Pex3p-Myc or Myc-Pex16p, similar results were obtained with both proteins labelling the spherical and the tubular membrane structures (Figure 3.18 J-O). In contrast to Pex19p and Pex3p, Myc-Pex16p sometimes exhibited a less prominent labelling of the tubules. Also a co-expressed Myc-tagged version of Pex12p, a zinc RING finger protein supposed to be involved in the recycling of the Pex5p receptor for matrix proteins, was found on all membranes of the TPAs (Figure 3.19). Furthermore, Pex14p, an essential component of the docking/translocation machinery for matrix proteins was detected on globular and (less prominent) on tubular membranes (Figure 3.18 A-C).

These findings clearly demonstrate that different PMPs are targeted or distributed to distinct regions within the TPAs and maintain specific membrane localization, although the globular and tubular membrane compartments form a continuum (Figure 3.19). PMPs with a metabolic function (e. g. PMP70, PMP22/Pxmp2) are predominantly localized to the spherical domains of the TPAs, which in addition are import-competent for peroxisomal matrix proteins. Pex11pβ, which promotes peroxisome elongation and division, is exclusively localized to the tubular membrane extensions. On the other hand, peroxins involved in membrane biogenesis and PMP import such as Pex19p, Pex3p and Pex16p are found on both the spherical and the tubular membrane compartments. The data further support that the globular domains of the TPAs represent a mature, import-competent peroxisomal structure, whereas the tubular extensions represent a pre-

peroxisomal membrane compartment which contains major PMPs required for membrane expansion, but has not (yet) acquired import competence for matrix proteins.

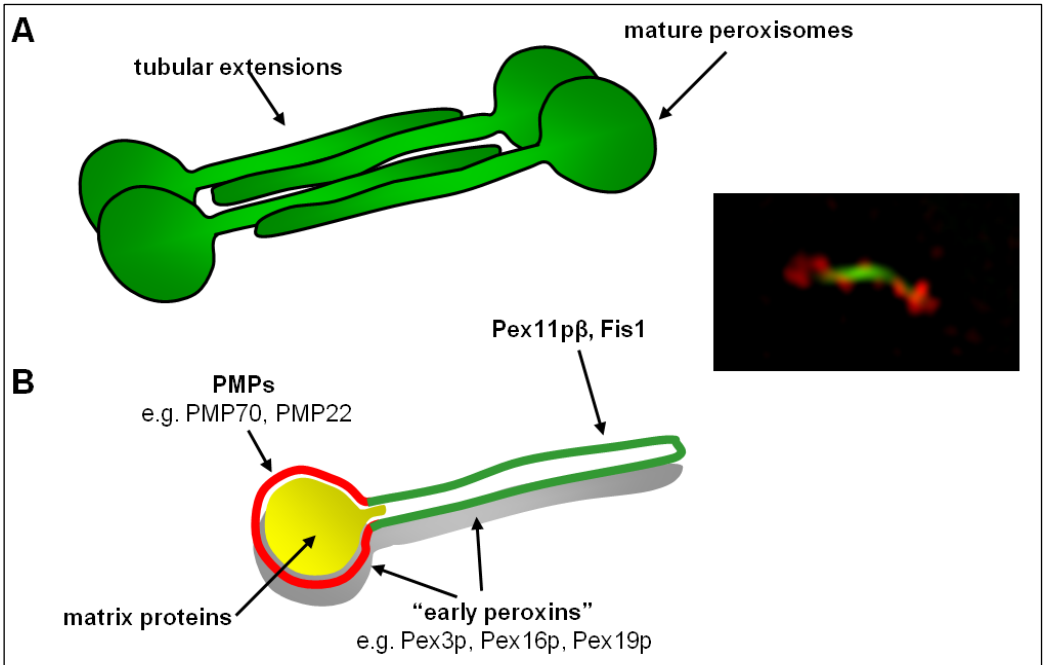

C

Protein	Function	Localization, Membrane topology	Globular domain	Tubular membrane extension
ACBD5	Lipid metabolism	PO membrane (1 TMD)	+	-
Pex3p	PMP import	PO membrane, N-terminally anchored	+	+
Pex11pα	PO Proliferation	PO membrane, 2 TMD	+	-/±
Pex11pβ	PO Proliferation	PO membrane, 2 TMD	-	+
Pex11pγ	PO Proliferation	PO membrane, 2 TMD	+	-/±
Pex12p	Matrix import, RING protein	PO membrane, 2 TMD	+	+
Pex14p	Matrix import	PO membrane, peripheral protein	+	±
Pex16p	PMP import	PO membrane, 2 TMD	+	+/±
Pex19p	PMP import, chaperone	Cytosol, PO membrane associated	+	+
PMP22	Pore	PO membrane, 4 TMD	+	-
PMP70	ABC transporter	PO membrane, 6 TMD	+	-
Fis1	Division	Mito & PO membrane, C-terminally anchored	-	+
DsRed-Peroxi	-	PO matrix	+	-

Figure 3.19: Schematic view of TPA organization
(A) TPAs are formed out of tubular extensions emerging from globular, mature peroxisome. **(B-C)** Overview of the distinct localization of peroxisomal proteins in TPA domains. Mito, mitochondria; PO, peroxisome; TMD, transmembrane domain. ± indicates weak labelling.

3.3.7 Tubular membrane extensions are formed by pre-existing peroxisomes

The import competent, globular domains of the TPAs can either be interpreted as new peroxisomes which are about to form at the endings of the tubular membrane structures. Alternatively, the import competent organelle-like structures might represent mature, pre-existing peroxisomes which give rise to the formation of tubular membrane extensions. To distinguish between these two alternative possibilities COS-7 cells were transfected with Pex11pβ-YFP using electroporation, which allows detection of the expressed protein early on after transfection. A time course experiment was performed, and cells were fixed 1 to 6 hours after electroporation and processed for immunofluorescence using antibodies directed to PMP70 (Figure 3.20 A-G). Interestingly, at early time points Pex11pβ-YFP was targeted to pre-existing, spherical peroxisomes positive for PMP70. A complete co-localization of Pex11pβ-YFP and PMP70 staining was observed in the majority of the cells expressing Pex11pβ-YFP (Figure 3.20 A-D). Shortly after, small nose-like tubular extensions were observed to form at one side of the spherical peroxisomes (Figure 3.20 E-F). These extensions were positive for Pex11pβ-YFP, but did not show labelling for PMP70. After longer periods of time, the Pex11pβ-YFP-positive membrane extensions became more prominent and elongated (Figure 3.20 G). These membrane extensions were highly dynamic (Figure 3.21 and Movie 2). More importantly, Pex11pβ-YFP appeared to concentrate in the growing tubular extensions. Later on, the elongated peroxisomes started to form TPAs (Figure 3.21). Within these TPAs, Pex11pβ-YFP was predominantly localized in the tubular membrane extensions and no longer in the globular (PMP70-positive) peroxisomes attached to them. Peroxisomal constriction and division was completely abolished, and single, spherical peroxisomes were no longer observed.

Expression of Pex11pβ-Myc has been shown to induce peroxisome elongation, and to promote constriction and division of the elongated peroxisomes into small spherical organelles (Schrader et al. 1998b). The time course experiment was repeated with Pex11pβ-Myc (Figure 3.20 H-M). Like Pex11pβ-YFP, Pex11pβ-Myc first localized to spherical PMP70-positive peroxisomes. After about 60 minutes small, nose-like Pex11pβ-Myc-positive (but PMP70-negative) extensions arose from the spherical peroxisomes. In contrast to Pex11pβ-YFP, the tubular extensions were observed to segment and constrict showing a “beads on a string”-like appearance (Figure 3.20 K-M).

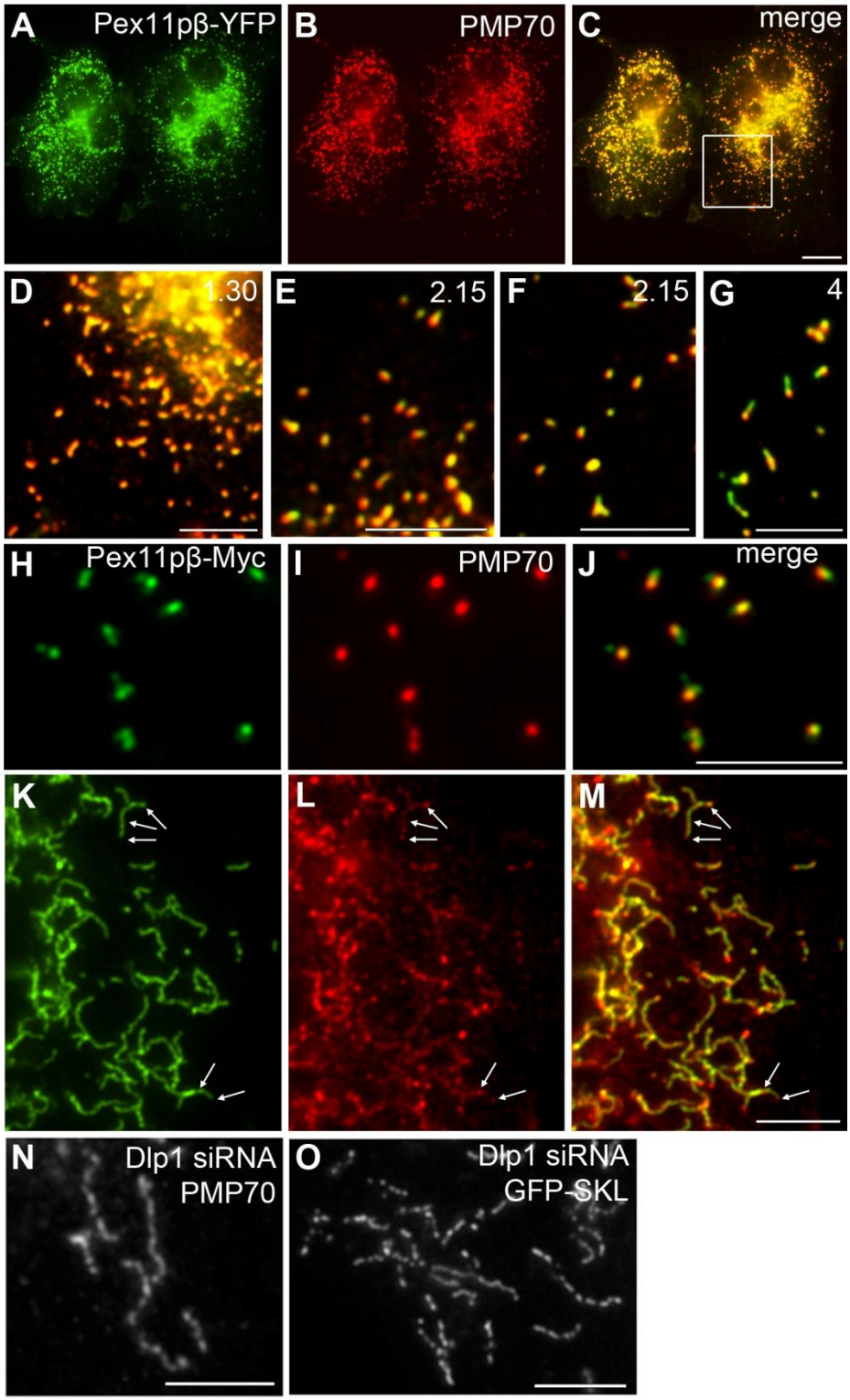

Figure 3.20: Tubular membrane extensions are formed by pre-existing peroxisomes
Time-course experiments of COS-7 cells transiently transfected with Pex11pβ-YFP (A-G) or Pex11pβ-Myc (H-M) by electroporation. Cells were fixed at different time points after transfection and peroxisomes were labeled with anti-PMP70. Note that early on Pex11pβ-YFP (A-G) or Pex11pβ-Myc (H-J) are targeted to pre-existing, spherical peroxisomes (positive for PMP70) where they induce small nose-like extensions. In the case of Pex11pβ-Myc, the tubular extensions continue to segment and constrict showing a "beads on a string"-like appearance (K-M, arrows). At this stage, the "beads" become positive for PMP70. **(N-O)** Silencing of DLP1 by siRNA results in the accumulation of tubular but constricted peroxisomes with the "beads" positive for PMP70 or matrix proteins (GFP-SKL). Bars, 10 µm (A-C), 5 µm (D-O).

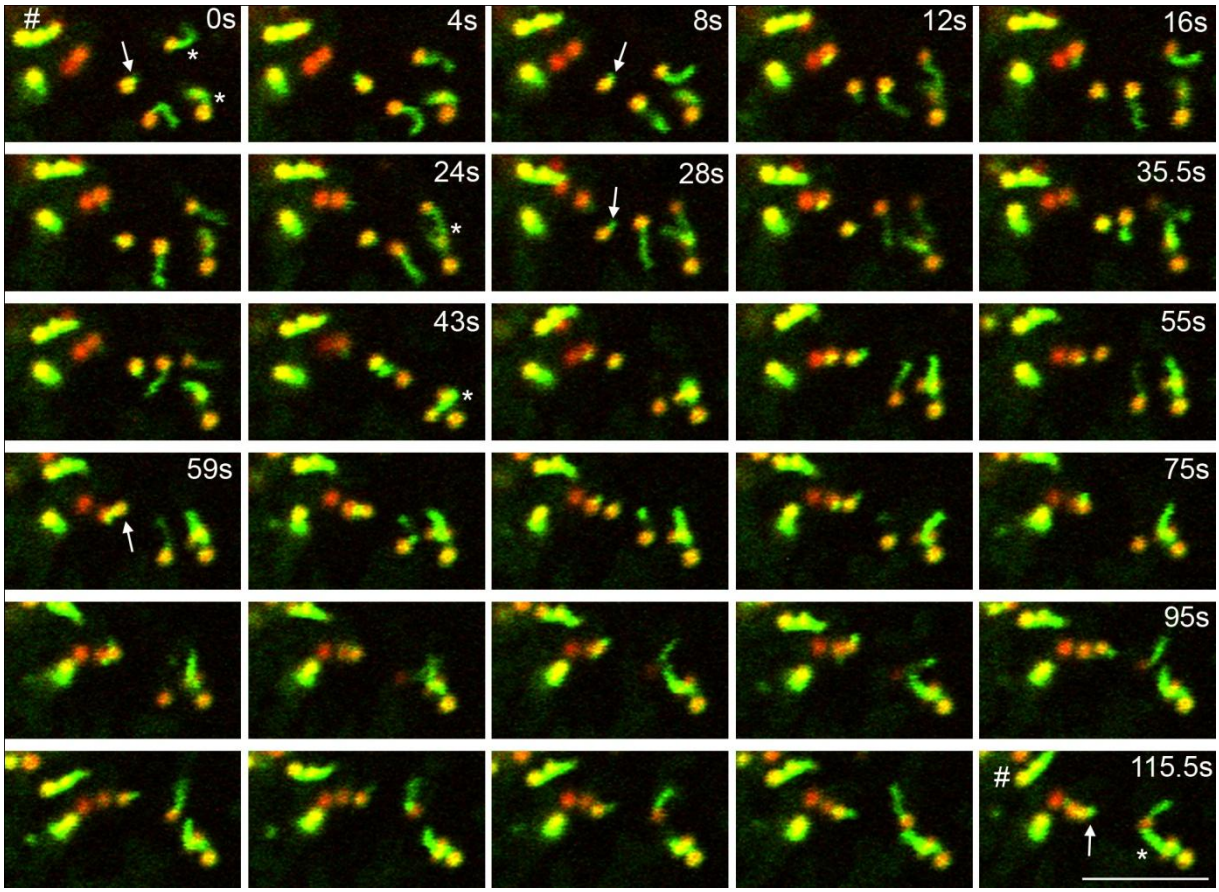

Figure 3.21: Peroxisomal tubular extensions are dynamic
COS-7 cells were co-transfected with mRuby-PTS1 (matrix, red) and Pex11pβ-YFP (green) and live cell imaging was performed at 37°C and 5% CO_2 4 hours after transfection. A small TPA (#) does not change its appearance during image acquisition. Two elongated peroxisomes (*) first interact with each other (24 seconds) and finally align with each other (43 seconds) to form a TPA. A single peroxisome (arrow) forms and retracts a tubular extension (e.g. 8 and 28 seconds) and interacts with other peroxisomes (e.g. 59 seconds) but separates again. See also Movie 2. Bar, 5 µm.

To investigate the import of matrix proteins into the pre-existing and newly formed peroxisomal structures upon overexpression of Pex11pβ-Myc, we applied the HaloTag technology (Huybrechts et al. 2009; Los et al. 2008). This method allows e.g. the sequential staining of a tagged protein with different synthetic ligands and thereby the identification of different protein pools. Using an approach with several staining pulses, a pool of newly synthesized protein could be distinguished from the pre-existing proteins. COS-7 cells expressing HaloTag-catalase were first incubated with the cell-permeable HaloTag TMR ligand (red), then transfected with Pex11pβ-Myc (stained blue), and immediately cultivated in the presence of the cell-permeable HaloTag R110 Direct ligand (green) (Figure 3.22). Spherical peroxisomes positive for both HaloTag-catalase ligands were detected. Interestingly, Pex11pβ-Myc positive tubules protruding from those were initially negative for catalase. Occasionally, newly imported catalase (green) was seen at the tubule tips (Figure 3.22 A). Later on, constricted tubules were observed, which contained only newly imported HaloTag-catalase (in the "beads"), whereas the globular

peroxisomes attached contained both pre-imported and newly imported HaloTag-catalase (Figure 3.22 B).

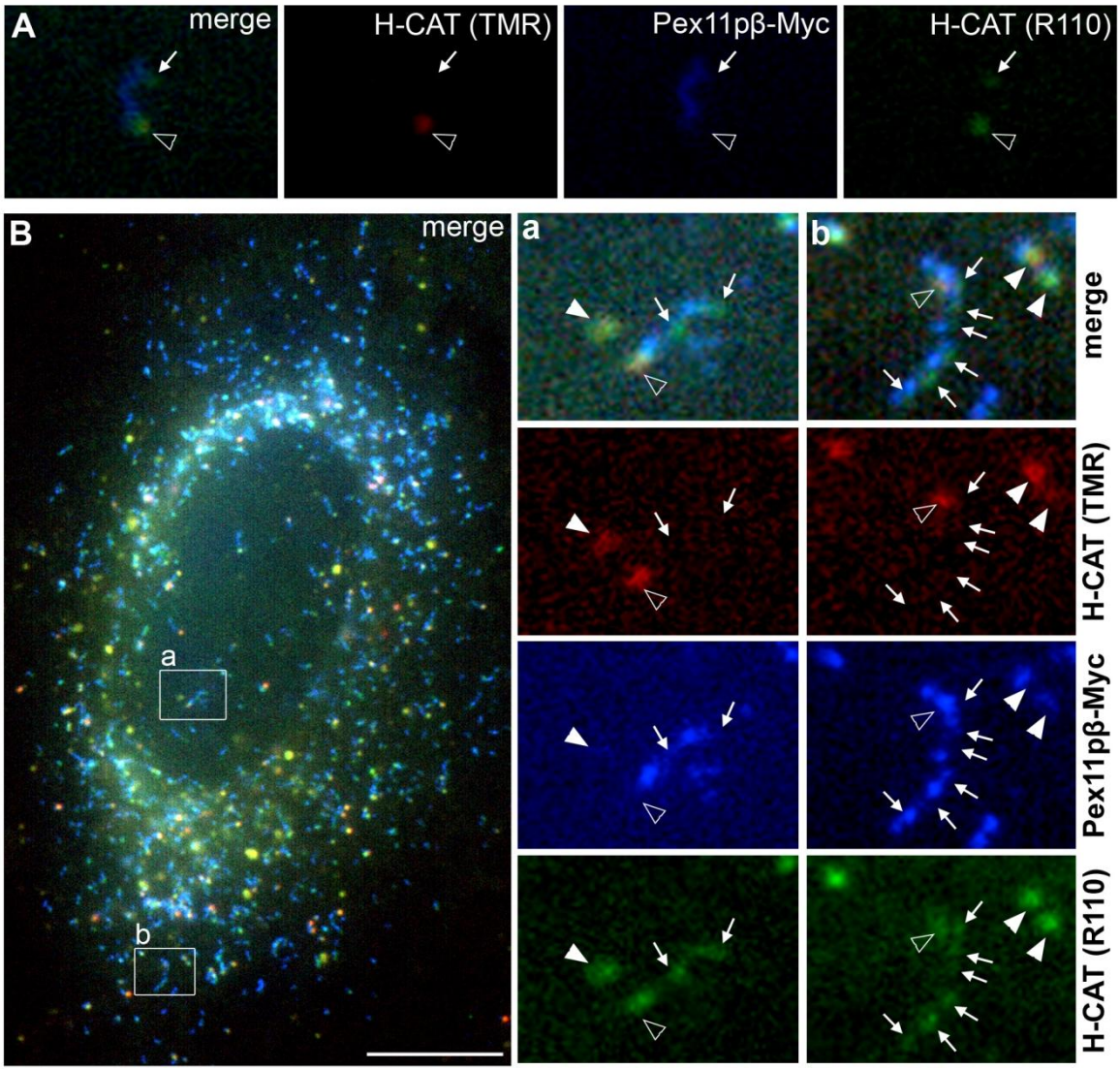

Figure 3.22: Peroxisomes formed by Pex11pβ-Myc overexpression contain newly imported catalase
COS-7 cells expressing HaloTag-catalase were incubated for 48 hours with the cell-permeable HaloTag TMR ligand (red), transfected with Pex11pβ-Myc and immediately cultivated in the presence of the cell-permeable HaloTag R110 Direct ligand (green). Cells were fixed after 24 hours and processed for immunofluorescence using anti-Myc and Alexa 350-coupled antibodies (blue). **(A)** Pex11pβ-Myc positive tubule with newly imported catalase (green) at the tubule tip (arrow) and within the attached pre-existing peroxisome (open arrowhead). **(B)** Dividing tubules/"beads on a string" (arrows) containing only newly imported HaloTag-catalase (green). Note that the globular (pre-existing) peroxisomes (open arrowheads) attached (A, B) contain both pre-imported and newly imported HaloTag-catalase. Closed arrowheads point to peroxisomes which are not elongated or constricted but positive for pre-imported and newly imported HaloTag-catalase. **(a, b)** Higher magnification view of boxed regions in B. Bar, 10 µm.

As reported before (Schrader et al. 1998b), Pex11pβ-Myc was absent from the bead-like structures, but was found in between at the constriction sites (Figure 3.20 K-M and Figure 3.22 B, a and b). Later on (>12-24h), fission into small spherical peroxisomes was observed (Figure 3.13). Please note that the latter is inhibited by silencing of DLP1 and

results in the accumulation of elongated but constricted membranes (Koch et al. 2004). Interestingly, the "beads" within these membranes are positive for matrix and membrane proteins (Figure 3.20 N-O) (Koch et al. 2004) indicating that loss of DLP1 function blocks at a later stage than Pex11pβ-YFP. In contrast to Pex11pβ-YFP, the formation of TPAs was not observed after expression of Pex11pβ-Myc or silencing of DLP1.

These findings demonstrate that Pex11pβ initially localizes to the membranes of pre-existing peroxisomes where it initiates the formation of a tubular membrane extension. This membrane extension is enriched in Pex11pβ, but not yet positive (import competent) for PMP70 or matrix proteins. In contrast to Pex11pβ-Myc, expression of Pex11pβ-YFP appears to act like a "dominant-negative" mutant which abolishes division of the tubular membranes as well as further PMP insertion and matrix protein import or redistribution into the forming, bead-like peroxisomes. Furthermore, the formation of TPAs occurs at later time points.

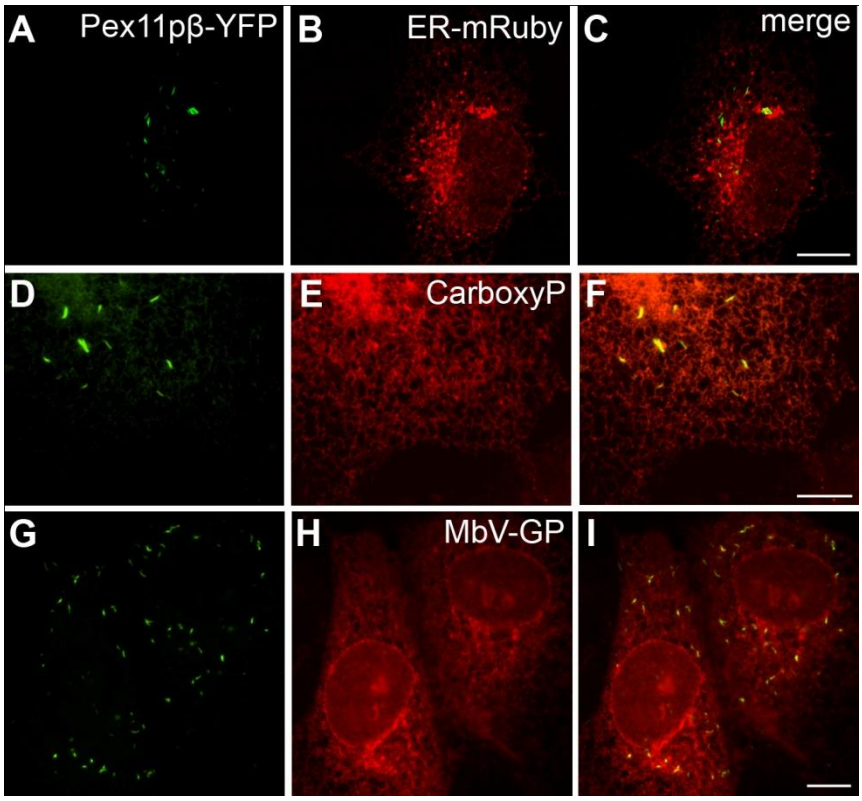

Figure 3.23: TPAs do not co-localize with markers for the endoplasmic reticulum
COS-7 cells were co-transfected with Pex11pβ-YFP (left panel) and ER-mRuby-KDEL (A-C), carboxypeptidase A (D-F) or Marburg virus glycoprotein (G-I) and stained with the respective antibodies (carboxypeptidase A or Marburg virus glycoprotein). Pex11pβ-YFP-induced TPAs did not co-localize with ER-mRuby-KDEL or overexpressed secretory proteins, which accumulated in the ER. **(A-C)** Confocal images. Bars, 10 µm.

As an involvement of the ER in peroxisomal biogenesis and/or protein targeting to the peroxisomes is discussed (1.2.3), co-labelling studies with ER marker proteins were performed. Pex11pβ-YFP was co-expressed with ER-mRuby-KDEL (Kredel et al. 2009), carboxypeptidase A or a glycoprotein of the Marburg virus (MBGV-GP; Becker et al. 1996;

Koch et al. 2004) in COS-7 cells. Carboxypeptidase A is a pancreatic zymogen usually entering the exocrine pathway (Kraehenbuhl et al. 1977). These exogenous, ER-targeted secretory proteins accumulate in COS-7 cells in the ER and the expression was performed to be able to detect even rather transient connections between TPAs and the ER. TPAs were never labelled by any of the ER markers, thus representing a membrane compartment distinct from the ER (Figure 3.23).

To exclude the possibility of TPAs either originating from or connecting to other organelles, co-labelling with Golgi (p115) and mitochondrial (Mito-RFP) markers was performed. Pex11pβ-YFP-induced TPAs did not co-localize with any of the organelle markers (Figure 3.24). TPAs were sometimes observed to localize in the Golgi region (Figure 3.24 G-I), but this was not statistically significant.

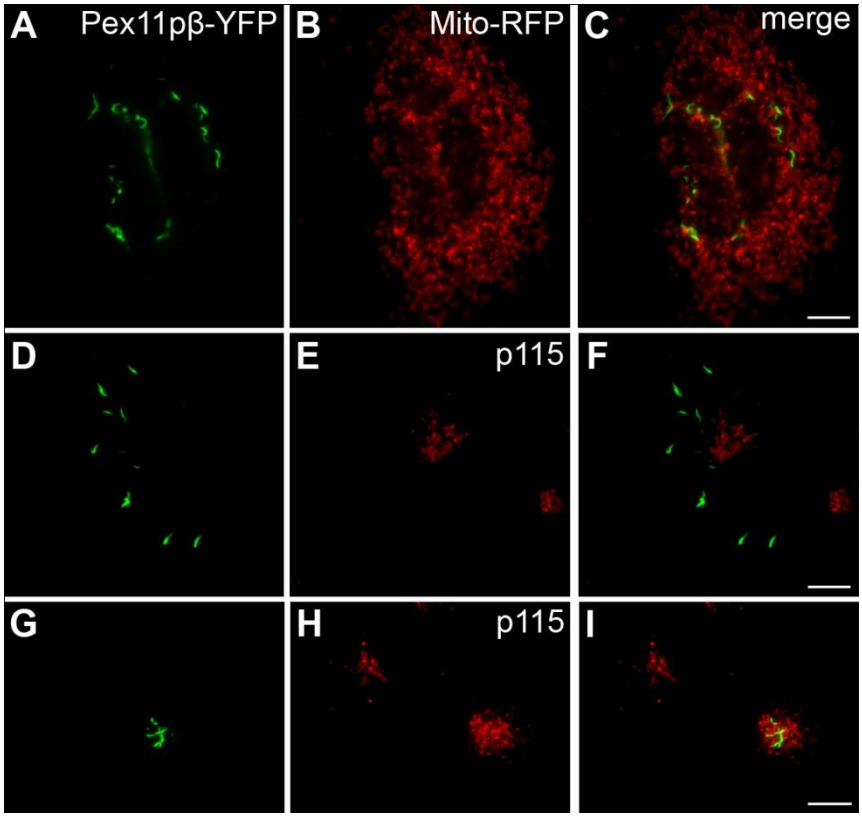

Figure 3.24: TPAs do not co-localize with markers for the Golgi complex or mitochondria
COS-7 cells were co-transfected with Pex11pβ-YFP (left panel) and Mito-RFP (A-C) or with Pex11pβ-YFP alone (D-I). After fixation cells were stained with antibodies directed to p115 (D-I). Pex11pβ-YFP-induced TPAs did not co-localize with Mito-RFP (mitochondria) or p115 (Golgi complex). TPAs were sometimes observed to localize in the Golgi region (G-I), but this was not statistically significant. Bars, 10 µm.

3.3.8 TPA formation is also induced by manipulation of hFis1

Besides Pex11pβ, expression of hFis1 has also been reported to promote peroxisome division and multiplication (Kobayashi et al. 2007; Koch et al. 2005). Moreover, hFis1 has been suggested to interact with Pex11pβ or/and to be recruit to peroxisomes via Pex11-proteins in plants (Kobayashi et al. 2007; Lingard et al. 2008). After co-

expression of Pex11pβ-YFP and Myc-Fis1, the latter was predominantly targeted to the tubular membrane extensions of the TPAs, but not to the globular organelle structures (Figure 3.25 A-F). Like Pex11pβ-Myc (Figure 3.18), Myc-Fis1 was not sufficient to overcome the block in peroxisomal division.

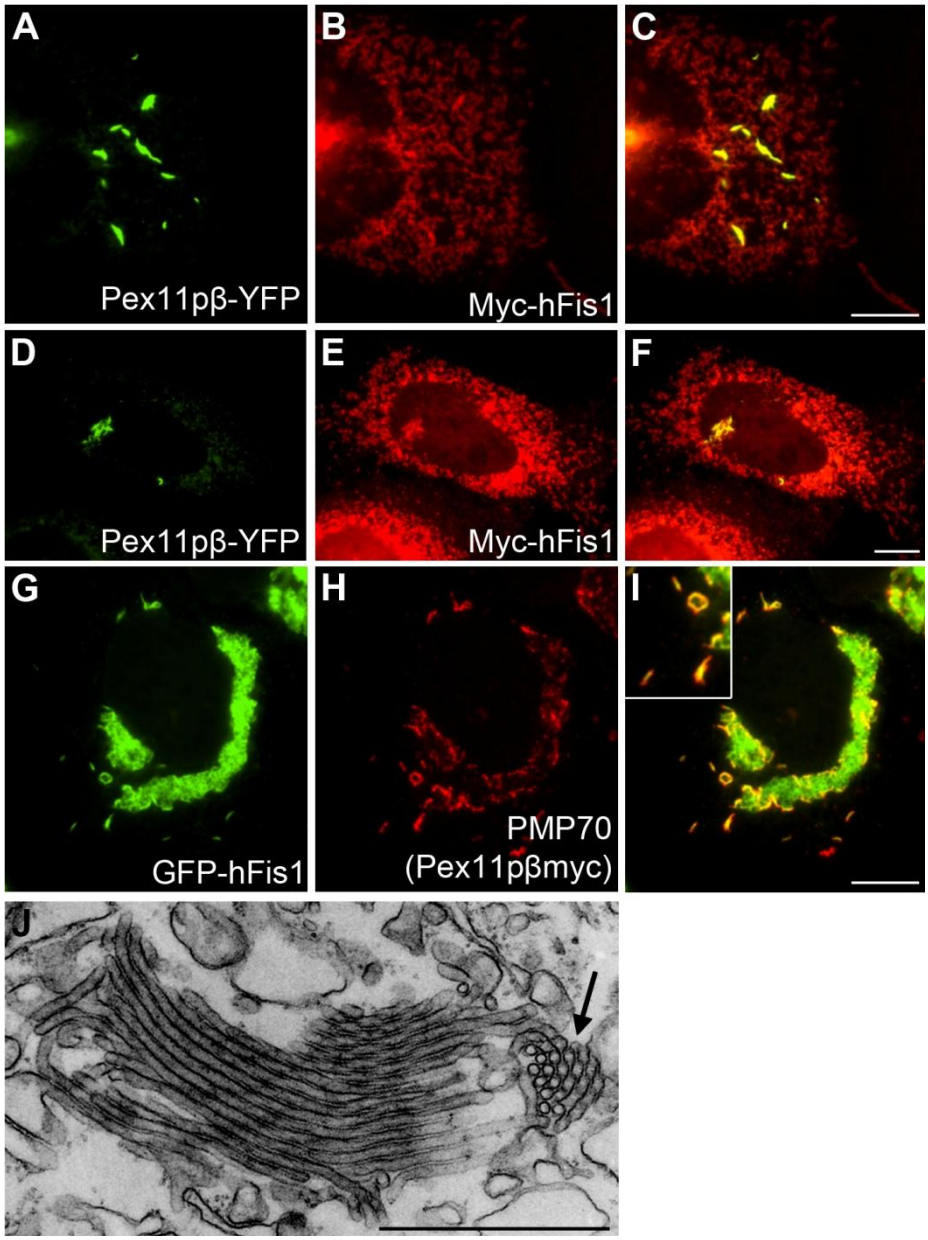

Figure 3.25: TPAs can also be induced by GFP-Fis1 and Pex11pβ-Myc
COS-7 cells were either co-transfected with Myc-hFis1 and Pex11pβ-YFP (A-F) or GFP-hFis1 and Pex11pβ-Myc (G-I) and stained with anti-PMP70 (H) or anti-Myc antibodies (A-F). GFP-Fis1/Pex11pβ-Myc co-expression results in TPA formation with both proteins co-localizing to the tubular structures. Note the formation of mitochondrial accumulations induced by GFP-hFis1 described before. Myc-hFis1 localizes to mitochondria and tubular extensions of TPAs induced by Pex11pβ-YFP. **(J)** Ultrastructure of TPAs induced by co-expression of GFP-hFis1 and Pex11pβ-Myc. Arrow, cross section. Bars, 10 µm (A-I), 500 nm (J).

It was previously reported that co-expression of Fis1 and Pex11pβ changed the uniform intracellular distribution of peroxisomes (Koch et al. 2005). Co-expression of a GFP-tagged Fis1 (GFP-Fis1) and Pex11pβ-Myc (but not expression of GFP-Fis1 or Pex11pβ-Myc alone) resulted in the formation of tubular peroxisomal accumulations and a block in peroxisomal division. Furthermore, GFP-Fis1 and Pex11pβ-Myc were observed to co-localize on these structures. These findings were re-evaluated and it was discovered that those accumulations were similar to TPAs formed by Pex11pβ-YFP (Figure 3.25 G-I). This notion was confirmed by ultrastructural studies of GFP-Fis1/Pex11pβ-Myc transfected cells (Figure 3.25 J). Labelling for PMP70 (or matrix proteins, not shown) revealed that the spherical organelle structures at the end of the tubules represented mature peroxisomes, whereas GFP-Fis1 and Pex11pβ-Myc co-localized along the tubular membrane extensions (Figure 3.25 G-I). These observations highlight that TPAs can also be generated independently of Pex11pβ-YFP, and they further support the suggested interactive roles of Fis1 and Pex11pβ. It is tempting to speculate that specific manipulations of either Fis1 or Pex11pβ disturb the assembly of a functional constriction/fission complex inhibiting peroxisomal division, thus promoting TPA formation.

3.3.9 Pex11pβ but not Pex11pα and Pex11pγ induces TPA formation when co-expressed with YFP-Pex11pβ

Studies on Pex11 proteins in fungi, plants and mammals revealed that there are different degrees of redundancy and overlap of function between the distinct isoforms (1.3.3) (Li et al. 2002a; Lingard et al. 2008; Lingard & Trelease 2006; Orth et al. 2007; Rottensteiner et al. 2003b; Schrader et al. 1998b; Tam et al. 2003) and that all Pex11 proteins form homo-dimers or -oligomers (Li & Gould 2003; Marshall et al. 1996; Rottensteiner et al. 2003b; Tam et al. 2003). Furthermore, all five Pex11 isoforms of plants (and two yeast proteins) have been shown to form heteromers (Lingard et al. 2008; Rottensteiner et al. 2003b; Tam et al. 2003). In this regard, co-expression studies of the different mammalian Pex11p isoforms were conducted.

While Myc-tagged Pex11pβ was observed to completely co-localize with Pex11pβ-YFP in the tubular structures of the induced TPAs (section 3.3.6, Figure 3.18 D-F), neither Myc-Pex11pα nor Myc-Pex11pγ appeared to co-localize with Pex11pβ-YFP in the tubular membrane extensions of TPAs after co-expression (Figure 3.26). Both Pex11p isoforms

were mainly found in the globular structures of the TPAs and only a small amount of protein was localized in the tubules. These observations do not support the idea of overlapping functions or hetero-oligomerization of Pex11pβ with the other two isoforms, and may suggest that they are acting at different steps in the peroxisomal biogenesis process. To gain further insight into the heteromer formation and oligomerization of the Pex11 proteins, different biochemical approaches such as co-immunoprecipitations, cross-linking experiments, and protein complex analysis with native gels were applied. Due to difficulties in our experimental setups these issue could not yet be addressed successfully. Future experiments regarding heteromer formation may benefit from the utilization of other methods, for example split-GFP/BiFC (Lingard et al. 2008).

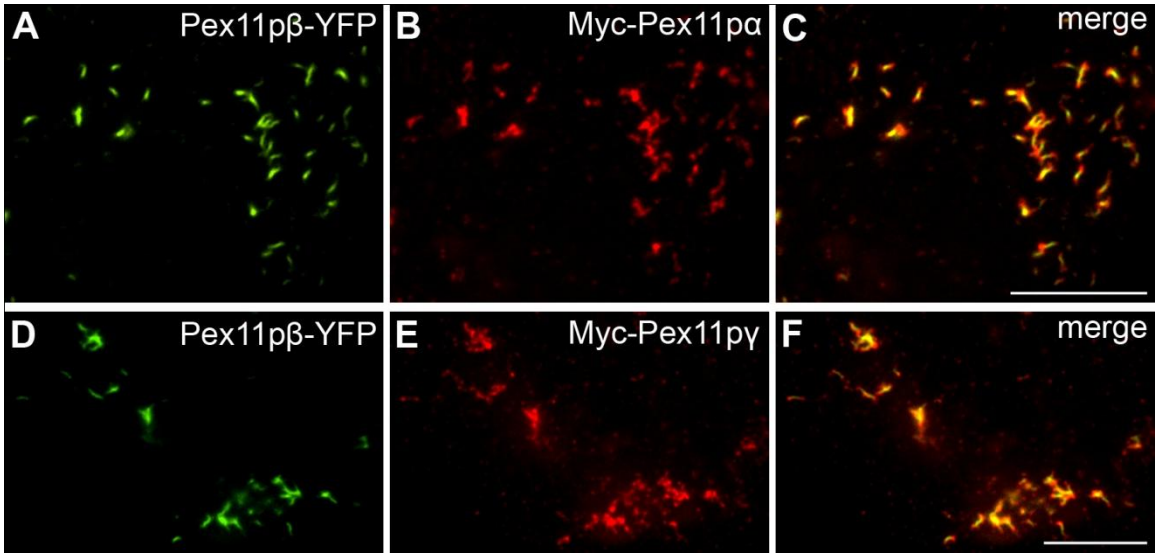

Figure 3.26: Pex11pα and Pex11pγ are targeted to globular structures of TPAs
COS-7 cells were co-transfected with Pex11pβ-YFP and Myc-Pex11pα (A-C) or Myc-Pex11pγ (D-F) and processed for immunofluorescence using an anti-Myc antibody. Pex11pβ-YFP induced the formation of TPAs and was localized in tubular structures. Myc-Pex11pα and Myc-Pex11pγ showed a rather punctuate staining pattern and were mainly targeted to spherical structures at the end of the tubules. Bars, 10 µm.

As described above (3.3.2), only C-terminal and not N-terminal fusion of Pex11pβ with YFP blocked peroxisome division and induced the formation of TPAs (Figure 3.14 and Figure 3.27 A and B). From cells expressing YFP-Pex11pβ at most 18.5 ± 7.7% exhibited TPAs, compared to 95.5 ± 4.4% of the cells transfected with Pex11pβ-YFP (Figure 3.27 C and Figure 3.13 G). However, when YFP-Pex11pβ was co-expressed with Myc-tagged Pex11pβ the number of cells with TPAs increased dramatically (79.0 ± 7.6%; Figure 3.27 C, G-I). YFP-Pex11pβ and Myc-Pex11pβ co-localized in the tubular structures of the TPAs. In contrast, co-expression of YFP-Pex11pβ with Myc-Pex11pα or Myc-Pex11pγ did not result in TPA formation (Figure 3.27 D-F and J-L). Peroxisomes exhibited a tubular

morphology with YFP-Pex11pβ localizing to the tubules, whereas both Myc-tagged Pex11pα and Pex11pγ were found in the spherical domains at one end of the tubules (Figure 3.27 insets in F and L).

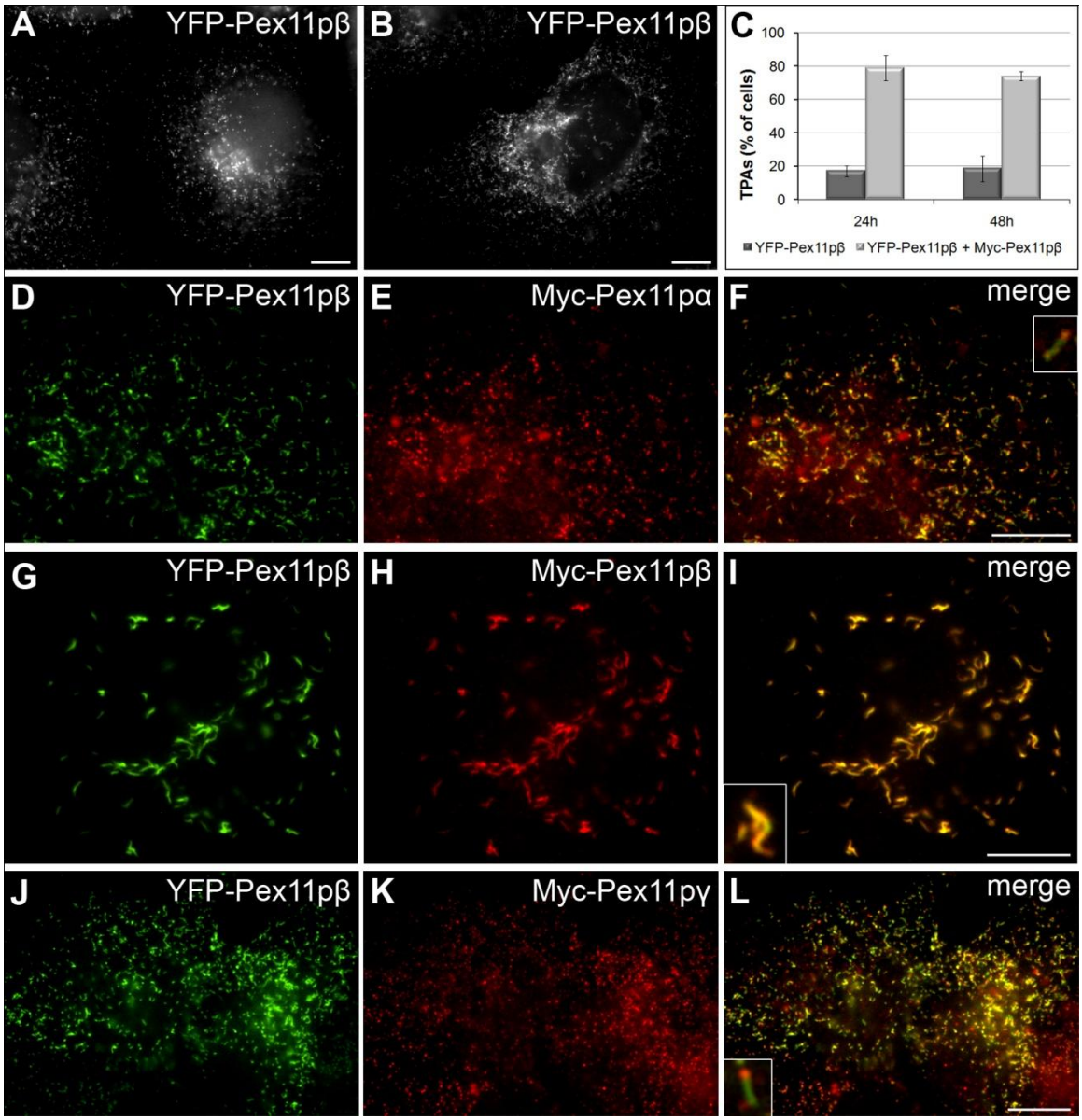

Figure 3.27: YFP-Pex11pβ can lead to TPA formation only when co-expressed with Myc-Pex11pβ
(A-B) YFP-Pex11pβ expressing cells with spherical (A) or tubular (B) peroxisomal morphology. **(C)** Quantitative evaluation of TPA formation in cells expressing YFP-Pex11pβ alone or co-expressing YFP-Pex11pβ and Myc-Pex11pβ. Cells were fixed 24 and 48 hours after transfection and transfected cells with TPAs were counted. Note the strong increase of TPAs in co-transfected cells. Data are expressed as mean ± SD. **(D-F)** Co-expression of YFP-Pex11pβ and Myc-Pex11pα. Peroxisomes were tubular with YFP-Pex11pβ localizing in the tubules while Myc-Pex11pα was mainly found in spherical endings of the tubules (inset). **(G-I)** Co-expression of YFP-Pex11pβ and Myc-Pex11pβ. Cells had TPAs instead of spherical or tubular peroxisomes and proteins were co-localizing in the tubules (inset). **(J-L)** Co-expression of YFP-Pex11pβ and Myc-Pex11pγ. Peroxisomes were tubular with YFP-Pex11pβ localizing in the tubules while Myc-Pex11pγ was mainly found in spherical endings of the tubules (inset). Bars, 10 μm.

In this approach, neither Pex11pα nor Pex11pγ acted in the same way as Pex11pβ – as they were not able to induce TPAs in concert with YFP-Pex11pβ. Moreover, they did not co-localize with Pex11pβ-YFP within the TPAs. Therefore TPA formation appears to be a specific function of Pex11pβ. Additionally, this data confirm that TPA formation is not caused by inaccessibility of the C-terminus of Pex11pβ by fusion to a tag, as also the co-expression of N-terminal Myc- and YFP-tagged Pex11pβ results in TPA formation. The block in the assembly of the division machinery must have other, yet unclear mechanistic or structural reasons, which may be based on the amount of Pex11pβ and its degree of homo-oligomerization. The alignment of peroxisomal tubules to each other, which leads to TPA formation, might only occur under conditions of high Pex11pβ (or Pex11pβ and hFis1) levels combined with a bulky tag, i.e. under circumstances with a disturbed assembly of a Pex11pβ-hFis1 complex.

3.3.10 Pex11pγ has higher membrane mobility than Pex11pβ

The endoplasmic reticulum is an organelle with diverse morphologies, reaching from a network of branching tubules to big cisternae such as the nuclear envelope, but also the formation of stacked membrane arrays has been observed (Snapp et al. 2003). Recently, a class of membrane proteins involved in the formation of tubular ER structures, reticulons and DP1/Yop1p, has been identified (Hu et al. 2008; Voeltz et al. 2006). Interestingly, proteins of the reticulon family form immobile oligomers in the tubular ER (Shibata et al. 2008) while the so called organized smooth ER (OSER) is formed by low affinity protein interactions of highly mobile membrane proteins (Snapp et al. 2003). In this regard it was interesting to determine the membrane mobility of the two tubule/TPA-inducing Pex11p isoforms (Pex11pβ and Pex11pγ) and FRAP (fluorescence recovery after photobleaching) experiments were performed. This technique allows measurement and comparison of the mobility of fluorescent-tagged proteins in a membrane. In a live-cell setup a certain area of the cell (region of interest, ROI; here a part of a peroxisomal tubule) expressing a fluorophore-tagged protein is bleached and the fluorescence recovery in this region is measured. Recovery occurs by lateral diffusion of non-bleached proteins from the surrounding membrane into the ROI. The time or degree of recovery depends on the mobility of the protein in the membrane.

FRAP experiments with Pex11pβ-YFP showed that the protein has very low mobility in the peroxisomal membrane. In a time period of 100 seconds at most 20% of the fluores-

cence intensity was recovered (Figure 3.28 B and D). In a long time observation slow regaining of fluorescence was only seen after 35 minutes and even after 70 minutes recovery was not complete (data not shown).

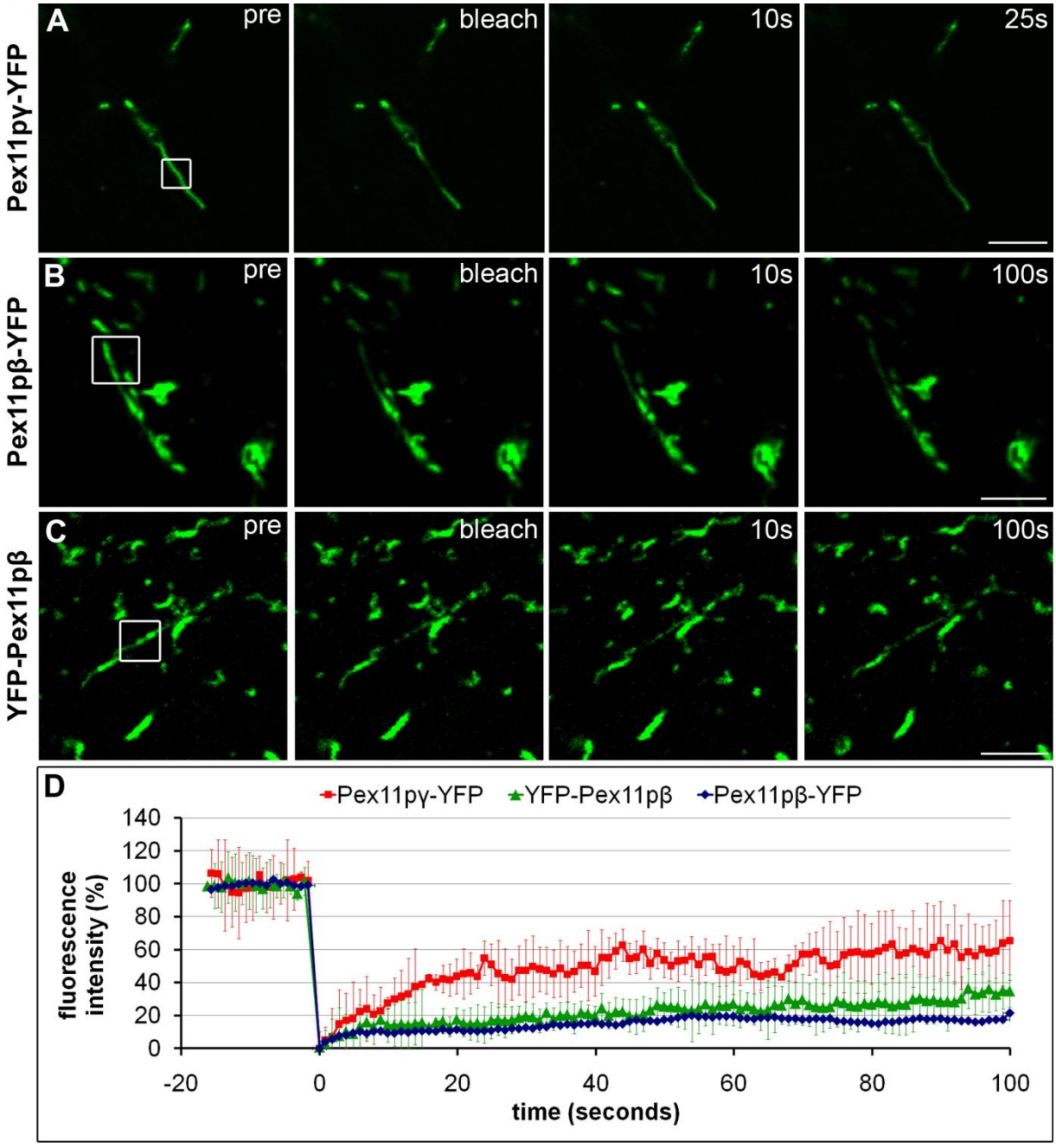

Figure 3.28: Pex11pβ protein with low membrane mobility
(A-C) Pex11pγ-YFP (A), Pex11pβ-YFP (B), or YFP-Pex11pβ (C) was expressed in COS-7 cells and after 24 hours FRAP experiments were performed by bleaching of a ROI (boxed areas in the left panels). Typical images acquired before (pre) and after the photobleach (bleach) for the times indicated are shown. **(D)** Plot of fluorescence intensities normalized to prebleach values (100%) over time. Fluorescence recovery was determined by intensity measurement of the ROI. Minimum intensity was set 0%. Data are presented as means ± SD (n = 4-6). Bleach at t = 0 seconds. Photobleaching by image acquisition was normalized using a non-bleached area. Bars, 5 µm.

To exclude that the low membrane mobility of Pex11pβ was only caused by the formation of TPAs, we repeated the experiments with YFP-Pex11pβ which does not induce TPA formation (Figure 3.27). N-terminally tagged Pex11pβ present in peroxisomal tubules showed only a small increase in final fluorescence recovery (25-30%, Figure 3.28 C-D), demonstrating that the membrane mobility properties of Pex11pβ do not depend on its presence in peroxisomal tubules or TPAs.

Next we studied the membrane mobility of Pex11pγ in peroxisomal tubules. Fluorescence of Pex11pγ-YFP recovered up to 45% of the initial value in a time period of 25 seconds. Afterwards an increase up to 60% prebleach fluorescence intensity was achieved (Figure 3.28 A and D), and a complete redistribution of the fluorescence over the entire tubule was observed, demonstrating that maximum recovery was already achieved. Thus, Pex11pγ shows higher membrane mobility than Pex11pβ.

3.3.11 Summary

It was discovered that a Pex11pβ-YFP fusion protein can be used as a specific tool to further dissect peroxisomal growth and division. Pex11pβ-YFP inhibited peroxisomal segmentation and division, but instead resulted in the formation of pre-peroxisomal membrane structures composed of globular domains and tubular extensions. Peroxisomal matrix and membrane proteins were targeted to distinct regions of the peroxisomal structures. Pex11pβ-mediated membrane formation was initiated at the pre-existing peroxisome, indicating that growth and division follows a multistep maturation pathway.

3.4 Hypertubulation of peroxisomes

The plasticity of the peroxisomal compartment is demonstrated by its ability to proliferate in response to a wide range of stimuli. In the liver of rodents peroxisome proliferation is observed for example after partial hepatectomy (Yamamoto & Fahimi 1987) or after feeding with proliferative compounds, the so-called peroxisome proliferators (e.g. hypolipidemic drugs like clofibrate and plasticizers like DEHP; Fahimi et al. 1982; Hess et al. 1965; Reddy & Lalwani 1983; Svoboda & Azarnoff 1966). Most, but not all, peroxisome proliferators act via the PPAR transcription factors (1.2.4.1) which induce a number of PEX genes. Peroxisomes can proliferate by growth and division, i.e. tubulation and subsequent fission of peroxisomes. In cultured mammalian cells tubular peroxisomes can be induced by a number of stimuli, for example by addition of peroxisomal substrates (e.g. polyunsaturated fatty acids, arachidonic acid), growth factors, ROS (created e.g. by UV irradiation or addition of H_2O_2), or by low cell densities (Schrader et al. 1998a; Schrader et al. 1999). The formation of elongated peroxisomes appears to be tightly associated with the metabolic state of the cell, and the formation of small tubular extensions (peroxules) has been demonstrated to be a local stress response to ROS in plants (Sinclair et al. 2009). Thus, it is not clear if the occurrence of tubular peroxisomes always represents a proliferative state of the peroxisomal compartment. Moreover, also the loss of the microtubule skeleton, the inhibition of DLP1 or hFis1 function, or the overexpression of Pex11 proteins leads to the formation of tubular peroxisomes (Koch et al. 2004; Koch et al. 2003; Schrader et al. 1996). Of the mammalian Pex11 proteins only Pex11pα - which does not induce elongated peroxisomes – can be induced via PPARs, whereas the regulation of the other two isoforms (β and γ) is unknown (see 1.3.3 and 3.2). It is not clear, how elongating effects are exerted, which signals or effector proteins might be involved in or required for this process, and how the effectors are regulated.

3.4.1 Cumulative effects of Pex11pβ expression, DLP1 silencing, and microtubule depolymerisation on peroxisomal elongation

Depolymerisation of microtubules has been shown to induce the formation of elongated peroxisomes. Although peroxisomes are still able to divide, the lack of microtubules in-

terferes with a uniform distribution of peroxisomes and results in the formation of peroxisomal aggregates (Figure 3.29 D and E, arrows) (Schrader et al. 1996).

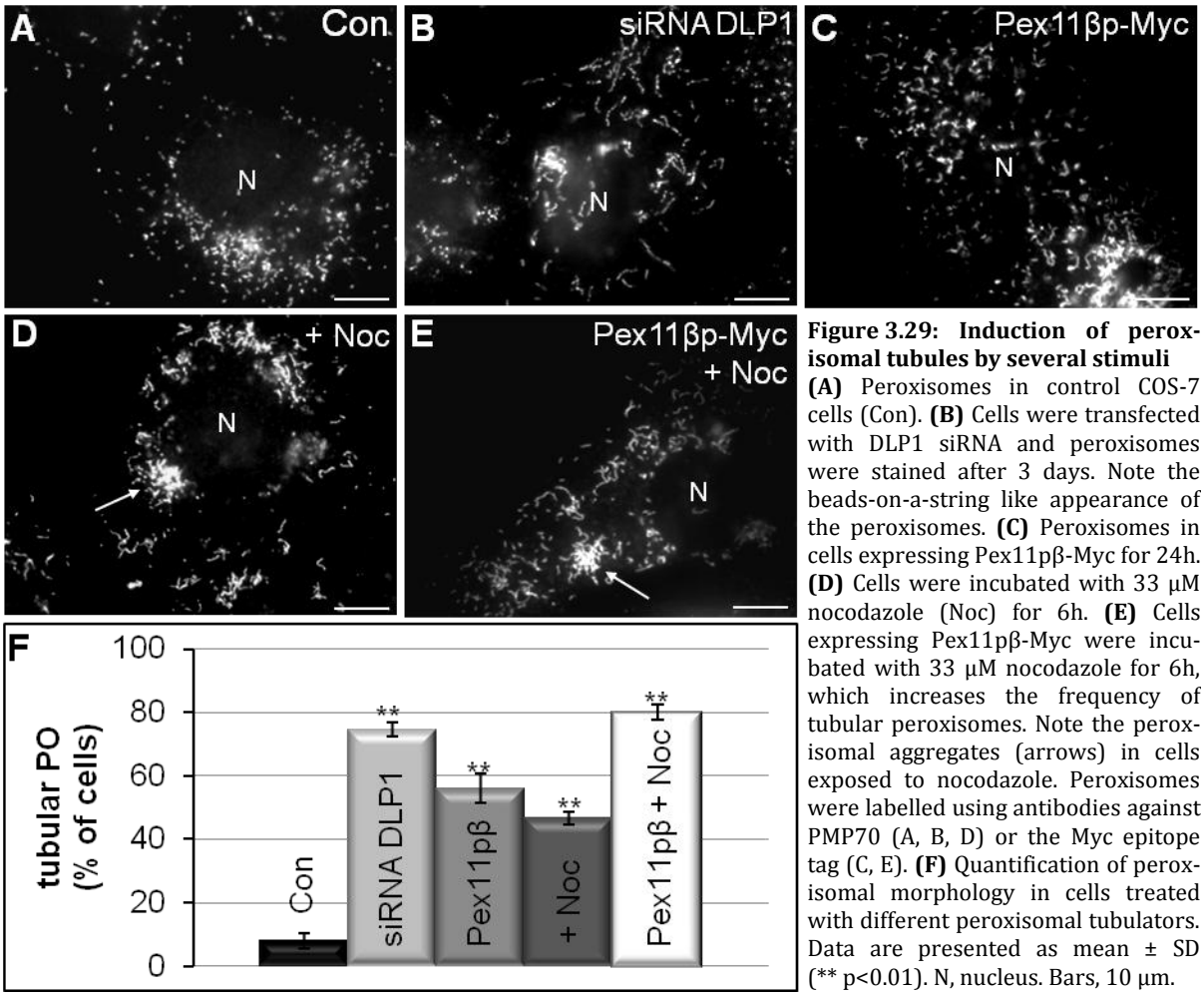

Figure 3.29: Induction of peroxisomal tubules by several stimuli
(A) Peroxisomes in control COS-7 cells (Con). **(B)** Cells were transfected with DLP1 siRNA and peroxisomes were stained after 3 days. Note the beads-on-a-string like appearance of the peroxisomes. **(C)** Peroxisomes in cells expressing Pex11pβ-Myc for 24h. **(D)** Cells were incubated with 33 µM nocodazole (Noc) for 6h. **(E)** Cells expressing Pex11pβ-Myc were incubated with 33 µM nocodazole for 6h, which increases the frequency of tubular peroxisomes. Note the peroxisomal aggregates (arrows) in cells exposed to nocodazole. Peroxisomes were labelled using antibodies against PMP70 (A, B, D) or the Myc epitope tag (C, E). **(F)** Quantification of peroxisomal morphology in cells treated with different peroxisomal tubulators. Data are presented as mean ± SD (** $p<0.01$). N, nucleus. Bars, 10 µm.

The combination of Pex11pβ overexpression with microtubule depolymerisation leads to an increased formation of elongated tubules, compared to both solitary stimuli (80.0 ± 2.3% of the cells compared to 56.0 ± 4.6% for Pex11pβ expression and 46.69 ± 1.9% for nocodazole; Figure 3.29 E and F). A similar number of cells with elongated peroxisomes was achieved by DLP1 silencing with siRNA (75.5 ± 3.7%; Figure 3.29 B and F) (Boll & Schrader 2005; Koch et al. 2004). Based on these observations a more detailed study on the effects of the combination of several tubulation stimuli was performed, in order to understand which factors mediate the formation of elongated peroxisomes.

The expression of Pex11pβ in cells already silenced for DLP1 exerts an additional elongating effect on peroxisomes (Figure 3.30 C) (Koch et al. 2004) sometimes leading to very long and thin peroxisomes (Figure 3.30 D). As other organelles, such as e.g. the Golgi, cannot maintain their shape without the presence of a supporting cytoskeleton

(Cole et al. 1996; Johnson et al. 1980; Swanson et al. 1987; Terasaki et al. 1986), it was interesting to examine if microtubule depolymerisation leads to fragmentation of those very long peroxisomal tubules (Figure 3.30 D).

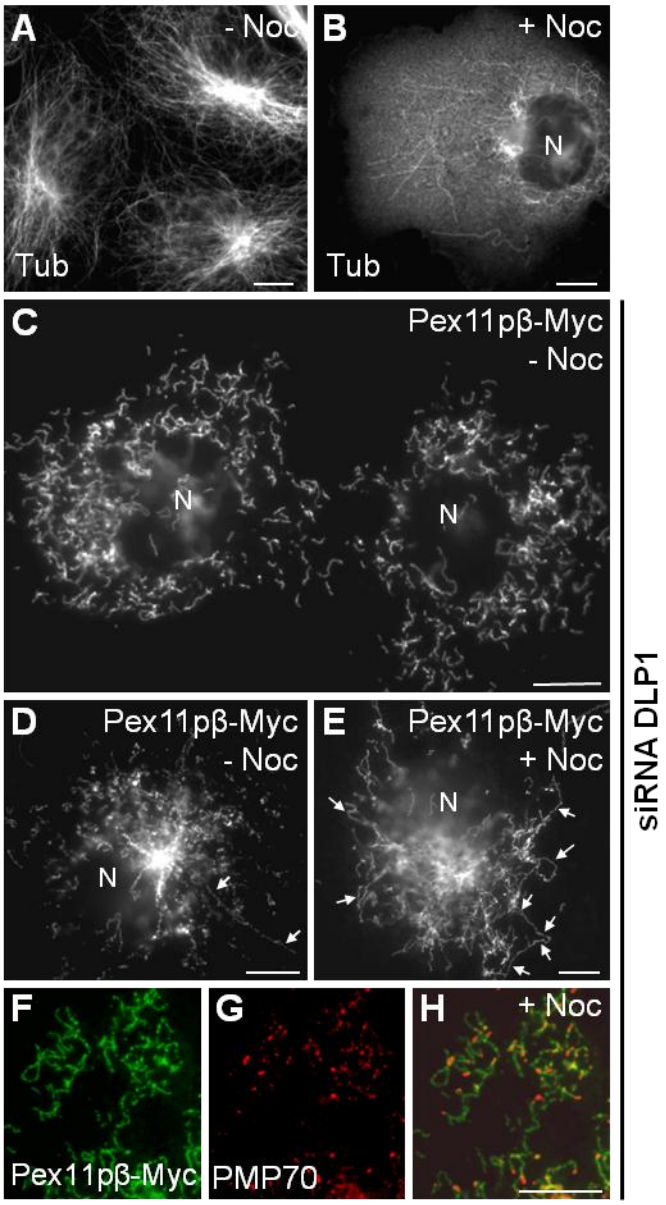

Figure 3.30: Cumulative effects on peroxisomal elongation by Pex11pβ expression, DLP1 silencing, and microtubule depolymerisation
(A) Microtubules in COS-7 cells stained with an anti-αTubulin antibody. **(B)** COS-7 cells were incubated with 33 µM nocodazole for 6 hours and stained with an anti-αTubulin antibody. Most of the microtubules are depolymerised. **(C-D)** COS-7 cells were transfected with DLP1 siRNA and re-transfected with Pex11pβ-Myc after 24 hours. Peroxisomes were labelled with an antibody against PMP70. **(E-H)** Cells were treated as in (C-D) and additionally incubated with nocodazole. Note the occurrence of numerous strongly elongated peroxisomal tubules (arrows). (F-H) Higher magnification view. Note that structures positive for PMP70 (G, H) are mainly spherical and located at one end of the tubules. N, nucleus. Bars, 10 µm.

Cells transfected with DLP1 siRNA and Pex11pβ-Myc were incubated for 6 hours with nocodazole. The microtubule depolymerisation increased the occurrence of very long and thin peroxisomes drastically and did not induce fragmentation of elongated peroxisomes (Figure 3.30 E-H). In almost all cells the peroxisomal morphology was changed to extremely elongated structures (up to 50 µm) spanning throughout the whole cell (Figure 3.30 E). Most of the tubular peroxisomes appeared to be segmented, which is typically seen after DLP1 silencing (Koch et al. 2004). PMP70, a peroxisomal membrane

protein, was mainly found in spherical structures at the end of the tubules, consistent with previous data (Figure 3.8 D-F) (Schrader et al. 1998b).

These observations demonstrate that the stability of preformed peroxisomal tubules does not depend on the microtubule skeleton; in contrast, peroxisomal tubules even become longer after the loss of microtubules. Furthermore, the combined application of several peroxisome elongating stimuli exerts a cumulative effect on the formation of tubular peroxisomes and, by increasing tubule length (and number), induces peroxisome hypertubulation.

3.4.2 Induction of reticular peroxisomal structures

Expression of a dominant-negative DLP1 mutant deficient in GTP hydrolysis (K38A) abolishes peroxisome division and leads to the formation of tubular peroxisomes. Upon co-expression with Pex11pβ-Myc DLP1-K38A induces hypertubulation of peroxisomes (Koch et al. 2003). Additionally, DLP1-K38A promotes the formation of tubulo-reticular "networks" of peroxisomes (Figure 3.31 A) (Koch et al. 2003). It is likely that the formation of a peroxisomal network requires the fusion of elongated peroxisomes. To investigate if the formation or maintenance of the peroxisomal network depends on the microtubule cytoskeleton, COS-7 cells were co-transfected with Pex11pβ-Myc and GFP-DLP1-K38A and after 24 hours the microtubules were depolymerised by incubation with nocodazole. Interestingly, the tubulo-reticular peroxisomal networks were not dispersed by microtubule depolymerisation. Instead, an increased number of cells with networks was observed (26.76 ± 7.2% compared to 12.67 ± 2.7% in controls; Figure 3.31 C-F). The peroxisomal networks were highly branched and spread throughout the whole cell, nicely visible in Figure 3.31 E. GFP-DLP1-K38A was observed to assemble into cytoplasmic aggregates as described before (Koch et al. 2003; Yoon et al. 2001) (Figure 3.31 B and D).

Similar to the combination of DLP1 silencing with Pex11pβ expression and nocodazole treatment described above, the depolymerisation of microtubules also acts as an additional elongation-enhancing stimulus on DLP1-K38A/Pex11pβ co-expression. The effects of the co-expression (tubulation of peroxisomes and formation of tubulo-reticular networks) were pronounced after applying a further tubulation stimulus – the depolymerisation of microtubules. The lack of the peroxisome-supporting cytoskeleton does

not interfere with the maintenance of complex long and branched peroxisomal structures.

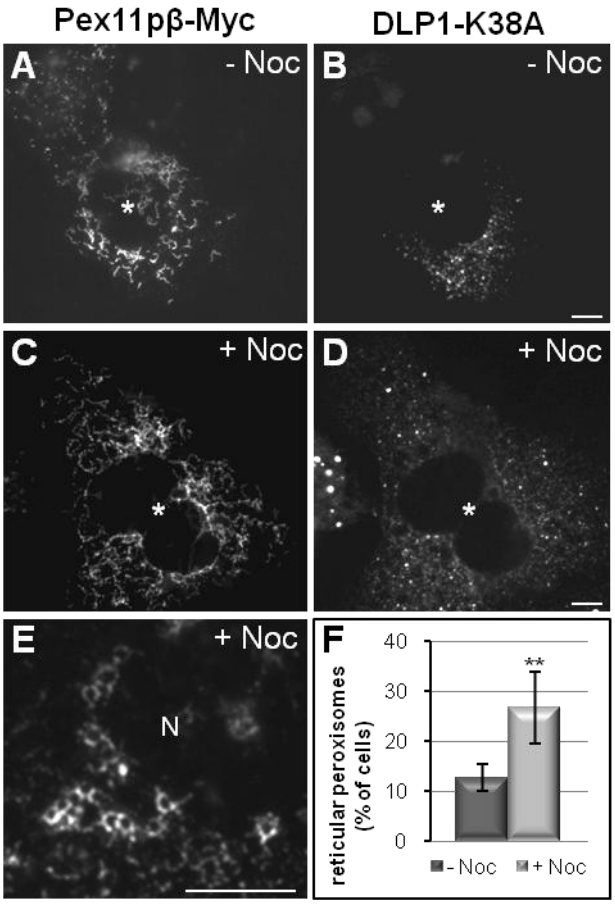

Figure 3.31: Enhanced formation of reticular peroxisomal structures by co-expression of Pex11pβ and DLP1-K38A combined with microtubule depolymerisation
(A-B) COS-7 cells expressing Pex11pβ-Myc (A) and GFP-DLP1-K38A (B). **(C-E)** Cells expressing Pex11pβ-Myc (C and E) and GFP-DLP1-K38A (D) were additionally incubated with 33 µM nocodazole for 6 hours. Note the enhanced elongation and rather reticular appearance of peroxisomes. Asterisks mark co-transfected cells. **(F)** Quantification of peroxisomal morphology in co-transfected cells, in control cells (-Noc) and after depolymerisation of microtubules (+Noc). Data are presented as mean ± SD (** $p<0.01$). N, nucleus. Bars, 10 µm.

3.4.3 Silencing of DLP1 induces long and branched TPAs, which are stable without microtubules

To further characterize the effects of simultaneous induction of different peroxisomal morphologies, the studies were continued with the Pex11pβ-YFP construct. The expression of this constructs results in the formation of tubular peroxisomal accumulations (TPAs) and inhibits the fission into small spherical peroxisomes (3.3). The co-expression of Pex11pβ-YFP with GFP-DLP1-K38A did not affect the morphological appearance of the TPAs (Figure 3.32 A). This supports the assumption that Pex11pβ-YFP blocks peroxisomal division at an early time point before the (DLP1-containing) fission complex is assembled at the peroxisomal membrane. Additional depolymerisation of the microtubules did not dissolve the TPAs but had an (slight) enhancing effect on their length (Figure 3.32 B). When DLP1 was silenced before expression of Pex11pβ-YFP TPAs were still formed but their morphology was altered. TPAs appeared to be longer, thinner and

less rigid and were often found to be aligned to each other, creating a branched appearance (Figure 3.32 C-E). PMP70 is localized to the globular endings of the TPAs, creating an "apple tree-like" appearance. It appeared as if the long and thin peroxisomal tubules induced by silencing of DLP1 accumulated or attach to one another upon the expression of Pex11pβ-YFP. This also demonstrates that the elongated peroxisomes induced by the fission block after DLP1 silencing are import competent for Pex11pβ-YFP. Additional depolymerisation of microtubules led to an increase in length of these thin and branched TPAs but did not disturb the general morphology or lead to a collapse of the structures (Figure 3.32 F-H).

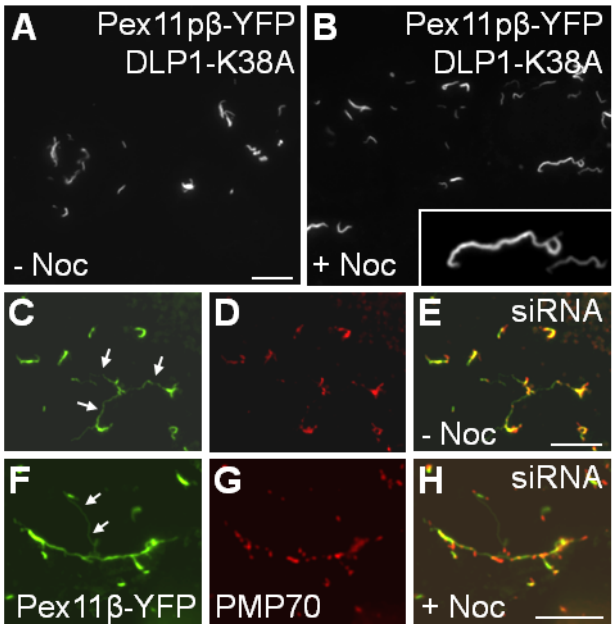

Figure 3.32: TPAs formed after DLP1/Drp1 silencing are stable without microtubules
(A-B) COS-7 cells were co-transfected with Pex11pβ-YFP and DLP1-K38A and additionally incubated with nocodazole (B). Note the increase in length of the TPAs after microtubule depolymerisation (B) compared to control (A). **(C-E)** COS-7 cells were transfected with DLP1 siRNA and after 48 hours re-transfected with Pex11pβ-YFP. After 24 hours cells were subjected to indirect immunofluorescence using an antibody against PMP70 (D). Note the rather thin and long appearance of TPAs (arrows) and the formation of branches in the TPAs. Structures positive for PMP70 are spherical and found at the end of peroxisomal tubules. **(F-H)** Cells were treated as in (C-E) and additionally incubated with nocodazole for 6 hours. The TPAs have a similar morphological appearance as in (C-E), but appear to be longer. Bars, 10 µm.

3.4.4 Formation of TPAs does not require the microtubule cytoskeleton

To examine if the formation of TPAs requires an intact microtubule network, microinjection studies were performed. This method allowed pre-incubation of the cells with nocodazole (for 2 hours), followed by transfection with Pex11pβ-YFP by injection of the plasmid into the nucleus. At this time point the microtubule cytoskeleton was clearly depolymerised (data not shown). Other transfection methods depend on an intact microtubule network for internalizing the DNA and were therefore not applicable (2.8.4). 24 hours after microinjection of Pex11pβ-YFP no differences in TPA formation were observed comparing control cells and cells pre-incubated with the microtubule-depolymerising agent (Figure 3.33).

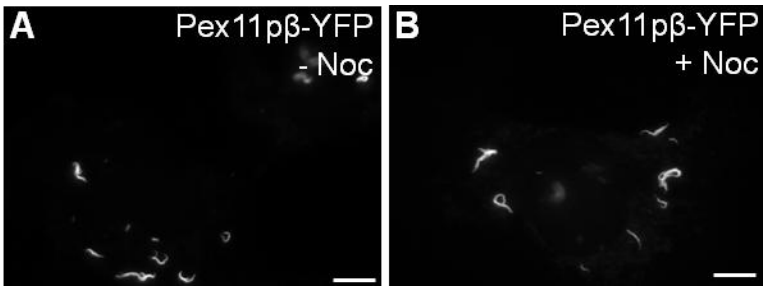

Figure 3.33: Formation of TPAs after microinjection of Pex11pβ-YFP into microtubule-depleted cells
COS-7 cells were transfected with Pex11pβ-YFP by microinjection of the DNA into the nucleus and fixed after 24 hours. **(B)** Prior to microinjection cells were pre-incubated with nocodazole for 2 hours and the incubation continued until fixation. Note that TPAs are formed under both conditions. Bars, 10 µm.

This demonstrates that microtubule-dependent movements of peroxisomes are not required for the formation of the tubular accumulations and that the basic random/oscillating movement of the peroxisomes is sufficient for TPA formation. In addition, targeting of Pex11pβ to the peroxisomes is a microtubule-independent process. TPAs seem to have self-stabilizing properties acting from the beginning and they never require a supporting skeleton, neither for formation nor for maintenance.

3.4.5 Peroxisome hypertubulation is not caused by Pex11 upregulation

In order to understand how depolymerisation of the microtubule cytoskeleton by application of nocodazole induces and enhances the formation of tubular peroxisomes, a semi-quantitative PCR (SQ-PCR) approach was applied. Total mRNA was isolated from control cells or from cells incubated with nocodazole for 3, 6 and 18 hours, respectively, and transcribed into cDNA. SQ-PCRs were performed to determine the mRNA levels of the three Pex11 isoforms. Interestingly, none of the Pex11 mRNA levels was increased after nocodazole treatment; the mRNA levels of Pex11α, Pex11β and Pex11γ did not change in comparison to non-treated cells (Figure 3.34 and personal communication N. A. Bonekamp, University of Aveiro, Portugal).

Due to the cumulative effects inducing hypertubulation, it is likely to assume that the different tubulation stimuli work via different signalling pathways and do not activate the same tubulation effector. Pex11pβ, the only effector known so far, is already highly abundant in the peroxisomal membrane as a result of its overexpression. Thus, it is improbable that a further upregulation of the Pex11pβ level is responsible for the enhanced peroxisomal tubulation, as could be confirmed by SQ-PCR. Furthermore, also

Pex11pγ, which was shown to induce peroxisome elongation in this study (section 3.2.1), is not upregulated and thus does not mediate peroxisome hypertubulation.

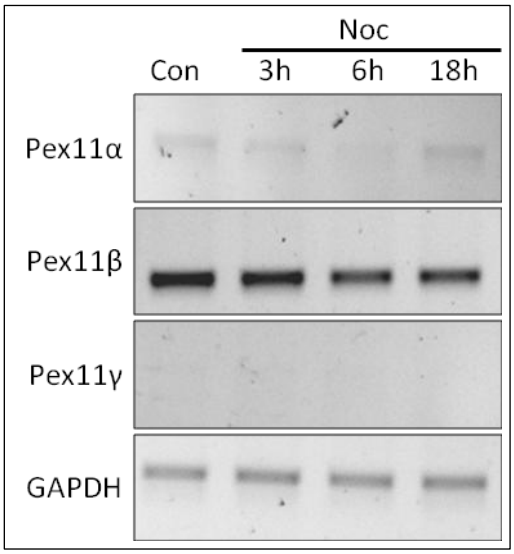

Figure 3.34: Depolymerisation of microtubules does not affect Pex11 mRNA levels
mRNA levels of Pex11α, Pex11β, Pex11γ, and GAPDH (Glyceraldehyde 3-phosphate dehydrogenase, as control) in cells incubated for 3, 6, or 18 hours with nocodazole (Noc) or untreated cells (Con) were determined by SQ-PCR. Note that mRNA levels are not increased after nocodazole treatment. Pex11γ-levels are below the detection limit under all conditions.

Elevated ROS levels have been shown to induce the formation of elongated peroxisomes (Schrader et al. 1999) and work from our laboratory showed that the application of nocodazole leads to a slight increase of oxidative stress in COS-7 cells (measured by an assay based on the ROS-sensitive fluorophore DCF). ROS might for example be released from mitochondria damaged by microtubule depolymerisation. However, combined application of nocodazole with antioxidants reduced ROS but did not inhibit the formation of tubular peroxisomes (personal communication S. Pinho, University of Aveiro, Portugal). This indicates that microtubule depolymerisation itself, but not ROS production, is the major cause for peroxisomal elongation.

3.4.6 Summary

It was demonstrated that the microtubule cytoskeleton is not required for the formation and stability of peroxisomal tubules, networks or TPAs. Depolymerisation of microtubules in addition to overexpression of Pex11pβ and/or inhibition of DLP1 function enhances the induction of tubular and reticular peroxisomes observed by these manipulations alone. Moreover, the simultaneous application of multiple tubulation stimuli results in hypertubulation of peroxisomes, indicating that different signals exert additive effects on peroxisome growth and division (Figure 4.4). Other elongating effectors than (upregulation of) the Pex11 proteins are likely to be involved in the formation of elongated peroxisomes.

4 DISCUSSION

Peroxisomes are essential organelles involved in numerous metabolic pathways (section 1.1.2), and defects in peroxisome functions or in peroxisomal biogenesis can lead to severe disorders (section 1.1.3). Although growth and division of peroxisomes has been intensively studied since many years, the details of this process are still not fully elucidated and hotly debated (Delille et al. 2009; Fujiki et al. 2006; Hettema & Motley 2009; Kunau 2005; Mullen & Trelease 2006; Nagotu et al. 2010; Platta & Erdmann 2007; Schrader & Fahimi 2008; Tabak et al. 2008). While peroxisomes are known to be able to multiply by growth and division, the contribution of peroxisomal *de novo* biogenesis (from the ER) to peroxisome multiplication could not yet be fully defined, and a number of different models for peroxisome biogenesis have been proposed. Furthermore, comprehension of the molecular components involved in growth and division is still limited. Three proteins have been identified to be key components of the peroxisomal division machinery: Pex11pβ, hFis1, and DLP1. These components are evolutionary conserved. Pex11pβ has been shown to promote peroxisome proliferation by induction of tubular peroxisomes, which are subsequently divided into new spherical peroxisomes. DLP1 and hFis1 were shown to be required for division, with hFis1 being the membrane adaptor for the GTPase DLP1, which in turn mediates final membrane scission. Interestingly, both hFis1 and DLP1 are likewise involved in the division of mitochondria, demonstrating a close interrelationship of both organelles. Thus, peroxisomes and mitochondria appear to be closely associated (Schrader & Yoon 2007). They do not only cooperate in regard to metabolic functions, but also share components of their division machineries.

hFis1 belongs to the family of TA proteins, whose membrane targeting and insertion mechanisms are not yet understood. The dual targeting of hFis1 to peroxisomes and mitochondria further complicates the import mechanism, given that specificity in the targeting to two different organelle membranes must be achieved. Regulative mechanisms for the dual targeting as well as sorting signals or the (putative) proteinaceous import factors involved are so far unknown.

Pex11pβ is not the only protein implicated in peroxisome proliferation; as a matter of fact a family of Pex11-type peroxisome proliferators (PPPs) exists in all species. Mammals possess three PPPs, the Pex11p isoforms Pex11pα, Pex11pβ, and Pex11pγ. It is not clear, which advantage the presence of several PPPs provides, and which roles the different isoforms play. Redundancy or specialized functions of the isoforms have not yet

been studied in detail. Furthermore, the biochemical properties of the Pex11 proteins are still a matter of debate. Efforts to dissect the growth and division process of peroxisomes have so far been focussed on the manipulation of DLP1 and hFis1 function, acting late in the growth and division process. A dissection of peroxisomal growth and division by manipulation of Pex11pβ, which is supposed to act early on in this process, has not yet been performed. Likewise, the signals and effectors mediating proliferation and morphological changes of peroxisomes are largely unknown. The role of the cytoskeleton in peroxisome biogenesis and morphogenesis is only partly understood.

4.1 Pex19p-mediated peroxisomal import of hFis1

Aim of this study was to understand the dual targeting of hFis1 to peroxisomes and mitochondria. In particular, the identification of import factors and targeting signals was intended, as well as gaining insights into regulative aspects of the dual targeting.

The import of peroxisomal membrane proteins is scarcely understood. Three peroxins, Pex3p, Pex16p, and Pex19p, have been implicated in this process (Girzalsky et al. 2010). While Pex19p appears to be a predominantly cytosolic protein, Pex3p and Pex16p are integral proteins of the peroxisomal membrane. Pex19p is thought to function as a cytosolic import receptor for PMPs and/or to provide chaperone activity and thus prevent protein aggregation. It binds numerous PMPs and appears to deliver them to Pex3p in the peroxisomal membrane, which is suggested to serve as a docking factor for the Pex19p-cargo complex. The function of Pex16p is less clear; it might represent the tethering or membrane assembly factor for Pex3p. The membrane insertion mechanisms for PMPs are not known (see section 1.2.2).

Tail-anchored proteins, such as hFis1, are supposed to utilize targeting mechanisms different from other membrane proteins. Their import does not require known components of the translocation machineries. Even unassisted insertion of TA proteins into mitochondrial and ER membranes has been described (Brambillasca et al. 2006; Kemper et al. 2008; Setoguchi et al. 2006). Insertion into the lipid bilayer might occur spontaneously, and targeting specificity could be mediated by the lipid composition of the respective membrane. Other studies propose an involvement of special proteins or chaperones for the import of TA proteins into the ER membrane (Abell et al. 2007; Stefanovic & Hegde 2007). Data regarding the targeting of TA proteins to peroxisomes are scarce and come from studies in yeast or plants (Elgersma et al. 1997; Mullen et al. 1999; Mullen &

Trelease 2000; Nito et al. 2001), where an indirect targeting to peroxisomes via the ER has been observed.

In this study firm evidence is provided that targeting of hFis1 to peroxisomes is mediated by Pex19p. Thus, peroxisomal TA proteins appear to use a protein-based sorting machinery which is shared with other PMPs. Similar results have been obtained in a study investigating the targeting of the TA protein Pex26p and its yeast homologue Pex15p (Halbach et al. 2006). In immunoprecipitation studies an interaction of Pex19p and hFis1 has been shown (Figure 3.1). Furthermore, by utilization of hFis1 deletion mutants, the mPTS of hFis1 could be restricted to a region comprising 26 amino acids at the very C-terminus (Figure 3.3). This region contains the TMD and five amino acids forming the intraorganellar tail. Removal of this tail disturbed Pex19p binding as well as peroxisomal and mitochondrial targeting (Figure 3.2) (Koch et al. 2005; Yoon et al. 2003). In agreement, an *in silico* search predicts a Pex19p binding site within the TMD of hFis1 (amino acids 136-145) (Rottensteiner et al. 2004; Schluter et al. 2010). Two additional potential binding sites are predicted in the cytosolic, N-terminal part of hFis1 (amino acids 52-61 and 91-100). However, the prediction matrix was developed for yeast proteins and the results obtained for mammalian proteins should be regarded with caution. Based on the experimental data the putative additional binding sites appear to be non-essential and might mediate rather weak interactions which assist in targeting and/or folding.

An overall positive charge in the tail of hFis1, provided by two lysine residues (K149 and K151), has been shown to be required for mitochondrial targeting (Stojanovski et al. 2004). In contrast, peroxisomal targeting as well as Pex19p binding does not depend on the presence of these lysine residues (Figure 3.3 and Figure 3.4). This finding is somehow puzzling, as positively charged amino acids have also been shown to be part of Pex19p binding regions (Halbach et al. 2005; Rottensteiner et al. 2004). As Pex19p binding to hFis1 does not appear to depend on a specific signal sequence, it can be speculated that the positively charged amino acids located N-terminally of the TMD might provide sufficient charge in a full length protein (Figure 1.8).

The Pex19-dependent targeting of hFis1 was further supported by data obtained using Pex19p siRNA. Knock down of Pex19p decreased the targeting of (overexpressed) hFis1 to peroxisomes, but not to mitochondria (Figure 3.6). As mitochondrial targeting of hFis1 does not require Pex19p, its unassisted insertion into the mitochondrial membrane cannot be excluded. It was shown that integration of TA proteins into the mito-

chondrial membrane, among them yeast Fis1, does not require known import components, and an implication of the membrane lipid composition has been postulated (Kemper et al. 2008; Setoguchi et al. 2006). The mitochondrial outer membrane contains very low amounts of ergosterol (ergosterol/phospholipid ratio 0.02), similar to peroxisomes (0.03), but in contrast to ER and plasma membrane (0.18 and 0.46, respectively) (Schneiter et al. 1999). Therefore, a well defined lipid composition might play a crucial role in (spontaneous) insertion of TA proteins into membranes. However, mitochondrial TA proteins have been shown to compete with each other for delivery to mitochondria, indicating the involvement of a limiting factor in protein folding and/or tail-mediated targeting (Setoguchi et al. 2006).

hFis1 is suggested to be the key player for recruiting DLP1 to both, the peroxisomal and mitochondrial membrane. Increasing hFis1 levels induces the fragmentation of both organelles. Therefore, the organelles might have to compete for recruitment of hFis1, e.g. under conditions of proliferation or multiplication. It is likely that recruitment and/or function of hFis1 is regulated or controlled. An unknown chaperone might fulfil this function for mitochondrial targeting, which competes with Pex19p for hFis1 binding and therefore for recruitment out of the cytosolic pool. A function for chaperones in targeting of TA proteins to the ER has been suggested (Abell et al. 2007), although they might not be required for proteins with low hydrophobic TMDs (Brambillasca et al. 2006). However, overexpression of Pex19p did not lead to a shift of hFis1 targeting towards peroxisomes (Figure 3.7). Another rate-limiting factor for hFis1 insertion into the peroxisomal membrane is likely to be involved. A good candidate would be Pex3p, the membrane docking factor for Pex19p.

Pex19p-dependent PMPs have been shown to be mistargeted to other organelles in the absence of Pex19p. PMP34 is targeted to non-peroxisomal compartments such as the ER (Jones et al. 2004) and the TA protein Pex26p is mistargeted to mitochondria under these conditions (Halbach et al. 2006). It was not possible to detect if the amount of hFis1 targeted to mitochondria is increased after knock down of Pex19p. However, hFis1 was not mistargeted to the ER (or other structures), although the ER membrane is thought to be the “default membrane” for TA proteins in case other targeting signals/factors are missing (Borgese et al. 2007). hFis1 also did not appear to travel to peroxisomes via the ER, as it has been hypothesized before (Elgersma et al. 1997; Mullen et al. 1999; Mullen & Trelease 2000; Nito et al. 2001), but is rather inserted into the peroxisomal membrane directly. ER targeting of hFis1 has only been observed after replace-

ment of the two C-terminal lysine residues, which removed the mitochondrial but not peroxisomal targeting signal. Again, this observation points to a rate-limited import into the peroxisomal membrane, as not all hFis1 (whose mitochondrial targeting is inhibited) is integrated into the peroxisomal membranes.

Recently, another pathway potentially involved in targeting of peroxisomal proteins has been discovered. A subpopulation of vesicles derived from mitochondria (MDVs) has been described to fuse with peroxisomes (Neuspiel et al. 2008). However, a role for MDVs in hFis1 targeting appears to be unlikely, given that MDVs fuse only with a small subpopulation of peroxisomes while hFis1 is found in all peroxisomes (Kobayashi et al. 2007; Koch et al. 2005). Furthermore, hFis1 has not been shown to be a prominent cargo of MDVs. Mitochondrial and peroxisomal targeting of hFis1 rather appear to be independent events.

A second TA protein targeted to peroxisomes and mitochondria was discovered recently (Gandre-Babbe & van der Bliek 2008). Interestingly, a role for Mff in the division process of both organelles has been suggested. No data have been obtained regarding the dual targeting of Mff, but a Pex19p binding site could be predicted (amino acids 170-179) (Delille & Schrader 2008). This region does not include the putative TMD of Mff (amino acids 199-216) and an involvement of Pex19p in Mff targeting needs to be experimentally tested.

In summary, two different mechanisms could apply for the dual targeting of hFis1 to peroxisomes and mitochondria. As Pex19p acts as cytosolic receptor for hFis1 in directing it to the peroxisomal membrane, a competing mitochondrial receptor might function in a similar way in mitochondrial targeting (Figure 4.1 A). On the other hand, the mitochondrial outer membrane might be the default target of hFis1, whereas only a minor part of the hFis1 pool is recruited to peroxisomes by Pex19p (Figure 4.1 B). In both cases the peroxisomal import appears to be regulated by an additional rate-limiting factor. This function could be fulfilled by a protein of the import machinery, such as Pex3p, or by a component of the division complex. However, targeting specificity to mitochondria has to be achieved to prevent inappropriate insertion e.g. into the ER membrane. This could also rely on a yet unidentified protein in the mitochondrial membrane that enhances the insertion by trapping hFis1. Alternatively, the native outer membrane might contain lipid domains or other structural elements that facilitate the insertion of hFis1 and/or stabilize the inserted protein (Kemper et al. 2008).

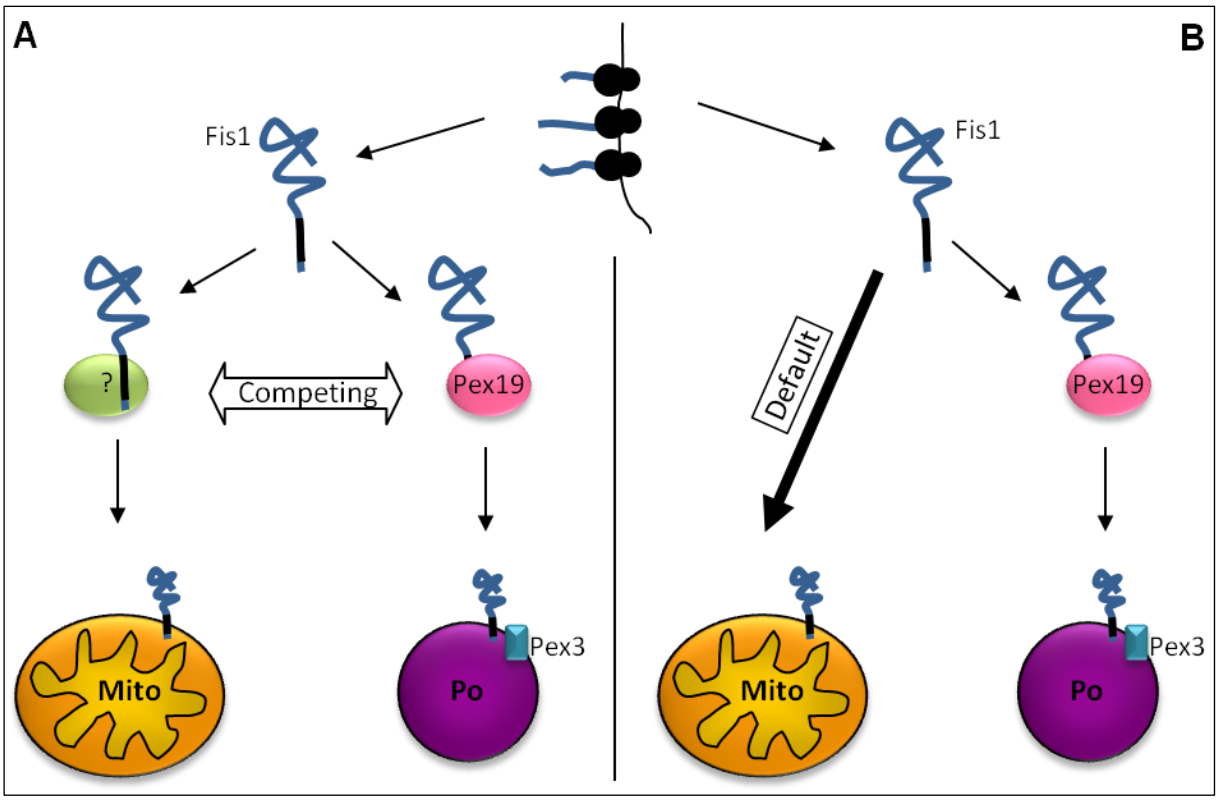

Figure 4.1: Models for the targeting of hFis1 to peroxisomes and mitochondria
(A) Targeting might be regulated by two cytosolic receptors competing with each other for hFis1 binding and its targeting to mitochondria (Mito) or peroxisomes (Po), respectively. The peroxisomal receptor is Pex19p. **(B)** Mitochondrial targeting could be the default way for hFis1, while parts of the hFis1 pool are bound by Pex19p and targeted to peroxisomes. In both scenarios peroxisomal import rate-limiting factors are likely to be involved (e.g. Pex3p).

4.2 Characterization of the mammalian Pex11 proteins

Proteins of the Pex11p family are remarkable in many respects. They are the only known proteins of the division machinery which are unique for peroxisomes and not shared with mitochondria. In mammals, they are the only proteins known to be involved in proliferation of peroxisomes, i.e. in regulation of peroxisome number and size. They are able to deform the peroxisomal membrane and to induce the formation of peroxisomal tubules. Apart from that, little is known about the functions of Pex11 proteins. All species tested so far possess several Pex11p isoforms, but little is known about the specific functions of these isoforms. Furthermore, the biochemical properties of Pex11 proteins are still unclear. Therefore, this study intended to deepen the understanding of the Pex11 protein family by a comparative characterization of the three mammalian Pex11p isoforms. It was thought to investigate the different Pex11 proteins under comparable experimental conditions, and to test the influence of different tags and deletions on Pex11p functions and the peroxisomal morphology.

4.2.1 Insights into the functions of Pex11 protein – elongation and constriction of peroxisomes

Pex11pβ is the Pex11 protein which has been studied most extensively and it exerts the most prominent effect on peroxisomes. Overexpression of Pex11pβ induces the formation of elongated peroxisomes (tubules). Subsequently, these tubules obtain a "striped" appearance, as Pex11pβ and e.g. matrix proteins are segregated from each other resulting in an alternating staining ("beads on a string"). This protein segregation appears to correlate with constriction of the peroxisomal tubules visible in ultrastructural studies (Grabenbauer et al. 2000; Koch et al. 2004; Lay et al. 2006). Pex11pβ is thought to be concentrated at the constriction sites (see also section 4.3.3). Next, the constricted tubules are divided resulting in the formation of spherical peroxisomes. These observations led to the definition of the Pex11pβ-induced growth and division process as a multistep pathway. However, two other Pex11p isoforms exist in mammals. Interestingly, the only isoform responding to peroxisome proliferators with an increase of protein levels is Pex11pα. But peroxisome proliferation induced by most – not all – proliferating agents does not depend on Pex11pα, at least in mice (Li et al. 2002a). A knockout of Pex11pα does not affect mice, in contrast to Pex11pβ whose loss results in neonatal lethality and ZS-like symptoms (Li et al. 2002b). Overexpression of Pex11pα was de-

scribed to rarely induce peroxisome proliferation and no increased elongation of peroxisomes has been observed (Abe et al. 1998; Schrader et al. 1998b). This data were confirmed in the present study. Nevertheless, segregation from matrix proteins similar to Pex11pβ was detected (Figure 3.8). Even small tubules were observed to have an alternating protein composition. This phenotype was not induced by overexpression of the third isoform, Pex11pγ. Conversely, Pex11pγ induced massive peroxisome elongation, just as strong as Pex11pβ (Figure 3.8 and Figure 3.9). While the number of cells with peroxisomal tubules induced by Pex11pβ decreased after 24 to 48 hours, due to the division into small peroxisomes, Pex11pγ-induced tubules persisted even 72 hours. The subsequent decrease of cells with tubular peroxisomes could be due to plasmid dilution and the resulting decrease in protein levels, or due to division of the tubular peroxisomes into spherical ones, although a massive increase in peroxisome number was not observed. Interestingly, peroxisomal tubules induced by Pex11pγ completely co-localized with matrix markers (Figure 3.8). During formation of elongated peroxisomes induced by Pex11pβ an intermediate state of globular peroxisomes positive for matrix proteins and tubular extension positive for Pex11pβ is observed (Figure 3.8). This was not seen after expression of Pex11pγ. Please note that peroxisome-elongating properties of Pex11pβ were not affected by the usage of tags at either site of the protein. The N-terminal Myc-tagged version used in this study induced peroxisome elongation and proliferation just as strong as the C-terminal tagged variant described before (Schrader et al. 1998b). In summary, the three Pex11 proteins appear to partially overlap in their functions, at least in regard to the phenotypes induced. Protein segregation – probably linked to membrane constriction (see below) – can be induced by Pex11pα and Pex11pβ, while tubule formation is induced by Pex11pβ and Pex11pγ. It should be noted that endogenous Pex11pγ levels are very low in most rat tissues tested, except liver (Li et al. 2002a). Pex11pβ is constitutive and equally expressed in all tissues.

4.2.2 Lipid binding and the different Pex11p C-termini

The Pex11p isoforms differ in their sensitivity to the detergent Triton X-100. Pex11pβ is the most and Pex11pγ the least sensitive protein, while the sensitivity of Pex11pα is placed in between those two. The sensitivity becomes apparent through diminished or absent signals in immunofluorescence studies, even in formaldehyde fixed samples (Figure 3.10). In previous biochemical approaches Triton X-100 could likewise not be

used with Pex11pβ and Pex11pα (Li & Gould 2003), but the reasons remained unclear. The Triton X-100 sensitivity might be explained by the lipid solubilising properties of the detergent. Amino acid sequence similarities between *Sc*Pex11p and PPARs, which bind to lipid ligands, point towards an ability of Pex11 proteins to bind lipids (Barnett et al. 2000). Therefore, Triton X-100 might influence the lipid binding properties of Pex11pβ (and Pex11pα) or replace the lipids and extract the proteins out of the membrane. The different Triton X-100 sensitivities could therefore reflect distinct lipid or membrane binding characteristics of the Pex11p isoforms. The different degrees of membrane extraction cannot be explained by different degrees of fixation by formaldehyde, as the respective number of lysine residues (which are cross-linked by formaldehyde) does not correlate with the sensitivities observed. If Pex11 proteins are indeed able to bind lipids directly has to be experimentally tested. However, such lipid interactions could relate to membrane constricting activities, which are likely to require actual wedging of the outer membrane leaflet or remodelling of the lipid composition inside the membrane. This hypothesis is supported by the observation that Pex11pγ, the only Pex11p isoform not sensitive to Triton X-100, does not induce membrane constriction/protein segregation.

Consistent with the proposed membrane topology of the mammalian Pex11 proteins (Figure 1.7 and Figure 1.9), removal of 30 C-terminal amino acids including the second putative transmembrane domain affects the peroxisomal targeting of the Pex11p isoforms, although to different degrees (section 3.3.3). Interestingly, deletion of the small C-terminal domain exposed in the cytosol had different effects on the respective isoforms. While Myc-Pex11pαΔ8 was not detectable, expression of Myc-Pex11pβΔ5 resulted in a delayed peroxisome elongation compared to the full length protein. Induction of peroxisomal tubules by Myc-Pex11pγΔ11, however, was hardly affected compared to the full length variant. The differences observed between the isoforms may allow some speculations about the function of the proteins or protein domains. The C-terminus of Pex11pα contains a dilysine motif, which was suggested to mediate coatamer binding (Passreiter et al. 1998). Although mutation of this motif did not affect function of *Tb*Pex11p (Maier et al. 2000), removal of the full C-terminus of Pex11pα appears to have more drastic effects, as it inhibits proper protein targeting (section 3.3.3). Additionally, the stability of the protein might be impaired. The fact that truncated Pex11pβ still promotes peroxisome proliferation, although delayed, might be explained by homo-oligomerization with endogenous Pex11pβ protein. Note that the C-terminus of Pex11pβ is most likely not

required for its homo-oligomerization but for interactions with hFis1 (Kobayashi et al. 2007). In contrast, tubulation activity of Pex11pγ does not appear to require its C-terminus. Homo-oligomerization with endogenous Pex11pγ is rather unlikely, due to its low expression levels (Figure 3.34).

In conclusion, it appears that the Pex11p isoforms having a segregating/membrane constricting activity (Pex11pα and Pex11pβ) are more strongly affected by C-terminal truncations than the isoform solely inducing tubular peroxisomes (Pex11pγ). The same applies to the Triton X-100 sensitivity, indicating that putative lipid-binding properties differ between Pex11pα/Pex11pβ on one hand and Pex11pγ on the other hand. It can be hypothesized that those two functions/characteristics are related, i.e. that tubule constriction (and subsequent protein segregation) is achieved by lipid remodelling through Pex11pα/Pex11pβ.

4.2.3 Membrane mobility and tubule motility

Tubulation of membranes does not only occur at peroxisomes, but also at other organelles such as the ER. Interestingly, the reticulon and DP1/Yop1p protein family has been implicated in the formation of tubular ER structures (Hu et al. 2008; Voeltz et al. 2006). These proteins are able to induce tubulation of liposomes *in vitro* and have been shown to form immobile oligomers in the tubular ER (Shibata et al. 2008). Furthermore, also stacked ER membrane arrays have been observed, which resemble somehow the TPAs induced by Pex11pβ-YFP (see section 4.3.1). The formation of the so called organized smooth ER (OSER) has been linked to interactions of highly mobile membrane proteins (Snapp et al. 2003). In this regard the membrane mobility properties of the tubule-inducing Pex11p isoforms were of interest. It was shown by FRAP experiments that Pex11pβ and Pex11pγ are rather low mobile membrane proteins (Figure 3.28). Pex11pγ, however, has the higher membrane mobility and a complete redistribution of Pex11pγ-YFP along peroxisomal tubules in around 25-40 seconds was observed. YFP-tagged Pex11pβ, on the other hand, did not completely redistribute over the tubule surface. Nevertheless, the membrane mobility of Pex11pβ was hardly influenced by the formation of TPAs, indicating that Pex11pβ molecules are not locked inside the TPA membranes (e.g. by increased oligomerization or interactions with proteins of the apposing membrane) and that protein flow within the membrane is still possible. In summary, the general low membrane mobility of Pex11 proteins suggests that the mecha-

nisms for tubule (and TPA) formation rather resemble the activity of reticulon than of OSER-inducing ER proteins.

Spherical peroxisomes are known to bind to and move along microtubules in mammals (section 1.2.4.3) (Huber et al. 1999; Rapp et al. 1996; Schrader et al. 1996; Schrader et al. 2000; Thiemann et al. 2000; Wiemer et al. 1997). Peroxisome motility is required for positioning of peroxisomes and for maintenance of their uniform intracellular distribution. It was shown here that highly elongated peroxisomal tubules induced by Pex11pγ are likewise able to move within the cell, although movement had only been described for rather short tubules before (<3 µm; Schrader et al. 2000). Tubules were highly motile and appeared to crawl along tracks, most probably along the microtubule cytoskeleton. Peroxisomal tubules also bent, as if they would pass over towards a crossing track and appeared to branch – which is most likely resulting from the alignment of two (or more) tubules along each other. These observations suggest that proteins localized along the entire peroxisomal tubule interact with the cytoskeleton e.g. via motor proteins. Alternatively, those connection sites could be localized exclusively at the tubule tip and pull the rest of the peroxisome throughout the cell. However, the bidirectional movements observed are difficult to explain by the latter model. It is unknown which proteins mediate the binding of peroxisomes to microtubules or to the motor proteins required for movement. An involvement of a cytosolic factor peripherally associated with peroxisomes and an additional peroxisomal membrane protein has been suggested by *in vitro* studies (Schrader et al. 1996; Thiemann et al. 2000). The microtubule binding appeared to be independent of motor proteins and is likely to include a CLIP-like protein (Thiemann et al. 2000). Interestingly, the Pex11-related protein Pex25p of *S. cerevisiae* was shown to interact with Rho1p, an actin-organizing protein (Marelli et al. 2004). Two other peroxisomal yeast proteins, Inp1p and Inp2p, have been identified to bind to the cell cortex or to the type V myosin Myo2p, respectively, and are required for proper organelle inheritance (section 1.2.4.3) (Fagarasanu et al. 2006; Fagarasanu et al. 2005; Saraya et al. 2010). Studies in plants, however, suggest that at least emanation of so-called peroxules – thin membrane extensions – could also be achieved by sequestration of existing ER tubules and retro-flow of peroxisomal proteins into the ER (Sinclair et al. 2009). However, it is difficult to imagine how such a mechanism should apply for membrane proteins, such as Pex11pγ studied here.

4.3 Pex11pβ-mediated growth and division of mammalian peroxisomes follows a maturation pathway

4.3.1 Pex11pβ-YFP – a novel tool to study peroxisome growth and division

Previously, only late events of the peroxisomal growth and division process could be studied, mainly by manipulation (e.g. knock down) of DLP1 and hFis1 (Koch et al. 2004; Koch et al. 2003; Koch et al. 2005). Thus, it was intended here to study the early events in this process, namely by manipulation of Pex11pβ. Pex11 proteins are – as described above – important for peroxisome morphogenesis. Pex11pβ expression promotes peroxisome elongation and division in mammalian cells (Li & Gould 2002; Schrader et al. 1998b), whereas *PEX11β* mice exhibit a reduced number of peroxisomes (Li et al. 2002b). In this work, the formation of a special peroxisomal compartment induced by manipulated Pex11pβ is described. Interestingly, the addition of a monomeric YFP to the C-terminus of Pex11pβ did not interfere with peroxisome elongation, but resulted in the formation of tubular peroxisomal membrane accumulations (named TPAs), which had lost their ability to constrict or divide (Figure 3.13). TPAs consist out of highly ordered elongated peroxisomal membranes which originate from pre-existing peroxisomes (Figure 3.16). The formation of TPAs leaves the cell with only few large peroxisomal structures, while all other (spherical) peroxisomes disappear. TPAs are not induced by other GFP-tagged peroxisomal membrane proteins, such as Pex3p-GFP, either alone or in combination with Pex11pβ-Myc. Also expression of the YFP-tagged isoform Pex11pα (Pex11pα-YFP) or N-terminal YFP-tagged Pex11pβ did not result in TPA formation or inhibition of peroxisome division (Figure 3.14). However, co-expression of Pex11pβ with GFP-hFis1 also led to formation of TPAs, as well as co-expression of N-terminal YFP-tagged Pex11pβ together with Myc-tagged Pex11pβ (but not Pex11pα or Pex11pγ) (Figure 3.25 and Figure 3.27). When Pex11pβ-YFP was targeted to mitochondria in *PEX19*-deficient fibroblasts, no clustering of mitochondria was observed (data not shown), indicating that TPA formation depends on the localization of Pex11pβ (and not e.g. Pex11pα) at the peroxisomal (and not the mitochondrial) membrane in combination with a bulky tag.

First, TPA formation was thought to result from a specific block of the (cytosolic) C-terminus of Pex11pβ and it was tested if removal of the C-terminus (and therefore its inaccessibility) would also lead to TPA formation. C-terminal deletions did not induce

TPAs but rather delayed peroxisome proliferation in comparison to the full length protein (Δ5, see section 4.2.2). Further truncation (Δ30 or Δ60) abrogated peroxisome elongation completely (Figure 3.14). These observations indicate that the morphological alterations were not merely the result of an inaccessibility of the C-terminus itself. Pex11pβ-YFP appeared to act like a "dominant-negative mutant" which blocks the Pex11pβ-induced peroxisome proliferation at a certain stage. The proper assembly of a functional constriction/division complex might be inhibited – most likely due to sterical hindrance.

In a previous study an interaction of Pex11pβ and hFis1 has been demonstrated (Kobayashi et al. 2007). The N-terminal domain of Pex11pβ was shown to be required for Pex11pβ homo-oligomerization and for peroxisome multiplication, while the C-terminus of Pex11pβ was required for binding of hFis1. A coordinated, interactive role of hFis1 and Pex11pβ is likely and interactions of Pex11 proteins with Fis1 were also shown in plants (Lingard et al. 2008). This is supported by the observations that both hFis1 and Pex11pβ co-localized in the membrane extensions of the TPAs, and that co-expression of GFP-hFis1 and Pex11pβ-Myc promoted TPA induction (Figure 3.25).

Pex11pβ-YFP appeared to initially inhibit the peroxisome constriction or segmentation, which subsequently leads to formation of stacked membranes by alignment of the tubular membrane extension along each other. The stacking could be mediated by weak or low affinity binding between the cytoplasmic domains of proteins on apposing peroxisomal membranes, which might accumulate upon the block by Pex11pβ-YFP. Such low affinity bindings have been described to result in OSER formation (Snapp et al. 2003) (section 4.2.3). The interactions are not mediated by the YFP-tag as such, as a monomeric YFP incapable of dimer formation has been used. Furthermore, formation of similar peroxisomal accumulations was also observed after fusion of Pex11pβ to another monomeric tag (HaloTag) of similar size (data not shown). The putative interactions between apposing membrane proteins might be of physiological significance, for example during peroxisome morphogenesis, organelle or peroxisome interactions, or transfer of lipids or other compounds (via the ER).

Altogether, the generated Pex11pβ-YFP fusion protein represents a specific and useful novel tool to further dissect the peroxisome multiplication and to investigate the early events in the peroxisome growth and division process.

4.3.2 New insights in Pex11pβ-mediated growth and division

An important finding of this work exploiting the Pex11pβ-YFP fusion protein is the observation that Pex11pβ-mediated growth (elongation) and division of peroxisomes follows a multistep maturation pathway. Starting at pre-existing peroxisomes membrane extensions enriched in Pex11pβ are formed. These membrane tubules become positive for the so-called "early peroxins" Pex3p, Pex16p, and Pex19p required for peroxisomal membrane protein import (Figure 3.18 and Figure 3.19). Other PMPs, such as PMP70 or PMP22, and matrix proteins are absent from the tubules and only found in the globular (mature) peroxisomes giving rise to the membrane extensions (Figure 3.17, Figure 3.18 and Figure 3.22). As Pex11pβ appears to act as a dominant-negative mutant, it blocks the subsequent constriction/segmentation and division of the tubular membrane compartment, which is e.g. observed after expression of Pex11pβ-Myc. The Pex11pβ-YFP mediated block or delay in the correct assembly of the constriction/division machinery is likely to inhibit the import of newly synthesized matrix proteins and PMPs into the membrane extensions as well. In contrast, proper import of matrix proteins and PMPs in the segmented, "beads on a string"-like peroxisomes is observed in controls expressing Pex11pβ-Myc. The import of newly synthesized matrix proteins into the "beads" was nicely shown by application of the HaloTag technology (Figure 3.22). Thus, it is proposed that the assembly of the constriction/division complex is a prerequisite for the proper assembly (or activation) of the protein import machinery for peroxisomal matrix proteins and other PMPs. These results demonstrate that the Pex11pβ-mediated growth and division of peroxisomes occurs by a maturation pathway (Figure 4.2) following several steps:

1) Pex11pβ-mediated formation of a peroxisomal subdomain at one side of pre-existing peroxisomes;
2) growth or extension of this subdomain resulting in a peroxisomal membrane compartment which contains some PMPs but no (active) import machinery for matrix proteins;
3) segmentation and constriction of the tubular extension, which requires Pex11pβ, hFis1 and maybe other components, but not DLP1;
4) assembly or activation of the import machinery followed by import of PMPs and matrix proteins;
5) final division into spherical peroxisomes by DLP1.

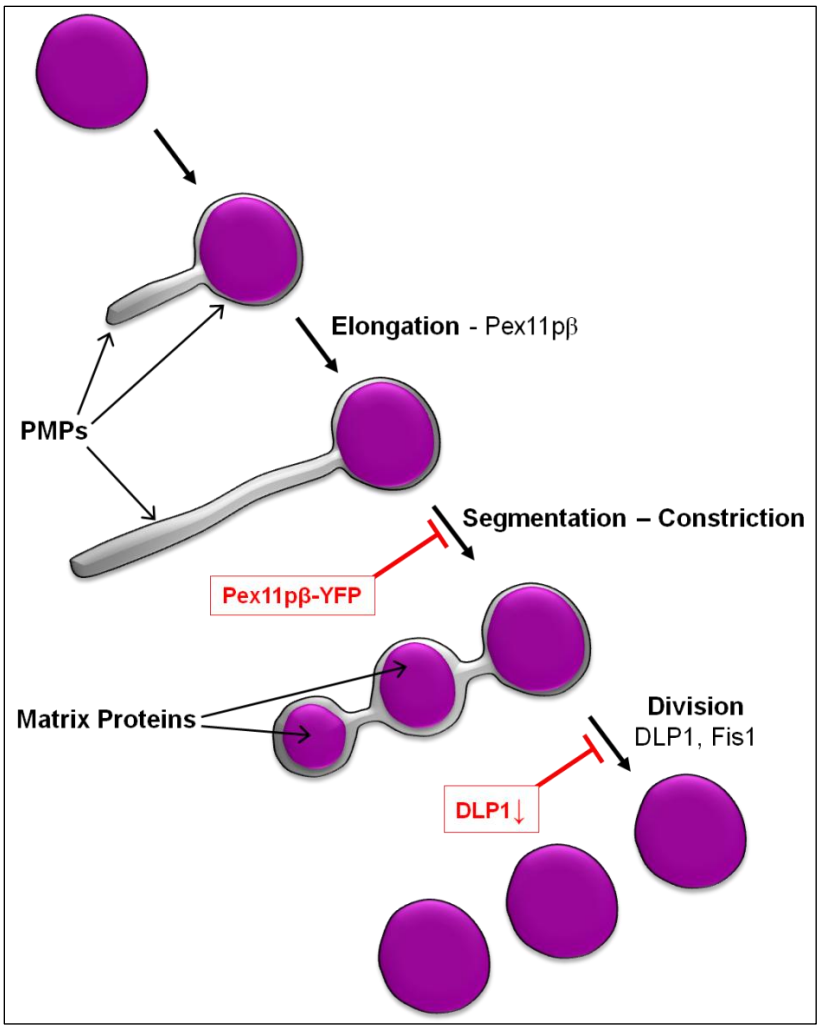

Figure 4.2: Peroxisome multiplication by growth and division follows a multistep maturation pathway
Pex11pβ mediates the formation of a tubular membrane extension emerging from one side of a spherical, mature peroxisome. The membrane extension grows and acquires a distinct set of PMPs, but is negative for matrix proteins. Afterwards, the membrane extension segments and constricts. This step can be inhibited by expression of Pex11pβ-YFP which keeps the peroxisomes in an elongated stage and results in TPA formation. The constricted peroxisomal tubule imports other PMPs and matrix proteins and is finally divided by hFis1 and DLP1 into several spherical peroxisomes. Silencing of DLP1 inhibits fission resulting in the accumulation of constricted peroxisomal tubules positive for PMPs and matrix proteins (Koch et al. 2004).

Similar maturation pathways which are commonly initiated by the formation of an early peroxisomal membrane compartment and its stepwise conversion into a mature, metabolically active peroxisome compartment have been proposed for peroxisomal growth/division in yeast (Veenhuis et al. 2000) and in some aspects also resemble ER-dependent peroxisome maturation (Titorenko & Rachubinski 2009; van der Zand et al. 2006). In those models, maturation is achieved by selective and stepwise import of certain PMPs, membrane lipids and matrix proteins.

The observations of the present study clearly demonstrate that growth and division of mammalian peroxisomes (at least the process mediated by Pex11pβ) is more complex than simple division of a pre-existing organelle and *per se* represents a process of biogenesis.

Interestingly, it was observed that the tubular membrane compartment apparently has to segment/constrict in order to import other PMPs and matrix proteins. The block exerted e.g. by Pex11pβ-YFP appears to interfere with the assembly of a functional con-

striction/division complex, but not with membrane extension. Interestingly, silencing of DLP1, which acts later on during final membrane scission, leads do accumulation of elongated peroxisomes which are still constricted but contain peroxisomal matrix and membrane proteins (Koch et al. 2004). These results suggest that the consecutive steps of the peroxisomal growth and division process are linked to each other, and may be triggered by the assembly of distinct machineries at the peroxisomal membrane. In this regard it is interesting to note that tubular peroxisomes with bulbous domains have also been observed after overexpression of *Sc*Pex25p in a *S. cerevisiae pex11/pex25/pex27* triple deletion strain. Furthermore, protein import was impaired by the triple deletion and cells were not able to grow on fatty acids (Rottensteiner et al. 2003b).

PMPs display distinct localizations inside the TPAs – at the tubular extension or the globular domains – although the two compartments show membrane continuity. This observation raises the questions which specific mechanisms restrict the mobility of PMPs and inhibit diffusion into the other compartment. This might be mediated by protein oligomerization, but might also involve a specific lipid environment. In *Y. lipolytica* a role for lipid microdomains in peroxisome maturation has been proposed (Boukh-Viner et al. 2005; Titorenko & Rachubinski 2009), and a similar mechanism might apply here. Furthermore, caveolin-1, a protein known to be associated with lipid microdomains forming caveolae, was recently shown to be enriched in the peroxisomal membrane of rat hepatocytes (Woudenberg et al. 2010).

It appears that Pex11pβ-YFP is a valuable tool to enrich or accumulate tubular peroxisomal membranes and might therefore be helpful for specific isolation and analysis of these structures in future experiments. Besides restriction of the mobility of existing proteins in the TPA membrane, also a specific targeting or sorting of PMPs to the globular or extended tubular membrane domain must be achieved. Pex11pβ and hFis1 are likely to be directly targeted to (tubular) peroxisomes in a Pex19p-dependent manner (Jones et al. 2004; Rottensteiner et al. 2004; this study). No evidence for localization to the ER has been obtained. The targeting is likely to occur at the correct subcompartmental site, regulated e.g. by assembly of the import machineries. If the targeting would occur indirectly via ER-derived pre-peroxisomal vesicular carriers (section 1.2.2) with distinct cargos, the distinct protein localizations would require a specific targeting and fusion of these carriers with the respective TPA domains. They must have the ability to distinguish between globular and tubular membrane domains prior to fusion.

Alternatively, subsequent sorting mechanisms within the peroxisomal membranes could exist.

Membrane growth and extension is expected to involve the transfer of lipids to peroxisomes. A so far unanswered question is how growing peroxisomes are supplied with membrane phospholipids. These lipids are synthesized in the ER and they need to be transported in an efficient manner towards peroxisomes. Three potential mechanisms could apply: A) an ER-derived vesicular transfer; B) membrane-membrane interactions with ER subdomains and a protein-based lipid transfer, resembling lipid transfer to mitochondria; C) direct luminal interactions which might be of transient nature (Figure 4.3). Although luminal connections between the ER and TPAs have not been observed, even after massive overexpression of secretory proteins (Figure 3.23), existence of those connections cannot be rigorously denied. Direct luminal connections to ER subdomains have been observed in mouse dendritic cells by three-dimensional image reconstruction (Geuze et al. 2003; Tabak et al. 2003). However, a recent report points towards a nonvesicular ER-to-peroxisome transfer of phospholipids (Raychaudhuri & Prinz 2008), and a close association of peroxisomes and the smooth ER has been frequently observed (Grabenbauer et al. 2000; Novikoff & Shin 1964; Yamamoto & Fahimi 1987; Zaar et al. 1987).

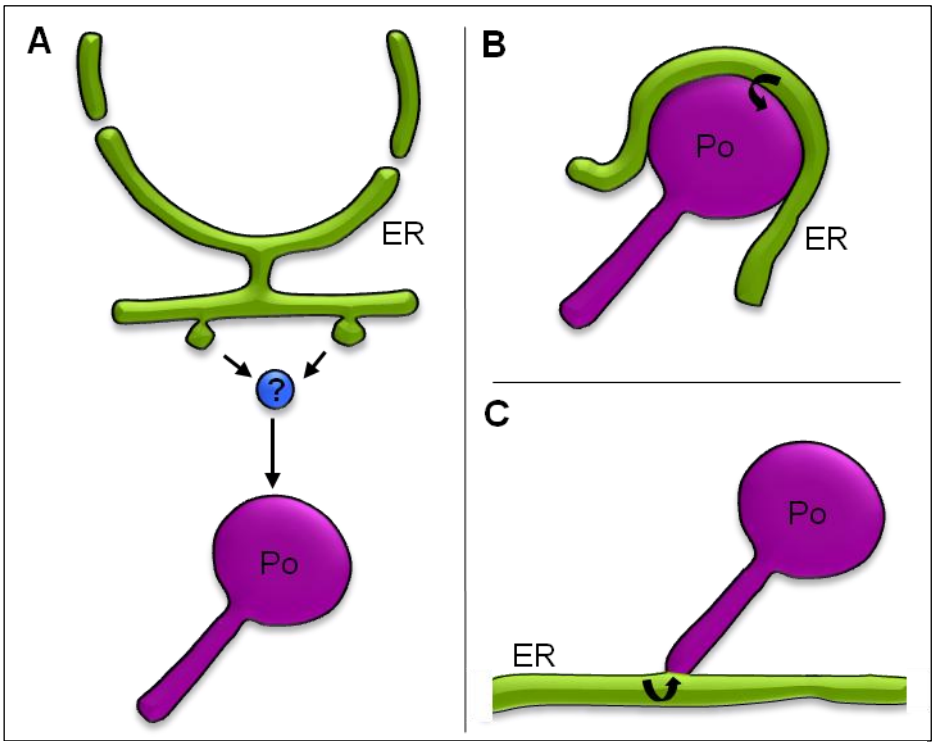

Figure 4.3: Models for lipid transfer from the ER to peroxisomes
(A) Lipids could be transferred to peroxisomes (Po) from the ER via vesicular carriers. **(B)** Lipid transfer could occur via membrane-membrane interactions. **(C)** Direct (transient?) luminal connections could mediate lipid transfer.

Remarkably, the formation of new spherical peroxisomes is inhibited in COS-7 cells containing TPAs (Figure 3.13). We have demonstrated that this is due to a block in the division of pre-existing peroxisomes. However, recent studies in yeast and mammalian cells have shown that peroxisomes can multiply either by division or by *de novo* formation (Hoepfner et al. 2005; Kim et al. 2006; Motley & Hettema 2007; Nagotu et al. 2008b). Whereas in yeast peroxisomes only form *de novo* in the absence of pre-existing peroxisomes and multiply by division in wild-type cells (Motley et al. 2008; Nagotu et al. 2008b), *de novo* formation and multiplication by division has been proposed to occur simultaneously in mammalian cells (Kim et al. 2006). As the formation of new spherical peroxisomes was not observe here, we might face a situation similar to yeast, where only the complete loss of peroxisomes triggers *de novo* formation. Alternatively, Pex11pβ might be required for *de novo* formation as well suggesting an overlap in the components involved. Recent data by Kim et al. (2006) suggested that *de novo* formation is the major pathway for peroxisome multiplication. The study was based on the assumption that all daughter organelles formed by division of pre-existing peroxisomes contain components of their mother peroxisome. However, in the present work it is demonstrated that (Pex11pβ-mediated) peroxisome growth and division is a maturation pathway which includes the import of new proteins into the forming organelles (Figure 3.22). The existence of condition-specific symmetric divisions of peroxisomes can not be excluded. Very recently, Huybrechts et al. (2009) have shown that peroxisome fission is a non-symmetric event, which was similarly observed in early studies of peroxisome proliferation in the regenerating rat liver (Yamamoto & Fahimi 1987). In *H. polymorpha* non-symmetric peroxisome division appears to be the general mechanism (Nagotu et al. 2008b).

4.3.3 Pex11pβ – a "morphogenic" peroxin?

Different models on how Pex11p might affect peroxisome number have been proposed (Lingard & Trelease 2006; Orth et al. 2007; Thoms & Erdmann 2005), but in many cases it is still unclear how this effect is exerted. The data presented herein strongly suggest that Pex11 proteins – at least Pex11pβ – are "morphogenic" proteins. It is responsible for the generation of a tubular peroxisomal subcompartment which is a pre-requisite for subsequent peroxisome division and multiplication. New evidence is provided that Pex11pβ initiates the formation of a membrane extension at one side of a pre-existing

peroxisome, promotes/induces membrane elongation, and, more importantly, also partitions into peroxisome membrane tubules. Noteworthy, within the "beads on a string"-like structures, Pex11pβ also concentrates at the constriction sites between the "beads" prior to membrane fission. Thus, it might mediate a narrowing of the tubular membranes (see section 4.2) to support exclusion of PMPs and matrix proteins from these regions and to prepare the ground for the assembly of the division machinery. Analogous, in a *H. polymorpha dnm1* deletion strain concentration of *Hp*Pex11p at the basis of tubular peroxisomal extensions has been observed and the formation of tubular extension required *Hp*Pex11p (Nagotu et al. 2008b). Interestingly, the Pex11pβ-YFP induced membranous tubules had a diameter of 35 to 60 nm, resembling the diameter of peroxisomal constriction sites observed before (20-60 nm) (Koch et al. 2004; Lay et al. 2006; Luers et al. 1993; Yamamoto & Fahimi 1987). These tubular extensions appear to be narrower than peroxisomal tubules observed under normal conditions, without overexpression of Pex11pβ (70-150 nm in HepG2 cells respectively 150-300 nm in tissues) (Grabenbauer et al. 2000; Yamamoto & Fahimi 1987). This implies that Pex11pβ might indeed be involved in determining the curvature of the peroxisomal membrane. Interestingly, Pex11pβ (or Pex11 proteins) shares some properties with the reticulon and DP1/Yop1p protein family, which shapes the tubular ER (Hu et al. 2008; Shibata et al. 2008; Voeltz et al. 2006). Both types of proteins generate long unbranched tubules and localize or partition preferentially to tubular membranes. They are expressed ubiquitously and are abundant proteins (yeast and trypanosomes) (Erdmann & Blobel 1995; Lorenz et al. 1998). Furthermore, they form homo- and hetero-oligomers. The cytoskeleton (microtubules) is unnecessary to determine and maintain the shape of tubular peroxisomes, as proposed for the ER tubules. Tubular peroxisomes and TPAs can even be formed in the absence of microtubules (Figure 3.33), and peroxisome elongation is even promoted by microtubule depolymerisation (section 3.4). Reticulons are supposed to induce membrane curvature as oligomers by insertion of hydrophobic domains only into the outer membrane leaflet. The reticulon homology domains (RHD) are composed out of two unusual long (30-35 amino acids) hydrophobic regions flanking a hydrophilic loop (Yang & Strittmatter 2007), which are supposed to form hairpin-like, wedge-shaped structures inducing and stabilizing highly curved membranes. Interestingly, reticulons have been shown to interact with a number of proteins, among them SNARE and Bcl proteins both belonging to the class of TA proteins (Yang & Strittmatter 2007). However, there are no sequence homologies between Pex11 and reticulon proteins and

there is no direct evidence for hairpin-like structures in Pex11 proteins, although the mammalian Pex11p isoforms possess two hydrophobic domains. The sensitivity to Triton X-100 (sections 3.2.2 and 4.2.2) might point to an unusual membrane topology of Pex11pβ (and Pex11pα), indicating that it is not deeply embedded into the lipid bilayer. Thus, Pex11pβ might possess a similar membrane topology as reticulons and by "wedging" itself into the outer membrane leaflet creating high peroxisomal membrane curvature. This hypothesis needs to be addressed by more sophisticated *in vitro* experiments, which were until now hampered by toxicity and low solubility of (recombinant) Pex11pβ.

Pex11pβ appears to be a peroxisomal scaffold or structural protein that forms and stabilizes highly curved peroxisomal membrane tubules. These properties are likely to depend on the abundance of Pex11pβ and its degree of oligomerization. For proper organelle constriction and fission, the interaction with other compounds (e.g. hFis1) is required. Reversible post-translational modifications, such as phosphorylation (Knoblach & Rachubinski 2010), might regulate the activity of Pex11pβ, for example by favouring an oligomeric form. The other Pex11p isoforms might as well be involved, and a concerted action of all three proteins could be required. However, hetero-oligomerization has so far only been described for plant and some yeast Pex11 proteins. The ability to mediate the formation of TPAs appears to be restricted to Pex11pβ, as only co-expression of YFP-Pex11pβ with Myc-Pex11pβ, and not with Myc-Pex11pα or Myc-Pex11pγ, resulted in TPA formation (Figure 3.27). It appears that the formation of long tubular extensions (and their subsequent alignment) can only be induced by high Pex11pβ levels (combined with a bulky tag) and not by combination of Pex11pβ with one of the other Pex11p isoforms. These data do not support hetero-oligomerization of the Pex11p isoforms. Future experiments, utilizing for example the split-GFP technology, should give further insight into the implication of the other Pex11 isoforms.

4.4 Is there Pex11p-independent elongation and proliferation of peroxisomes?

The occurrence of polymorphic peroxisomes, such as e.g. spherical, tubular and reticular peroxisomes, is a main characteristic of these organelles. Those morphologies can be induced by numerous metabolic or other proliferation-inducing stimuli, as well as by manipulation of components of the growth and division machinery (Schrader & Fahimi 2006b). It is likely that a change of the peroxisomal morphology – besides the described intermediate states in peroxisome proliferation – provides the cell with a certain (metabolic) advantage, for example by increasing the membrane surface. In line with this, formation of membranous extensions, so-called peroxules, has been shown to be a local response to oxidative stress in plants (Sinclair et al. 2009). Long-term or strong oxidative stress, on the other hand, led to formation of tubular peroxisomes and subsequent division. This has likewise been described for mammalian cells (Schrader et al. 1999). Furthermore, overexpression of *Pc*Pex11p in *P. chrysogenum* induced peroxisome elongation and increased penicillin production, although the levels of the biosynthetic enzymes were not affected (Kiel et al. 2005). This may be explained by increased fluxes across the enlarged membrane. Nevertheless, elongation of peroxisomes is an indicator for proliferation/growth and division of peroxisomes (Figure 1.6). In yeast and plants, some data regarding the (nuclear) regulation of Pex11p-mediated peroxisome proliferation have been obtained (Kaur & Hu 2009). It was shown that light-induced proliferation of peroxisomes depends on *At*Pex11b, and that expression of *At*Pex11b is induced via the action of the far-red light photoreceptor phytochrome A and direct binding of the HY5 homolog transcription factor to the *AtPEX11b* promoter (Desai & Hu 2008). In *S. cerevisiae,* the nuclear receptors Oaf1p/Pip2p induce in presence of oleic acids (at least) the PPPs Pex11p and Pex25p by binding to the ORE in their promoters (Gurvitz & Rottensteiner 2006; Rottensteiner et al. 2003a; Rottensteiner et al. 1996). Also Adr1p, which binds to the upstream activation sequence 1 (UAS1), appears to play a role (Gurvitz et al. 2001; Rottensteiner et al. 2003c). In mammals, however, the signalling pathways appear to be more complicated, since peroxisome proliferation induced via classical PPAR-dependent proliferators does not involve transcriptional upregulation of the Pex11 proteins (Abe & Fujiki 1998; Abe et al. 1998; Li et al. 2002a; Schrader et al. 1998b; Tanaka et al. 2003).

In this study, it is shown that a combined application of several tubulation-inducing stimuli results in hypertubulation of peroxisomes. Hypertubulation is defined as a strong increase in number and/or length of elongated peroxisomes. This phenomenon has been described before, e.g. by combining inhibition of DLP1 function with Pex11pβ overexpression (Koch et al. 2004). Interestingly, it was shown here that hypertubulation is further pronounced by additional depolymerisation of microtubules. Although it was known that microtubule depolymerisation results in formation of tubular peroxisomes (Schrader et al. 1996), hyperproliferative effects have not been observed before. Remarkably, other organelles (e.g. mitochondria, lysosomes and the Golgi) tend to lose their shape, i.e. they collapse or fragment, upon loss of their supporting cytoskeleton (Cole et al. 1996; Johnson et al. 1980; Swanson et al. 1987; Terasaki et al. 1986). In contrast, the effect on peroxisomes is to increase non-spherical – tubular or reticular – morphologies. The observations made here give some clues about the signalling pathways involved in regulation of peroxisomal growth and division (Figure 4.4). Several lines of evidence point towards a direct cause of peroxisome elongation by loss of the microtubules as such. Pex11 proteins are the only molecular components known to be able to induce peroxisome tubulation in mammals. But expression levels, at least on mRNA basis, are not affected by microtubule depolymerisation. This was tested by determination of the Pex11α, Pex11β, and Pex11γ mRNA levels by SQ-PCR. None of the isoforms was induced upon depolymerisation of microtubules by incubation with nocodazole (Figure 3.34). An increase in protein level of the Pex11p isoforms, e.g. resulting from an increased stability, could not be analyzed due to restrictions in the availability of specific antibodies. However, it is rather unlikely that an upregulation of Pex11 proteins induces the observed hypertubulation, as Pex11pβ levels are already high due to its overexpression by a CMV promoter plasmid.

Another stimulus known to induce the formation of tubular peroxisome is the increase of ROS. Interestingly, it was observed that microtubule depolymerisation leads to a slight increase of ROS production in COS-7 cells (section 3.4.5). This effect may be caused by a release of ROS from mitochondria, which are likely to be affected by microtubule depolymerisation, since their dynamics as well as fusion and fission events are disturbed. However, the simultaneous application of antioxidants reduced ROS levels but had no effect on the formation of tubular peroxisomes. Thus, microtubule depolymerisation as such appears to cause hypertubulation of peroxisomes, independent from ROS production in the cell.

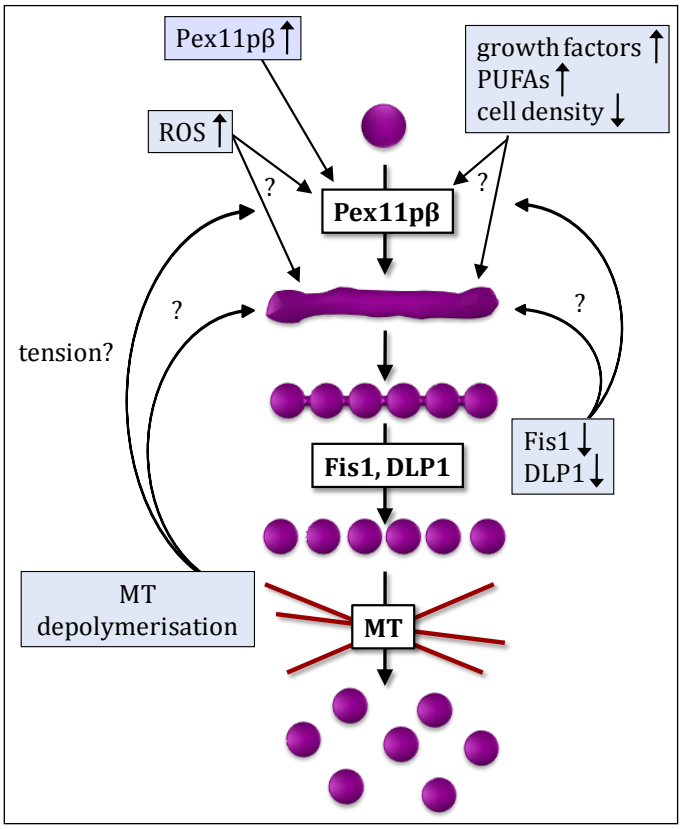

Figure 4.4: Model of the signals inducing peroxisomal tubulation
Peroxisomal tubules can be induced by different factors such as polyunsaturated fatty acids (PUFAs), growth factors, ROS or low cell densities. Also manipulation of the division machinery (Fis1 or DLP1) as well as depolymerisation of the microtubule cytoskeleton (MT) leads to tubulation of peroxisomes. Peroxisomal tubules can be induced via Pex11pβ, but different signalling pathways inducing peroxisomal tubules independent of Pex11pβ/Pex11 proteins may exist (indicated by question marks).

But why does a loss of microtubules lead to peroxisome proliferation? It could be due to mechanistic reasons including tension, or, respectively, the lack of tension. This would mean that peroxisomes require the presence of or the attachment to microtubules to maintain a spherical morphology. Elongated peroxisomes would consequently represent the "relaxed" form, which can exist independently of any forces or support provided by the microtubule cytoskeleton. This hypothesis is challenged by the observation that only a subset of the peroxisomes present in a cell (10 to 15%; Schrader et al. 2003) display microtubule-dependent motility, while the majority shows wriggling movement. The latter ones are, nevertheless, likely to be bound to microtubules as well (Schrader et al. 1996; Schrader et al. 2000). As discussed above (4.2.3), peroxisomal proteins mediating the microtubule association have not been identified yet. Inhibition or depletion of those proteins could provide further information regarding the induction of peroxisome hypertubulation. If a loss of microtubule attachment results in the same phenotype, a mechanistic basis for peroxisome tubulation would be supported. Motor proteins (e.g. dynein) mediating peroxisome motility are not required for microtubule binding and their inhibition does not affect peroxisomal morphology (Schrader et al. 2000). Besides a facilitated formation of tubular peroxisomes after microtubule depolymerisation, also a reduced fission process could be responsible for peroxisome hypertubulation. Since

division of tubular peroxisomes is not inhibited and segmentation of tubular peroxisomes is microtubule-independent, this seems rather unlikely and the fission process might, if affected at all, only be slowed down (Schrader et al. 1996; Schrader et al. 1998b).

Studies from *A. thaliana* suggest that peroxisomes replicate (duplicate) in a cell cycle-associated manner, which requires cooperative action of *At*Pex11c, *At*Pex11d, and *At*-Pex11e to promote peroxisome elongation and recruitment of Fis1b before mitosis (Lingard et al. 2008). It can be speculated that microtubule depolymerisation may mimic a cell cycle-associated remodelling of the microtubules and thus give a signal inducing peroxisome multiplication. A cell cycle-associated Pex11p-mediated proliferation of peroxisomes is supported by the observation that overexpression of cyclin-dependent kinase Phos85p resulted in hyperphosphorylation of *Sc*Pex11p and peroxisome proliferation (Knoblach & Rachubinski 2010). However, a correlation between the duplication of peroxisomes and cell division has not yet been observed in mammalian cells. Other cell growth-inducing conditions or signals might be mimicked/activated by microtubule depolymerisation, which induce peroxisome proliferation.

Peroxisome hypertubulation could be mediated by signals resulting in post-translational modifications of e.g. Pex11pβ. Phosphorylation has been shown to regulate *Sc*Pex11p activity in yeast, but there are so far no data regarding phosphorylation of the mammalian Pex11p isoforms. However, the residues suggested to be phosphorylated in *Sc*Pex11p are not conserved among species (Figure 1.9). Besides influencing protein activity, post-translational modifications could also affect the protein stability, e.g. by increased/diminished targeting to the proteasome or degradation of peroxisomes. Several studies suggest that dimerization influences the activity of Pex11 proteins. Lingard et al. (2008) propose a model where homo/hetero-oligomerization events (of *At*Pex11c, d, and e) within the peroxisome membrane promote peroxisome elongation in plants. In yeast, however, monomeric *Sc*Pex11p was suggested to be the active species promoting peroxisome tubulation and proliferation, while redox-sensitive homo-dimerization appeared to inhibit peroxisome proliferation (Marshall et al. 1996). Kobayashi et al. (2007) favour a model where homo-oligomerization of Pex11pβ is a prerequisite for formation of Pex11pβ-enriched patches on peroxisome membranes and assembly of the fission machinery. Thus, post-translational modifications affecting the degree of oligomerization of the Pex11 proteins are likely to regulate peroxisome tubulation and proliferation.

Altogether, it was shown that the simultaneous application of multiple tubulation stimuli results in hypertubulation of peroxisomes. This indicates that different signals exert additive effects on peroxisome growth and division. These signals do not induce transcriptional upregulation of Pex11pβ, the most prominent peroxisome elongation factor, or of other Pex11p isoforms. Thus, peroxisome hypertubulation involves additional effector proteins or mechanisms (Figure 4.4). Besides unknown proteinaceous components, these may be mechanistic, microtubule-dependent effects or post-translational modifications influencing e.g. Pex11p oligomerization and its (hyper-) activation.

4.5 Future perspectives

Besides the new insights this work provided into many aspects of the peroxisomal growth and division process, a number of new questions has been raised.

There is a close connection of peroxisomes and mitochondria and the dual targeting of one shared component was studied. It was shown that peroxisomal targeting of hFis1 depends on Pex19p, but it is still unclear if the mitochondrial import requires a proteinaceous component as well. Identification or exclusion of such a mitochondrial import factor will furthermore help to understand the regulation of the dual targeting of hFis1 to peroxisomes and mitochondria, and thereby the regulation of peroxisomal division. Moreover, it is likely that also Mff, another TA protein targeted to both organelles and involved in their division, is targeted to peroxisomes in a Pex19p-dependent manner. However, this has to be proven experimentally and might as well lead to a better understanding of the general membrane targeting mechanisms of TA proteins. Another exciting question is, if the division of peroxisomes and mitochondria occurs coordinated, e.g. under special metabolic conditions or linked to the cell cycle.

Many species tested contain several Pex11p isoforms and the mammalian ones, Pex11pα, Pex11pβ, and Pex11pγ, were characterized in a comparative manner in this study. It was shown that they induce different morphological changes and have partial overlapping functions. Future experiments should focus on the regulation of the distinct isoforms, as only Pex11pα can be induced via PPARs. Pex11pγ appears to be a low-abundant protein and its function might therefore be very specific, e.g. restricted to developmental stages of specific organs. As Pex11 proteins of plants (and yeast) have been shown to be able to form hetero-oligomers, this possibility should be (re-)examined for the mammalian isoforms. Utilization of *in vivo* technologies such as split-GFP/BiFC will facilitate those studies, in comparison to the *in vitro* methods applied previously. Furthermore, it should be tested if Pex11pβ (and Pex11pγ) is able to induce tubulation of liposomes, as it has been observed for reticulon proteins (Hu et al. 2008). This knowledge will help to understand the biochemical properties and the mode of function of Pex11 proteins. Furthermore, structural information is required to comprehend their functions on a molecular level. It should be examined if Pex11 proteins are indeed capable of lipid binding, how they are exactly inserted into the peroxisomal membrane, and if Pex11pβ (and Pex11pα) are involved in the constriction of peroxisomal membranes. Otherwise, the search for a peroxisomal (and mitochondrial) constriction factor should

be continued. A good candidate might be Mff. Understanding the constriction mechanisms in the process of peroxisomal growth and division will simultaneously lead to a better understanding of the protein segregation observed. Also the issue of (transient) connections of peroxisomes with the ER or ER-subdomains should be addressed, these putative connections would likewise require protein segregation mechanisms. Furthermore, (post-translational) modifications of Pex11p proteins, such as phosphorylation, should be investigated in detail. It is likely that those modifications play a major role in regulation of the growth and division machinery. As shown by the hypertubulation of peroxisomes, little is known about other effectors besides Pex11pβ, or signalling pathways, which induce peroxisome elongation. In general, the advantages tubular peroxisomes provide to the cell, apart from peroxisome proliferation, should be investigated, to further understand how and why changes in peroxisome morphology may influence the (metabolic) state of the cell and therefore have an impact on health and disease. Despite their strong implication in peroxisome proliferation, nothing is known about the role of Pex11 proteins in diseases. Peroxisomal defects have been connected e.g. to carcinogenesis, neurodegeneration and aging. Understanding the function of the Pex11 proteins and of the growth and division machinery will provide clues in regard to how peroxisomal morphology and dynamics influence peroxisomal functions as well as developmental and physiological processes.

5 SUMMARY

Peroxisomes are multifunctional organelles involved in various metabolic processes. Peroxisomal malfunctions lead to numerous mostly severe disorders, rendering peroxisomes essential for human health and development. Peroxisomal abundance can be adjusted to the cellular needs, since peroxisomes have the capacity to proliferate or to be degraded. Peroxisomes multiply by growth and division, but can also form *de novo* via the endoplasmic reticulum. Peroxisomal growth and division is a multistep process involving peroxisome elongation, constriction and final fission. The molecular components and mechanisms mediating the formation, growth, division and dynamics of peroxisomes are far from being understood. Pex11pβ, DPL1 and hFis1 were previously identified as the first molecular components involved in proliferation and division of peroxisomes in mammals. Pex11pβ mediates peroxisome elongation, while hFis1 serves as membrane adaptor for DLP1 responsible for division of the organelles. Surprisingly, DLP1 and hFis1 are involved in both mitochondrial and peroxisomal division. Aim of this study was to further reveal the molecular mechanisms of peroxisomal proliferation and division.

First, the dual targeting of hFis1, a tail-anchored protein, was studied. It was demonstrated for the first time that peroxisomal but not mitochondrial targeting of hFis1 depends on Pex19p, a peroxisomal import factor. An essential binding region for Pex19p was located within the last 26 C-terminal amino acids of hFis1. The basic amino acids in the very C-terminus are not essential for Pex19p binding and peroxisomal targeting but are instead required for mitochondrial targeting. Since overexpression of Pex19p alone was not sufficient to shift the targeting of hFis1 to peroxisomes, further regulative mechanisms are likely to be involved. The findings indicate that targeting of hFis1 to peroxisomes and mitochondria are independent events and support a direct, Pex19p-dependent targeting of peroxisomal tail-anchored proteins.

Furthermore, Pex11pβ and its isoforms Pex11pα and Pex11pγ have been studied. Pex11 proteins are the only proteins known to induce peroxisome elongation and proliferation in mammals, and it is assumed that they are key components in the regulation of peroxisome abundance. In this study, a comparative characterization of the Pex11p isoforms was performed for the first time. Differently tagged and truncated versions were generated and alterations of peroxisome formation and division were monitored. Interestingly, it was shown that the Pex11 proteins have (only) partially overlapping functions.

Pex11pβ expression is known to induce formation of tubular peroxisomes, followed by segmentation of the tubules before they are divided by the division machinery. It was demonstrated here that Pex11pγ promotes tubulation of peroxisomes similar to Pex11pβ, but does not induce subsequent segmentation of the peroxisomal tubules. Pex11pα, on the other hand, induces only a segregation of peroxisomal proteins. Thus, Pex11pα and Pex11pγ appear to fulfil different functions, which are combined in Pex11pβ. Furthermore, the Pex11 proteins show different sensitivities to the detergent Triton-X 100, which is likely to be related with different lipid binding properties, which might in turn explain their capacities to deform membranes.

Several signals inducing peroxisome elongation (e.g. microtubule depolymerisation) were examined, and it was demonstrated that multiple simultaneous stimuli result in hypertubulation of peroxisomes. The hypertubulation was not mediated by transcriptional upregulation of the Pex11 proteins. This additive effect indicates that complex regulation and activation mechanisms of the Pex11 proteins exist (e.g. post-translational modifications), and/or that other effectors than Pex11pβ are able to mediate elongation of peroxisomal membranes.

Moreover, it was discovered that a Pex11pβ-YFP fusion protein can be used as a specific tool to further dissect the growth and division process at early time points. Pex11pβ-YFP inhibits peroxisomal segmentation and division, but instead results in formation of pre-peroxisomal membrane structures composed out of globular domains and tubular extensions. These structures were characterized in detail. Interestingly, peroxisomal matrix and membrane proteins were targeted to distinct regions of the peroxisomal structures. Performing time-course and import assays, it was shown that Pex11pβ-mediated membrane formation was initiated at the pre-existing peroxisome. This indicates that growth and division of peroxisomes follows a multistep maturation pathway and that formation of mammalian peroxisomes is more complex than simple division of a pre-existing organelle.

In this study, the early steps of the peroxisomal growth and division process have been characterized in detail for the first time. The findings give new insights into the general processes of peroxisome formation by growth and division, and indicate the involvement of new, not yet characterized processes (e.g. in protein sorting) at the peroxisomal membrane.

6 ZUSAMMENFASSUNG

Peroxisomen sind multifunktionale Zellorganellen, die in eine Vielzahl von metabolischen Prozessen involviert sind. Peroxisomale Dysfunktionen führen zu verschiedensten zum Teil schwerwiegenden Erkrankungen. Peroxisomen sind für die Entwicklung und Gesundheit des Menschen essentiell. Die Anzahl der Peroxisomen kann den jeweiligen Anforderungen durch Proliferation oder Degradation der Organellen angepasst werden. Peroxisomen vermehren sich durch Wachstum und Teilung, sie können aber auch de novo aus dem Endoplasmatischen Retikulum gebildet werden. Der Wachstums- und Teilungsprozess besteht aus mehreren Schritten: Elongation, Segmentierung und anschließende Durchschnürung der peroxisomalen Tubuli. Die genauen Mechanismen und molekularen Komponenten der Wachstums- und Teilungsmaschinerie sind noch weitestgehend unbekannt. Die ersten identifizierten Säugerproteine sind Pex11pβ, hFis1 und DLP1. Pex11pβ vermittelt die peroxisomale Elongation, während hFis1 der Membranandapter für DLP1 ist, welches wiederum die Organellen teilt. Interessanterweise sind hFis1 und DLP1 gleichermaßen an der Teilung der Mitochondrien beteiligt. Ziel dieser Arbeit war es nun die molekularen Mechanismen der peroxisomalen Proliferation und Teilung weiter aufzuklären.

Zunächst wurde das duale Targeting von hFis1, einem C-terminal verankerten Protein, untersucht. Es konnte gezeigt werden, dass Pex19p, ein peroxisomaler Importfaktor, an hFis1 bindet und das peroxisomale Targeting von hFis1 vermittelt. Pex19p wird hingegen nicht für den mitochondrialen Import benötigt. Die Binderegion von Pex19p konnte auf die C-terminalen 26 Aminosäuren eingegrenzt werden. Des Weiteren wurde gezeigt, dass basische Aminosäuren im C-Terminus von hFis1 zwar für den mitochondrialen Import von Nöten sind, der peroxisomale Import und die Bindung von Pex19p erforderte diese Aminosäuren hingegen nicht. Weitere Regulationsmechanismen scheinen zu existieren, da das peroxisomale Targeting von hFis1 nicht mittels Überexpression von Pex19p gesteigert werden konnte. Die erzielten Ergebnisse lassen den Schluss zu, dass das Targeting von hFis1 zu Peroxisomen und Mitochondrien zwei unabhängige Prozesse sind. Zudem scheinen C-terminal verankerte Proteine direkt und Pex19p-abhängig in die peroxisomale Membran inseriert zu werden.

Des Weiteren wurde Pex11pβ sowie dessen beide Isoformen Pex11pα und Pex11pγ untersucht. Pex11-Proteine sind die einzig bekannten Proteine, die im Säuger die Elongation und Proliferation von Peroxisomen induzieren; sie erfüllen daher (vermutlich) eine

Schlüsselfunktion in der Regulation der Peroxisomenanzahl. Hier wurde zum ersten Mal eine vergleichende Charakterisierung der Pex11p-Isoformen durchgeführt. Unterschiedlich getaggte und trunkierte Konstrukte wurden generiert und deren Auswirkungen auf die Bildung und Teilung der Peroxisomen untersucht. Bemerkenswert ist, dass die drei Pex11-Proteine (nur) teilweise überlappende Funktionen haben. Durch Pex11pβ induzierte peroxisomale Tubuli segmentieren (bevor sie geteilt werden). Pex11pγ bewirkt ebenfalls die Ausbildung von Tubuli, diese werden allerdings nicht segmentiert. Die Expression von Pex11pα führt hingegen ausschließlich zu einer Segregation der peroxisomalen Proteine. Die beiden unterschiedlichen Funktionen von Pex11pα und Pex11pγ scheinen daher in Pex11pβ vereint zu sein. Zusätzlich zeigen die Pex11-Proteine unterschiedlich starke Sensitivität für das Detergens Triton-X 100, was mit unterschiedlichen Lipidbindeeigenschaften zusammenhängen könnte, die wiederum die membrandeformierenden Fähigkeiten erklären würden.

Es wurden zudem unterschiedliche Signale, die zu Elongation von Peroxisomen führen (wie z.B. Mikrotubulidepolymerisation), untersucht und es konnte gezeigt werden, dass multiple Stimuli zu einer Hypertubulation der Peroxisomen führen. Diese wird allerdings nicht durch transkriptionelle Hochregulation der Pex11-Proteine vermittelt. Dies weist darauf hin, dass weitere Proteine eine Elongation von Peroxisomen induzieren können und/oder dass andere regulatorische Prozesse wie z.B. posttranslationale Modifikationen an der Tubulation der Peroxisomen beteiligt sind.

Ferner wurde entdeckt, dass das Fusionsprotein Pex11pβ-YFP als spezifisches Werkzeug für die Entschlüsselung früher Ereignisse im Wachstums- und Teilungsprozess der Peroxisomen genutzt werden kann. Pex11pβ-YFP inhibiert die Segmentierung und Teilung der Peroxisomen. Es führt zur Bildung von pre-peroxisomalen Strukturen, die aus globulären Domänen und tubulären Membranfortsätzen aufgebaut sind. Diese Strukturen wurden detailliert charakterisiert. Interessanterweise sind die peroxisomalen Matrix- und Membranproteine in definierten Regionen lokalisiert. Es konnte mit Hilfe von *time-course* und Importstudien gezeigt werden, dass die von Pex11pβ induzierten Membranfortsätze von schon vorhandenen Peroxisomen ausgehen. Dies zeigt, dass der Wachstums- und Teilungsprozess der Peroxisomen ein mehrschrittiger Reifungsvorgang ist. Die Bildung von Peroxisomen im Säuger ist somit komplexer als die simple Durchschnürung einer existenten Organelle.

In dieser Arbeit wurden insbesondere die frühen Schritte des peroxisomalen Wachstums- und Teilungsprozesses erstmals detailliert charakterisiert. Die erzielten Befunde

werfen ein neues Licht auf den generellen Prozess der Bildung von Peroxisomen durch Wachstum und Teilung und weisen auf neue, noch nicht charakterisierte Vorgänge (z.B. bei der Proteinsortierung) an der peroxisomalen Membran hin.

7 REFERENCES

Abe I & Fujiki Y. (1998)
cDNA cloning and characterization of a constitutively expressed isoform of the human peroxin Pex11p. *Biochem Biophys Res Commun* 252(2): 529-533.

Abe I, Okumoto K, Tamura S & Fujiki Y. (1998)
Clofibrate-inducible, 28-kDa peroxisomal integral membrane protein is encoded by PEX11. *FEBS Lett* 431(3): 468-472.

Abell BM, Rabu C, Leznicki P, Young JC & High S. (2007)
Post-translational integration of tail-anchored proteins is facilitated by defined molecular chaperones. *J.Cell Sci.* 120(Pt 10): 1743-1751.

Alberts B, Johnson A, Lewis J, Raff M, Roberts K & Walter P. (2002)
Molecular biology of the cell. New York, Garland Science.

Andrade-Navarro MA, Sanchez-Pulido L & McBride HM. (2009)
Mitochondrial vesicles: an ancient process providing new links to peroxisomes. *Curr Opin Cell Biol* 21(4): 560-567.

Angermuller S & Fahimi HD. (1981)
Selective cytochemical localization of peroxidase, cytochrome oxidase and catalase in rat liver with 3,3'-diaminobenzidine. *Histochemistry* 71(1): 33-44.

Angermuller S, Bruder G, Volkl A, Wesch H & Fahimi HD. (1987)
Localization of xanthine oxidase in crystalline cores of peroxisomes. A cytochemical and biochemical study. *Eur J Cell Biol* 45(1): 137-144.

Antonenkov VD. (1989)
Dehydrogenases of the pentose phosphate pathway in rat liver peroxisomes. *Eur J Biochem* 183(1): 75-82.

Arimura S, Fujimoto M, Doniwa Y, Kadoya N, Nakazono M, Sakamoto W & Tsutsumi N. (2008)
Arabidopsis ELONGATED MITOCHONDRIA1 is required for localization of DYNAMIN-RELATED PROTEIN3A to mitochondrial fission sites. *Plant Cell* 20(6): 1555-1566.

Azevedo JE & Schliebs W. (2006)
Pex14p, more than just a docking protein. *Biochim Biophys Acta* 1763(12): 1574-1584.

Baes M & Aubourg P. (2009)
Peroxisomes, myelination, and axonal integrity in the CNS. *Neuroscientist* 15(4): 367-379.

Baird GS, Zacharias DA & Tsien RY. (2000)
Biochemistry, mutagenesis, and oligomerization of DsRed, a red fluorescent protein from coral. *Proc Natl Acad Sci U S A* 97(22): 11984-11989.

Barnett P, Tabak HF & Hettema EH. (2000)
Nuclear receptors arose from pre-existing protein modules during evolution. *Trends Biochem Sci* 25(5): 227-228.

Bassnett S & Mataic D. (1997)
Chromatin degradation in differentiating fiber cells of the eye lens. *J Cell Biol* 137(1): 37-49.

Baumgart E, Schad A, Volkl A & Fahimi HD. (1997)
Detection of mRNAs encoding peroxisomal proteins by non-radioactive in situ hybridization with digoxigenin-labelled cRNAs. *Histochem Cell Biol* 108(4-5): 371-379.

Becker S, Klenk HD & Muhlberger E. (1996)
Intracellular transport and processing of the Marburg virus surface protein in vertebrate and insect cells. *Virology* 225(1): 145-155.

Beilharz T, Egan B, Silver PA, Hofmann K & Lithgow T. (2003)
Bipartite signals mediate subcellular targeting of tail-anchored membrane proteins in Saccharomyces cerevisiae. *J.Biol.Chem.* 278(10): 8219-8223.

Bellu AR, Komori M, van der Klei IJ, Kiel JA & Veenhuis M. (2001)
Peroxisome biogenesis and selective degradation converge at Pex14p. *J Biol Chem* 276(48): 44570-44574.

Bellu AR, Salomons FA, Kiel JA, Veenhuis M & Van Der Klei IJ. (2002)
Removal of Pex3p is an important initial stage in selective peroxisome degradation in Hansenula polymorpha. *J Biol Chem* 277(45): 42875-42880.

Bentley P, Calder I, Elcombe C, Grasso P, Stringer D & Wiegand HJ. (1993)
Hepatic peroxisome proliferation in rodents and its significance for humans. *Food Chem Toxicol.* 31(11): 857-907.

Berger J & Gartner J. (2006)
X-linked adrenoleukodystrophy: clinical, biochemical and pathogenetic aspects. *Biochim Biophys Acta* 1763(12): 1721-1732.

Bernhard W & Rouiller C. (1956)
Microbodies and the problem of mitochondrial regeneration in liver cells. *J Biophys Biochem Cytol.* 2(4, Suppl): 355-360.

Bleazard W, McCaffery JM, King EJ, Bale S, Mozdy A, Tieu Q, Nunnari J & Shaw JM. (1999)
The dynamin-related GTPase Dnm1 regulates mitochondrial fission in yeast. *Nat Cell Biol* 1(5): 298-304.

Boll A & Schrader M. (2005)
Elongation of peroxisomes as an indicator for efficient dynamin-like protein 1 knock down in mammalian cells. *J Histochem Cytochem* 53(8): 1037-1040.

Bonekamp NA, Volkl A, Fahimi HD & Schrader M. (2009)
Reactive oxygen species and peroxisomes: struggling for balance. *Biofactors* 35(4): 346-355.

Borgese N, Colombo S & Pedrazzini E. (2003)
The tale of tail-anchored proteins: coming from the cytosol and looking for a membrane. *J.Cell Biol.* 161(6): 1013-1019.

Borgese N, Brambillasca S & Colombo S. (2007)
How tails guide tail-anchored proteins to their destinations. *Curr Opin Cell Biol* 19(4): 368-375.

Boukh-Viner T, Guo T, Alexandrian A, et al. (2005)
Dynamic ergosterol- and ceramide-rich domains in the peroxisomal membrane serve as an organizing platform for peroxisome fusion. *J Cell Biol* 168(5): 761-773.

Brambillasca S, Yabal M, Soffientini P, Stefanovic S, Makarow M, Hegde RS & Borgese N. (2005)
Transmembrane topogenesis of a tail-anchored protein is modulated by membrane lipid composition. *Embo J.* 24(14): 2533-2542.

Brambillasca S, Yabal M, Makarow M & Borgese N. (2006)
Unassisted translocation of large polypeptide domains across phospholipid bilayers. *J Cell Biol* 175(5): 767-777.

Braverman N, Chen L, Lin P, et al. (2002)
Mutation analysis of PEX7 in 60 probands with rhizomelic chondrodysplasia punctata and functional correlations of genotype with phenotype. *Hum Mutat* 20(4): 284-297.

Brites P, Waterham HR & Wanders RJ. (2004)
Functions and biosynthesis of plasmalogens in health and disease. *Biochim Biophys Acta.* 1636(2-3): 219-231.

Brocard C & Hartig A. (2006)
Peroxisome targeting signal 1: is it really a simple tripeptide? *Biochim Biophys Acta* 1763(12): 1565-1573.

Brocard CB, Boucher KK, Jedeszko C, Kim PK & Walton PA. (2005)
Requirement for microtubules and dynein motors in the earliest stages of peroxisome biogenesis. *Traffic.* 6(5): 386-395.

Brosius U & Gartner J. (2002)
Cellular and molecular aspects of Zellweger syndrome and other peroxisome biogenesis disorders. *Cell Mol Life Sci* 59(6): 1058-1069.

Brown TW, Titorenko VI & Rachubinski RA. (2000)
Mutants of the Yarrowia lipolytica PEX23 gene encoding an integral peroxisomal membrane peroxin mislocalize matrix proteins and accumulate vesicles containing peroxisomal matrix and membrane proteins. *Mol Biol Cell.* 11(1): 141-152.

Burnette WN. (1981)
"Western blotting": electrophoretic transfer of proteins from sodium dodecyl sulfate--polyacrylamide gels to unmodified nitrocellulose and radiographic detection with antibody and radioiodinated protein A. *Anal Biochem* 112(2): 195-203.

Camoes F, Bonekamp NA, Delille HK & Schrader M. (2009)
Organelle dynamics and dysfunction: A closer link between peroxisomes and mitochondria. *J Inherit Metab Dis* 32(2): 163-180.

Carvalho AF, Pinto MP, Grou CP, Alencastre IS, Fransen M, Sa-Miranda C & Azevedo JE. (2007)
Ubiquitination of mammalian Pex5p, the peroxisomal import receptor. *J Biol Chem* 282(43): 31267-31272.

Casteels M, Foulon V, Mannaerts GP & Van Veldhoven PP. (2003)
Alpha-oxidation of 3-methyl-substituted fatty acids and its thiamine dependence. *Eur J Biochem* 270(8): 1619-1627.

Chang J, Mast FD, Fagarasanu A, Rachubinski DA, Eitzen GA, Dacks JB & Rachubinski RA. (2009)
Pex3 peroxisome biogenesis proteins function in peroxisome inheritance as class V myosin receptors. *J Cell Biol* 187(2): 233-246.

Chuong SD, Park NI, Freeman MC, Mullen RT & Muench DG. (2005)
The peroxisomal multifunctional protein interacts with cortical microtubules in plant cells. *BMC Cell Biol.* 6: 40.

Cimini A, Moreno S, D'Amelio M, et al. (2009)
Early Biochemical and Morphological Modifications in the Brain of a Transgenic Mouse Model of Alzheimer's Disease: A Role for Peroxisomes. *J Alzheimers Dis* In Press.

Cole NB, Sciaky N, Marotta A, Song J & Lippincott-Schwartz J. (1996)
Golgi dispersal during microtubule disruption: regeneration of Golgi stacks at peripheral endoplasmic reticulum exit sites. *Mol Biol Cell* 7(4): 631-650.

Colombo SF, Longhi R & Borgese N. (2009)
The role of cytosolic proteins in the insertion of tail-anchored proteins into phospholipid bilayers. *J Cell Sci* 122(Pt 14): 2383-2392.

Cooper TG & Beevers H. (1969)
Beta oxidation in glyoxysomes from castor bean endosperm. *J Biol Chem* 244(13): 3514-3520.

Dammai V & Subramani S. (2001)
The human peroxisomal targeting signal receptor, Pex5p, is translocated into the peroxisomal matrix and recycled to the cytosol. *Cell* 105(2): 187-196.

Danpure CJ. (2006)
Primary hyperoxaluria type 1: AGT mistargeting highlights the fundamental differences between the peroxisomal and mitochondrial protein import pathways. *Biochim Biophys Acta* 1763(12): 1776-1784.

De Duve C & Baudhuin P. (1966)
Peroxisomes (microbodies and related particles). *Physiol Rev* 46(2): 323-357.

Delille HK. (2006)
Untersuchungen zum dualen Transport von hFis1 zu Peroxisomen und Mitochondrien. *Institut für klinische Zytobiologie und Zytopathologie, Philipps-Universität Marburg*. Diplomarbeit.

Delille HK, Bonekamp NA & Schrader M. (2006)
Peroxisomes and disease - an overview. *Int J Biomed Sci* 2(4): 308-314.

Delille HK & Schrader M. (2008)
Targeting of hFis1 to peroxisomes is mediated by Pex19p. *J Biol Chem* 283(45): 31107-31115.

Delille HK, Alves R & Schrader M. (2009)
Biogenesis of peroxisomes and mitochondria: linked by division. *Histochem Cell Biol* 131(4): 441-446.

Depreter M, Espeel M & Roels F. (2003)
Human peroxisomal disorders. *Microsc Res Tech* 61(2): 203-223.

Desai M & Hu J. (2008)
Light induces peroxisome proliferation in Arabidopsis seedlings through the photoreceptor phytochrome A, the transcription factor HY5 HOMOLOG, and the peroxisomal protein PEROXIN11b. *Plant Physiol* 146(3): 1117-1127.

Dhaunsi GS, Gulati S, Singh AK, Orak JK, Asayama K & Singh I. (1992)
Demonstration of Cu-Zn superoxide dismutase in rat liver peroxisomes. Biochemical and immunochemical evidence. *J Biol Chem* 267(10): 6870-6873.

Distel B, Erdmann R, Gould SJ, et al. (1996)
A unified nomenclature for peroxisome biogenesis factors. *J Cell Biol* 135(1): 1-3.

Dodt G, Warren D, Becker E, Rehling P & Gould SJ. (2001)
Domain mapping of human PEX5 reveals functional and structural similarities to Saccharomyces cerevisiae Pex18p and Pex21p. *J Biol Chem* 276(45): 41769-41781.

Dohm JA, Lee SJ, Hardwick JM, Hill RB & Gittis AG. (2004)
Cytosolic domain of the human mitochondrial fission protein fis1 adopts a TPR fold. *Proteins* 54(1): 153-156.

Dunn WA, Jr., Cregg JM, Kiel JA, van der Klei IJ, Oku M, Sakai Y, Sibirny AA, Stasyk OV & Veenhuis M. (2005)
Pexophagy: the selective autophagy of peroxisomes. *Autophagy* 1(2): 75-83.

Eitzen GA, Szilard RK & Rachubinski RA. (1997)
Enlarged peroxisomes are present in oleic acid-grown Yarrowia lipolytica overexpressing the PEX16 gene encoding an intraperoxisomal peripheral membrane peroxin. *J Cell Biol.* 137(6): 1265-1278.

Elbashir SM, Harborth J, Lendeckel W, Yalcin A, Weber K & Tuschl T. (2001)
Duplexes of 21-nucleotide RNAs mediate RNA interference in cultured mammalian cells. *Nature* 411(6836): 494-498.

Elgersma Y, Kwast L, van den Berg M, Snyder WB, Distel B, Subramani S & Tabak HF. (1997)
Overexpression of Pex15p, a phosphorylated peroxisomal integral membrane protein required for peroxisome assembly in S.cerevisiae, causes proliferation of the endoplasmic reticulum membrane. *Embo J* 16(24): 7326-7341.

Erdmann R & Blobel G. (1995)
Giant peroxisomes in oleic acid-induced Saccharomyces cerevisiae lacking the peroxisomal membrane protein Pmp27p. *J Cell Biol* 128(4): 509-523.

Erdmann R & Schliebs W. (2005)
Opinion: Peroxisomal matrix protein import: the transient pore model. *Nat Rev Mol Cell Biol* 6(9): 738-742.

Fagarasanu A, Fagarasanu M, Eitzen GA, Aitchison JD & Rachubinski RA. (2006)
The Peroxisomal Membrane Protein Inp2p Is the Peroxisome-Specific Receptor for the Myosin V Motor Myo2p of Saccharomyces cerevisiae. *Dev Cell.* 10(5): 587-600.

Fagarasanu A, Fagarasanu M & Rachubinski RA. (2007)
Maintaining peroxisome populations: a story of division and inheritance. *Annu Rev Cell Dev Biol* 23: 321-344.

Fagarasanu M, Fagarasanu A, Tam YY, Aitchison JD & Rachubinski RA. (2005)
Inp1p is a peroxisomal membrane protein required for peroxisome inheritance in Saccharomyces cerevisiae. *J Cell Biol* 169(5): 765-775.

Fahimi HD. (1968)
Cytochemical localization of peroxidase activity in rat hepatic microbodies (peroxisomes). *J Histochem Cytochem* 16(8): 547-550.

Fahimi HD. (1969)
Cytochemical localization of peroxidatic activity of catalase in rat hepatic microbodies (peroxisomes). *J Cell Biol.* 43(2): 275-288.

Fahimi HD, Reinicke A, Sujatta M, Yokota S, Ozel M, Hartig F & Stegmeier K. (1982)
The short- and long-term effects of bezafibrate in the rat. *Ann N Y Acad Sci* 386: 111-135.

Fahimi HD. (2009)
Peroxisomes: 40 years of histochemical staining, personal reminiscences. *Histochem Cell Biol* 131(4): 437-440.

Fang Y, Morrell JC, Jones JM & Gould SJ. (2004)
PEX3 functions as a PEX19 docking factor in the import of class I peroxisomal membrane proteins. *J Cell Biol* 164(6): 863-875.

Farre JC & Subramani S. (2004)
Peroxisome turnover by micropexophagy: an autophagy-related process. *Trends Cell Biol.* 14(9): 515-523.

Faust PL, Banka D, Siriratsivawong R, Ng VG & Wikander TM. (2005)
Peroxisome biogenesis disorders: the role of peroxisomes and metabolic dysfunction in developing brain. *J Inherit Metab Dis* 28(3): 369-383.

Feige JN, Gelman L, Michalik L, Desvergne B & Wahli W. (2006)
From molecular action to physiological outputs: Peroxisome proliferator-activated receptors are nuclear receptors at the crossroads of key cellular functions. *Prog Lipid Res.* 45(2): 120-159.

Ferdinandusse S, Meissner T, Wanders RJ & Mayatepek E. (2002)
Identification of the peroxisomal beta-oxidation enzymes involved in the degradation of leukotrienes. *Biochem Biophys Res Commun* 293(1): 269-273.

Ferdinandusse S, Ylianttila MS, Gloerich J, Koski MK, Oostheim W, Waterham HR, Hiltunen JK, Wanders RJ & Glumoff T. (2006)
Mutational spectrum of D-bifunctional protein deficiency and structure-based genotype-phenotype analysis. *Am J Hum Genet* 78(1): 112-124.

Fourcade S, Lopez-Erauskin J, Galino J, et al. (2008)
Early oxidative damage underlying neurodegeneration in X-adrenoleukodystrophy. *Hum Mol Genet* 17(12): 1762-1773.

Fransen M, Wylin T, Brees C, Mannaerts GP & Van Veldhoven PP. (2001)
Human pex19p binds peroxisomal integral membrane proteins at regions distinct from their sorting sequences. *Mol.Cell Biol.* 21(13): 4413-4424.

Frederick SE & Newcomb EH. (1969)
Cytochemical localization of catalase in leaf microbodies (peroxisomes). *J.Cell Biol.* 43(2): 343-353.

Fujiki Y, Matsuzono Y, Matsuzaki T & Fransen M. (2006)
Import of peroxisomal membrane proteins: The interplay of Pex3p- and Pex19p-mediated interactions. *Biochim Biophys Acta* 1763(12): 1639-1646.

Fujimoto M, Arimura S, Mano S, et al. (2009)
Arabidopsis dynamin-related proteins DRP3A and DRP3B are functionally redundant in mitochondrial fission, but have distinct roles in peroxisomal fission. *Plant J* 58(3): 388-400.

Gandre-Babbe S & van der Bliek AM. (2008)
The Novel Tail-anchored Membrane Protein Mff Controls Mitochondrial and Peroxisomal Fission in Mammalian Cells. *Mol Biol Cell* 19(6): 2402-2412.

Gatto GJJ, Geisbrecht BV, Gould SJ & Berg JM. (2000)
Peroxisomal targeting signal-1 recognition by the TPR domains of human PEX5. *Nat.Struct.Biol.* 7(12): 1091-1095.

Geuze HJ, Murk JL, Stroobants AK, Griffith JM, Kleijmeer MJ, Koster AJ, Verkleij AJ, Distel B & Tabak HF. (2003)
Involvement of the endoplasmic reticulum in peroxisome formation. *Mol Biol Cell* 14(7): 2900-2907.

Ghaedi K, Tamura S, Okumoto K, Matsuzono Y & Fujiki Y. (2000)
The peroxin pex3p initiates membrane assembly in peroxisome biogenesis. *Mol Biol Cell* 11(6): 2085-2102.

Girzalsky W, Saffian D & Erdmann R. (2010)
Peroxisomal protein translocation. *Biochim Biophys Acta* In Press.

Glebov OO & Nichols BJ. (2004)
Lipid raft proteins have a random distribution during localized activation of the T-cell receptor. *Nat Cell Biol* 6(3): 238-243.

Glover JR, Andrews DW & Rachubinski RA. (1994)
Saccharomyces cerevisiae peroxisomal thiolase is imported as a dimer. *Proc Natl Acad Sci U S A* 91(22): 10541-10545.

Gorgas K, Teigler A, Komljenovic D & Just WW. (2006)
The ether lipid-deficient mouse: tracking down plasmalogen functions. *Biochim Biophys Acta* 1763(12): 1511-1526.

Gotte K, Girzalsky W, Linkert M, Baumgart E, Kammerer S, Kunau WH & Erdmann R. (1998)
Pex19p, a farnesylated protein essential for peroxisome biogenesis. *Mol.Cell Biol.* 18(1): 616-628.

Gould SG, Keller GA & Subramani S. (1987)
Identification of a peroxisomal targeting signal at the carboxy terminus of firefly luciferase. *J Cell Biol* 105(6 Pt 2): 2923-2931.

Gould SJ, Keller GA, Hosken N, Wilkinson J & Subramani S. (1989)
A conserved tripeptide sorts proteins to peroxisomes. *J.Cell Biol.* 108(5): 1657-1664.

Grabenbauer M, Satzler K, Baumgart E & Fahimi HD. (2000)
Three-dimensional ultrastructural analysis of peroxisomes in HepG2 cells. Absence of peroxisomal reticulum but evidence of close spatial association with the endoplasmic reticulum. *Cell Biochem Biophys* 32(Spring): 37-49.

Grou CP, Carvalho AF, Pinto MP, Wiese S, Piechura H, Meyer HE, Warscheid B, Sa-Miranda C & Azevedo JE. (2008)
Members of the E2D (UbcH5) family mediate the ubiquitination of the conserved cysteine of Pex5p, the peroxisomal import receptor. *J Biol Chem* 283(21): 14190-14197.

Grou CP, Carvalho AF, Pinto MP, Alencastre IS, Rodrigues TA, Freitas MO, Francisco T, Sa-Miranda C & Azevedo JE. (2009a)
The peroxisomal protein import machinery - a case report of transient ubiquitination with a new flavor. *Cell Mol Life Sci* 66(2): 254-262.

Grou CP, Carvalho AF, Pinto MP, Huybrechts SJ, Sa-Miranda C, Fransen M & Azevedo JE. (2009b)
Properties of the ubiquitin-pex5p thiol ester conjugate. *J Biol Chem* 284(16): 10504-10513.

Gurvitz A, Hiltunen JK, Erdmann R, Hamilton B, Hartig A, Ruis H & Rottensteiner H. (2001)
Saccharomyces cerevisiae Adr1p governs fatty acid beta-oxidation and peroxisome proliferation by regulating POX1 and PEX11. *J Biol Chem.* 276(34): 31825-31830. Epub 32001 Jun 31828.

Gurvitz A & Rottensteiner H. (2006)
The biochemistry of oleate induction: transcriptional upregulation and peroxisome proliferation. *Biochim Biophys Acta* 1763(12): 1392-1402.

Halbach A, Lorenzen S, Landgraf C, Volkmer-Engert R, Erdmann R & Rottensteiner H. (2005)
Function of the PEX19-binding site of human adrenoleukodystrophy protein as targeting motif in man and yeast. PMP targeting is evolutionarily conserved. *J.Biol.Chem.* 280(22): 21176-21182.

Halbach A, Landgraf C, Lorenzen S, Rosenkranz K, Volkmer-Engert R, Erdmann R & Rottensteiner H. (2006)
Targeting of the tail-anchored peroxisomal membrane proteins PEX26 and PEX15 occurs through C-terminal PEX19-binding sites. *J Cell Sci* 119(Pt 12): 2508-2517.

Hara-Kuge S & Fujiki Y. (2008)
The peroxin Pex14p is involved in LC3-dependent degradation of mammalian peroxisomes. *Exp Cell Res* 314(19): 3531-3541.

Hess R, Staubli W & Riess W. (1965)
Nature of the hepatomegalic effect produced by ethyl-chlorophenoxy-isobutyrate in the rat. *Nature.* 208(13): 856-858.

Hettema EH & Motley AM. (2009)
How peroxisomes multiply. *J Cell Sci* 122(Pt 14): 2331-2336.

Heymans HS, Schutgens RB, Tan R, van den Bosch H & Borst P. (1983)
Severe plasmalogen deficiency in tissues of infants without peroxisomes (Zellweger syndrome). *Nature* 306(5938): 69-70.

High S & Abell BM. (2004)
Tail-anchored protein biosynthesis at the endoplasmic reticulum: the same but different. *Biochem.Soc.Trans.* 32(Pt 5): 659-662.

Hinshaw JE. (2000)
Dynamin and its role in membrane fission. *Annu Rev Cell Dev Biol.* 16: 483-519.

Hoepfner D, van den Berg M, Philippsen P, Tabak HF & Hettema EH. (2001)
A role for Vps1p, actin, and the Myo2p motor in peroxisome abundance and inheritance in Saccharomyces cerevisiae. *J Cell Biol* 155(6): 979-990.

Hoepfner D, Schildknegt D, Braakman I, Philippsen P & Tabak HF. (2005)
Contribution of the endoplasmic reticulum to peroxisome formation. *Cell* 122(1): 85-95.

Hogenboom S, Tuyp JJ, Espeel M, Koster J, Wanders RJ & Waterham HR. (2004)
Mevalonate kinase is a cytosolic enzyme in humans. *J Cell Sci* 117(Pt 4): 631-639.

Honsho M, Tamura S, Shimozawa N, Suzuki Y, Kondo N & Fujiki Y. (1998)
Mutation in PEX16 is causal in the peroxisome-deficient Zellweger syndrome of complementation group D. *Am J Hum Genet.* 63(6): 1622-1630.

Honsho M, Hiroshige T & Fujiki Y. (2002)
The membrane biogenesis peroxin Pex16p. Topogenesis and functional roles in peroxisomal membrane assembly. *J.Biol.Chem.* 277(46): 44513-44524.

Hruban Z & Swift H. (1964)
Uricase: Localization in Hepatic Microbodies. *Science* 146: 1316-1318.

Hu J, Shibata Y, Voss C, Shemesh T, Li Z, Coughlin M, Kozlov MM, Rapoport TA & Prinz WA. (2008)
Membrane proteins of the endoplasmic reticulum induce high-curvature tubules. *Science* 319(5867): 1247-1250.

Huber CM, Saffrich R, Ansorge W & Just WW. (1999)
Receptor-mediated regulation of peroxisomal motility in CHO and endothelial cells. *Embo J* 18(20): 5476-5485.

Hulshagen L, Krysko O, Bottelbergs A, et al. (2008)
Absence of functional peroxisomes from mouse CNS causes dysmyelination and axon degeneration. *J Neurosci* 28(15): 4015-4027.

Huybrechts SJ, Van Veldhoven PP, Brees C, Mannaerts GP, Los GV & Fransen M. (2009)
Peroxisome dynamics in cultured mammalian cells. *Traffic* 10(11): 1722-1733.

Hwang YT, Pelitire SM, Henderson MP, Andrews DW, Dyer JM & Mullen RT. (2004)
Novel targeting signals mediate the sorting of different isoforms of the tail-anchored membrane protein cytochrome b5 to either endoplasmic reticulum or mitochondria. *Plant Cell* 16(11): 3002-3019.

Immenschuh S & Baumgart-Vogt E. (2005)
Peroxiredoxins, oxidative stress, and cell proliferation. *Antioxid Redox Signal* 7(5-6): 768-777.

Islinger M, Luers GH, Li KW, Loos M & Volkl A. (2007)
Rat liver peroxisomes after fibrate treatment. A survey using quantitative mass spectrometry. *J Biol Chem* 282(32): 23055-23069.

Islinger M, Li KW, Seitz J, Volkl A & Luers GH. (2009)
Hitchhiking of Cu/Zn superoxide dismutase to peroxisomes--evidence for a natural piggyback import mechanism in mammals. *Traffic* 10(11): 1711-1721.

Issemann I & Green S. (1990)
Activation of a member of the steroid hormone receptor superfamily by peroxisome proliferators. *Nature.* 347(6294): 645-650.

Issemann I, Prince RA, Tugwood JD & Green S. (1993)
The peroxisome proliferator-activated receptor:retinoid X receptor heterodimer is activated by fatty acids and fibrate hypolipidaemic drugs. *J Mol Endocrinol* 11(1): 37-47.

Ito S & Karnovsky MJ. (1968)
Formaldehyde-glutaraldehyde fixatives containing trinitro compunds. *J Cell Biol* 39: 168-169 (abstract).

Iwata J, Ezaki J, Komatsu M, Yokota S, Ueno T, Tanida I, Chiba T, Tanaka K & Kominami E. (2006)
Excess peroxisomes are degraded by autophagic machinery in mammals. *J Biol Chem* 281(7): 4035-4041.

Jansen GA & Wanders RJ. (2006)
Alpha-oxidation. *Biochim Biophys Acta* 1763(12): 1403-1412.

Jedd G & Chua NH. (2000)
A new self-assembled peroxisomal vesicle required for efficient resealing of the plasma membrane. *Nat.Cell Biol.* 2(4): 226-231.

Jedd G & Chua NH. (2002)
Visualization of peroxisomes in living plant cells reveals acto-myosin-dependent cytoplasmic streaming and peroxisome budding. *Plant Cell Physiol.* 43(4): 384-392.

Johnson LV, Walsh ML & Chen LB. (1980)
Localization of mitochondria in living cells with rhodamine 123. *Proc Natl Acad Sci U S A* 77(2): 990-994.

Jones JM, Morrell JC & Gould SJ. (2004)
PEX19 is a predominantly cytosolic chaperone and import receptor for class 1 peroxisomal membrane proteins. *J Cell Biol* 164(1): 57-67.

Jourdain I, Sontam D, Johnson C, Dillies C & Hyams JS. (2008)
Dynamin-dependent biogenesis, cell cycle regulation and mitochondrial association of peroxisomes in fission yeast. *Traffic* 9(3): 353-365.

Karnik SK & Trelease RN. (2007)
Arabidopsis peroxin 16 trafficks through the ER and an intermediate compartment to pre-existing peroxisomes via overlapping molecular targeting signals. *J Exp Bot* 58(7): 1677-1693.

Kassmann CM, Lappe-Siefke C, Baes M, et al. (2007)
Axonal loss and neuroinflammation caused by peroxisome-deficient oligodendrocytes. *Nat Genet* 39(8): 969-976.

Kaur N & Hu J. (2009)
Dynamics of peroxisome abundance: a tale of division and proliferation. *Curr Opin Plant Biol* 12(6): 781-788.

Kemper C, Habib SJ, Engl G, Heckmeyer P, Dimmer KS & Rapaport D. (2008)
Integration of tail-anchored proteins into the mitochondrial outer membrane does not require any known import components. *J Cell Sci* 121(Pt 12): 1990-1998.

Kiel JA, van der Klei IJ, van den Berg MA, Bovenberg RA & Veenhuis M. (2005)
Overproduction of a single protein, Pc-Pex11p, results in 2-fold enhanced penicillin production by Penicillium chrysogenum. *Fungal Genet Biol* 42(2): 154-164.

Kiel JA, Veenhuis M & van der Klei IJ. (2006)
PEX genes in fungal genomes: common, rare or redundant. *Traffic.* 7(10): 1291-1303.

Kiernan JA. (2000)
Formaldehyde, formalin, paraformaldehyde and glutaraldehyde: What they are and what they do. *Microscopy Today* 8(1): 8-12.

Kikuchi M, Hatano N, Yokota S, Shimozawa N, Imanaka T & Taniguchi H. (2004)
Proteomic analysis of rat liver peroxisome: presence of peroxisome-specific isozyme of Lon protease. *J Biol Chem* 279(1): 421-428.

Kim PK, Mullen RT, Schumann U & Lippincott-Schwartz J. (2006)
The origin and maintenance of mammalian peroxisomes involves a de novo PEX16-dependent pathway from the ER. *J Cell Biol.* 173(4): 521-532.

Knoblach B & Rachubinski RA. (2010)
Phosphorylation-dependent activation of peroxisome proliferator protein PEX11 controls peroxisome abundance. *J Biol Chem* 285(9): 6670-6680.

Kobayashi S, Tanaka A & Fujiki Y. (2007)
Fis1, DLP1, and Pex11p coordinately regulate peroxisome morphogenesis. *Exp Cell Res* 313(8): 1675-1686.

Koch A, Thiemann M, Grabenbauer M, Yoon Y, McNiven MA & Schrader M. (2003)
Dynamin-like protein 1 is involved in peroxisomal fission. *J Biol Chem* 278(10): 8597-8605.

Koch A, Schneider G, Luers GH & Schrader M. (2004)
Peroxisome elongation and constriction but not fission can occur independently of dynamin-like protein 1. *J Cell Sci* 117(Pt 17): 3995-4006.

Koch A, Yoon Y, Bonekamp NA, McNiven MA & Schrader M. (2005)
A role for fis1 in both mitochondrial and peroxisomal fission in Mammalian cells. *Mol Biol Cell* 16(11): 5077-5086.

Kraehenbuhl JP, Racine L & Jamieson JD. (1977)
Immunocytochemical localization of secretory proteins in bovine pancreatic exocrine cells. *J Cell Biol* 72(2): 406-423.

Kragt A, Voorn-Brouwer T, van den Berg M & Distel B. (2005)
Endoplasmic reticulum-directed Pex3p Routes to peroxisomes and restores peroxisome formation in a Saccharomyces cerevisiae pex3Delta strain. *J Biol Chem* 280(40): 34350-34357.

Kredel S, Oswald F, Nienhaus K, Deuschle K, Rocker C, Wolff M, Heilker R, Nienhaus GU & Wiedenmann J. (2009)
mRuby, a bright monomeric red fluorescent protein for labeling of subcellular structures. *PLoS One* 4(2): e4391.

Krikken AM, Veenhuis M & van der Klei IJ. (2009)
Hansenula polymorpha pex11 cells are affected in peroxisome retention. *FEBS J* 276(5): 1429-1439.

Krivit W. (2004)
Allogeneic stem cell transplantation for the treatment of lysosomal and peroxisomal metabolic diseases. *Springer Semin Immunopathol* 26(1-2): 119-132.

Kulic IM, Brown AE, Kim H, Kural C, Blehm B, Selvin PR, Nelson PC & Gelfand VI. (2008)
The role of microtubule movement in bidirectional organelle transport. *Proc Natl Acad Sci U S A* 105(29): 10011-10016.

Kunau WH, Buhne S, de la Garza M, Kionka C, Mateblowski M, Schultz-Borchard U & Thieringer R. (1988)
Comparative enzymology of beta-oxidation. *Biochem Soc Trans* 16(3): 418-420.

Kunau WH. (2005)
Peroxisome biogenesis: end of the debate. *Curr Biol.* 15(18): R774-776.

Kunze M, Pracharoenwattana I, Smith SM & Hartig A. (2006)
A central role for the peroxisomal membrane in glyoxylate cycle function. *Biochim Biophys Acta* 1763(12): 1441-1452.

Kural C, Kim H, Syed S, Goshima G, Gelfand VI & Selvin PR. (2005)
Kinesin and dynein move a peroxisome in vivo: a tug-of-war or coordinated movement? *Science* 308(5727): 1469-1472.

Kuravi K, Nagotu S, Krikken AM, Sjollema K, Deckers M, Erdmann R, Veenhuis M & van der Klei IJ. (2006)
Dynamin-related proteins Vps1p and Dnm1p control peroxisome abundance in Saccharomyces cerevisiae. *J Cell Sci.* 119(Pt 19): 3994-4001.

Kyhse-Andersen J. (1984)
Electroblotting of multiple gels: a simple apparatus without buffer tank for rapid transfer of proteins from polyacrylamide to nitrocellulose. *J Biochem Biophys Methods* 10(3-4): 203-209.

Laemmli UK. (1970)
Cleavage of structural proteins during the assembly of the head of bacteriophage T4. *Nature* 227(259): 680-685.

Lay D, L Grosshans B, Heid H, Gorgas K & Just WW. (2005)
Binding and functions of ADP-ribosylation factor on mammalian and yeast peroxisomes. *J Biol Chem* 280(41): 34489-34499.

Lay D, Gorgas K & Just WW. (2006)
Peroxisome biogenesis: Where Arf and coatomer might be involved. *Biochim Biophys Acta* 1763(12): 1678-1687.

Lazarow PB & De Duve C. (1976)
A fatty acyl-CoA oxidizing system in rat liver peroxisomes; enhancement by clofibrate, a hypolipidemic drug. *Proc Natl Acad Sci U S A* 73(6): 2043-2046.

Lazarow PB & Fujiki Y. (1985)
Biogenesis of peroxisomes. *Annu Rev Cell Biol* 1: 489-530.

Lazarow PB. (1987)
The role of peroxisomes in mammalian cellular metabolism. *J Inherit Metab Dis* 10(Suppl 1): 11-22.

Lazarow PB. (2003)
Peroxisome biogenesis: advances and conundrums. *Curr Opin Cell Biol* 15(4): 489-497.

Lazarow PB. (2006)
The import receptor Pex7p and the PTS2 targeting sequence. *Biochim Biophys Acta* 1763(12): 1599-1604.

Lefebvre P, Chinetti G, Fruchart JC & Staels B. (2006)
Sorting out the roles of PPAR alpha in energy metabolism and vascular homeostasis. *J Clin Invest* 116(3): 571-580.

Leighton F, Coloma L & Koenig C. (1975)
Structure, composition, physical properties, and turnover of proliferated peroxisomes. A study of the trophic effects of Su-13437 on rat liver. *J Cell Biol* 67(2PT.1): 281-309.

Li X, Baumgart E, Dong GX, Morrell JC, Jimenez-Sanchez G, Valle D, Smith KD & Gould SJ. (2002a)
PEX11alpha Is Required for Peroxisome Proliferation in Response to 4-Phenylbutyrate but Is Dispensable for Peroxisome Proliferator-Activated Receptor Alpha-Mediated Peroxisome Proliferation. *Mol Cell Biol* 22(23): 8226-8240.

Li X, Baumgart E, Morrell JC, Jimenez-Sanchez G, Valle D & Gould SJ. (2002b)
PEX11 beta deficiency is lethal and impairs neuronal migration but does not abrogate peroxisome function. *Mol Cell Biol* 22(12): 4358-4365.

Li X & Gould SJ. (2002)
PEX11 promotes peroxisome division independently of peroxisome metabolism. *J Cell Biol* 156(4): 643-651.

Li X & Gould SJ. (2003)
The dynamin-like GTPase DLP1 is essential for peroxisome division and is recruited to peroxisomes in part by PEX11. *J Biol Chem* 278(19): 17012-17020.

Lingard MJ & Trelease RN. (2006)
Five Arabidopsis peroxin 11 homologs individually promote peroxisome elongation, division without elongation, or aggregation. *J. Cell Sci.* 119: 1961-1972.

Lingard MJ, Gidda SK, Bingham S, Rothstein SJ, Mullen RT & Trelease RN. (2008)
Arabidopsis PEROXIN11c-e, FISSION1b, and DYNAMIN-RELATED PROTEIN3A Cooperate in Cell Cycle-Associated Replication of Peroxisomes. *Plant Cell* 20(6): 1567-1585.

Lippincott-Schwartz J, Snapp E & Kenworthy A. (2001)
Studying protein dynamics in living cells. *Nat Rev Mol Cell Biol* 2(6): 444-456.

Lorenz P, Maier AG, Baumgart E, Erdmann R & Clayton C. (1998)
Elongation and clustering of glycosomes in Trypanosoma brucei overexpressing the glycosomal Pex11p. *Embo J* 17(13): 3542-3555.

Los GV, Encell LP, McDougall MG, et al. (2008)
HaloTag: a novel protein labeling technology for cell imaging and protein analysis. *ACS Chem Biol* 3(6): 373-382.

Lottspeich F & Engels JW. (2006)
Bioanalytik. München, Spektrum, Akademischer Verlag.

Luers G, Hashimoto T, Fahimi HD & Volkl A. (1993)
Biogenesis of peroxisomes: isolation and characterization of two distinct peroxisomal populations from normal and regenerating rat liver. *J Cell Biol* 121(6): 1271-1280.

Maier AG, Schulreich S, Bremser M & Clayton C. (2000)
Binding of coatomer by the PEX11 C-terminus is not required for function. *FEBS Lett* 484(2): 82-86.

Mano S, Nakamori C, Hayashi M, Kato A, Kondo M & Nishimura M. (2002)
Distribution and characterization of peroxisomes in Arabidopsis by visualization with GFP: dynamic morphology and actin-dependent movement. *Plant Cell Physiol.* 43(3): 331-341.

Mano S, Nakamori C, Kondo M, Hayashi M & Nishimura M. (2004)
An Arabidopsis dynamin-related protein, DRP3A, controls both peroxisomal and mitochondrial division. *Plant J* 38(3): 487-498.

Marelli M, Smith JJ, Jung S, et al. (2004)
Quantitative mass spectrometry reveals a role for the GTPase Rho1p in actin organization on the peroxisome membrane. *J Cell Biol* 167(6): 1099-1112.

Marshall PA, Krimkevich YI, Lark RH, Dyer JM, Veenhuis M & Goodman JM. (1995)
Pmp27 promotes peroxisomal proliferation. *J Cell Biol* 129(2): 345-355.

Marshall PA, Dyer JM, Quick ME & Goodman JM. (1996)
Redox-sensitive homodimerization of Pex11p: a proposed mechanism to regulate peroxisomal division. *J Cell Biol.* 135(1): 123-137.

Marzioch M, Erdmann R, Veenhuis M & Kunau WH. (1994)
PAS7 encodes a novel yeast member of the WD-40 protein family essential for import of 3-oxoacyl-CoA thiolase, a PTS2-containing protein, into peroxisomes. *EMBO J* 13(20): 4908-4918.

Mathur J, Mathur N & Hulskamp M. (2002)
Simultaneous visualization of peroxisomes and cytoskeletal elements reveals actin and not microtubule-based peroxisome motility in plants. *Plant Physiol* 128(3): 1031-1045.

Matsui M, Yamamoto A, Kuma A, Ohsumi Y & Mizushima N. (2006)
Organelle degradation during the lens and erythroid differentiation is independent of autophagy. *Biochem Biophys Res Commun* 339(2): 485-489.

Matsumoto N, Tamura S & Fujiki Y. (2003)
The pathogenic peroxin Pex26p recruits the Pex1p-Pex6p AAA ATPase complexes to peroxisomes. *Nat Cell Biol* 5(5): 454-460.

Matsuzaki T & Fujiki Y. (2008)
The peroxisomal membrane protein import receptor Pex3p is directly transported to peroxisomes by a novel Pex19p- and Pex16p-dependent pathway. *J Cell Biol* 183(7): 1275-1286.

Matsuzono Y, Kinoshita N, Tamura S, et al. (1999)
Human PEX19: cDNA cloning by functional complementation, mutation analysis in a patient with Zellweger syndrome, and potential role in peroxisomal membrane assembly. *Proc Natl Acad Sci U S A.* 96(5): 2116-2121.

Matsuzono Y & Fujiki Y. (2006)
In vitro transport of membrane proteins to peroxisomes by shuttling receptor Pex19p. *J Biol Chem* 281(1): 36-42.

Matsuzono Y, Matsuzaki T & Fujiki Y. (2006)
Functional domain mapping of peroxin Pex19p: interaction with Pex3p is essential for function and translocation. *J.Cell Sci.* 119(Pt 17): 3539-3550.

Matz MV, Fradkov AF, Labas YA, Savitsky AP, Zaraisky AG, Markelov ML & Lukyanov SA. (1999)
Fluorescent proteins from nonbioluminescent Anthozoa species. *Nat Biotechnol* 17(10): 969-973.

McNew JA & Goodman JM. (1994)
An oligomeric protein is imported into peroxisomes in vivo. *J Cell Biol* 127(5): 1245-1257.

Meijer WH, van der Klei IJ, Veenhuis M & Kiel JA. (2007)
ATG genes involved in non-selective autophagy are conserved from yeast to man, but the selective Cvt and pexophagy pathways also require organism-specific genes. *Autophagy* 3(2): 106-116.

Michels PA, Moyersoen J, Krazy H, Galland N, Herman M & Hannaert V. (2005)
Peroxisomes, glyoxysomes and glycosomes. *Mol Membr Biol* 22(1-2): 133-145.

Miyata N & Fujiki Y. (2005)
Shuttling mechanism of peroxisome targeting signal type 1 receptor Pex5: ATP-independent import and ATP-dependent export. *Mol Cell Biol* 25(24): 10822-10832.

Moody DE & Reddy JK. (1976)
Morphometric analysis of the ultrastructural changes in rat liver induced by the peroxisome proliferator SaH 42-348. *J Cell Biol* 71(3): 768-780.

Moody DE, Reddy JK, Lake BG, Popp JA & Reese DH. (1991)
Peroxisome proliferation and nongenotoxic carcinogenesis: commentary on a symposium. *Fundam Appl Toxicol* 16(2): 233-248.

Moser HW, Mahmood A & Raymond GV. (2007)
X-linked adrenoleukodystrophy. *Nat Clin Pract Neurol* 3(3): 140-151.

Motley A, Hettema E, Distel B & Tabak H. (1994)
Differential protein import deficiencies in human peroxisome assembly disorders. *J Cell Biol* 125(4): 755-767.

Motley AM & Hettema EH. (2007)
Yeast peroxisomes multiply by growth and division. *J Cell Biol* 178(3): 399-410.

Motley AM, Ward GP & Hettema EH. (2008)
Dnm1p-dependent peroxisome fission requires Caf4p, Mdv1p and Fis1p. *J Cell Sci* 121(Pt 10): 1633-1640.

Mozdy AD, McCaffery JM & Shaw JM. (2000)
Dnm1p GTPase-mediated mitochondrial fission is a multi-step process requiring the novel integral membrane component Fis1p. *J Cell Biol* 151(2): 367-380.

Muench DG & Mullen RT. (2003)
Peroxisome dynamics in plant cells: a role for the cytoskeleton. *Plant Science* 164: 307-315.

Mullen RT, Lisenbee CS, Miernyk JA & Trelease RN. (1999)
Peroxisomal membrane ascorbate peroxidase is sorted to a membranous network that resembles a subdomain of the endoplasmic reticulum. *Plant Cell* 11(11): 2167-2185.

Mullen RT & Trelease RN. (2000)
The sorting signals for peroxisomal membrane-bound ascorbate peroxidase are within its C-terminal tail. *J.Biol.Chem.* 275(21): 16337-16344.

Mullen RT & Trelease RN. (2006)
The ER-peroxisome connection in plants: development of the "ER semi-autonomous peroxisome maturation and replication" model for plant peroxisome biogenesis. *Biochim Biophys Acta* 1763(12): 1655-1668.

Muller WH, Bovenberg RA, Groothuis MH, Kattevilder F, Smaal EB, Van der Voort LH & Verkleij AJ. (1992)
Involvement of microbodies in penicillin biosynthesis. *Biochim Biophys Acta* 1116(2): 210-213.

Munck JM, Motley AM, Nuttall JM & Hettema EH. (2009)
A dual function for Pex3p in peroxisome formation and inheritance. *J Cell Biol* 187(4): 463-471.

Muntau AC, Mayerhofer PU, Paton BC, Kammerer S & Roscher AA. (2000)
Defective peroxisome membrane synthesis due to mutations in human PEX3 causes Zellweger syndrome, complementation group G. *Am J Hum Genet.* 67(4): 967-975.

Muntau AC, Roscher AA, Kunau WH & Dodt G. (2003)
The interaction between human PEX3 and PEX19 characterized by fluorescence resonance energy transfer (FRET) analysis. *Eur J Cell Biol* 82(7): 333-342.

Nagotu S, Krikken AM, Otzen M, Kiel JA, Veenhuis M & van der Klei IJ. (2008a)
Peroxisome fission in Hansenula polymorpha requires Mdv1 and Fis1, two proteins also involved in mitochondrial fission. *Traffic* 9(9): 1471-1484.

Nagotu S, Saraya R, Otzen M, Veenhuis M & van der Klei IJ. (2008b)
Peroxisome proliferation in Hansenula polymorpha requires Dnm1p which mediates fission but not de novo formation. *Biochim Biophys Acta* 1783(5): 760-769.

Nagotu S, Veenhuis M & van der Klei IJ. (2010)
Divide et impera: the dictum of peroxisomes. *Traffic* 11(2): 175-184.

Neuspiel M, Schauss AC, Braschi E, Zunino R, Rippstein P, Rachubinski RA, Andrade-Navarro MA & McBride HM. (2008)
Cargo-selected transport from the mitochondria to peroxisomes is mediated by vesicular carriers. *Current Biology* 18(2): 102-108.

Nguyen T, Bjorkman J, Paton BC & Crane DI. (2006)
Failure of microtubule-mediated peroxisome division and trafficking in disorders with reduced peroxisome abundance. *J Cell Sci.* 119(Pt 4): 636-645.

Nito K, Yamaguchi K, Kondo M, Hayashi M & Nishimura M. (2001)
Pumpkin peroxisomal ascorbate peroxidase is localized on peroxisomal membranes and unknown membranous structures. *Plant Cell Physiol* 42(1): 20-27.

Nito K, Kamigaki A, Kondo M, Hayashi M & Nishimura M. (2007)
Functional classification of Arabidopsis peroxisome biogenesis factors proposed from analyses of knockdown mutants. *Plant Cell Physiol* 48(6): 763-774.

Novikoff AB & Shin WY. (1964)
The endoplasmic reticulum in the Golgi zone and its relations to microbodies, Golgi apparatus, and autophagic vacuoles in rat liver cells. *J Microscopy* 3: 187-206.

Novikoff AB & Goldfischer S. (1969)
Visualization of peroxisomes (microbodies) and mitochondria with diaminobenzidine. *J Histochem Cytochem* 17(10): 675-680.

Opperdoes FR. (1988)
Glycosomes may provide clues to the import of peroxisomal proteins. *Trends Biochem.Sci.* 13(7): 255-260.

Orth T, Reumann S, Zhang X, Fan J, Wenzel D, Quan S & Hu J. (2007)
The PEROXIN11 protein family controls peroxisome proliferation in Arabidopsis. *Plant Cell* 19(1): 333-350.

Otera H, Harano T, Honsho M, Ghaedi K, Mukai S, Tanaka A, Kawai A, Shimizu N & Fujiki Y. (2000)
The mammalian peroxin Pex5pL, the longer isoform of the mobile peroxisome targeting signal (PTS) type 1 transporter, translocates the Pex7p.PTS2 protein complex into peroxisomes via its initial docking site, Pex14p. *J Biol Chem* 275(28): 21703-21714.

Passreiter M, Anton M, Lay D, Frank R, Harter C, Wieland FT, Gorgas K & Just WW. (1998)
Peroxisome biogenesis: involvement of ARF and coatomer. *J Cell Biol* 141(2): 373-383.

Peters JM, Cheung C & Gonzalez FJ. (2005)
Peroxisome proliferator-activated receptor-alpha and liver cancer: where do we stand? *J Mol Med.* 83(10): 774-785.

Pinto MP, Grou CP, Alencastre IS, Oliveira ME, Sa-Miranda C, Fransen M & Azevedo JE. (2006)
The import competence of a peroxisomal membrane protein is determined by Pex19p before the docking step. *J Biol Chem* 281(45): 34492-34502.

Pitts KR, Yoon Y, Krueger EW & McNiven MA. (1999)
The dynamin-like protein DLP1 is essential for normal distribution and morphology of the endoplasmic reticulum and mitochondria in mammalian cells. *Mol Biol Cell* 10(12): 4403-4417.

Platta HW, Grunau S, Rosenkranz K, Girzalsky W & Erdmann R. (2005)
Functional role of the AAA peroxins in dislocation of the cycling PTS1 receptor back to the cytosol. *Nat Cell Biol* 7(8): 817-822.

Platta HW, El Magraoui F, Schlee D, Grunau S, Girzalsky W & Erdmann R. (2007)
Ubiquitination of the peroxisomal import receptor Pex5p is required for its recycling. *J Cell Biol* 177(2): 197-204.

Platta HW & Erdmann R. (2007)
Peroxisomal dynamics. *Trends Cell Biol* 17(10): 474-484.

Platta HW, El Magraoui F, Baumer BE, Schlee D, Girzalsky W & Erdmann R. (2009)
Pex2 and pex12 function as protein-ubiquitin ligases in peroxisomal protein import. *Mol Cell Biol* 29(20): 5505-5516.

Poirier Y, Antonenkov VD, Glumoff T & Hiltunen JK. (2006)
Peroxisomal beta-oxidation--a metabolic pathway with multiple functions. *Biochim Biophys Acta* 1763(12): 1413-1426.

Praefcke GJ & McMahon HT. (2004)
The dynamin superfamily: universal membrane tubulation and fission molecules? *Nat Rev Mol Cell Biol* 5(2): 133-147.

Prasher DC, Eckenrode VK, Ward WW, Prendergast FG & Cormier MJ. (1992)
Primary structure of the Aequorea victoria green-fluorescent protein. *Gene* 111(2): 229-233.

Purdue PE & Lazarow PB. (2001)
Peroxisome biogenesis. *Annu Rev Cell Dev Biol* 17: 701-752.

Pyper SR, Viswakarma N, Yu S & Reddy JK. (2010)
PPARalpha: energy combustion, hypolipidemia, inflammation and cancer. *Nucl Recept Signal* 8: e002.

Rabu C, Schmid V, Schwappach B & High S. (2009)
Biogenesis of tail-anchored proteins: the beginning for the end? *J Cell Sci* 122(Pt 20): 3605-3612.

Rao MS & Reddy JK. (1987)
Peroxisome proliferation and hepatocarcinogenesis. *Carcinogenesis* 8(5): 631-636.

Rapaport D. (2003)
Finding the right organelle. Targeting signals in mitochondrial outer-membrane proteins. *EMBO Rep* 4(10): 948-952.

Rapp S, Saffrich R, Anton M, Jakle U, Ansorge W, Gorgas K & Just WW. (1996)
Microtubule-based peroxisome movement. *J Cell Sci* 109(Pt 4): 837-849.

Rayapuram N & Subramani S. (2006)
The importomer--a peroxisomal membrane complex involved in protein translocation into the peroxisome matrix. *Biochim Biophys Acta* 1763(12): 1613-1619.

Raychaudhuri S & Prinz WA. (2008)
Nonvesicular phospholipid transfer between peroxisomes and the endoplasmic reticulum. *Proc Natl Acad Sci U S A* 105(41): 15785-15790.

Reddy JK, Azarnoff DL & Hignite CE. (1980)
Hypolipidaemic hepatic peroxisome proliferators form a novel class of chemical carcinogens. *Nature* 283(5745): 397-398.

Reddy JK, Warren JR, Reddy MK & Lalwani ND. (1982)
Hepatic and renal effects of peroxisome proliferators: biological implications. *Ann N Y Acad Sci* 386: 81-110.

Reddy JK & Lalwani ND. (1983)
Carcinogenesis by hepatic peroxisome proliferators: Evaluation of the risk of hypolipidemic drugs and industrial plasticizers to humans. *CRC Critical Rev. Tox.* 12: 1-58.

Reddy JK & Hashimoto T. (2001)
Peroxisomal beta-oxidation and peroxisome proliferator-activated receptor alpha: an adaptive metabolic system. *Annu Rev Nutr.* 21: 193-230.

Rehling P, Skaletz-Rorowski A, Girzalsky W, Voorn-Brouwer T, Franse MM, Distel B, Veenhuis M, Kunau WH & Erdmann R. (2000)
Pex8p, an intraperoxisomal peroxin of Saccharomyces cerevisiae required for protein transport into peroxisomes binds the PTS1 receptor pex5p. *J Biol Chem* 275(5): 3593-3602.

Reumann S & Weber AP. (2006)
Plant peroxisomes respire in the light: Some gaps of the photorespiratory C(2) cycle have become filled-Others remain. *Biochim Biophys Acta* 1763(12): 1496-1510.

Rhodin J. (1954)
Correlation of ultrastructural organization and function in normal experimentally changed convoluted tubule cells of the mouse kidney. *Ph. D. thesis*. Stockholm, Aktiebolaget Godvil.

Rokka A, Antonenkov VD, Soininen R, et al. (2009)
Pxmp2 is a channel-forming protein in Mammalian peroxisomal membrane. *PLoS One* 4(4): e5090.

Rottensteiner H, Kal AJ, Filipits M, Binder M, Hamilton B, Tabak HF & Ruis H. (1996)
Pip2p: a transcriptional regulator of peroxisome proliferation in the yeast Saccharomyces cerevisiae. *Embo J.* 15(12): 2924-2934.

Rottensteiner H, Hartig A, Hamilton B, Ruis H, Erdmann R & Gurvitz A. (2003a)
Saccharomyces cerevisiae Pip2p-Oaf1p regulates PEX25 transcription through an adenine-less ORE. *Eur J Biochem.* 270(9): 2013-2022.

Rottensteiner H, Stein K, Sonnenhol E & Erdmann R. (2003b)
Conserved function of pex11p and the novel pex25p and pex27p in peroxisome biogenesis. *Mol Biol Cell* 14(10): 4316-4328.

Rottensteiner H, Wabnegger L, Erdmann R, Hamilton B, Ruis H, Hartig A & Gurvitz A. (2003c)
Saccharomyces cerevisiae PIP2 mediating oleic acid induction and peroxisome proliferation is regulated by Adr1p and Pip2p-Oaf1p. *J Biol Chem.* 278(30): 27605-27611. Epub 22003 May 27614.

Rottensteiner H, Kramer A, Lorenzen S, Stein K, Landgraf C, Volkmer-Engert R & Erdmann R. (2004)
Peroxisomal membrane proteins contain common Pex19p-binding sites that are an integral part of their targeting signals (mPTS). *Mol Biol Cell* 15: 3406-3417.

Roux A, Uyhazi K, Frost A & De Camilli P. (2006)
GTP-dependent twisting of dynamin implicates constriction and tension in membrane fission. *Nature* 441(7092): 528-531.

Roux A, Koster G, Lenz M, Sorre B, Manneville JB, Nassoy P & Bassereau P. (2010)
Membrane curvature controls dynamin polymerization. *Proc Natl Acad Sci U S A*.

Rucktaschel R, Thoms S, Sidorovitch V, et al. (2009)
Farnesylation of pex19p is required for its structural integrity and function in peroxisome biogenesis. *J Biol Chem* 284(31): 20885-20896.

Sacksteder KA & Gould SJ. (2000)
The genetics of peroxisome biogenesis. *Annu Rev Genet* 34: 623-652.

Sacksteder KA, Jones JM, South ST, Li X, Liu Y & Gould SJ. (2000)
PEX19 binds multiple peroxisomal membrane proteins, is predominantly cytoplasmic, and is required for peroxisome membrane synthesis. *J Cell Biol* 148(5): 931-944.

Sakai Y, Koller A, Rangell LK, Keller GA & Subramani S. (1998)
Peroxisome degradation by microautophagy in Pichia pastoris: identification of specific steps and morphological intermediates. *J Cell Biol* 141(3): 625-636.

Sakai Y, Oku M, van der Klei IJ & Kiel JA. (2006)
Pexophagy: Autophagic degradation of peroxisomes. *Biochim Biophys Acta* 1763(12): 1767-1775.

Santos MJ, Imanaka T, Shio H, Small GM & Lazarow PB. (1988)
Peroxisomal membrane ghosts in Zellweger syndrome--aberrant organelle assembly. *Science* 239(4847): 1536-1538.

Santos MJ, Quintanilla RA, Toro A, Grandy R, Dinamarca MC, Godoy JA & Inestrosa NC. (2005)
Peroxisomal proliferation protects from beta-amyloid neurodegeneration. *J Biol Chem.* 280(49): 41057-41068.

Saraya R, Cepinska MN, Kiel JA, Veenhuis M & van der Klei IJ. (2010)
A conserved function for Inp2 in peroxisome inheritance. *Biochim Biophys Acta* In Press.

Schewe T, Halangk W, Hiebsch C & Rapoport SM. (1975)
A lipoxygenase in rabbit reticulocytes which attacks phospholipids and intact mitochondria. *FEBS Lett* 60(1): 149-152.

Schluter A, Fourcade S, Ripp R, Mandel JL, Poch O & Pujol A. (2006)
The evolutionary origin of peroxisomes: an ER-peroxisome connection. *Mol Biol Evol* 23(4): 838-845.

Schluter A, Real-Chicharro A, Gabaldon T, Sanchez-Jimenez F & Pujol A. (2010)
PeroxisomeDB 2.0: an integrative view of the global peroxisomal metabolome. *Nucleic Acids Res* 38(Database issue): D800-805.

Schneiter R, Brugger B, Sandhoff R, et al. (1999)
Electrospray ionization tandem mass spectrometry (ESI-MS/MS) analysis of the lipid molecular species composition of yeast subcellular membranes reveals acyl chain-based sorting/remodeling of distinct molecular species en route to the plasma membrane. *J Cell Biol* 146(4): 741-754.

Schnell DJ & Hebert DN. (2003)
Protein translocons: multifunctional mediators of protein translocation across membranes. *Cell* 112(4): 491-505.

Schrader M, Baumgart E, Volkl A & Fahimi HD. (1994)
Heterogeneity of peroxisomes in human hepatoblastoma cell line HepG2. Evidence of distinct subpopulations. *Eur J Cell Biol* 64(2): 281-294.

Schrader M, Burkhardt JK, Baumgart E, Luers G, Spring H, Volkl A & Fahimi HD. (1996)
Interaction of microtubules with peroxisomes. Tubular and spherical peroxisomes in HepG2 cells and their alterations induced by microtubule-active drugs. *Eur J Cell Biol* 69(1): 24-35.

Schrader M, Krieglstein K & Fahimi HD. (1998a)
Tubular peroxisomes in HepG2 cells: selective induction by growth factors and arachidonic acid. *Eur J Cell Biol* 75(2): 87-96.

Schrader M, Reuber BE, Morrell JC, Jimenez-Sanchez G, Obie C, Stroh TA, Valle D, Schroer TA & Gould SJ. (1998b)
Expression of PEX11beta mediates peroxisome proliferation in the absence of extracellular stimuli. *J Biol Chem* 273(45): 29607-29614.

Schrader M, Wodopia R & Fahimi HD. (1999)
Induction of tubular peroxisomes by UV irradiation and reactive oxygen species in HepG2 cells. *J Histochem Cytochem* 47(9): 1141-1148.

Schrader M, King SJ, Stroh TA & Schroer TA. (2000)
Real time imaging reveals a peroxisomal reticulum in living cells. *J Cell Sci* 113(Pt 20): 3663-3671.

Schrader M, Thiemann M & Fahimi HD. (2003)
Peroxisomal motility and interaction with microtubules. *Microsc Res Tech* 61(2): 171-178.

Schrader M & Fahimi HD. (2004)
Mammalian peroxisomes and reactive oxygen species. *Histochem Cell Biol* 122(4): 383-393.

Schrader M. (2006)
Shared components of mitochondrial and peroxisomal division. *Biochim Biophys Acta* 1763(5-6): 531-541.

Schrader M & Fahimi HD. (2006a)
Peroxisomes and oxidative stress. *Biochim Biophys Acta* 1763(12): 1755-1766.

Schrader M & Fahimi HD. (2006b)
Growth and division of peroxisomes. *Int Rev Cytol* 255: 237-290.

Schrader M & Yoon Y. (2007)
Mitochondria and peroxisomes: Are the 'Big Brother' and the 'Little Sister' closer than assumed? *Bioessays* 29(11): 1105-1114.

Schrader M & Fahimi HD. (2008)
The peroxisome: still a mysterious organelle. *Histochem Cell Biol* 129(4): 421-440.

Schroder LA, Glick BS & Dunn WA. (2007)
Identification of pexophagy genes by restriction enzyme-mediated integration. *Methods Mol Biol* 389: 203-218.

Schumann U & Subramani S. (2008)
Special delivery from mitochondria to peroxisomes. *Trends Cell Biol* 18(6): 253-256.

Serasinghe MN & Yoon Y. (2008)
The mitochondrial outer membrane protein hFis1 regulates mitochondrial morphology and fission through self-interaction. *Exp Cell Res* 314(19): 3494-3507.

Setoguchi K, Otera H & Mihara K. (2006)
Cytosolic factor- and TOM-independent import of C-tail-anchored mitochondrial outer membrane proteins. *Embo J* 25(24): 5635-5647.

Shen YQ & Burger G. (2009)
Plasticity of a key metabolic pathway in fungi. *Funct Integr Genomics* 9(2): 145-151.

Shibata H, Kashiwayama Y, Imanaka T & Kato H. (2004)
Domain architecture and activity of human Pex19p, a chaperone-like protein for intracellular trafficking of peroxisomal membrane proteins. *J.Biol.Chem.* 279(37): 38486-38494.

Shibata Y, Voss C, Rist JM, Hu J, Rapoport TA, Prinz WA & Voeltz GK. (2008)
The reticulon and DP1/Yop1p proteins form immobile oligomers in the tubular endoplasmic reticulum. *J Biol Chem* 283(27): 18892-18904.

Sinclair AM, Trobacher CP, Mathur N, Greenwood JS & Mathur J. (2009)
Peroxule extension over ER defined paths constitutes a rapid subcellular response to hydroxyl stress. *Plant J* 59(2): 231-242.

Singh AK, Dhaunsi GS, Gupta MP, Orak JK, Asayama K & Singh I. (1994)
Demonstration of glutathione peroxidase in rat liver peroxisomes and its intraorganellar distribution. *Arch Biochem Biophys* 315(2): 331-338.

Singh I. (1996)
Mammalian peroxisomes: metabolism of oxygen and reactive oxygen species. *Ann N Y Acad Sci* 804: 612-627.

Smirnova E, Griparic L, Shurland DL & van der Bliek AM. (2001)
Dynamin-related protein Drp1 is required for mitochondrial division in mammalian cells. *Mol Biol Cell* 12(8): 2245-2256.

Smith JJ, Marelli M, Christmas RH, et al. (2002)
Transcriptome profiling to identify genes involved in peroxisome assembly and function. *J Cell Biol* 158(2): 259-271.

Snapp EL, Hegde RS, Francolini M, Lombardo F, Colombo S, Pedrazzini E, Borgese N & Lippincott-Schwartz J. (2003)
Formation of stacked ER cisternae by low affinity protein interactions. *J Cell Biol* 163(2): 257-269.

Snyder WB, Koller A, Choy AJ & Subramani S. (2000)
The peroxin Pex19p interacts with multiple, integral membrane proteins at the peroxisomal membrane. *J.Cell Biol.* 149(6): 1171-1178.

Soukupova M, Sprenger C, Gorgas K, Kunau WH & Dodt G. (1999)
Identification and characterization of the human peroxin PEX3. *Eur J Cell Biol* 78(6): 357-374.

South ST & Gould SJ. (1999)
Peroxisome synthesis in the absence of preexisting peroxisomes. *J Cell Biol* 144(2): 255-266.

South ST, Sacksteder KA, Li X, Liu Y & Gould SJ. (2000)
Inhibitors of COPI and COPII do not block PEX3-mediated peroxisome synthesis. *J Cell Biol* 149(7): 1345-1360.

South ST, Baumgart E & Gould SJ. (2001)
Inactivation of the endoplasmic reticulum protein translocation factor, Sec61p, or its homolog, Ssh1p, does not affect peroxisome biogenesis. *Proc Natl Acad Sci U S A* 98(21): 12027-12031.

Stamer K, Vogel R, Thies E, Mandelkow E & Mandelkow EM. (2002)
Tau blocks traffic of organelles, neurofilaments, and APP vesicles in neurons and enhances oxidative stress. *J Cell Biol.* 156(6): 1051-1063. Epub 2002 Mar 1018.

Staubli W, Schweizer W, Suter J & Weibel ER. (1977)
The proliferative response of hepatic peroxidomes of neonatal rats to treatment with SU-13 437 (nafenopin). *J Cell Biol* 74(3): 665-689.

Stefanovic S & Hegde RS. (2007)
Identification of a targeting factor for posttranslational membrane protein insertion into the ER. *Cell* 128(6): 1147-1159.

Steinberg S, Jones R, Tiffany C & Moser A. (2008)
Investigational methods for peroxisomal disorders. *Curr Protoc Hum Genet* Chapter 17: Unit 17.16.

Steinberg SJ, Dodt G, Raymond GV, Braverman NE, Moser AB & Moser HW. (2006)
Peroxisome biogenesis disorders. *Biochim Biophys Acta* 1763(12): 1733-1748.

Stojanovski D, Koutsopoulos OS, Okamoto K & Ryan MT. (2004)
Levels of human Fis1 at the mitochondrial outer membrane regulate mitochondrial morphology. *J Cell Sci* 117(Pt 7): 1201-1210.

Suzuki M, Jeong SY, Karbowski M, Youle RJ & Tjandra N. (2003)
The solution structure of human mitochondria fission protein Fis1 reveals a novel TPR-like helix bundle. *J Mol Biol* 334(3): 445-458.

Suzuki M, Neutzner A, Tjandra N & Youle RJ. (2005)
Novel structure of the N terminus in yeast Fis1 correlates with a specialized function in mitochondrial fission. *J Biol Chem* 280(22): 21444-21452.

Svoboda DJ & Azarnoff DL. (1966)
Response of hepatic microbodies to a hypolipidemic agent, ethyl chlorophenoxyisobutyrate (CPIB). *J Cell Biol* 30(2): 442-450.

Swanson J, Bushnell A & Silverstein SC. (1987)
Tubular lysosome morphology and distribution within macrophages depend on the integrity of cytoplasmic microtubules. *Proc Natl Acad Sci U S A* 84(7): 1921-1925.

Sweitzer SM & Hinshaw JE. (1998)
Dynamin undergoes a GTP-dependent conformational change causing vesiculation. *Cell* 93(6): 1021-1029.

Swinkels BW, Gould SJ, Bodnar AG, Rachubinski RA & Subramani S. (1991)
A novel, cleavable peroxisomal targeting signal at the amino-terminus of the rat 3-ketoacyl-CoA thiolase. *Embo J.* 10(11): 3255-3262.

Tabak HF, Murk JL, Braakman I & Geuze HJ. (2003)
Peroxisomes start their life in the endoplasmic reticulum. *Traffic* 4(8): 512-518.

Tabak HF, Hoepfner D, Zand A, Geuze HJ, Braakman I & Huynen MA. (2006)
Formation of peroxisomes: present and past. *Biochim Biophys Acta* 1763(12): 1647-1654.

Tabak HF, van der Zand A & Braakman I. (2008)
Peroxisomes: minted by the ER. *Curr Opin Cell Biol* 20(4): 393-400.

Tam YY & Rachubinski RA. (2002)
Yarrowia lipolytica cells mutant for the PEX24 gene encoding a peroxisomal membrane peroxin mislocalize peroxisomal proteins and accumulate membrane structures containing both peroxisomal matrix and membrane proteins. *Mol Biol Cell.* 13(8): 2681-2691.

Tam YY, Torres-Guzman JC, Vizeacoumar FJ, Smith JJ, Marelli M, Aitchison JD & Rachubinski RA. (2003)
Pex11-related proteins in peroxisome dynamics: a role for the novel peroxin Pex27p in controlling peroxisome size and number in Saccharomyces cerevisiae. *Mol Biol Cell* 14(10): 4089-4102.

Tam YY, Fagarasanu A, Fagarasanu M & Rachubinski RA. (2005)
Pex3p Initiates the Formation of a Preperoxisomal Compartment from a Subdomain of the Endoplasmic Reticulum in Saccharomyces cerevisiae. *J Biol Chem* 280(41): 34933-34939.

Tanaka A, Okumoto K & Fujiki Y. (2003)
cDNA cloning and characterization of the third isoform of human peroxin Pex11p. *Biochem Biophys Res Commun.* 300(4): 819-823.

Terasaki M, Chen LB & Fujiwara K. (1986)
Microtubules and the endoplasmic reticulum are highly interdependent structures. *J Cell Biol* 103(4): 1557-1568.

Terlecky SR, Koepke JI & Walton PA. (2006)
Peroxisomes and aging. *Biochim Biophys Acta* 1763(12): 1749-1754.

Thiemann M, Schrader M, Volkl A, Baumgart E & Fahimi HD. (2000)
Interaction of peroxisomes with microtubules. In vitro studies using a novel peroxisome-microtubule binding assay. *Eur J Biochem* 267(20): 6264-6275.

Thoms S & Erdmann R. (2005)
Dynamin-related proteins and Pex11 proteins in peroxisome division and proliferation. *Febs J* 272(20): 5169-5181.

Titorenko VI & Rachubinski RA. (1998)
Mutants of the yeast Yarrowia lipolytica defective in protein exit from the endoplasmic reticulum are also defective in peroxisome biogenesis. *Mol Cell Biol* 18(5): 2789-2803.

Titorenko VI, Nicaud JM, Wang H, Chan H & Rachubinski RA. (2002)
Acyl-CoA oxidase is imported as a heteropentameric, cofactor-containing complex into peroxisomes of Yarrowia lipolytica. *J Cell Biol* 156(3): 481-494.

Titorenko VI & Rachubinski RA. (2009)
Spatiotemporal dynamics of the ER-derived peroxisomal endomembrane system. *Int Rev Cell Mol Biol* 272: 191-244.

Toro AA, Araya CA, Cordova GJ, et al. (2009)
Pex3p-dependent peroxisomal biogenesis initiates in the endoplasmic reticulum of human fibroblasts. *J Cell Biochem* 107(6): 1083-1096.

Towbin H, Staehelin T & Gordon J. (1979)
Electrophoretic transfer of proteins from polyacrylamide gels to nitrocellulose sheets: procedure and some applications. *Proc Natl Acad Sci U S A* 76(9): 4350-4354.

Tsien RY. (1998)
The green fluorescent protein. *Annu Rev Biochem* 67: 509-544.

Tugwood JD, Issemann I, Anderson RG, Bundell KR, McPheat WL & Green S. (1992)
The mouse peroxisome proliferator activated receptor recognizes a response element in the 5' flanking sequence of the rat acyl CoA oxidase gene. *EMBO J* 11(2): 433-439.

Urquhart AJ, Kennedy D, Gould SJ & Crane DI. (2000)
Interaction of Pex5p, the type 1 peroxisome targeting signal receptor, with the peroxisomal membrane proteins Pex14p and Pex13p. *J Biol Chem* 275(6): 4127-4136.

Van Ael E & Fransen M. (2006)
Targeting signals in peroxisomal membrane proteins. *Biochim Biophys Acta* 1763(12): 1629-1638.

van den Bosch H, Schutgens RB, Wanders RJ & Tager JM. (1992)
Biochemistry of peroxisomes. *Annu Rev Biochem* 61: 157-197.

van der Klei IJ & Veenhuis M. (2006a)
PTS1-independent sorting of peroxisomal matrix proteins by Pex5p. *Biochim Biophys Acta* 1763(12): 1794-1800.

van der Klei IJ & Veenhuis M. (2006b)
Yeast and filamentous fungi as model organisms in microbody research. *Biochim Biophys Acta* 1763(12): 1364-1373.

van der Zand A, Braakman I, Geuze HJ & Tabak HF. (2006)
The return of the peroxisome. *J Cell Sci.* 119(Pt 6): 989-994.

van Kuppeveld FJ, van der Logt JT, Angulo AF, van Zoest MJ, Quint WG, Niesters HG, Galama JM & Melchers WJ. (1992)
Genus- and species-specific identification of mycoplasmas by 16S rRNA amplification. *Appl Environ Microbiol* 58(8): 2606-2615.

van Leyen K, Duvoisin RM, Engelhardt H & Wiedmann M. (1998)
A function for lipoxygenase in programmed organelle degradation. *Nature* 395(6700): 392-395.

van Roermund CW, Tabak HF, van Den Berg M, Wanders RJ & Hettema EH. (2000)
Pex11p plays a primary role in medium-chain fatty acid oxidation, a process that affects peroxisome number and size in Saccharomyces cerevisiae. *J Cell Biol* 150(3): 489-498.

Veenhuis M, Mateblowski M, Kunau WH & Harder W. (1987)
Proliferation of microbodies in Saccharomyces cerevisiae. *Yeast* 3(2): 77-84.

Veenhuis M, Salomons FA & Van Der Klei IJ. (2000)
Peroxisome biogenesis and degradation in yeast: a structure/function analysis. *Microsc Res Tech.* 51(6): 584-600.

Veenhuis M, Kiel JA & Van Der Klei IJ. (2003)
Peroxisome assembly in yeast. *Microsc Res Tech.* 61(2): 139-150.

Vizeacoumar FJ, Torres-Guzman JC, Tam YY, Aitchison JD & Rachubinski RA. (2003)
YHR150w and YDR479c encode peroxisomal integral membrane proteins involved in the regulation of peroxisome number, size, and distribution in Saccharomyces cerevisiae. *J Cell Biol.* 161(2): 321-332.

Vizeacoumar FJ, Torres-Guzman JC, Bouard D, Aitchison JD & Rachubinski RA. (2004)
Pex30p, Pex31p, and Pex32p form a family of peroxisomal integral membrane proteins regulating peroxisome size and number in Saccharomyces cerevisiae. *Mol Biol Cell* 15(2): 665-677.

Voeltz GK, Prinz WA, Shibata Y, Rist JM & Rapoport TA. (2006)
A class of membrane proteins shaping the tubular endoplasmic reticulum. *Cell* 124(3): 573-586.

Voncken F, van Hellemond JJ, Pfisterer I, Maier A, Hillmer S & Clayton C. (2003)
Depletion of GIM5 causes cellular fragility, a decreased glycosome number, and reduced levels of ether-linked phospholipids in trypanosomes. *J Biol Chem.* 278(37): 35299-35310. Epub 32003 Jun 35226.

Voorn-Brouwer T, Kragt A, Tabak HF & Distel B. (2001)
Peroxisomal membrane proteins are properly targeted to peroxisomes in the absence of COPI- and COPII-mediated vesicular transport. *J Cell Sci* 114(Pt 11): 2199-2204.

Walton PA, Hill PE & Subramani S. (1995)
Import of stably folded proteins into peroxisomes. *Mol.Biol.Cell* 6(6): 675-683.

Wanders RJ & Waterham HR. (2005)
Peroxisomal disorders I: biochemistry and genetics of peroxisome biogenesis disorders. *Clin Genet.* 67(2): 107-133.

Wanders RJ & Waterham HR. (2006a)
Peroxisomal disorders: the single peroxisomal enzyme deficiencies. *Biochim Biophys Acta* 1763(12): 1707-1720.

Wanders RJ, Ferdinandusse S, Brites P & Kemp S. (2010)
Peroxisomes, lipid metabolism and lipotoxicity. *Biochim Biophys Acta* 1801(3): 272-280.

Wanders RJA & Waterham HR. (2006b)
Biochemistry of mammalian peroxisomes revisited. *Annu. Rev. Biochem.* 75: 295-332.

Waterham HR, Koster J, van Roermund CW, Mooyer PA, Wanders RJ & Leonard JV. (2007)
A lethal defect of mitochondrial and peroxisomal fission. *N Engl J Med* 356(17): 1736-1741.

Wattenberg B & Lithgow T. (2001)
Targeting of C-terminal (tail)-anchored proteins: understanding how cytoplasmic activities are anchored to intracellular membranes. *Traffic* 2(1): 66-71.

Weller S, Gould SJ & Valle D. (2003)
Peroxisome biogenesis disorders. *Annu Rev Genomics Hum Genet* 4: 165-211.

Wells RC, Picton LK, Williams SC, Tan FJ & Hill RB. (2007)
Direct binding of the dynamin-like GTPase, Dnm1, to mitochondrial dynamics protein Fis1 is negatively regulated by the Fis1 N-terminal arm. *J Biol Chem* 282(46): 33769-33775.

Wessel D & Flugge UI. (1984)
A method for the quantitative recovery of protein in dilute solution in the presence of detergents and lipids. *Anal.Biochem.* 138(1): 141-143.

White AL, Modaff P, Holland-Morris F & Pauli RM. (2003)
Natural history of rhizomelic chondrodysplasia punctata. *Am J Med Genet A* 118A(4): 332-342.

Wiemer EA, Wenzel T, Deerinck TJ, Ellisman MH & Subramani S. (1997)
Visualization of the peroxisomal compartment in living mammalian cells: dynamic behavior and association with microtubules. *J Cell Biol* 136(1): 71-80.

Williams C & Distel B. (2006)
Pex13p: docking or cargo handling protein? *Biochim Biophys Acta* 1763(12): 1585-1591.

Williams C, van den Berg M, Geers E & Distel B. (2008)
Pex10p functions as an E3 ligase for the Ubc4p-dependent ubiquitination of Pex5p. *Biochem Biophys Res Commun* 374(4): 620-624.

Woodward AW & Bartel B. (2005)
The Arabidopsis peroxisomal targeting signal type 2 receptor PEX7 is necessary for peroxisome function and dependent on PEX5. *Mol Biol Cell* 16(2): 573-583.

Woudenberg J, Rembacz KP, van den Heuvel FA, et al. (2010)
Caveolin-1 is enriched in the peroxisomal membrane of rat hepatocytes. *Hepatology* 51(5): 1744-1753.

Yamamoto K & Fahimi HD. (1987)
Three-dimensional reconstruction of a peroxisomal reticulum in regenerating rat liver: evidence of interconnections between heterogeneous segments. *J Cell Biol* 105(2): 713-722.

Yan M, Rayapuram N & Subramani S. (2005)
The control of peroxisome number and size during division and proliferation. *Curr Opin Cell Biol* 17: 376-383.

Yang F, Moss LG & Phillips GN, Jr. (1996)
The molecular structure of green fluorescent protein. *Nat Biotechnol* 14(10): 1246-1251.

Yang X, Purdue PE & Lazarow PB. (2001)
Eci1p uses a PTS1 to enter peroxisomes: either its own or that of a partner, Dci1p. *Eur J Cell Biol* 80(2): 126-138.

Yang YS & Strittmatter SM. (2007)
The reticulons: a family of proteins with diverse functions. *Genome Biol* 8(12): 234.

Yokota S, Oda T & Fahimi HD. (2001)
The role of 15-lipoxygenase in disruption of the peroxisomal membrane and in programmed degradation of peroxisomes in normal rat liver. *J Histochem Cytochem.* 49(5): 613-622.

Yokota S. (2003)
Degradation of normal and proliferated peroxisomes in rat hepatocytes: regulation of peroxisomes quantity in cells. *Microsc Res Tech* 61(2): 151-160.

Yokota S, Haraguchi CM & Oda T. (2008)
Induction of peroxisomal Lon protease in rat liver after di-(2-ethylhexyl)phthalate treatment. *Histochem Cell Biol* 129(1): 73-83.

Yokota S & Fahimi HD. (2009)
Degradation of excess peroxisomes in mammalian liver cells by autophagy and other mechanisms. *Histochem Cell Biol* 131(4): 455-458.

Yoon Y, Pitts KR, Dahan S & McNiven MA. (1998)
A novel dynamin-like protein associates with cytoplasmic vesicles and tubules of the endoplasmic reticulum in mammalian cells. *J Cell Biol* 140(4): 779-793.

Yoon Y & McNiven MA. (2001)
Mitochondrial division: New partners in membrane pinching. *Curr Biol* 11(2): R67-70.

Yoon Y, Pitts KR & McNiven MA. (2001)
Mammalian dynamin-like protein DLP1 tubulates membranes. *Mol Biol Cell* 12(9): 2894-2905.

Yoon Y, Krueger EW, Oswald BJ & McNiven MA. (2003)
The mitochondrial protein hFis1 regulates mitochondrial fission in mammalian cells through an interaction with the dynamin-like protein DLP1. *Mol Cell Biol* 23(15): 5409-5420.

Yu T, Fox RJ, Burwell LS & Yoon Y. (2005)
Regulation of mitochondrial fission and apoptosis by the mitochondrial outer membrane protein hFis1. *J Cell Sci* 118(Pt 18): 4141-4151.

Zaar K, Volkl A & Fahimi HD. (1987)
Association of isolated bovine kidney cortex peroxisomes with endoplasmic reticulum. *Biochim Biophys Acta* 897(1): 135-142.

Zaar K, Volkl A & Fahimi HD. (1991)
Purification of marginal plates from bovine renal peroxisomes: identification with L-alpha-hydroxyacid oxidase B. *J Cell Biol* 113(1): 113-121.

Zhang X-C & Hu J-P. (2008)
FISSION1A and FISSION1B Proteins Mediate the Fission of Peroxisomes and Mitochondria in Arabidopsis. *Mol Plant* 1(6): 1036-1047.

Zhang X & Hu J. (2010)
The Arabidopsis chloroplast division protein DYNAMIN-RELATED PROTEIN5B also mediates peroxisome division. *Plant Cell* 22(2): 431-442.

Zutphen T, Veenhuis M & van der Klei IJ. (2008)
Pex14 is the sole component of the peroxisomal translocon that is required for pexophagy. *Autophagy* 4(1): 63-66.

8 APPENDIX

8.1 Abbreviations and definitions

8.1.1 Abbreviations

α	alpha
AAA	ATPases associated with diverse cellular activities
ABC	ATP-binding cassette
ACALD	adolescent/adult cerebral adrenoleukodystrophy
AGT	alanine glyoxylate aminotransferase
ALD	adrenoleukodystrophy
APS	ammonium persulphate
At, A. thaliana	*Arabidopsis thaliana*
ATP	Adenosine-5'-triphosphate
β	beta
BiFC	bimolecular fluorescence complementation
bp	base pair(s)
BSA	bovine serum albumin
°C	degree Celsius
CCALD	childhood cerebral adrenoleukodystrophy
CCD	charge-coupled device
cDNA	complementary DNA
CLSM	confocal laser scanning microscopy
CMV	cytomegalovirus
Con	control
DAB	3, 3'-diaminebenzidine
DBP	D-bifunctional protein
DCF	dichlorofluorescein
DEAE-Dextran	diethylaminoethyl dextran
DEPC	diethylpyrocarbonate
dH_2O	distilled water
DLP1	dynamin-like protein 1
DMEM	Dulbecco's modified Eagle medium
DMSO	dimethyl sulphoxide
DNA	deoxyribonucleic acid
DSP	dithiobis(succinimidyl propionate)
dT	deoxythymidine
DTT	dithiothreitol
E. coli	*Escherischia coli*
e.g.	*exempli gratia* (for example)
ECL	enhanced chemiluminescence
EDTA	ethylenediaminetetraacetic acid

EM	electron microscopy
ER	endoplasmic reticulum
et al.	*et alii* (and others)
F	Farad
FBS	fetal bovine serum
FRAP	fluorescence recovery after photobleaching
γ	gamma
x g	x 9.81 m s^{-2}
G	gauge (~ reciprocal inch)
g	gram
GAPDH	glyceraldehyde 3-phosphate dehydrogenase
GFP	green fluorescent protein
h	hour
Hp, H. polymorpha	*Hansenula polymorpha*
H. sapiens	*Homo sapiens*
HRP	horseradish peroxidase
i.e.	*id est* (which means)
IMF	immunofluorescence
IP	immunoprecipitation
IRD	infantile Refsum's disease
kb	kilo base pairs
kDa	kilo Dalton
l	litre
LC3	microtubule-associated protein I light chain 3
µ	micro (10^{-6})
m	metre
M	molar
m (prefix)	milli (10^{-3})
mc	monoclonal
MDV	mitochondria-derived vesicle
Mff	mitochondrial fission factor
min	minute
Mito	mitochondria
ml	millilitre
M-MuLV	*Moloney Murine Leukemia Virus*
mPTS	peroxisomal targeting signal of PMPs
mRNA	messenger RNA
n	nano (10^{-9})
N. crassa	*Neurospora crassa*
NALD	neonatal adrenoleukodystrophy
Ω	Ohm
ORE	oleate response element
p	pico (10^{-12})
P. chrysogenum	*Penicicilium chrysogenum*

P. pastoris	*Pichia pastoris*
PAGE	polyacrylamide gel electrophoresis
PAS	protein A-sepharose
PBD	peroxisome biogenesis disorder
PBS	phosphate buffered saline
PBS	phosphate buffered saline
pc	polyclonal
PCR	polymerase chain reaction
PCR	polymerase chain reaction
PED	peroxisomal enzyme deficiency
PEI	polyethylenimine
Pex	peroxin
PH	Pleckstrin homology
pH	negative decimal logarithm of hydrogen ion activity
PMP	peroxisomal membrane protein
PMSF	phenylmethylsulphonyl fluoride
PO	peroxisome
POLP	peroxisome-specific isoform of Lon protease
PPAR	peroxisome proliferator activated receptor
PPP	Pex11-type peroxisome proliferator
PTS	peroxisomal targeting signal
RCDP	Rhizomelic chondrodysplasia punctata
RE	restriction endonuclease
RHD	reticulon homology domains
RING	really interesting new gene
RISC	RNA-induced silencing complex
RNA	ribonucleic acid
RNAi	RNA interference
ROI	region of interest
ROS	reactive oxygen species
rpm	revolutions per minute
RT	reverse transcription/transcriptase
s/sec	second
Sc, *S. cerevisiae*	*Saccharomyces cerevisiae*
SD	standard deviation
SDS	sodium dodecyl sulphate
SH3	Src-Homology 3
siRNA	small interfering RNA
SQ-PCR	semi-quantitative RT-PCR
TA	tail-anchored
Tb, *T. brucei*	*Trypanosoma brucei*
TEMED	tetramethylethelenediamine
T_m	melting temperature
TMD	transmembrane domain

TPA	tubular peroxisomal accumulation
TPR	tetratricopeptide repeat
TRITC	tetramethylrhodamine 5 isothiocyanate
U	units
U	Unit
UT	untagged
UV	ultraviolet
V	volt
v/v	volume per volume
VLCFA	very long-chain fatty acids
Vps1	Vacuolar protein sorting-associated protein 1
w/v	weight per volume
WB	Western blot
WD	tryptophan-aspartic acid
X-ALD	X-linked adrenoleukodystrophy
YFP	yellow fluorescent protein
Yl, *Y. lipolytica*	*Yarrowia lipolytica*
ZS	Zellweger syndrome
ZSS	Zellweger syndrome spectrum

8.1.2 Unit definitions

KOD DNA polymerase:

One unit is defined as the amount of enzyme that will catalyze the incorporation of 10 nmol of dNTP into acid-insoluble form in 30 minutes at 75°C in a reaction containing 20 mM Tris-HCl (pH 7.5 at 25°C), 8 mM $MgCl_2$, 0.5 mM DTT, 50 µg/ml BSA, 150 µM each of dATP, dCTP, dGTP, dTTP and 150 µg/ml activated calf thymus DNA. (Novagen)

Ligase:

One unit is defined as the amount of enzyme required to give 50% ligation of *Hind*III fragments of λ DNA (5´ DNA termini concentration of 0.12 µM, 300- µg/ml) in a total reaction volume of 20 µl in 30 minutes at 16°C in 1x T4 DNA Ligase Reaction Buffer. (NEB)

Restriction enzymes:

One unit is defined as the amount of enzyme required to digest 1 µg of λ DNA in 1 hour at 37°C in a total reaction volume of 50 µl. (NEB)

Taq DNA polymerase:

One unit is defined as the amount of enzyme that will incorporate 15 nmol of dNTP into acid-insoluble material in 30 minutes at 75°C. (NEB)

8.2 Table of figures

8.3 Curriculum vitae

Diese Seite enthält persönliche Daten und ist daher nicht Bestandteil der Veröffentlichung.

8.4 Verzeichnis der akademischen Lehrer

Meine akademischen Lehrer in Marburg waren die Damen und Herren Professoren, Doktoren und Dozenten:

Dalpke
Daut
Dietrich
Eilers
Elsässer
Feuser
Garn
Garten
Gudermann
Hasilik
Hassel
Hilt
Huber
Hühnermann
Jacob
Junclas
Kirchner
Knöller
Koolmann
Kunz
Lang
Lill
Löffler
Lohoff
Lorberth
Maisner
Moll
Müller
Renkawitz-Pohl
Röhm
Röper
Schäfer
Schrader
Stöckmann
Voigt
Weihe
Westermann

8.5 Acknowledgements

First of all I would like to thank PD Dr. Michael Schrader for the exciting project, the pieces of advice in the curse of my work and the many fruitful discussions. I am very grateful for his trust, support and all the provided opportunities. They enabled me to make a lot of valuable experiences in Portugal, both scientifically and personally.

I would like to thank Prof Dr. Ralf Jacob for kindly being the supervisor of my thesis.

Many thanks to the members of the *Institut für Zytobiolgie und Zytopathologie* for their cooperation, in particular to Brigitte Agricola.

I would like to deeply thank all the members of the Schrader-lab, in particular Nina Anna Maria Bonekamp, who met the numerous scientific and non-scientific challenges with me, and Conni Rinn. Furthermore, I would like to thank all the great people that gave me such a warm welcome, support, scientific advices and a wonderful time in Portugal, especially Maria de Fátima Camões Sobral de Bastos, Sandra Isabel Moreira Pinto Vieira, Ana Sofia da Cunha Guimarães, María Gómez Lázaro, Miguel Ângelo Mouta Martins Aroso, Sara Luisa de Castro Esteves, and Maria João Ribeiro Cardoso. Muito obrigada por tudo!

Furthermore, I would like to thank all members of the *Centro de Biologia Celular* and the *Departamento de Biologia* in Aveiro for their big support.

I would also like to thank all the dear people and friends outside of the lab who accompanied me during my thesis, both in Portugal and from Germany.

Finally, I would like to thank my family, in particular my parents, sisters and aunt, and special thanks go to Thomas Kröger. I am very grateful for the big and caring support and the patience during the last years. It gave me the strength required for this work.

8.6 Ehrenwörtliche Erklärung (mit Publikationsliste)

Ich erkläre ehrenwörtlich, dass ich die dem Fachbereich Medizin Marburg zur Promotion eingereichte Arbeit mit dem Titel „Biogenesis of peroxisomes in mammalian cells: Characterization oft the Pex11 proteins and their role in peroxisomal growth and division“ selber und ohne fremde Hilfe verfasst, nicht andere als die angegebenen Quellen oder Hilfsmittel benutzt, alle vollständig oder sinngemäß übernommenen Zitate als solche gekennzeichnet sowie die Dissertation in der vorliegenden oder einer ähnlichen Form noch bei keiner anderen in- oder ausländischen Hochschule anlässlich eines Promotionsgesuchs oder zu anderen Prüfungszwecken eingereicht habe. Ich habe bisher an keiner Hochschule ein Gesuch um Zulassung zur Promotion eingereicht.

Marburg Hannah Delille

Teile der vorliegenden Arbeit wurden/werden wie folgt publiziert:

Delille HK & Schrader M. (2008)
Targeting of hFis1 to peroxisomes is mediated by Pex19p. *J Biol Chem* 283(45): 31107-31115.

Delille HK, Agricola B, Guimaraes SC, Borta H, Lüers GH, Fransen M, & Schrader M. (2010)
Pex11pβ-mediated growth and division of mammalian peroxisomes follows a maturation pathway. *J Cell Sci* (in press)

Delille HK, Guimaraes SC, Gomez-Lazaro M, Cardoso MJ, Rinn C & Schrader M. (2010)
Comparative analysis of Pex11p alpha, beta and gamma. (in Vorbereitung)

Delille HK, Bonekamp NB, Pinho S & Schrader M. (2010)
Hypertubulation of peroxisomes by multiple stimuli. (in Vorbereitung)

Reviews:

Delille HK, Bonekamp NA & Schrader M. (2006)
Peroxisomes and disease - an overview. *Int J Biomed Sci* 2(4): 308-314.

Delille HK, Alves R & Schrader M. (2009)
Biogenesis of peroxisomes and mitochondria: linked by division. *Histochem Cell Biol* 131(4): 441-446.

Camoes F, Bonekamp NA, Delille HK & Schrader M. (2009)
Organelle dynamics and dysfunction: A closer link between peroxisomes and mitochondria. *J Inherit Metab Dis* 32(2): 163-180.

Publizierte Abstracts:

Delille HK & Schrader M. (2008)
Targeting of hFis1 to peroxisomes is mediated by Pex19p. *Eur J Cell Biol* 87S1 (Suppl. 58) MS4-6

Delille HK & Schrader M. (2009)
Hypertubulation of peroxisomes by multiple stimuli. *Eur J Cell Biol* 88S1 (Suppl. 59) U-2

Posterpräsentationen:

Delille HK & Schrader M. (2008)
Targeting of hFis1 to peroxisomes is mediated by Pex19p. 31st Annual Meeting of the German Society for Cell Biology, Marburg

Delille HK & Schrader M. (2009)
Hypertubulation of peroxisomes by multiple stimuli. 32nd Annual Meeting of the German Society for Cell Biology, Konstanz

Delille HK & Schrader M. (2009)
Hypertubulation of peroxisomes by multiple stimuli. Sinal, 3rd National Meeting on Signal Transduction, Aveiro, Portugal

Delille HK, Bonekamp NA, Agricola B, Lüers GH & Schrader M. (2009)
Pex11pβ-induced growth and division of peroxisomes follows a maturation pathway. The EMBO Meeting, Amsterdam, Niederlande